MOLECULAR MODELLING AIDED DESIGN AND SYNTHESIS OF PHOTOCHROMIC DYES CONTAINING A PERMANENT CHROMOPHORE

Being a Thesis

presented by

AYESHA RASHEED (BSc., MSc.)

in application for

THE DEGREE OF DOCTOR OF PHILOSOPHY

to HERIOT-WATT University

The work embodied in this text was carried out at the Scottish Borders Campus, School of Textiles and Design.

January 2008

Abstract

Photochromic dyes are a very important and relatively novel class of dyes. The usual, though not exclusive, behaviour of these dyes is to show a reversible colour change from colourless to coloured when exposed to UV light. Among the photochromic dye classes, spirooxazines and naphthopyrans were selected for investigation. An attempt was made to construct molecules with a permanent chromophore (azo) in spirooxazines as well as naphthopyrans separately, with a view to providing a colour change from one colour to another. Three different isomers of dihydroxynaphthalene were used as one group of starting materials for the synthesis of spirooxazines with the introduction of the azo (hydrazone) chromophore by coupling. Other starting materials used were anthraquinones, naphthoquinones and pyrazolones. A range of molecular modelling techniques (molecular mechanics, MM2 and quantum mechanics, AM1) using the CAChe system, were applied to predict optimized geometrical conformations and energies of the ring-closed form and ring-opened merocyanine forms of all the dyes. PPP-MO calculations were also carried out to predict the potential colour of the dyes. The dyes were characterized using DSC, FTIR, NMR, UV-Visible spectroscopy and elemental analysis. The photochromic properties of one of the azospirooxazines was subjected to a detailed study under different experimental conditions, and showed a unique slow colour change from orange to grey.

Dedicated to my family

Acknowledgements

Many thanks are due to Dr R. M. Christie of the School of Textiles and Design, the Scottish Borders Campus for his guidance, expert supervision, and encouragement throughout my time in Galashiels. Thanks are also due to Professor R. Wardman as a co-supervisor and Dr K. M. Morgan for his expert advise on molecular modelling.

I am also thankful to Dr R. A. Spark and Mrs. M. Robson for their technical assistance.

Thanks are also due to Dr M. Heron of the University of Leeds, Department of Colour and Polymer Chemistry, for his advice during this research project.

My sincere thanks to the Worshipful Company of Dyers (London) for the award of studentship for PhD.

The help of library staff and the computer services of the Scottish Borders Campus is much appreciated. I would like to express my gratitude to Mrs. E. Drummond and Mr. and Mrs Leslie Steele for their help and care, as without their influence I would not have been able to enjoy my time here.

Special thanks are due to my mother and to all my family for their love and support throughout my time here.

TABLE OF CONTENTS

3 Results and discussion

1 Introduction

There is considerable interest in photochromic materials arising from the many potential applications which are associated with their ability to undergo reversible, light-induced colour change. Two chemical species showing reversible transformation differ from one another not only in the absorption spectra but in their physical and chemical properties as well. Photochromic materials are used most widely in ophthalmic sun-screening applications, and also find applications in security printing, optical recording and switching, solar energy storage, nonlinear optics and biological systems.[1-11] Spirooxazines are a particularly significant group of photochromic materials, due to their intense colour generation properties, good fatigue resistance and relative ease of synthesis. The existing range of products generally undergoes positive photochromism, a light-induced transition from colourless to coloured due to a ring-opening reaction.

The aim of this research work was to design, using computer-aided molecular modelling techniques, and synthesise spirooxazine dyes which also contain a permanent azo (hydrazone) chromophore, aimed to produce materials which undergo a photochromic change from one colour to another. It was anticipated that the observed colour changes, determined by the differences in the visible spectra of the ring-closed and ring-opened forms, would be significantly different from those given by physical mixtures of permanently coloured dyes and photochromic dyes, thus providing the potential for niche applications, for example in anti-counterfeit security printing and brand protection. Another direction of research was a reinvestigation and continuation of some results related to spirooxazines based on nitrosopyrazolones and the investigation of a secondary product which proved to be an N-oxide.

Two main photochromic families, spirooxazines and naphthopyrans, were selected for investigation and with molecular modelling carried out on the target molecules followed by synthesis of selected molecules. Different types of starting materials but with certain common features in attempts to synthesize spirooxazines. The modelling of the molecules involved geometry optimization with MM2 and the calculations of final energies, followed

by the calculation of the heats of formation obtained from AM1 calculations. The comparison of heat of formation values of ring closed and ring opened isomers helps in the prediction of photochromic behaviour of molecule. It is a useful predictive tool before proceeding to synthesis to provide information about the potential photochromic behaviour of the product.

The second chapter of this thesis describes the general principles of the theoretical background underlying this thesis with a detailed literature review. The chapter starts with an introduction to colour and constitution relationships. Basic concepts of the electromagnetic spectrum are followed by an explanation of the application of valence bond theory, and molecular orbital theory including the Pariser-Parr Pople Molecular Orbital method. Some discussion of more advanced molecular orbital is also given.

Photochromism is the main focus of the literature review, providing an overview of history and definitions followed by a review of the photochromic mechanisms.

Section 2.3 provides an overview of spirooxazines, one of the most important classes of photochromic dyes. An introduction and explanation of the spectral properties with reference to substitution effects and mechanisms is discussed. A discussion on properties such as photodegradation including the mechanism of formation of degradation products is given. Synthetic methods are briefly explained to illustrate different possible routes for preparation.

The principles governing in diazotization and azo coupling are outlined in section 2.4 outlined with appropriate reference to reaction conditions.

Naphthopyrans are similarly treated in a further sub-section of the literature review.

Section 2.6 describes about molecular modelling including molecular orbital theories.
The results of the investigation on the range of photochromic dyes investigation and a discussion of the compounds are found in Chapter 3. These sections are generally

structured to begin with molecular modelling, involving molecular mechanics (MM2) and Quantum mechanics calculations, which are used for the comparison of relative stabilities of the possible photomerocyanines and the prediction for potential photochromism respectively. The second sections deal with the prediction of λ_{max} values using the PPP-MO calculations. These calculations were used because of their versatility and general ability to correlate with experimental λ_{max} values although there are issues when compounds are non-planer. Discussion on syntheses is then accompanied by the analytical data from DSC, FTIR, ^{1}H NMR, mass spectrometry, UV-visible spectroscopy, and X-ray crystallography on selected molecules. The interesting photochromic behaviour of one azospirooxazine is investigated in detail.

Chapter 4 covers the overall conclusions that had been drawn from this investigation in terms of correlation of molecular modelling results with the results of compounds obtained from synthesis, prediction of merocyanine isomer and a comparison of the electronic spectral properties with the PPP-MO calculations.

Details of the experimental procedure are given in Chapter 5 while the extensive list of reference used within this study is given after Chapter 5. X-ray crystal structure data for azo-based spirooxazine is given in Appendix A and pyrazolone-based spirooxazines is provided in Appendices B and C respectively. Glossary of terms is given at the end.

2 Literature review

2.1 Colour and constitution

2.1.1 Colour

Colour is the visual perceptual property in which the brain recognizes the different qualities of light falling on the retina within an approximate wavelength range of 380-780 nm. The electromagnetic character of light was suggested by Maxwell and later, in 1905, Planck and Einstein developed the particle theory of electromagnetic radiation. Light was regarded as a stream of discrete energy particles or photons which travel with the velocity of the wave front in Maxwell's wave theory. Light can be characterized either by its wavelength or frequency in wave theory.

$$c = \upsilon\lambda$$

where c is the velocity of light, υ is the frequency and λ is the wavelength of light.

The particle theory deals with the characterization of monochromatic radiation by the energy of each photon. The energy of a photon can be related to the frequency of the wave by Planck's equation.

$$E = h\upsilon$$

h = Planck's constant which has a value of 6.63×10^{-34} J s.

The electromagnetic spectrum comprises the complete range of wavelengths of electromagnetic radiation. The spectrum starts from the short wavelength such as X-rays and γ rays to the long wavelength radiations such as radio waves. The visible region ranges from 380 nm to 780 nm. The electromagnetic spectrum is shown in Figure 1.

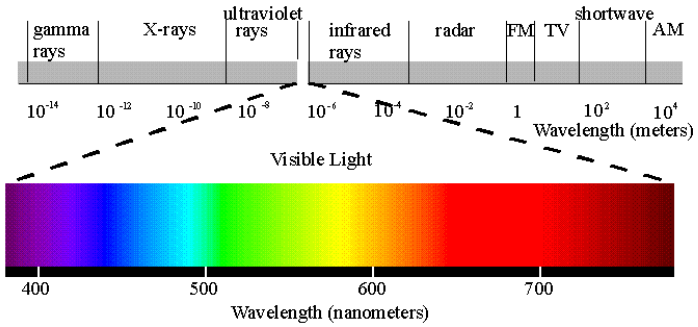

Figure 1: The electromagnetic spectrum.

Colouring materials normally termed as "colorants" include dyes and pigments. The solubility character distinguishes dyes from pigments, the former being soluble commonly in water while the latter are insoluble in their application medium. There are two ways to classify colorants, either according to their chemical structure or by their method of application. Colorants have the ability to absorb selectively radiation from the visible region. The absorption characteristics of a dye can be measured in solution by UV-visible absorption spectroscopy. The relationship between the absorbance **A** of a dye in solution and the concentration of an absorbing species can be expressed in the Lambert-Beer law and is usually written as:

$$\mathbf{A = \varepsilon cl}$$

ε = the molar extinction coefficient with units of l mol^{-1} cm^{-1}

c = concentration of solute, expressed in mol l^{-1}

l = path length of the sample (cm)

2.1.2 Developments in Theories of Colour and Constitution

(a) Classical Theories:

(i) 1865-1887

The relationship between colour and chemical constitution of dyes has long intrigued chemists. Kekule's structure of benzene was published in 1865 [12] and *p*-

benzoquinone was at that time the only coloured compound whose structure was known. One of the first contribution to the relationship between colour and constitution was proposed by Graebe and Liebermann in 1867.[13] The destruction of colour of known dyes by reduction led them to the conclusion that dyes are chemically unsaturated compounds. Witt, in 1876, [14] proposed a concept suggesting that dyes consist chemically of two groups, one of which was called the chromophore which can be defined as the group of atoms principally responsible for the colour of the dye. The part of the molecule possessing the chromophore was called the chromogen. Secondly there were groups called the auxochromes. The main function of an auxochrome was described as the enhancement of the colour.[15] Three years later, Nietzki suggested that a bathochromic shift was produced by the introduction of certain substituents such as methyl, ethyl or ethoxy etc.[16] The quinonoid theory of colour was proposed by Armstrong in 1887, which argued that coloured compounds are compounds which can be written in quinonoid form.[17]

(ii) 1904-1935

The first coloured free radical, the triphenylmethyl radical, was discovered by Gomberg in 1900 [18] and during research on this radical, the theory of halochromism was proposed by Baeyer, which proposed that a colourless compound may be rendered coloured on salt formation. In 1907, Baeyer [19] proposed the theory of tautomerism which states that there is a rapid oscillation between two tautomeric forms of a compound such as in the case of Doebner's violet **(1)** ⇌ **(1a)**, with a rapid flipping of the chloride ion from one amino group to another.

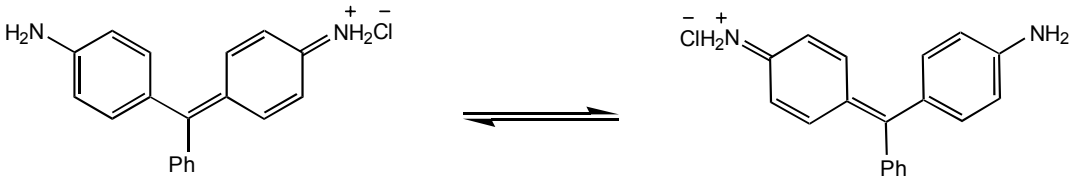

(1) **(1a)**

Scheme 1: Proposed tautomeric forms of Doebner's violet.

The theory of "chromotropy" suggested by Hantzsch, after working on indophenols and their coloured salts, provided the same conclusion as Baeyer's theory. Isorropesis was defined as a process where the colour was suggested to be the result of the breaking and reforming of the bonds during the oscillation from one tautomeric form to another as proposed by Baly in 1907. The understanding of colour and constitution relationships developed further as "Tautomeric Theory" was proposed by Watson in 1914.[20] This theory proposed tautomerism as the basic requirement to achieve a coloured molecule and also that the conjugated chain must exist in a quinonoid form in all the possible tautomers. The theories of Armstrong and Watson became untenable after the discovery of dyes without a quinonoid structure.

Adams and Rosenstein were the first to suggest the link between colour and the oscillation of electrons.[21] They rejected the concept of oscillation of atoms which gives rise to the absorption of infrared radiation. Bury, in 1935, highlighted the relationship between the colour of a dye and resonance.[22]

Baeyer's idea that the colour of Doebner's violet arose from the oscillation of atoms was refuted by Bury, who proposed that it was the electrons that moved and not the atoms, and that the movement of the electrons was explained by the concept of resonance i.e.

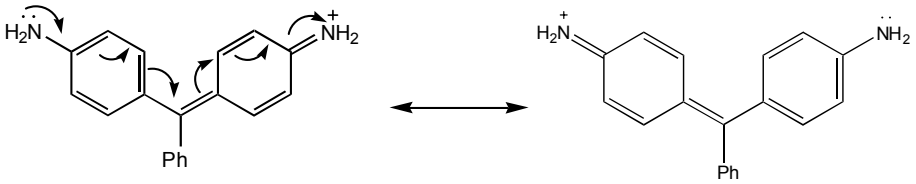

(2) **(2a)**

Scheme 2: Resonance in compound **(2)**.

Bury proposed that colour is due to the involvement of a chromogen in resonance in the molecule. The theory most similar to modern concepts was originally proposed by Lewis in 1916; [23] he described colour as the result of selective absorption of light by valence electrons. The frequency of oscillation was suggested to be synchronized with light of a definite frequency.

(b) Modern Theories

The modern theories of colour, namely Valence Bond (VB) Theory and Molecular Orbital (MO) Theory, evolved from the Einstein Planck quantum theory which stated that energy adopts quantized values and is not continuous. VB theory and MO theory differ in that the former is based on the valence electron pair being localized between specific atoms, while with the latter, electrons are considered as being distributed among a set of molecular orbitals of specific energies.

(i) Valence Bond Theory or Resonance Theory

The quantitative approach to valence bond theory, because of its failure in the application to larger molecules, was replaced by qualitative VB theory, pioneered by Heitler, London, Pauling and Slater shortly after the publication of Schrödinger's equation. The valence bond approach postulates a series of organic structures of a particular compound in which electrons are localized in bonds between atoms. The overall structure is considered to be a hybrid of the contributing forms. Two assumptions or approximations were made in order to apply the valence-bond approach to colour and constitution, which are:

(i) the ground electronic state of the dye resembles the most stable resonance form (s).
(ii) the first excited state of the dye resembles the less stable, charge-separated form (s).

A qualitative explanation of colour can be provided by an analysis of factors e.g. electronic and steric, which stabilize or destabilize the first excited state relative to the ground state. The bathochromicity of a dye is explained on the basis of Planck's relationship which determines that by decreasing the energy difference between the ground state and the first excited state, there is an increase in the wavelength absorbed by the dye. This effect can be explained by the example of compound **(3)** as shown in scheme 3.

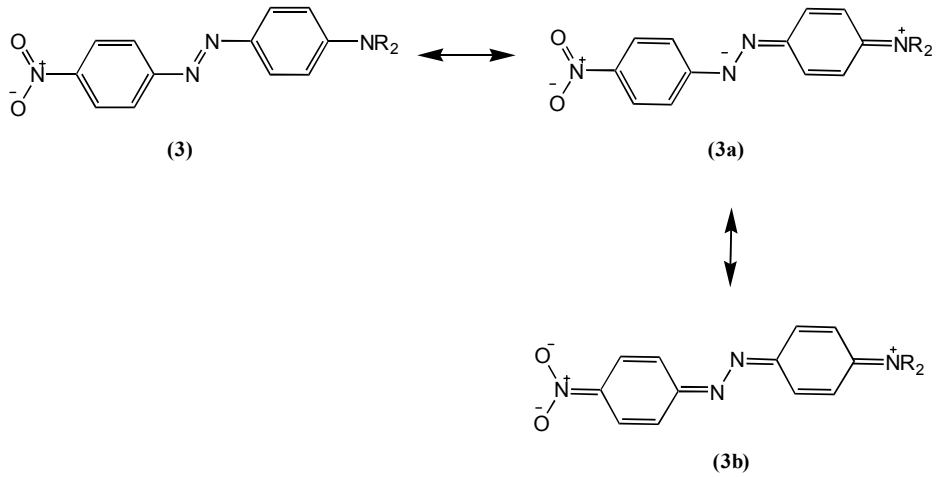

Scheme 3: The stabilization of compound **(3)** because of charge delocalization.

While charge-separated structures **(3a)** and **(3b)** contribute to the ground state of the dye, it is assumed that they make a greater contribution to the first excited state. In this case electron-donor groups and electron-acceptor groups are in the same molecule. The additional stabilization of the first excited state by charge delocalization onto the nitro group explains the strong bathochromicity compared with azobenzene derivatives without this group. The stabilization of the first excited state by lowering the energy causes a bathochromic shift. Steric and electronic effects can affect the colour of the dye. This is clearly illustrated for compounds **(4a)** and **(4b)**.

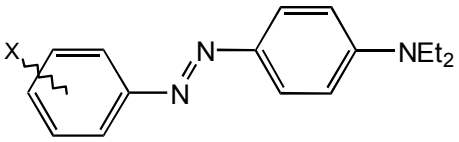

(4a), X=*o*-NO_2

(4b), X= *p*-NO_2

Figure 2: Structure of compounds **(4a)** and **(4b)**.

The *p*-nitro group produces a more pronounced bathochromic effect than *o*-nitro. The compound **(4b)** has a planar structure while **(4a)** is non-planar due to steric constraints

between the *o*-nitro group and the lone pair of the azo group. This arrangement causes the group to rotate out of plane. The rotation takes place between the carbon atom of the aromatic ring and the nitrogen atom of the NO_2 group. The rotation about the double bond requires more energy than the rotation about a single bond. The first excited state of compound **(4a)** in which this bond has considerable double bond character is destabilized relative to its ground state where the bond is closer to a single bond which results in the reduction in the bathochromic effect.

(ii) Molecular Orbital Theory

In molecular orbital theory, the electrons are considered as a form of electromagnetic radiation. The formation of an electronically excited state, due to the electronic distribution within a molecule results in the absorption of ultraviolet and visible light. The molecule can only exist in a series of discrete energy states according to quantum theory. When quanta of visible ultraviolet light are absorbed, the molecules are promoted to a higher energy state. The following equation relates the energy of radiation absorbed to the absorption frequency.

$$E_{\text{excited state}} - E_{\text{ground state}} = h\upsilon$$

Schrodinger's wave equation in its simplest form is written as

$$\mathbf{E\psi = H\,\psi}$$

Here ψ is the molecular orbital wave function, a function of the momenta and coordinates of all the electrons in the molecule, E is the energy associated with the molecular orbital, H is the Hamiltonian operator, a complex differential operator which operates on the molecular wavefunction (ψ). The mathematics of atomic orbital theory is complex and was first elaborated by Schrodinger by the following equation.

$$\frac{\partial^2\phi}{\partial x^2}+\frac{\partial^2\phi}{\partial y^2}+\frac{\partial^2\phi}{\partial z^2}+\frac{8\pi^2 m}{h^2}[E-U(x,y,z)]\phi=0$$

h = Planck's constant.

m = Mass of an electron.

U = Potential energy of the electron as a function of space co-ordinates x, y and z.

E = Total energy of the electron.

ϕ = The atomic wave function assigned to the electron.

The overlap of atomic orbitals generates molecular orbitals; σ-orbitals obtained as a result of direct overlap are low energy. The 'sideways' overlap gives rise to π- molecular orbitals. The extended conjugation of dyes contains a framework of σ-bonds with an associated π-system. The promotion of electrons from a π-orbital to an unoccupied π*-orbital gives rise to the lowest energy transition. The absorption of organic dyes and pigments in the UV and visible regions of the spectrum are mainly because of the π- π* transitions.

(iii) Hückel Molecular Orbital (HMO) Method

This is a method of obtaining one-electron orbital wave functions and energies. It involves the linear combination of atomic orbital procedures which assumes that a molecular orbital wave function can be expressed as a linear combination of atomic orbital (LCAO) wave functions. When light is absorbed in a conjugated system, only π electrons are involved in the electronic transition and σ bonds in the molecule remain unaffected; this is an important assumption for the HMO method which is a reasonable approximation. Electronic transition energies for the promotion of an electron from an occupied molecular orbital to an unoccupied higher energy orbital are provided by the HMO method. The values denoted as the resonance integral (β), are considered as empirical parameters. The HMO method is also used to calculate π electron charge densities (Q) and bond orders (P).

(iv) Π-electron charge densities (Q) and π- bond orders (P)

The charge distribution and bonding proportion in conjugated systems are also described by the method based on the LCAO assumption. In addition, the π-electrons are assumed to be independent of each other with no interaction between each pair. The HMO method is not particularly useful in quantitative correlation with spectral data for dyes.

This method works well for the polyenes or other hydrocarbons but works less well for molecules containing hetero atoms, e.g. O and N mainly because it takes no account of electron-electron interactions.

(v) Pariser, Parr and Pople (PPP) Molecular Orbital Method

This method is suitable for the treatment of conjugated and larger molecules and also contains approximations. Pariser and Parr [24] and Pople [25] methods retain the σ-π separation principle and LCAO approximation of the HMO method. In addition to this, inter-electronic repulsion effects are also taken into account. Advantages of this method over HMO or FEMO procedures include the ability to accommodate molecules with heteroatoms, the inclusion of molecular geometry [26] and the ability to distinguish between two states of the molecule (singlet and triplet). The procedure for PPP-MO calculations involves the following steps.

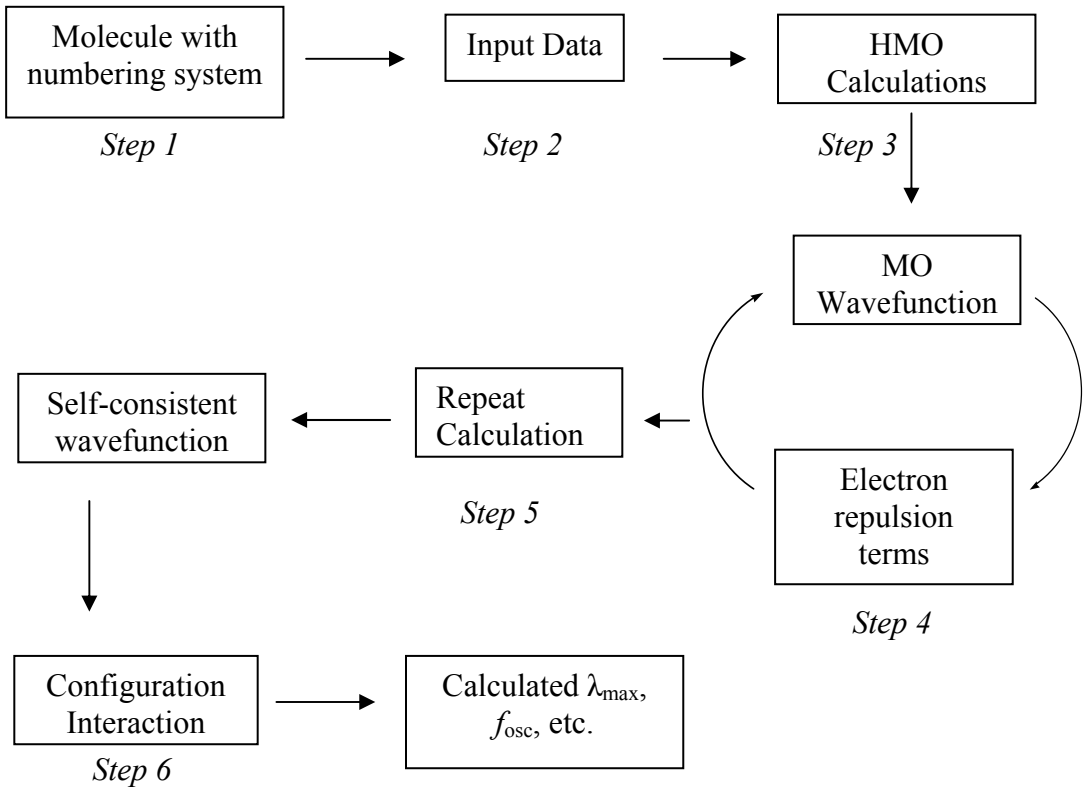

Scheme 4: The systematic scheme for PPP-MO calculation.

Step 1:

In the first step, all the atoms in the π-system of the molecule are numbered and the total number of π-electrons indicated.

Step 2:

As a second step, a combination of absolute values (bond angles, bond lengths, core charge) and semi-empirical values (valence state ionization potentials, electron affinities and bond resonance integrals) are used as input data for molecular orbital calculations. The specification of molecular geometry in terms of bond angles and bond lengths with the assignment of valence state ionization potential, electron affinity and bond resonance integral value (β) is the second step of calculations. The π-electron charge densities (Q) and π-bond order (P) are also required to be included for all the relevant atoms and bonds.

Step 3:

The electron densities and bond order determinations are only possible after the LCAO co-efficients for all the occupied orbital are known. To overcome this problem, an approximate set of LCAO co-efficients is obtained using a Hückel (HMO) calculation on the system and a set of molecular orbital wave function is obtained in the third step. The PPP parameters are based on the π-electron densities and bond orders determined in this way.

Step 4:

The fourth step is calculation of electronic interaction energies from the molecular orbital wave functions.

Step 5:

An improved set of co-efficients is obtained as a result of step 4 and a greater degree of consistency is obtained by the repetition of successive cycles. This iterative procedure is called a self-consistent field procedure which gives a more accurate set of molecular orbital energies which are used in the calculation of electronic transition energies.

Step 6:

As a last step in the calculation, configuration interaction (CI) is carried out to correlate the fact that molecular orbital energies may change after excitation and gives improved excited state data. The result of configuration interaction gives more accurate prediction of the absorption maximum.

Absorption maxima may be calculated by the PPP-MO method. In addition absorption intensities from oscillator strength values, absorption band widths and polarization directions can also be calculated.

By assuming a simple relationship between absorption band widths and Stoke's shift, this method has been successfully applied for the band-width calculation.[27] The dyes used in liquid crystal displays can be selected by the calculation of polarization direction.[28] The PPP-MO method is the most extensively used method for the prediction of colour properties.

(vi) Advanced MO Methods

In the PPP-MO method, the approximation of σ and π bond separate treatment becomes most evident in the case of non-planar molecules. Many molecular orbital methods which treat σ and π electrons simultaneously are known as "all-valence-electron" treatments. Pople and Segal [29] suggested the CNDO/1 method (i.e. complete neglect of differential overlap) followed by a modified version called CNDO/2.[30] These methods can be applied to small molecules and large organic molecules. Other all-valence-electron methods include the PNDO method (partial neglect of differential overlap) suggested by Dewar and Klopman, [31] the INDO method (intermediate neglect of differential overlap) [32] and finally a modification of INDO [33] called MINDO. The calculations involved in these methods are in principle more justifiable than PPP-MO because of their involvement of σ electrons. Because of the increased mathematical difficulties, their popularity is less than the PPP-MO method. ZINDO (Zerner's Intermediate Neglect of Differential Overlap), determines optimum geometry and electronic properties using valence-electron-only semi-empirical procedures and computes optimum geometries, bond orders, ionization potentials, electron affinities and electronic spectra.

2.2 Photochromism

2.2.1 History and development

Fritsche [34] is generally regarded as the first to observe the phenomenon of photochromism by the exposure of tetracene **(5)** to air and light which produced a colourless material with the regeneration of colour upon heating.

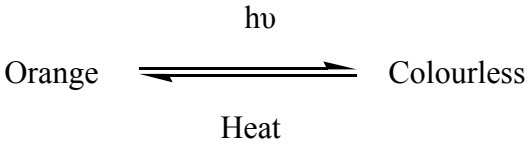

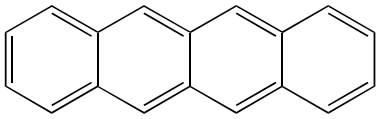

(5)

Figure 3: Structure of tetracene **(5)** with the colour change as shown.

Ter Meer [35] showed a colour change of yellow to red in the potassium salt of dinitromethane upon exposure to light. The photochromic character of benzalphenylhydrazone was first observed by Wislicenus [36] and later by Biltz.[37-39] The phenomenon in which a solid changes colour when exposed to light but reverts back to its original colour in dark was named "phototropy" by Marckwald [40] and was studied in benzo-1-naphthyridine and tetrachloro-1,2-naphthalenone **(6)**.[41]

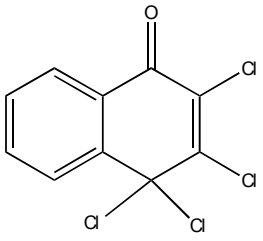

(6)

Figure 4: Structure of tetrachloro-1,2-naphthalenone (β-TCDHN)

The period from 1940 [1] to 1960 was important for photochromism with the development of a number of organic and inorganic photochromic compounds, assisted by advances in organic synthesis and the development of physical methods of characterisation such as NMR, UV, mass, IR spectroscopy and X-ray crystallography. The term "photochromism" was suggested by Hirshberg in 1950 for the light induced colour change in non-biological systems and he also suggested the possibility of photochromic compounds being used in optical memories.[42] A suggested application which attracted interest was the photochromic microimage (PCMI) process with the possibility of reduction of the 1245 pages of a Bible to an area of about $6cm^2$. The work of Hirshberg and Fischer is of note for the development and understanding of the mechanism of photochromism and the structures of the reactants, products and the intermediates. Photochromic materials are currently used most widely in ophthalmic sun-screening applications and also there are applications in security printing, optical recording and switching, solar energy storage, nonlinear optics and biological systems.[6, 43-48]

2.2.2 Definition and Process

"Photochromism" is defined as a light induced reversible transformation of chemical species between isomers having different absorption spectra. The word photochromism is a combination of two Greek words: Φωζ (photo) meaning light, and χρωμα (chroma) meaning colour, with the suffix (-ism) which means phenomenon. Most of the photochromic transformations are unimolecular in nature and can be represented as shown in Scheme 5.

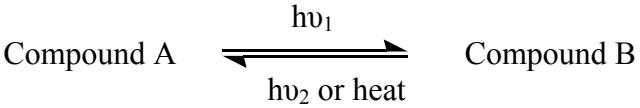

Scheme 5: Representation of a unimolecular photochromic system (positive photochromism).

The two isomers differ in their physical and chemical properties such as refractive indices, electronic distributions, geometric structures and dielectric constants in addition to their different absorption spectra. Compound A when irradiated converts into compound B. Reversibility is generally an important criterion for photochromism. Two types of photochromism are described on the basis of the nature of reverse reaction. If the reverse reaction occurs thermally, it is referred to as "*T*" type photochromism and if it occurs photochemically, it is known as "*P*" type photochromism.

The bimolecular reaction involving photocycloaddition reactions, where λ_{max} A > λ_{max} B, is called "negative" or inverse photochromism [49] when the compound is coloured in the dark and is bleached by UV-light. An example of the spectral outcome of a photochromic system is shown graphically in Figure 5.

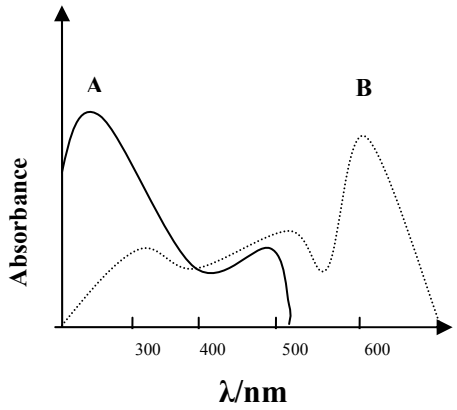

Figure 5: Graphic representation of a photochromic system.

Irreversible reactions leading to colour changes are generally considered as normal photochemical reactions, and not photochromism. Compound A is commonly referred to as in its "ground state" and after the influence of external stimulus ($h\upsilon_1$), the structure changes to the "excited state", compound B which is usually coloured and may have a life time from microseconds to weeks. However care must be exercised in the use of these terms because of confusion in their use in explaining the colour of individual species. The typical behaviour of a photochromic process is shown graphically in Figure 6.

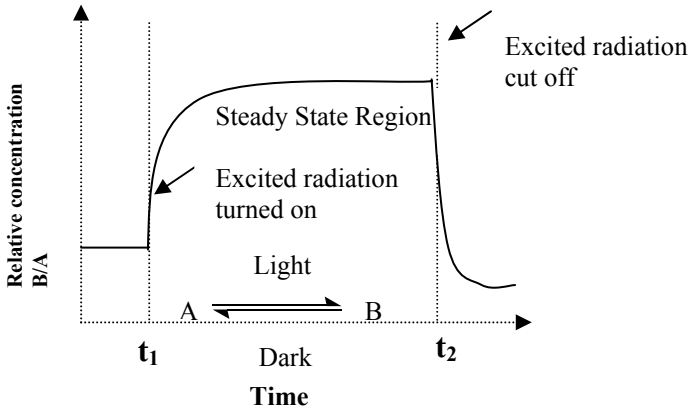

Figure 6: Graphic representation of a photochemical system.

The photochromic system initially consists of the A state of the molecule. When the exciting radiation is turned on at time t_1, a coloured form B is produced, whose concentration increases to a limiting value with time until a steady state of equilibrium $A \rightleftharpoons B$, is reached. The coloured form B reverts back to form A at time t_2, when the exciting radiation is removed, at a rate depending upon the kinetics of the dark reaction. The photochromic species after acquiring sufficient energy are activated and pass through an energy barrier to give compound B. The quantum yield is usually less than one as all the excited molecules may not undergo the conversion. The reverse reaction proceeds through a transition state of energy higher than that of the A and B states.

2.2.3 Photochromic mechanisms

Most photochromic systems are classified according to the nature of reaction such as reactions involving bond cleavage, tautomerism, oxidation-reduction reactions and *cis-trans* isomerization.

(a) Photochromic processes involving *cis-trans* isomerization [50]

The *cis-trans* isomerization process is shown in Scheme 6.

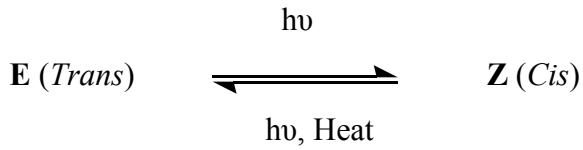

Scheme 6: *Cis-trans* isomerization process in photochromism.

The *cis-trans* isomerization process possesses the following characteristics:
(i) The *trans* isomer, in most cases, is thermodynamically more stable with a higher extinction coefficient, and absorbing at longer wavelength than the *cis*-isomer.

(ii) Most, E ⇌ Z isomerizations are reversible. The *cis*-isomer is converted back to the *trans*-isomer by a thermal (dark) process which may have a life time from milliseconds to months depending upon the solvents, temperature, pH and the chemical nature of the compound.

(iii) The quantum yield for such processes is temperature dependent, i.e. increases with the increase in temperature and in some cases is solvent sensitive.

Three different pathways are suggested for the conversion of *trans* isomer to the *cis*.
(i) The rotational mechanism, in which the π-bond is broken homolytically or heterolytically giving rise to a system which may rotate freely about the X-Y axis as shown in Figure 7.

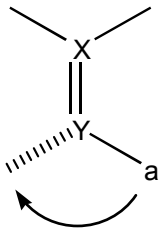

Figure 7: Rotational mechanism in *cis-trans* isomerization.

(ii) The inversion mechanism, which involves the inversion of substituents at the X=Y bond, as shown in Scheme 7.

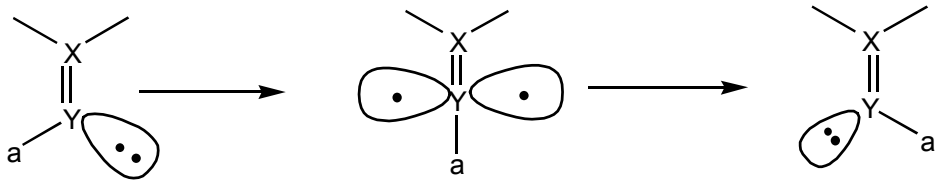

Scheme 7: Inversion mechanism in *cis-trans* isomerization.

One of the atoms forming the double bond requires an unshared electron pair or an unpaired electron in order to undergo an inverse mechanism.

(iii) The disassociation-recombination mechanism, where the breaking of a double bond and the recombination results in isomerization.

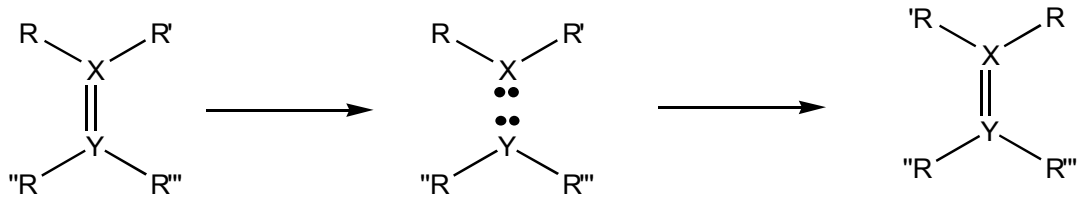

Scheme 8: Disassociation-recombination mechanism in *cis-trans* isomerization.

Thermal isomerization depends upon the energy levels of the ground states as well as the height of the transition energy barrier. The possibilities of thermal isomerization can be discussed as:

(i) If the activation energy barrier is small, the equilibrium is established thermally between both isomers and the reaction can proceed in both directions.

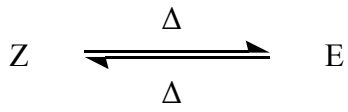

(ii) If the energy of the *cis*-isomer is greater than the *trans*, the thermal equilibrium is shifted towards the *trans*-isomer. When the activation energy barrier between two isomers is not too high then Z→E conversion can be observed.

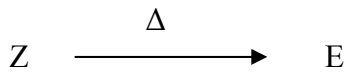

(iii) If the activation energy barrier is too high between two isomers then no thermal isomerization occurs.

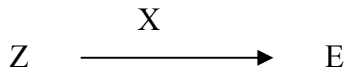

This type of photochromic reaction usually occurs in compounds such as alkenes where the C=C rotation gives rise to *cis-trans* isomerization. These reactions cause changes in parts of the spectrum with no visible change but are still classified as photochromism because the absorption spectra of the *cis* and *trans* isomers are significantly different. Important examples are found in some biological molecules, e.g., the isomerization of rhodopsin, the conversion of Schiff's base of 11-*cis*-retinal **(7)** with the protein opsin, to the *trans* isomer prelumirhodopsin **(8)** and the interconversion of tachysterol **(9)** to previtamin D **(10)**.(Schemes 9 & 10)

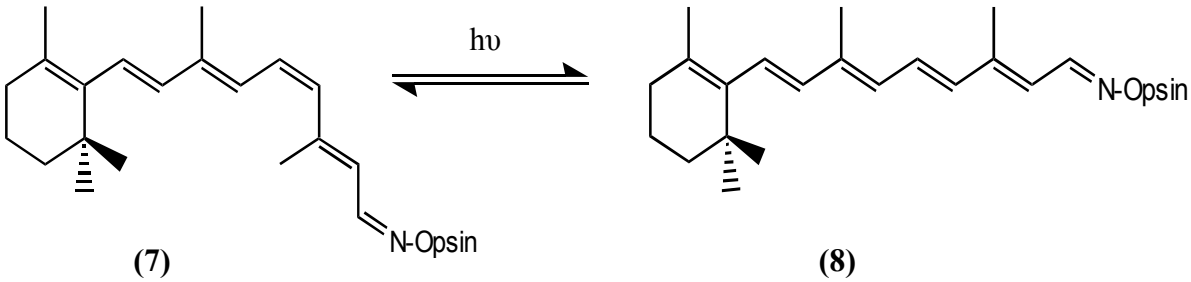

(7) **(8)**

Scheme 9: *Cis-trans* isomerization in rhodopsin.

Similarly, the conversion of tachysterol **(9)** to previtamin D **(10)** is shown in Scheme 10.

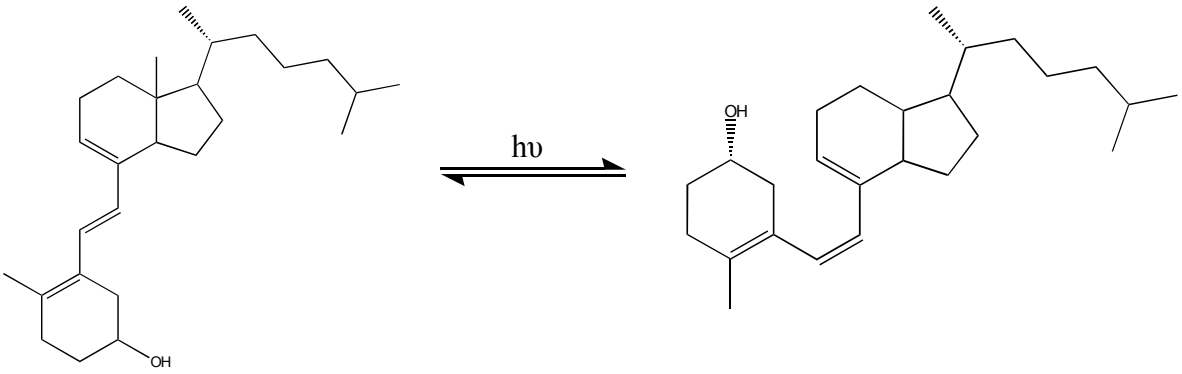

(9) **(10)**

Scheme 10: The interconversion of tachysterol **(9)** and previtamin D **(10)**.

(b) Photochromic processes involving cleavage (Heterolytic and Homolytic)

This type of cleavage occurs in most of the common organic compounds showing photochromism. The heterolytic cleavage of a single covalent bond of a photoactivated molecule occurs after excitation. The resulting charged moieties may exist as isolated ions or may remain connected by chemical bonding. The resulting species due to its structure may be relatively stable and may react thermally to regenerate the original molecule. Spiropyrans, spirooxazines, triarymethanes and polymethines are some of the classes of organic compounds which exhibit photochromism involving heterolytic cleavage.

In a spiropyran containing the 2-*H*-pyran ring, heterolytic cleavage of the 1,2-single bond of the pyran ring results in a zwitterion which is stabilized by resonance. The generalized reaction of spiropyran involved in photochromism is shown in Scheme 11.

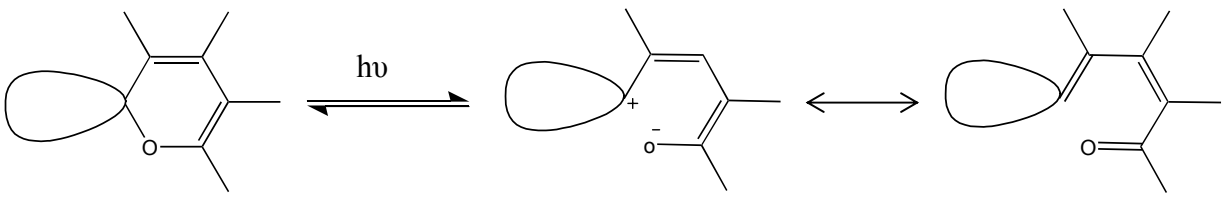

Scheme 11: The mechanism of photochromism in spiropyran.

In homolytic cleavage the bond dissociation is caused by energy absorption and localization of energy resulting in bond rupture. In thermal dissociation, the main cause of dissociation is the increase in vibrational, translational and rotational energy. Compounds such as hydrazines, pyrroles, sydnones and nitroso dimers exhibit this type of photochromism.
C-C bond cleavage by light is a widely used process in polymerization. The most powerful photoinitiators are benzyl and benzoin derivatives (ethers and ketals). Reversible C-C bond homolysis is presented by the bipyrrolyl system **(11)**.

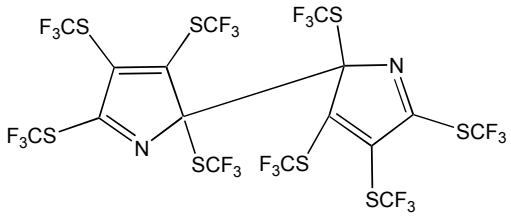

(11)

Figure 8: Structure of bipyrrolyl system.

It can be initiated photochemically and thermally.[51] Heating at 20^{o} C results in dissociation to radical species. These species on heating above the melting point causes rearrangement to the N-N linked isomer. Further photochemical data for compound **(11)** have not been reported.

(c) Photochromism based on tautomerism

The reversible interconversion of isomers differing in the location of a mobile H-atom is referred to as tautomerism. Photochromic tautomerism is essentially a photochemical shift in the equilibrium between two tautomers having different absorption spectra giving reversible colour change. In the tautomeric system illustrated in Scheme 8, the shift of the "Z" group induced by light between X and Y occurs due to a bond rearrangement giving different absorption spectra.

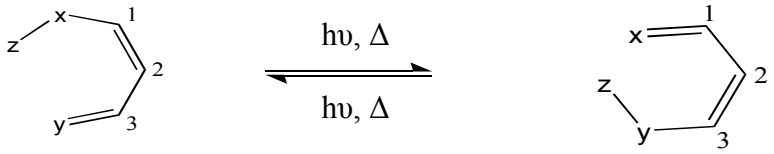

Scheme 12: The shift of Z group in a tautomeric system.

In photochromic tautomerism, exposure to light sources can result in a change in the relative concentrations of the isomers which may or may not reach thermal equilibrium readily. An illustration of different conditions is shown in Figure 9.

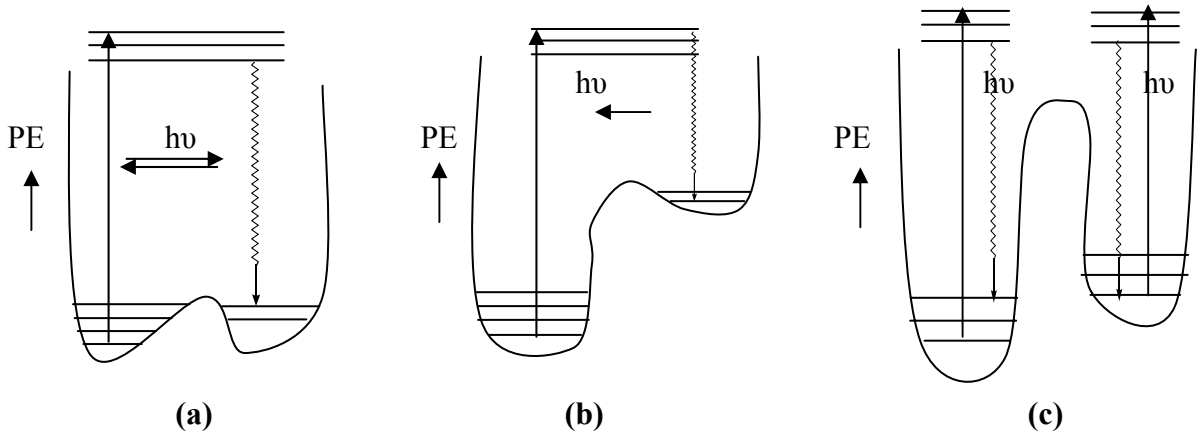

Figure 9: Potential energy diagram for photochromic tautomerism.

(a) Normal tautomeric situation, in which ready thermal interconversion of the isomers is possible because of the low potential energy barrier.
(b) Photochromic behaviour, where one isomer is dominant and the other isomer is formed photochemically and returns thermally to the most stable isomer.
(c) When the potential energy barrier is high between two isomers, the interconversion is achieved only by photoisomerization in each direction.
There are two types of photochromic tautomerism.[52]

(a) H-transfer tautomersim

This type of photochromic tautomerism possesses the following general characteristics.

(i) The intramolecular hydrogen transfer photolysis occurs through a six membered transition state.

(ii) Ortho substituted aromatic structures are thermally stable forms.

(iii) Quinonoid structures are produced by the photochemical hydrogen transfer.

(iv) When ortho substituents are polar, having increased reactivity than other groups then either a proton transfer can occur, if there is an acid-base relation between ortho groups or hydrogen abstraction reaction is favoured by an excited state.

A simple example [53] of H-transfer tautomerism is shown in Scheme 13.

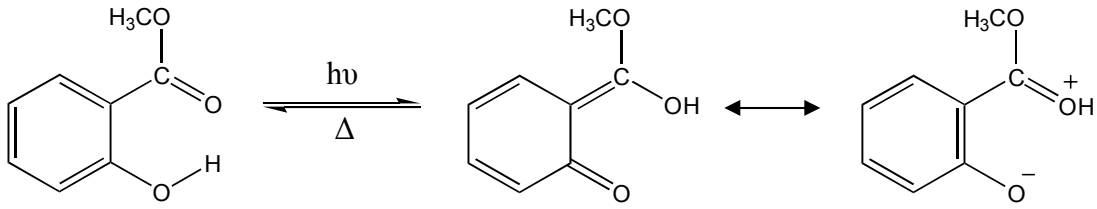

(12) **(13)**

Scheme 13: H-transfer tautomerism in compound **(12).**

(b) Photochromic valence tautomerism

A dynamic isomerism, in which the primary change is a shift in the position of the valence bonds, is called valence tautomerism. A change in the relative position of nuclei also takes place although it may be small or may not appear at all in the customary depiction of structure. The involvement of a monovalent atom or group in dynamic isomerism is called phototropy or anionotropy and if a multivalent atom or group is involved then it is termed as valence tautomerism. The main condition for valence tautomerism to occur is the capability of two structural moieties, which are joined together through a chain of atoms, to undergo reversible photoisomerization. Fulgides represents

one of the oldest group of photochromic compounds. Chemically these are derivatives of dimethylene-succinic anhydrides.

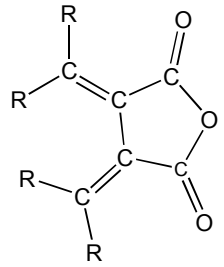

(14)

Figure 10: The structure of dialkyl-succinic anhydride.

In order to show photochromism, one of the substituents must be aromatic. The photogenerated valence tautomer may be a dihydronaphthalene derivative **(14)**, for example diphenylfulgide **(15)**, as shown in Scheme 14.

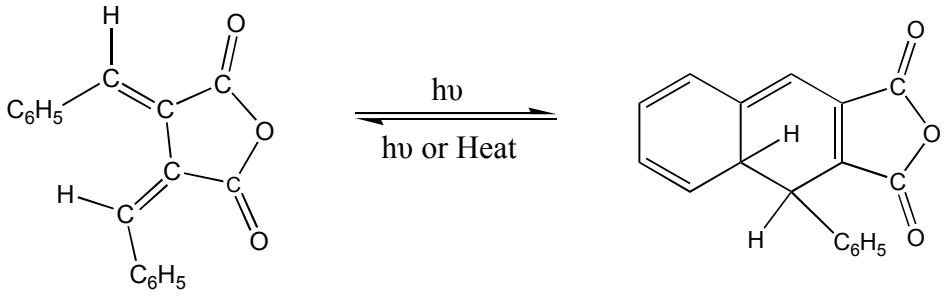

(15) **(16)**

Scheme 14: Photochromism of diphenylfulgide **(15)**.

Photocoloration of the crystals **(15)** occurs on irradiation at room temperature in a glass at -196^{o}C with original absorption peaks at 287 nm and 355 nm which after irradiation give new absorption peaks at 375 nm and 485 nm. Fading takes place upon warming to room temperature.

2.3 Spirooxazines

2.3.1 Introduction

Spirooxazines represent a very important class of photochromic compounds which can be defined as molecules containing a condensed ring-substituted 2*H*-[1,4]oxazine, in which the C-2 of the oxazine ring is involved in a spiro linkage.[54] Photochromism in spirooxazines is shown in Scheme 15.

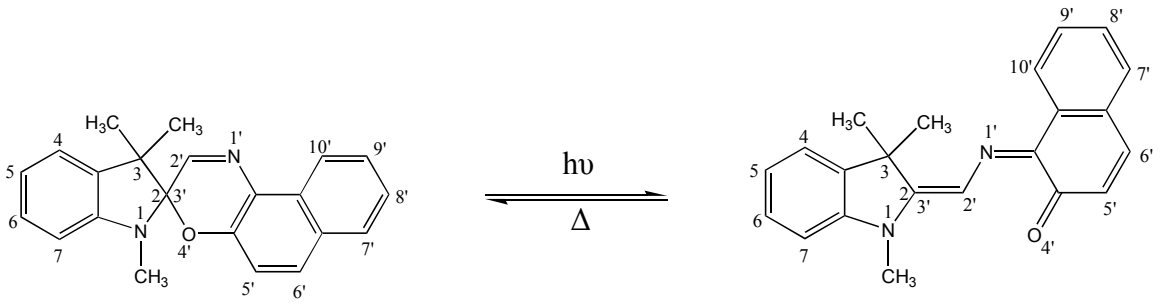

(17) **(18)**

Scheme 15: Photochromism in spirooxazine **(17)**.

Spirooxazines comprise two heterocyclic nearly planar moieties, indoline and naphthoxazine. These moieties are linked by a tetrahedral spiro-carbon which insulates the two π–electron systems from conjugation. Due to the lack of conjugation, the spiro compounds are pale yellow or colourless because the lowest electronic transitions of the molecule occur in the near UV region. Generally UV-A light (315-380 nm) is required for the photoactivation. After UV irradiation, the photo-cleavage (heterolytic) of the C-O spiro bond leads to the photochromism. The C-C bond rotates to give a photomerocyanine form, which is intensely coloured because of the absorption in the visible region, as shown in Scheme 15.

The photochromism in spirooxazines which is a two-step process was first studied by Fox. [55] The first step involves the shift of the electron density from the indoline group to the naphthoxazine ring. The rehybridization of the C_{spiro} atom leads to a reverse shift of electron density in the second step. In most of the spirooxazines, [56, 57] the structure of the spiro centre of the molecule is favourable for interaction between the lone pair of

electrons of N-1 and the σ* orbital of the C_{spiro}-O bond. The N-atom with the lone pair of electrons overlaps with the σ* orbital of (C_{spiro}-O). This overlapping leads to the shortening of the C(2)-N(1) bond and the elongation of the C(2)-O bond compared to the normal values observed in the five and six member rings.[58] The standard lengths of the C-N bond and C-O bond are 1.48 Å and 1.43 Å respectively. For compound **(17)**, the C_{spiro}-O bond length is 1.454 Å.

The nature of the electronic state of the nitrogen and oxygen atoms determines the efficiency of this interaction. For spiropyran, electron withdrawing substituents in the benzopyran ring gives strength to the interaction while electron donating groups weaken the interaction. The naphthoxazine and the indoline fragments are perpendicular to each other. The indoline ring in spirooxazine adopts an envelope confirmation with folding angles, along the N (2) -$C(CH_3)_2$ lines, in a range of 33.8°-39.9° as shown in Figure 11.[59]

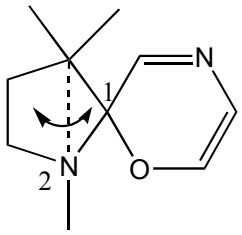

(19)

Figure 11: Folding angles in the indoline ring in spirooxazine.

In the colouration-decolouration process of photochromic spirooxazines a main problem is the photostability of the spiro compound or the merocyanine form. The degradation process also known as fatigue occurs during the reverse reaction. Spirooxazines commonly show better stability and fatigue resistance than other families of photochromic compounds such as spiropyrans.[60]

It has been seen that the introduction of an electron rich heteroatomic group at the indoline nitrogen, for example antioxidant groups such as 4-hydroxy-2,2,6,6-tetramethylpiperidinyloxy or 2,2,6,6,-tetramethyl-4-piperidinol (HOTEMP) as pendant groups provide higher fatigue resistance.[54, 61, 62]

2.3.2 Spectral Properties

(a) Photochromism in solution

Spirooxazines show photochromism when dissolved in solution or in a medium such as gel, plastic resins, or films. Generally, spirooxazines are not photochromic in the solid state but the photochromic property of solid spirooxazines in a microcrystalline powder state has been reported by Asahi and Masuhara.[63]

The transformation of the ring closed spirooxazine to the merocyanine or quinoidal form occurs upon irradiation by UV light. Spirooxazines are usually more soluble in aromatic hydrocarbons than in alcohols and aliphatic hydrocarbons.

(i) Absorption spectrum of the closed form

The structure of spirooxazine **(17)** is divided into two halves at the spiro linkage. The two halves are orthogonal and the absorption spectrum of spirooxazine **(17)** consists of localized transitions arising from a particular half of the molecule without interaction of the other half.[64] The electronic absorption spectra of the ring closed spirooxazines consist of localized π-π^* transitions in the UV region. Three absorption peaks with moderate intensity in the region above 280 nm are seen at 345 nm, 317 nm and 297 nm with respective molar absorptivities of 4.76×10^3 $M^{-1}cm^{-1}$, 6.78×10^3 M^{-1} cm^{-1} and $6.53 \times 10^3 M^{-1}$ cm^{-1}. In the far ultraviolet region, two further absorptions with maxima at 235 nm (5.43×10^4 $M^{-1}cm^{-1}$) and 203 nm (4.41×10^4 $M^{-1}cm^{-1}$) are seen. The spectral properties of spiropyrans studied by Tyer and Becker [65] led to conclusions similar to the spirooxazines. After the comparison of compound **(17)** with appropriate oxazine and indoline models, the absorption maxima at 345 and 317 nm are assigned to transitions localized in the oxazine part and the 297 and 235 nm absorption bands from the indoline part of the spirooxazine.

Substituted compounds show different UV-visible spectra.[66] The –OH derivatives **(20)** show broad absorption at 345 nm while benzothiazolyl substituted compounds **(21)** show a narrow absorption band in the region of 270-340 nm due to the electronic and vibronic transitions localized on the naphthoxazine part of the molecule.[67]

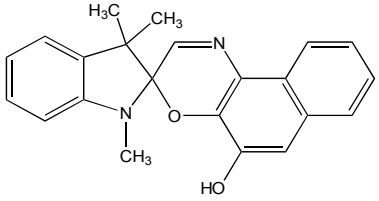

(20)

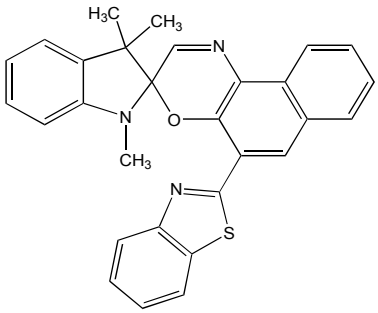

(21)

Figure 12: Structures of compounds **(20)** and **(21)**.

(ii) Absorption spectra of the merocyanine form

In general, in irradiated spirooxazine solution, the colour fades thermally and it becomes difficult to obtain a true absorption spectrum of the merocyanine form at room temperature. As the rate of thermal fading is significant compared to the time required to record the spectrum, it is difficult to obtain a solution which contains the coloured form only without the presence of the colourless form. Generally the thermal fading rate decreases with a decrease in temperature and for compound **(17)** it effectively stops below -60^{o}C. The absorption bands measured from the coloured form were 612 nm and 578 nm with 8.1 x 10^3 $M^{-1}cm^{-1}$ and 4.9 x 10^3 $M^{-1}cm^{-1}$ respective molar absorptivities. The photomerocyanine spectra, in most cases, are not single absorptions.[68-70] The absorption spectrum of the coloured form is affected by the polarity of the solvent. A hypsochromic shift is observed with a decrease in solvent polarity; e.g. for compound **(17)**, the absorption maxima is shifted from 612 nm to 590 nm and 555 nm as the solvent is changed from ethanol to toluene and cyclohexane respectively.

(b) Substitution effect on spirooxazines

(i) Substitution effect on the Naphthoxazine ring

The substitution of an alicyclic amino group at the 6'-position, as in compound **(22)**, causes a 30-40 nm hypsochromic shift in the visible absorption band.

Indolinospironaphthoxazine (NISO) gives a blue colour in poly (methyl methacrylate) matrix and 6'-piperidino-NISO yields a purple colour upon UV-irradiation.

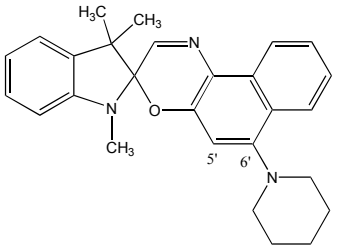

(22)

Figure 13: Structure of compound **(22).**

The quantum yield of the photochromic compounds depends on the presence of electron donating substituents in the 6'-position and the nature of the solvent. Non-polar solvents usually give a higher yield. A shift in the thermal equilibrium between the uncoloured and coloured species towards the coloured species is induced by the presence of the methoxy group at the 5' position.

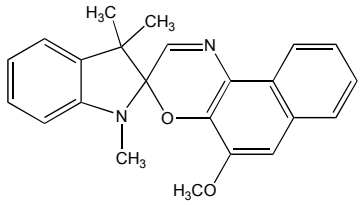

(23)

Figure 14: Structure of compound **(23)**.

(ii) Substitution effect on the Indoline ring

The attachment of an electron donating group to the spiroindolino moiety can cause an absorption shift, as shown by Rickwood et al.[71] Hypsochromic shifts of 10 and 18 nm was observed by the substitution of chloro and trifluoromethyl groups respectively at the 5-position of the spiroindolino moiety, as shown in Table 1.

Table 1: Substitution effect on the naphthoxazine moiety.

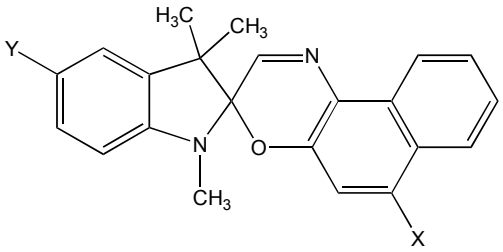

Compounds	**X**	**Y**	**λ_{max} in polyurethane (nm)**
24	Indolino	H	606
25	Piperidino	H	578
26	Piperidino	Cl	568
27	Piperidino	CF_3	560
28	Morpholino	H	580
29	Aziridino	H	574
30	Diethylamino	H	574

A hypsochromic shift of 64 nm was observed in the 4,6-bis-trifluoromethyl derivative **(33)**, by the incorporation of two electronegative centres on the indoline moiety plus a methoxy group at the 5' position relative to compound **(17)**.

Table 2: Effect of electronegative groups on the indoline moiety.

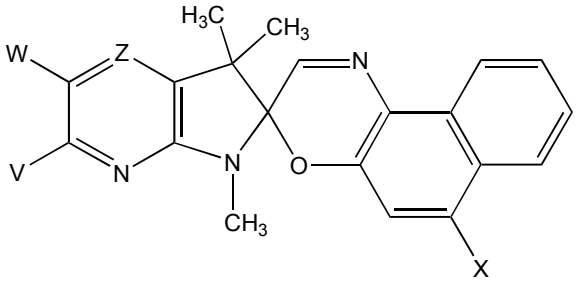

Compounds	X	Z	W	V	λ_{max} in polyurethane (nm)
31	Piperidino	CH	H	H	540
32	Piperidino	N	H	H	526
	Tetramethylguanidino	N	H	H	516
	Tetramethylguanidino	CH	CF_3	H	520
	Methoxy	CH	CF_3	H	522
	Methoxy	N	H	H	524
33	Methoxy	CCF_3	H	CF_3	510

(c) Mechanism of photochromic reactions

The photochromic reaction of spirooxazines was examined by Aramaki et al [72] using time-resolved Raman spectroscopy. The vibrational resonance Raman spectra of the merocyanine (MC) forms were recorded over a 50 ps-1.5 ns, and was found not to change during this interval. This confirmed that the ring opening reaction to form the merocyanine (MC) forms or the distribution of the merocyanine form was complete within 50-ps and also the distribution of isomers remained unchanged for at least 1.5 ns.[73]

The primary photochemical step after the excitation of the spirooxazines with UV light is the heterolytic bond cleavage between the spiro carbon and the neighbouring oxygen. The investigation of the primary ring opening reaction by picosecond time resolved absorption and emission spectroscopy was carried out by Schneider.[74] A non-planar intermediate is generated after the primary process and it relaxes very rapidly to a distribution of open forms which are similar in structure to the merocyanines. The build up time for a nonplanar intermediate is less than 2 ps which convert to the planar forms within 2 to 12 ps, depending upon the nature of substituents attached to the parent compound as well as the nature of the solvent. The photochemical formation of the merocyanine forms of different spirooxazines have been studied by Wilkinson.[75]

2.3.3 Photodegradation

Photochromism is a non-destructive process but side reactions do occur. Due to chemical degradation of a material, the performance is reduced over time and this is termed "fatigue". The major cause of degradation is oxidation.[76] The nitro derivatives of spirobenzopyrans, SP_{NO2}, show good colourability but lack sufficient durability for long term applications. The spirooxazines on the other hand have higher stability with respect to photooxidation. The resistance to the photochemical fatigue is usually determined by the reactivity of the excited states of the spiro and/or merocyanine forms. In the case of nitrospiropyrans (SP_{NO2}), a triplet state ($^3SP_{NO2}$) plays a very important role in the photocolouration process [77] whereas for other spiropyrans the excited singlet state is dominant in the photoreaction. Both conditions are shown in Scheme 16.

$$SP_{NO_2} \rightarrow {}^1SP_{NO_2} \rightarrow {}^3SP_{NO_2} \rightarrow MC$$

$$SP \rightarrow {}^1SP \rightarrow MC$$

Scheme 16: The involvement of the triplet and singlet state in the photochromism of spiropyrans.

The photodegradation of nitro-substituted spiropyrans involves the reaction of the unstable isomer **(34)** (*cis-cisoid*) isomer with solvent or impurities as suggested by Malkin et al [78] and Hirshburg et al [79]. (Scheme 17)

Photodegradation $\rightleftharpoons$ X $\rightleftharpoons$ MC $\longrightarrow$ MC Isomers

Scheme 17: The photodegradation of compound **(34)** and the usual formation of merocyanine isomers.

Photooxidation is the result of oxygen reacting with the triplet state of a spirooxazine or spiropyran. A thorough investigation on the nature of the isomer **(34)** has been reported in literature.[80] The structure of compound **(34)** is given in Figure 15.

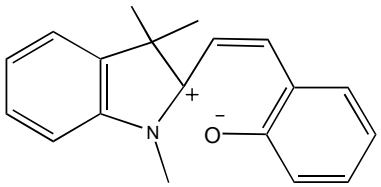

(34)

Figure15: Structure of the *cis-cisoid* isomer **(34)**.

The photodegradation of 6-nitro-BIPS **(35)** was first investigated by Gautron [81] in 1968.

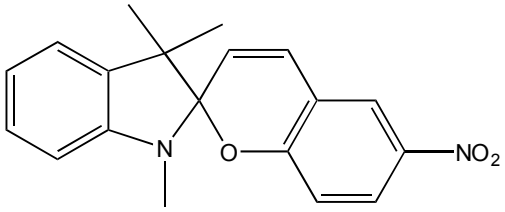

(35)

Figure 16: Structure of compound **(35)**, 6-nitro-benzoindolinospiropyran.

The extent of photodegradation is a function of light intensity and irradiation wavelength. The absorptions at 294 and 320 nm are the most effective in promoting degradation. Photocolouration is improved by increasing light energy whereas photostability decreases. Photodegradation and colourability often work in opposite ways. A more dilute solution has better colourability but poorer fatigue resistance. Guglielmetti and co-workers [82] reported, in 1993, a comparative study of 8-CH_3O-6-NO_2-BIPS **(36)**, spiro[indoline-naphthopyran] **(37)**, and spiro[indoline-naphthoxazine] **(38)**.

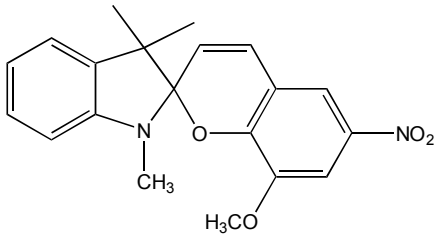

(36)

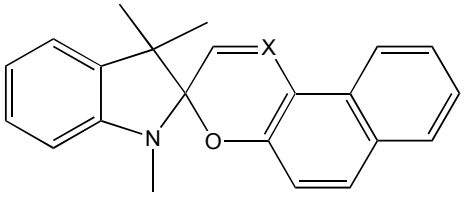

(37) SP; X=CH

(38) SO; X= N

Figure 17: Photochromic compounds **(36)**, **(37)** and **(38)**.

The common products yielded from the heterocyclic moiety, after the irradiation of aerated toluene solution (10^{-3}M) of photochromes **(36)**, **(37)** and **(38)**, were 3,3-dimethyloxindole **(40)**, 1,3,3-trimethyloxindole **(39)** and 1,2,3,4-tetrahydro-2,3-dioxo-4,4-dimethylquinoline **(41)**.

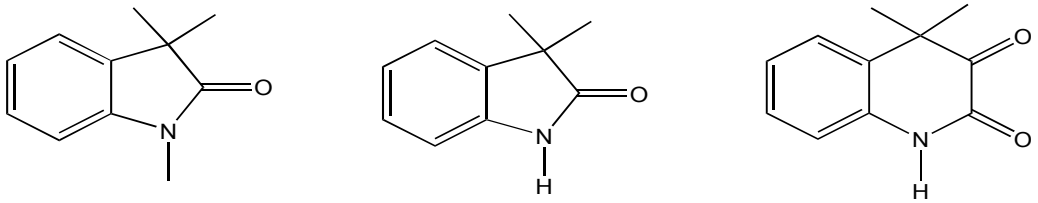

(39) **(40)** **(41)**

Figure 18: The structures of the products yielded after photodegradation of the heterocyclic part of compounds **(36)**, **(37)** and **(38)**.

The chromene moiety upon degradation gave the nitroaldehyde **(42)**, 1-formyl-2-naphthol **(43)**, and naphth[1,2-*d*]oxazole **(44)**.

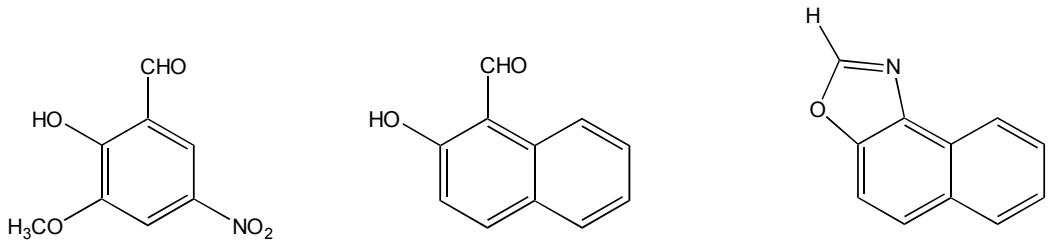

(42) **(43)** **(44)**

Figure 19: The structure of the products after chromene moiety degradation.

Photooxidation of spirooxazines: Mechanism

The spirooxazines are in general more stable than the spiropyrans. Guglielmetti and co-workers confirmed the results of Gautron on the photooxidation of compound **(37)**. The mechanism of photooxidation was not clear although it was suggested that it could be due to the interaction of a biradical form of the merocyanine with oxygen (O_2) or with singlet oxygen $^1O_2$. An experiment was carried out to check the hypothesis that spirooxazines or spiropyran could act as sensitizers by promoting the formation of singlet oxygen. Dichloromethane solutions of compounds **(36)** and **(37)** were excited with a frequency-tripled Nd-YAG laser (355 nm), and an emission was detected by a germanium diode to monitor the formation of $^1O_2$, through its luminescent emission at 1269 nm.[83] No emission at 1269 nm was detected which indicated that no $^1O_2$ was formed.

A comparison of the degradation products from spirooxazines and spiropyrans was made. Spirooxazine yielded more 1,3,3-trimethyloxindole **(39)** whereas the spiropyran gave more 3,3-dimethyloxindole **(40)**. The suggested mechanism was the attack of O_2^- on the indoleninium quaternary nitrogen atom, to give an adduct **(47)** in the case of spirooxazines. The rearrangement of the adduct **(47)** yielded 3,3-dimethyloxindole via N-formyl-3,3-dimethyloxindole **(48)** as shown in Scheme 18.

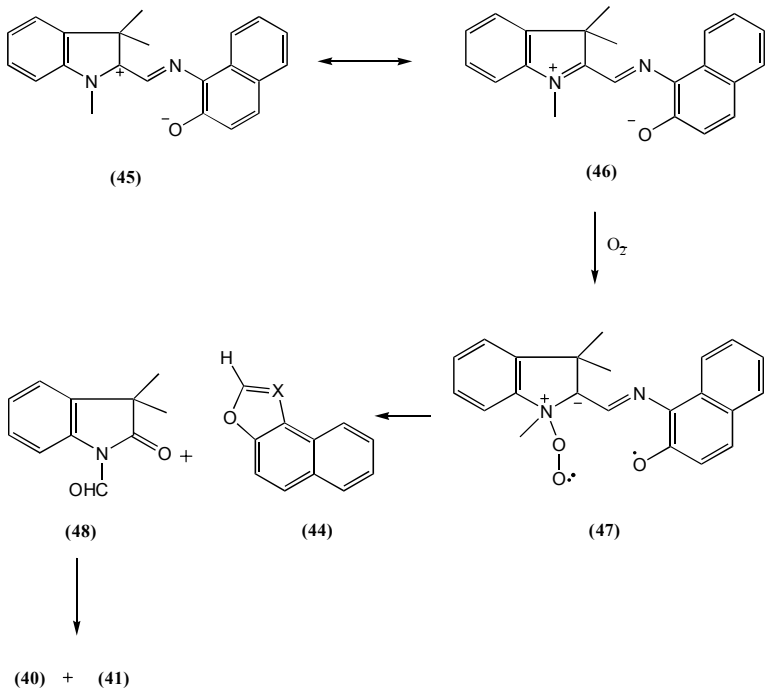

Scheme 18: The proposed mechanism for photooxidation in spirooxazine **(38)**.

Other products isolated after degradation of spirooxazine **(38)** were **(49)** and **(50)**.

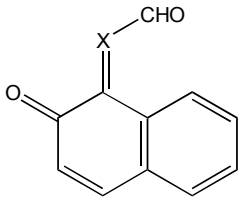

(49)

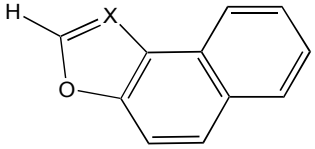

(50)

X=CH, N

Figure 20: The products from a photooxidation process of spirooxazine **(38)**.

1,3,3-Trimethyloxindole **(39)** was subjected to some experimental photodegradation conditions and it was observed that demethylation of **(39)** to 3,3-dimethyloxindole did not occur. Two possible mechanisms were proposed. Gugielmetti and co-workers suggested that peroxyl intermediate **(51)** is formed by the reaction of the merocyanine with molecular oxygen and then undergoes rearrangement. This rearrangement results in the conversion of the indolyl (N-CH_3) methyl group to a formyl group as shown in Scheme 19.

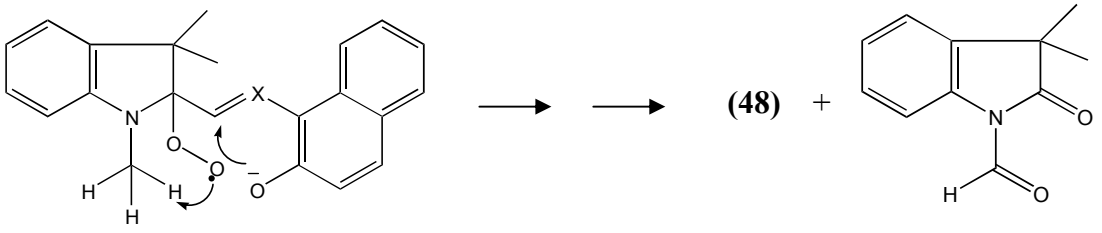

(51) **(52)**

(40)

Scheme 19: Gugielmetti's proposed mechanism for formation of 3,3-dimethyloxindole **(40)**.

Malatesta et al suggested another possible mechanism.[76] The excited zwitterionic form of merocyanine yields the superoxide radical anion O_2^- and the merocyanine radical cation

by a charge transfer to the molecular oxygen. A further reaction gives the same biradical / O_2^- adduct **(51)** as suggested by Guglielmetti. This mechanism is shown in Scheme 20.

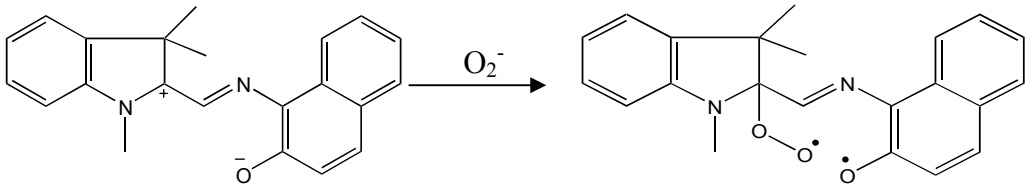

(46) **(53)**

Scheme 20: Proposed mechanism (Malatesta et al) for formation of 3,3-dimethyloxindole **(40)**.

Photodegradation under continuous irradiation at 365 nm was found not to be dependent on the presence of oxygen.[84] Reductive degradation has also been suggested in literature [85]; in the absence of oxygen the spirooxazine undergoes degradation in solution. The merocyanine form can also react with free radicals. The radical attacks the C5'=C6' double bond of the merocyanine and yields mono- and/or disubstituted free radical adducts as shown in Scheme 21.

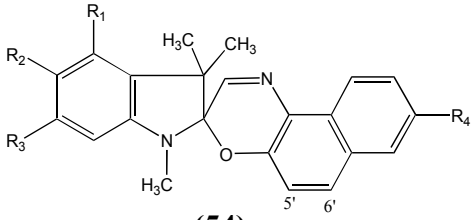

(54)

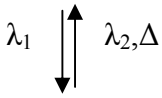

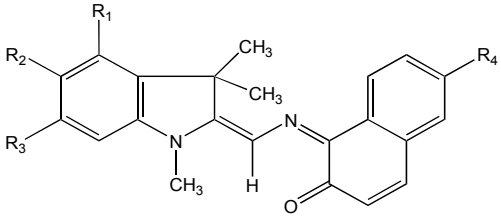

(55)

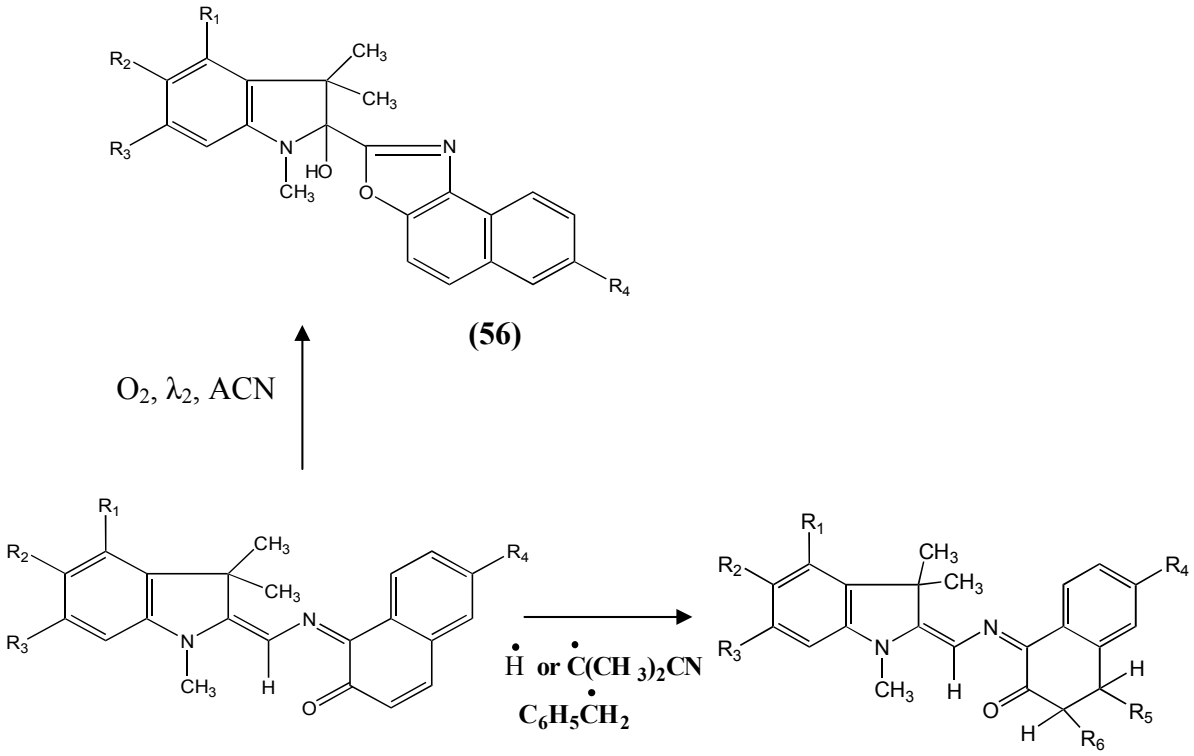

Scheme 21: Synthesis of mono and disubsitituted free radical adducts from the degradation of spirooxazine **(54)**.

2.3.4 Thermochromism

A thermally induced reversible colour change is called thermochromism. It was precisely defined by Day [86] as the "easily noticeable reversible colour change in the temperature range limited by the boiling point of each liquid, the boiling point of the solvent in case of solution or the melting point for solids".

Thermosolvatochromism [87] is the phenomenon exhibited when the thermochromism of a molecular system results from its association with another chemical species such as metal ion or proton or from modification of the medium by a thermal effect.

Thermochromism of spiropyrans was discovered in 1926. These compounds give a deep colour (red, purple or blue) on melting while on heating, the solution of spiropyran also

causes colouration. A mechanism for thermochromism was also proposed. A thermally sensitive equilibrium has been assumed to exist between the colourless spiroheterocyclic form and the open merocyanine like structure, obtained after the breaking of the C-O bond. (Scheme 22)

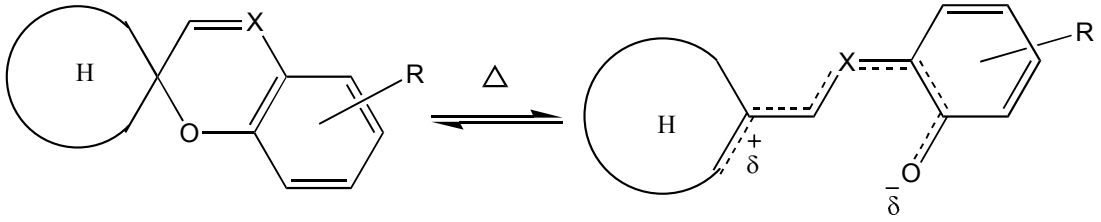

X= CH: Spiropyran **(58)**

X= N: Spirooxazine **(59)**

H= Heterocycle

Scheme 22: Thermochromism in the spiroheterocyclic compounds.

For the spirooxazines and spiropyrans, the most thermally stable photoinduced coloured forms and thermally formed species are indistinguishable spectroscopically and kinetically. The electronic distribution of the open form is situated between two resonance forms and the proximity to one form or the other depends upon the structure and the medium. (Scheme 23) For example, spiro[indoline-naphthopyrans] or spiro[indoline-naphthoxazine will be largely quinoidal whereas spiro[indoline-pyran] having a NO_2 group will be largely zwitterionic.[85, 88, 89]

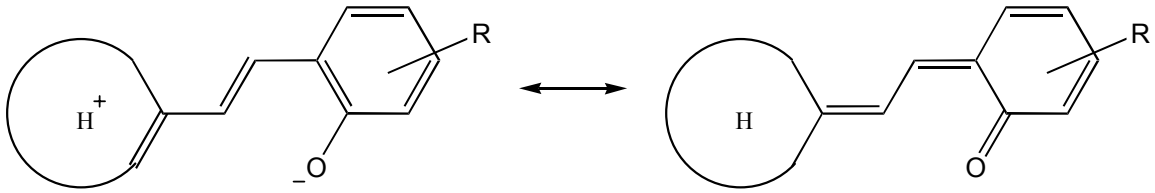

Scheme 23: The resonance forms of compound **(58)**.

Three thermochromic spirooxazines, reported in the literature, [90] are given below.

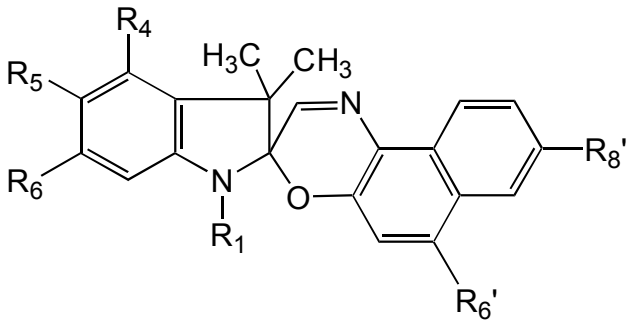

(60) $R^1 = CH_3$ $R^4 = R^5 = R^6 = R^{6'} = R^{8'} = H$

(61) $R^1 = R^4 = R^5 = CH_3$ $R^6 = R^{6'} = R^{8'} = H$

(62) $R^1 = CH_3$, $R^{6'}$ = N-piperidinyl, $R^4 = R^5 = R^6 = R^{8'} = H$

Figure 21: Structure of three thermochromic spirooxazines

2.3.5 Colourabilty and Solvatochromism

The ability of a colourless or a slightly coloured (pale yellow) photochromic material to develop colouration is called colourability. In dilute solutions, at a given wavelength, the initial absorbance "$A_o(\lambda)$" after photolysis is proportional to the colouration quantum yield (Φ_{col}), the molar absorption coefficient of coloured form (ε_B), and the concentration of the colourless form (C_A). [91]

$$A_o(\lambda) = k\, \Phi_{col}\, \varepsilon_B\, C_A$$

Here k is proportionality constant and includes photon flux. The colourability of the photomerocyanine was calculated from the absorbance value.[92, 85] The analysis showed that the colourability depended upon the quantum yield Φ_c of the colour forming reaction and ε of the visible absorption band. The absorbance of a series of photochromic colourless

compounds such as spirooxazines, spiropyrans, chromenes etc, is usually determined under standard conditions (concentration of the closed form ca. $2.5x10^{-5}$ M, in toluene solution at $25^{o}C$). It is also an indicator of their relative photochromic behaviour. The variation of the electronic spectroscopic properties such as absorption and emission of a chemical species, induced by solvent, is termed "solvatochromism".[93, 94]

The photochromic and solvatochromic properties of the spirooxazines are very sensitive to the donor/acceptor character and the position of the substituents.[95] A spirooxazine with an acceptor substituent on the naphthoxazine ring is called a "pull type" while the spirooxazines with a donor substituent on the indoline ring is termed as the "push type" compound. A push-pull type compound is obtained when the indoline ring bears a donor and the naphthoxazine ring possesses an acceptor group.[96]

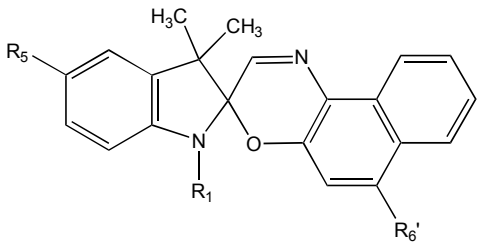

Compounds	**R_1**	**R_5**	**$R_{6'}$**
63	CH_3	OCH_3	CN
64	CH_3	$OC_{16}H_{33}$	CN
65	n-C_3H_7	OCH_3	CN
66	CH_3	H	H

Figure 22: The structures of spirooxazines **(63-66)**.

The solvatochromism of the open form of spirooxazines **(63-66)** was studied by Metelitsa et al.[67] The compounds **(63-65)** showed negative solvatochromism, in which the λ_{max} value decreased with an increase in the solvent polarity. However positive solvatochromism was observed in case of compound **(66)**, where a bathochromic shift was observed by increasing the solvent polarity. The λ_{max} values and the solvents used are given in Table 3.

Table 3: The solvent effect on compounds **(63-66)**

Compounds	λ_{max} nm (Toluene)	λ_{max} nm (Methanol)
63	661	649
64	662	651
65	662	655
66	596	613

The data in Table 3 shows negative solvatochromism with shifts of 12, 11 and 7 nm from toluene to methanol, for the open forms of compounds **63**, **64**, and **65** respectively. Positive solvatochromism with a shift of 17 nm was observed in the case of compound **(66)** when the solvent was changed from toluene to methanol.

2.3.6 Synthetic Methods

The condensation of an alkylidene heterocycle with an ortho-nitroso aromatic alcohol in a polar solvent such as methanol or ethanol is the most common method used for the synthesis of the spirooxazines. The general method of synthesis for the spirooxazine is given in Scheme 24.

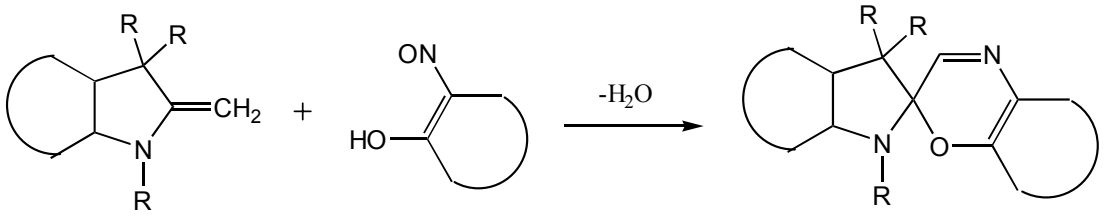

Scheme 24: General scheme for the synthesis of spirooxazines.

For thermally stable spirooxazines, the yield of the condensation reaction is about 30-50%. The yield was reported to improve to 70-75% by the use of substituted 2-methyleneindoline derivatives.[97] The successful synthesis of the spirooxazines was carried out by the use of ortho-nitroso aromatic alcohols such as 1-nitroso-2-naphthol, 5-nitroso-6-quinolinol and 9-nitroso-10-phenanthrol. Masahiro and Hosoda have also reported the synthesis of

photochromic spirooxazines in a patent.[98] The difficulty in obtaining a pure spirooxazine for characterization and the instability of many spirooxazines are the main reasons commonly given for their number being less than the corresponding spiropyrans. There are a few problems associated with the above method for synthesis of the spirooxazines which are highlighted below:

(i) There is a loss of material during the oximation reaction of 1,2-naphthoquinones, especially due to the low stability of the 1,2-naphthoquinones and the formation of two possible isomers.

(ii) The condensation reactions generally give a low yield for the spirooxazines.

The synthesis of the spirooxazines through the reaction of 2-hydroxyiminomethyl-1,3,3-trimethylindolenium perchlorate with 1-amino-2-naphthol hydrochloride has been documented by Japanese researchers in 1988 (Method 2).[99]
Minkin et al [100] described another method of synthesis for the spirooxazines starting from the oxidation of the Fischer's base. The ketene is considered to be the reactive carbonyl intermediate in the reaction mechanism. (Method 3) The important contribution of this method was a yield improvement. All three methods are illustrated in Scheme 25.

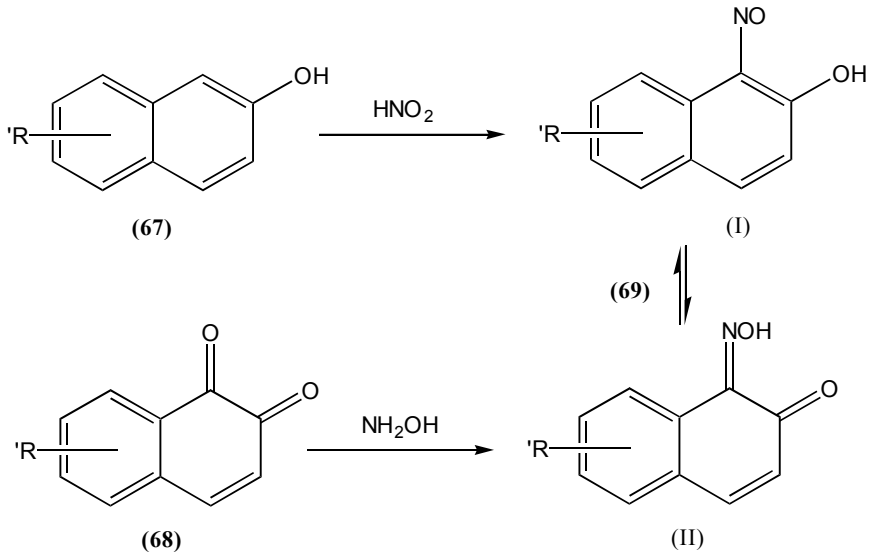

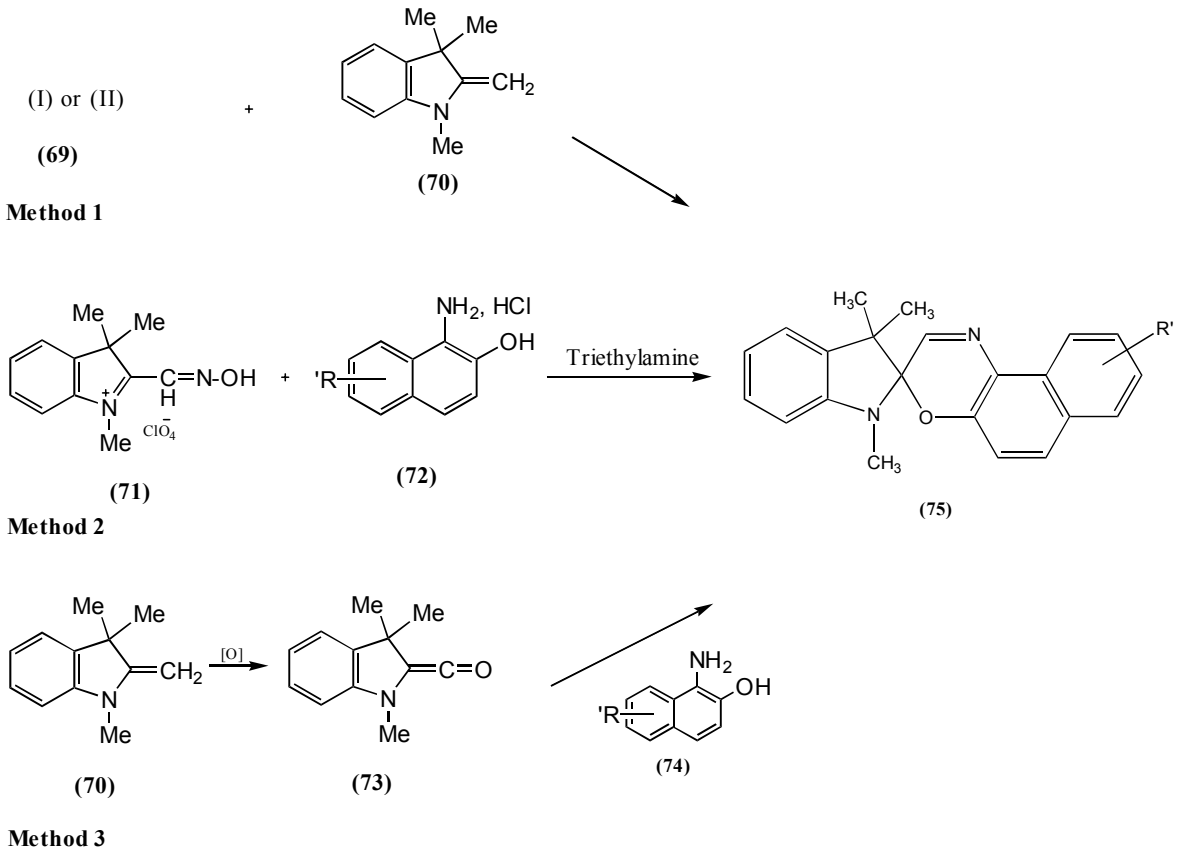

Scheme 25: Synthesis of the spirooxazine **(75)** by three different routes.

Microwave assisted synthesis of photochromic spirooxazine dyes under solvent free conditions is a fast and environmentally friendly method which has been reported in the literature.[101] The reaction was complete within a few minutes with 35-40% yield. I-Nitroso-2-naphthol, compound **(77)** and the catalyst were allowed to react in a microwave reactor. The scheme for the synthesis of the spirooxazine is given below.

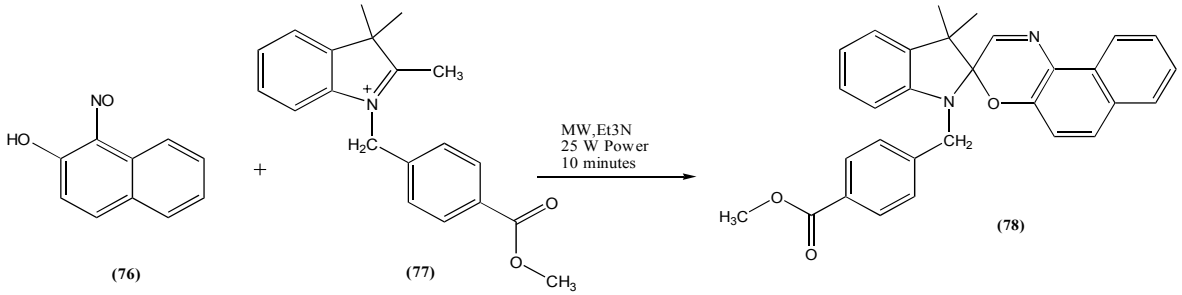

Scheme 26: Microwave assisted synthetic route to the photochromic dyes under solvent free conditions.

2.4 Diazotization and Azo coupling

2.4.1 Introduction to diazo compounds

The organic compounds containing two adjacent nitrogen atoms, one of which is attached to a carbon atom are called diazo compounds having the general formula $R_2C=N_2$. The electronic structure of diazo compounds involves a positive charge on the central nitrogen and a negative charge distributed between the terminal nitrogen and the α-carbon. Diazoketones and α-diazoesters are amongst the most stable diazo compounds since the negative charge is delocalized into the carbonyl group. In contrast, most alkyldiazo compounds are so unstable that they may be explosive. Diazomethane is the simplest example of a diazo compound. The general structure of a diazo compound is shown in Scheme 27.

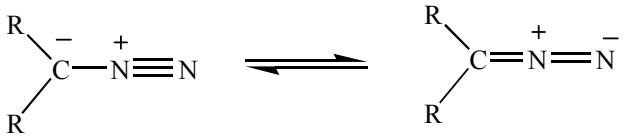

(79a) **(79b)**

Scheme 27: Structure of a diazo compound.

Aromatic diazo compounds were discovered by Griess in 1858 [102] and were name given that "diazo" in 1860.[103] Originally, the diazotization of picramic acid was carried out by Griess by passing nitrous gases, prepared by the reduction of nitric acid with starch or arsenious acid, into an alcoholic solution of the amine. (Scheme 28)

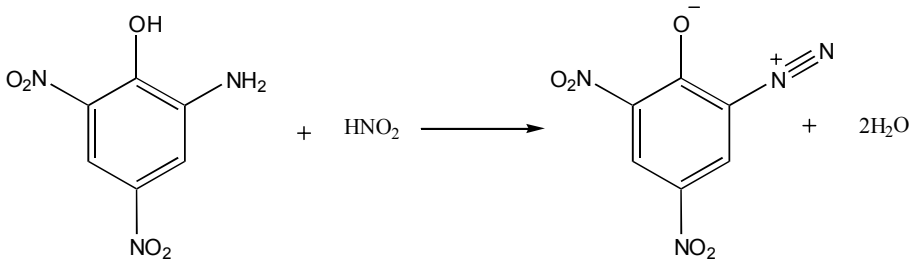

(80) **(81)**

Scheme 28: Diazotization of picramic acid **(80)**.

Regarding the nomenclature of the diazo compounds, different systems have been used. According to the International Union of Pure and Applied Chemistry, compounds of the form $RN_2^+X^-$ are named by adding the suffix "diazonium" to the name of the parent compound RH. The whole molecule is followed by the name of the anion X^- exemplified by benzenediazonium chloride. The parent compound is named by adding the prefix "diazo" if it contains the neutral group $=N_2$ attached by one atom to the carbon. e.g., diazomethane.

Diazo compounds are distinguished from azo compounds by the fact that the group X is not attached to the β–nitrogen atom by a link from the carbon atom (except for the cyanides) e.g., (E)-benzenediazohydroxide, C_6H_5-N=N-OH and (Z)-benzenediazocyanide, C_6H_5-N=N-CN. The term "diazo compounds" is also a generic name including neutral, cationic, anionic and radical compounds with the group $– N_2$ or $– N_2^-$, excluding the azo compounds, in which the $– N_2 –$ is attached to the carbon atom on both sides.

2.4.2 Diazotization

Diazotization is carried out by the reaction of a solution of a primary aromatic amine with sodium nitrite under acidic conditions at about 0^o C. The overall reaction is shown in Scheme 29.

$$Ar\text{-}NH_2 + 2HX + NaNO_2 \longrightarrow Ar\text{-}N_2X + NaX + 2H_2O$$

(X= Cl, Br, NO_3, HSO_4, etc.)

Scheme 29: General representation of a diazotization reaction.

During diazotization the solution should be distinctly acidic (pH<2), and according to Scheme 29, two equivalents of the mineral acid are essential for a smooth reaction. Under acidic conditions, the insoluble free amine ($Ar\text{-}NH_2$) is converted into its water soluble protonated form ($ArNH_3^+Cl^-$). An appropriate low pH is necessary for the following reasons:

(i) At higher pH, the equilibrium between the ammonium ion and amine is shifted in favour of the free base which is less soluble in water.

(ii) At lower concentration of hydrogen ion, the diazonium ion formed reacts with the free base to produce the triazene (diazoamino) compound.

(iii) At higher pH, the effective forms of the diazotizing agents are converted into ineffective forms, namely nitrous acid, HNO_2, and the nitrite ion, $-NO_2^-$.

Diazotization is commonly a quantitative reaction. The amount of sodium nitrite should not be in excess as the excess of nitrous acid exerts an unfavourable influence on the stability of the diazo solution, as shown by Gies and Pfeil in 1952.[104] Diazotization is usually carried out in the temperature range 0-5^oC. The low temperature is advantageous because of two reasons. Firstly, at higher temperatures, nitrous acid decomposes to give the oxides of nitrogen. Secondly, the diazonium salt is more stable at lower temperatures.[105] The diazonium cation decomposes readily with the evolution of nitrogen, giving phenols as the decomposition products as shown in Scheme 30.

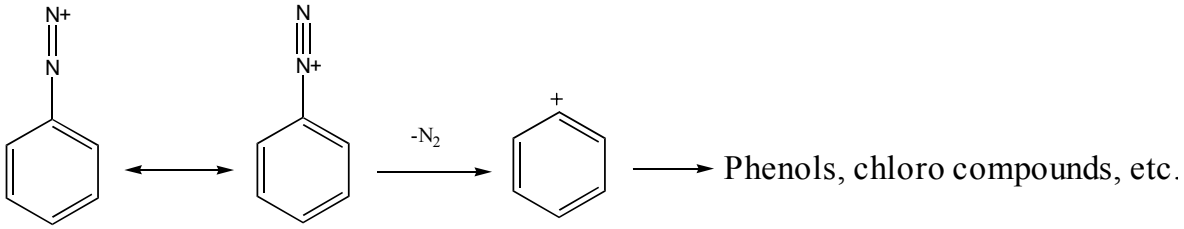

(82a) **(82b)** **(83)**

Scheme 30: Thermal decomposition of diazonium salts.

Diazotization of 1,2-diaminobenzene gives different products under different acid concentrations. If a dilute acid solution is used for the reaction, the 2-aminobenzene-1-diazonium ion is formed which undergoes an intramolecular N-azo coupling reaction to give 1,2,3-benzotriazole **(87)**. The diazotization under concentrated acidic conditions gives

the bisdiazonium ion **(86)**. In order to avoid intermolecular N- or C-coupling, 1,3- and 1,4-diamines must also be bisdiazotized in concentrated acid. The products formed under different acidic conditions are shown in Scheme 31.

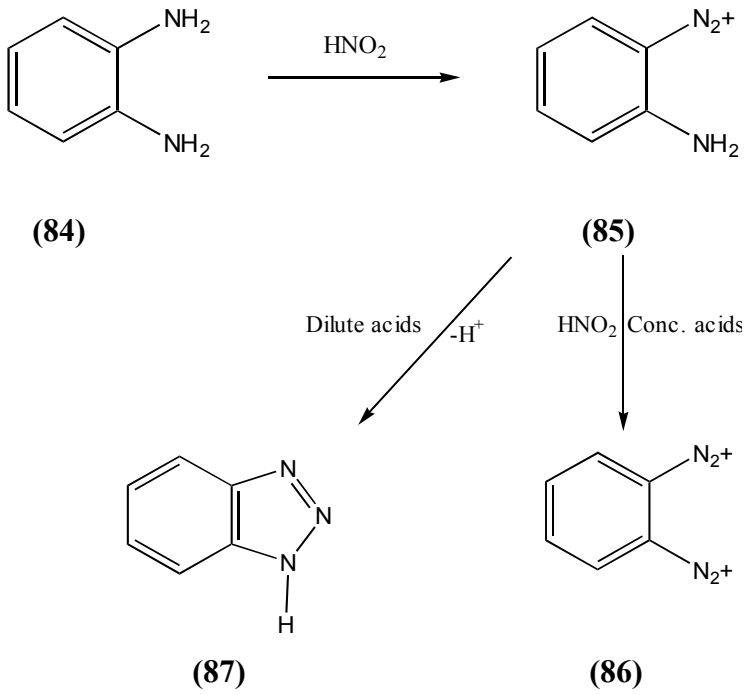

Scheme 31: Diazotization of compound **(84)** under different acid conditions.

After the completion of the diazotization reaction, the excess of nitrous acid is destroyed using sulphamic acid and this is usually done before the coupling reaction. The reaction is shown in Scheme 32.

$$NH_2SO_3H + HNO_2 \longrightarrow N_2 + H_2SO_4 + H_2O$$

Scheme 32: The reaction of sulphamic acid with nitrous acid.

The first step in the diazotization reaction is the N-nitrosation of the amine and the nitrosating species is represented by X-N=O. The common nitrosating species include the nitrosoacidium $\left(H_2O^+ - NO\right)$, ion nitrosyl chloride (NOCl) or the nitrosonium cation (NO+). The stages of the diazotization reaction following reaction with nitrosating species show tautomerism. The protonation of the nitrosating species and the subsequent removal of water lead to the diazo compound. (Scheme 33)

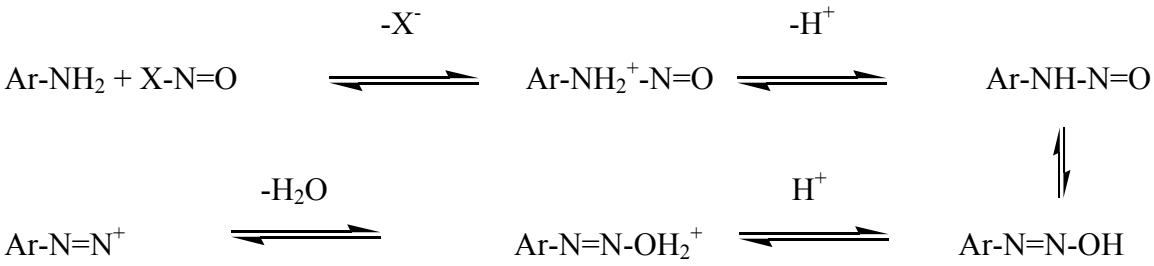

Scheme 33: Mechanism of diazotization.

2.4.3 Azo coupling

Azo coupling is a type of electrophilic aromatic substitution in which the diazonium cation (ArN_2^+) acts as an electrophile and the two aromatic compounds are coupled forming a -N=N- group. According to systematic IUPAC nomenclature, the azo coupling reactions are called arylazo-de-hydrogenation. The diazonium cations are weak electrophiles and will react with those coupling components which are highly activated to electrophilic attack by the presence of strongly electron releasing groups. The most common coupling components are phenols and the aromatic amines. β-ketoacid derivatives are another type of coupling component, in which the coupling takes place at an active methylene group.

A tautomeric equilibrium is seen in the azo compounds formed from coupling components containing hydroxy or primary or secondary amino groups. The reaction product of benzenediazonium ion with 2-naphthol is an example of the compounds showing such tautomerism.[106] The reaction procedure is given in Scheme 34.

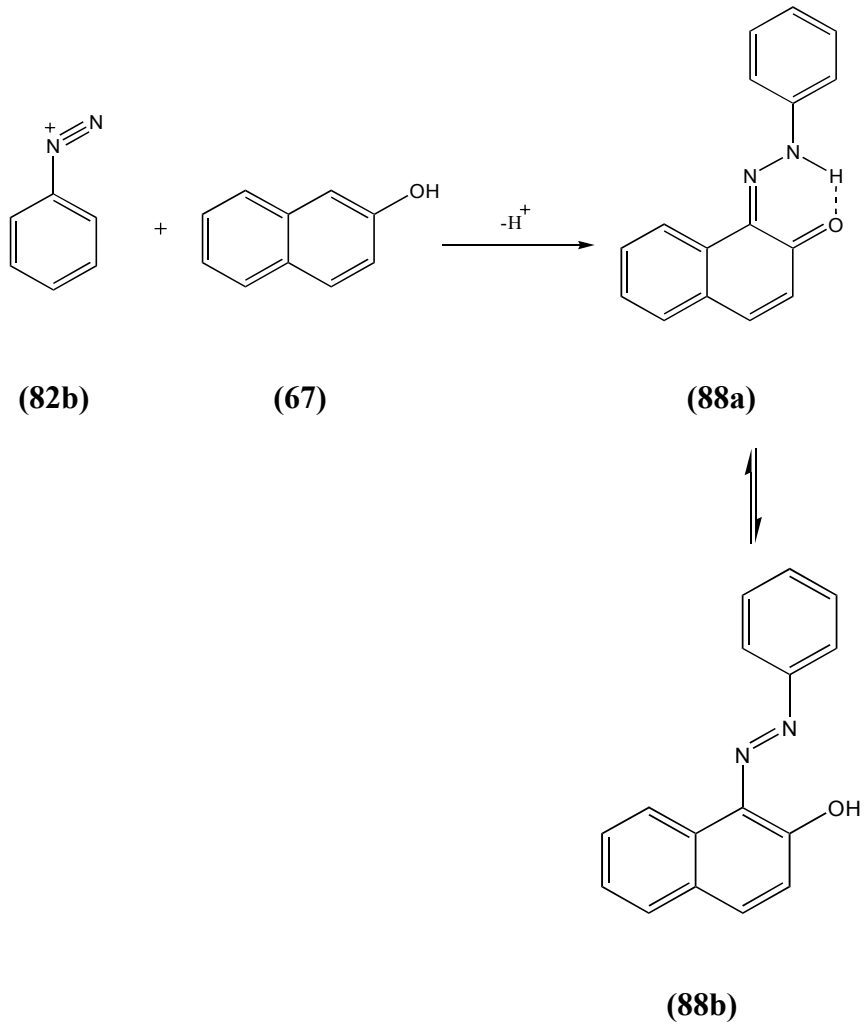

(82b) **(67)** **(88a)**

(88b)

Scheme 34: Tautomerism in azo compound **(88)**.

Another phenomenon associated with many of the commercial azo compounds is the formation of a hydrogen bond between the α-nitrogen atom of the diazonium ion and the OH or NH substituent in the *ortho* position of the reaction site in the coupling component. The azo and the hydrazone tautomers are stabilized by such bond formation by about 20 KJ mol^{-1} as seen from the pK_a values of the 1,2 and 1,4 isomers as shown in Figure 23.

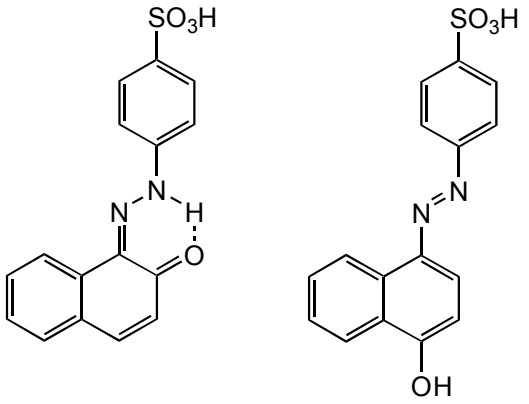

pKa= 11.4 pKa= 8.2

(89) **(90)**

Figure 23: Stabilization of the azo and the hydrazone tautomers.

Water is usually the reaction solvent for the azo coupling and a careful control of pH is necessary for optimizing the reaction. Phenols are coupled under alkaline conditions as the phenol is converted into the phenolate ion. The phenolate ion is more water soluble than the phenol itself and therefore facilitates the reaction. Another reason to facilitate the reaction is that the $-O^-$ group is a more powerful electron releasing group than the –OH group and therefore activates the system towards the electrophilic substitution. The diazonium compounds usually decompose under highly alkaline conditions and another possibility is the conversion of a diazo compound into the diazotate ion ($Ar\text{-}N{=}N\text{-}O^-$), which is less reactive than the diazonium cation. The coupling reactions for amines are usually carried out in a weakly acidic to neutral condition. Such a pH is selected which can maintain an equilibrium between the water soluble protonated form ($ArNH_3^+$) and the free amine ($ArNH_2$) which in turn is more reactive towards the azo coupling. The common coupling components used for the azo coupling are shown in Figure 24 with an indication of most likely coupling position.

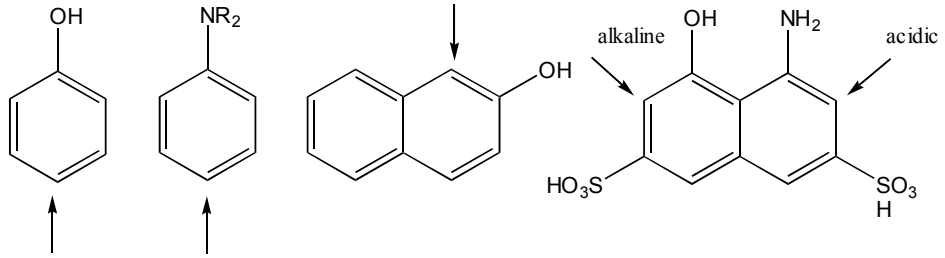

(91) **(92)** **(67)** **(93)**

Figure 24: Structure of the coupling components **(67, 91-93)**.

The diazonium cations are poor electrophiles and often relatively bulky species and therefore mainly para substitution takes place because the steric hindrance is at its weakest at this position. If the para position is already occupied by another substituent, ortho substitution occurs.

H-acid (1-amino-8-hydroxynaphthalene-3,6-disulphonic acid) can be taken as an example to discuss the position of coupling.[107] The coupling position for this coupling component is usually controlled by the pH range selection. The hydroxy group is converted into the phenolate ion under the alkaline conditions which is more electron releasing than the amino group and therefore the coupling is favoured at the position *ortho* to the hydroxy group. Under weakly acidic conditions the OH group exists as an un-ionized OH group, the amino group is more electron releasing and this favours coupling at the *ortho* position to the amino group.

Aromatic azo compounds are usually intensely coloured, as they possess an extensively conjugated π electron system. Many aromatic azo compounds are utilized as dyes and these dyes are called azo dyes. For textile use, azo dyes containing a sulfonic acid group (SO_3H^-) are commonly used in order to increase their water solubility and additional functional groups may be added to assist binding to textile fibres.

2.5 Naphthopyrans

2.5.1 Introduction

Naphthopyrans are also known as benzochromenes. The strict chemical terminology used for chromene is 2-*H*-1-benzopyran. The general structures of some of the naphthopyrans are given in Figure 25 where R_1 and R_2 are usually hydrogen.

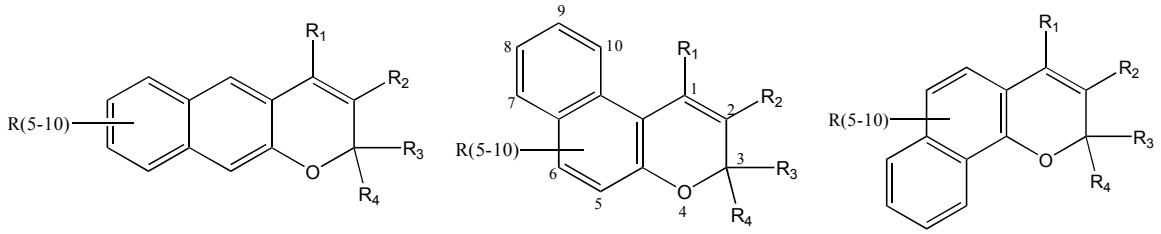

(94) **(95)** **(96)**

Figure 25: General structure of naphthopyrans **(94-96)**.

After UV-light irradiation, the uncoloured or faintly coloured molecules undergo an electrocyclic pyran ring opening with the cleavage of the sp^3 carbon to oxygen bond. The structural reorganization allows the photogenerated species to adopt more planar structures. The greater conjugation is responsible for absorption in the visible region of the spectrum. The coloured geometric isomers gradually electrocyclize to regenerate the colourless form on the cessation of the irradiation.[108] The photochromic reaction in the case of a naphthopyran is shown in Scheme 35.

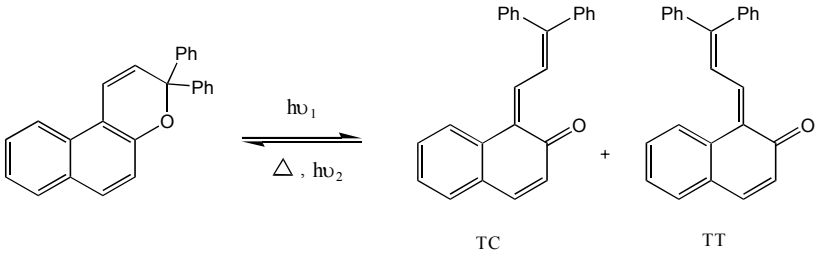

(97) **(98)** **(99)**

Scheme 35: Photochromism in the naphthopyran **(97)**.

The reverse reaction which occurs after the removal of the light source may be a thermal or a photoinduced process. The spectroscopic studies (NMR and UV) by Delbaere, Micheall and Vermeersch showed that the TC and TT forms were the main photoproducts at room temperature, the latter being the most thermally stable.[109] Naphthopyrans are widely applied in the manufacture of ophthalmic plastic lenses and solar protection glasses. [110, 111] Other applications involve the use of naphthopyrans in fuel markers [112] and security markers.[113] A great deal of research on naphthopyrans is proceeding. An important advance is the availability of the colour range, which was initially limited to orange/yellow colours and nowadays is extended to virtually any colour. A technical development to achieve the colour range involves the mixing of two or more photochromic dyes. To prevent the photochromic lenses from displaying different colours under varying exposure conditions, the photochromic dyes should have similar photochromic properties. The synthesis of biphotochromic naphthopyran molecules have also been reported in the literature.[114, 115]

2.5.2 Substituent effects on the naphthopyrans

The hydrogen atoms at the 1 and 2 positions are usually required because it is believed that alternative substitution leads to greatly diminished photochromism. The presence of substituents at these positions causes a steric inhibition of the bond rotation or isomerization. Compounds having a methyl group at these positions have been claimed in the literature.[116] The substitution of bromine at the 2-position of 3-*H*-naphtho[2,1-*b*]pyrans has been described by Gabbutt et al in 1994.[117] The reaction scheme for introduction of the bromine substitutent is given below.

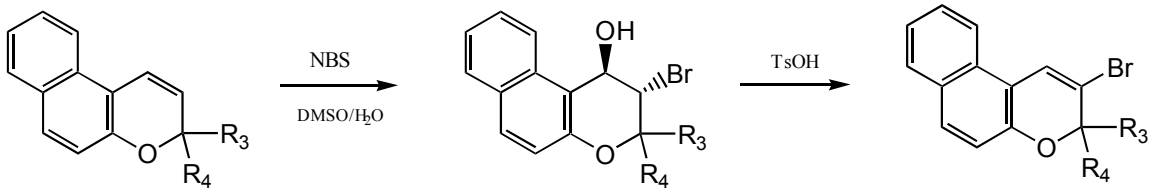

(100) **(101)** **(102)**

Scheme 36: Substitution of bromine in compound **(100)**.

The enhanced photochromism of the pyrans aryl substituted at the 3-position has been studied by Becker and Michel.[118] A comparison with the unsubstituted pyrans showed that the former had increased fatigue resistance. The photochromic properties of 3,3-diphenyl-3*H*-naphtho[2,1-*b*]pyrans and related compounds are given in Table 4.

Table 4: Photochromic properties of 3,3-diphenyl-3*H*-naphtho[2,1-*b*]pyrans imbibed into polymerizates of diethyleneglycolbis(allylcarbonate).

Compounds	**Phenyl substituents**	**λ_{max} (nm)**	**Fade $T_{1/2}$ (s)**
97	None	432	45
103	*p*-MeO	468	35
104	*p*-MeO, *p'*-MeO	480	40

The steric destabilization of the *trans* quinoidal form **(105)** is believed to be responsible for the rapid fade rates as illustrated in Figure 26.

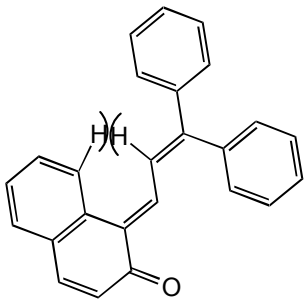

(105)

Figure 26: Structure of the *trans* quinoidal open form of 3,3-diphenyl-3*H*-naphtho[2,1-*b*]pyrans showing destabilization.

A substantial effect on the colour, intensity and fade rate has been observed by substitution on the phenyl ring of photoexcited 3,3-diphenyl-3*H*-naphtho[2,1-*b*]pyran. Electron donating groups at the *para* position result in a bathochromic shift in the visible spectrum. Substitution at the *meta* position of the aryl ring has a limited effect on the properties of the

coloured species because the *meta* position does not participate in the stabilization of the open form by resonance. The photochromic properties of the compounds **(106)** and **(107)** containing the two aryl groups together can be explained if these are considered as di-*ortho*-substituted 3,3-diphenyl-3*H*-naphtho[2,1-*b*]pyrans.[119] The structures of compounds **(106)** and **(107)** are given in Figure 27.

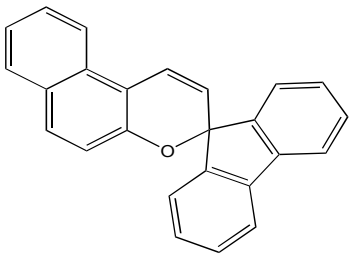

(106)

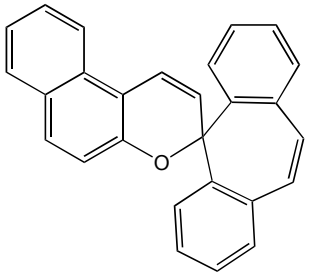

(107)

Figure 27: Structures of compounds **(106)** and **(107)**.

A hypsochromic shift of approximately 36nm in the UV spectrum of the ring closed form is observed when ether substituents, such as methoxy or ethoxy, are present at the 5-position of the pyran compound. The colour of the open form was not significantly affected by the 5-methoxy substitution. A bathochromic shift of 25nm was observed by the introduction of the 5-acetoxy group.[120] In compound **(108)**, the lengthening of the chromophore can be attributed to participation of the 5-substituent as shown in Figure 28.

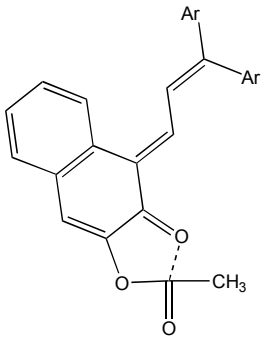

(108)

Figure 28: The participation of the 5-acetoxy group in the chromophore of the open form of compound **(108)**.

The substitution of the electron-donating substituents e.g. an alkoxy group at the 8-position of a 3*H*-naphtho[2,1-*b*]pyrans results in a bathochromic shift in both the UV spectrum of the ring closed form and the visible spectrum of the open form. The open form of the 8-methoxypyran has a resonance contribution from a zwitterionic form where the aromaticity is destroyed in both the rings and becomes a high energy species. The structure of the compound is shown in Figure 29.

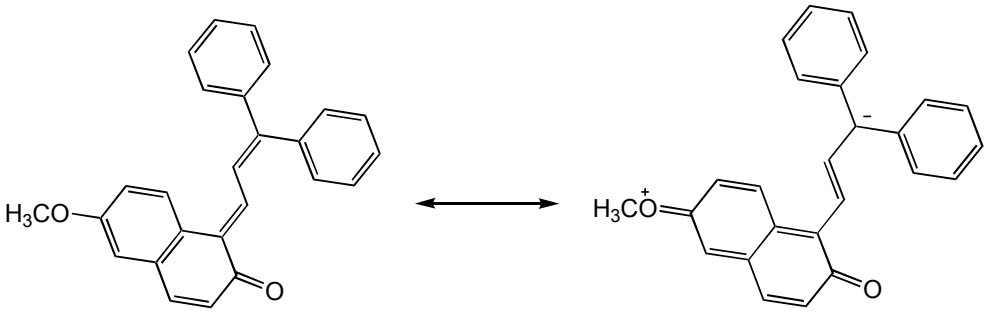

(109) **(110)**

Figure 29: The resonance forms of the open form of 8-methoxy-3*H*-naphtho[2,1-*b*]pyran.

2.5.3 Synthetic Methods

Different methods of synthesis of naphthopyrans are described in the literature.[121, 122] The naphthopyrans can be obtained by the reaction of propynols with a naphthol in toluene in the presence of the acidic alumina. The reaction sequence for the synthesis of compound **(117)** is given in Scheme 37.

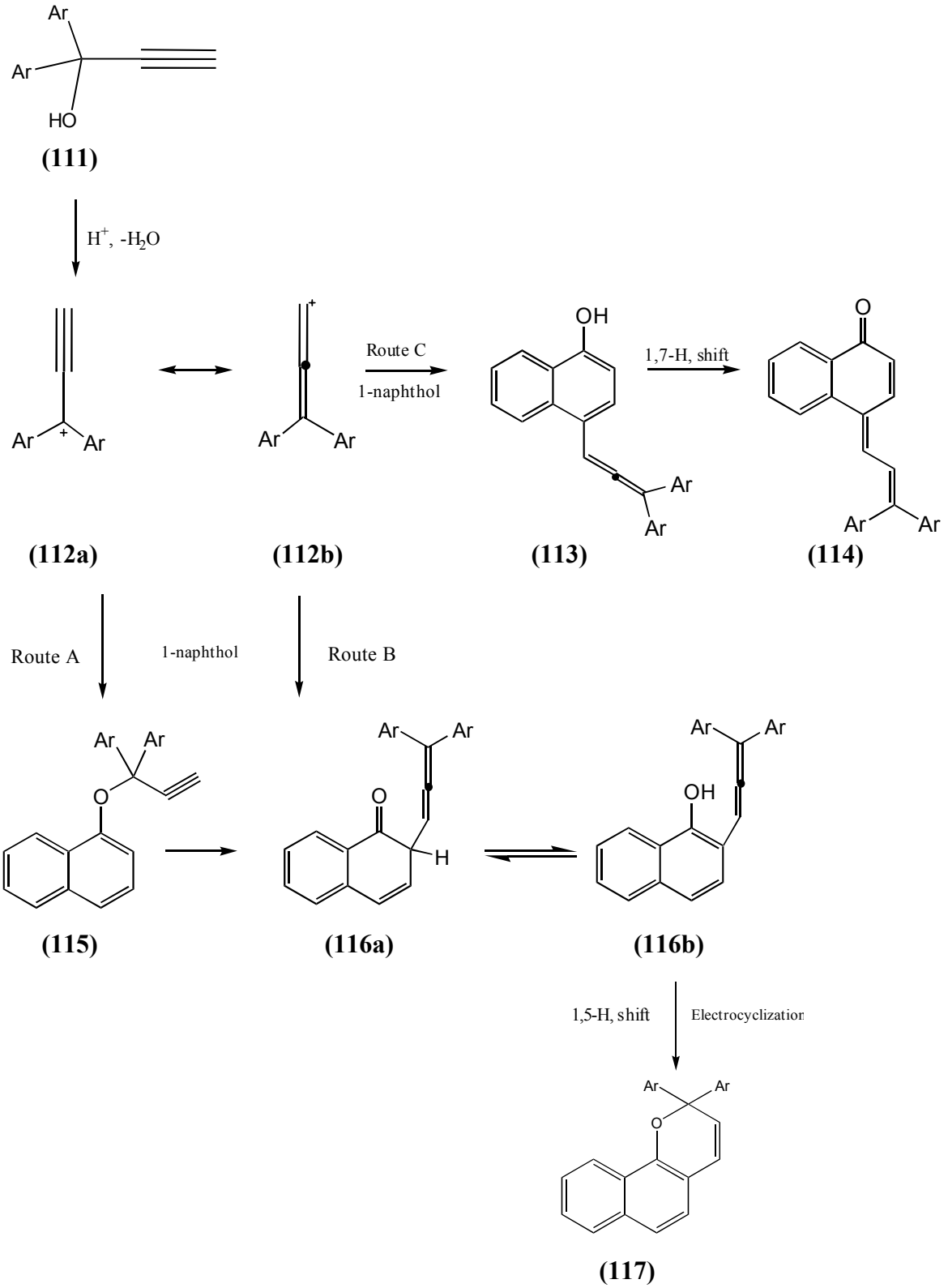

Scheme 37: Reaction scheme for synthesis of a naphthopyran **(117)**.

In the reaction mechanism described above, a carbocation is generated after protonation and the loss of water from the propynol **(111)**. Route A leads to the formation of naphthopyran **(117)**, which may be envisaged as proceeding via resonance from **(112a)** with 1-naphthol. The reaction first leads to compound **(115)** and, following a Claisen type [3,3] sigmatropic shift to compound **(116)**, which can exist in tautomeric forms. The 1,5-H shift and electrocyclization of compound **(116b)** provides a different compound **(117)** as shown in both routes A and B. In route C, the compound **(113)** undergoes a 1,7-H shift to give product **(114)**. The loss of aromaticity in compound **(114)** is balanced by the stabilization of the extended conjugation.[123] The use of NMR spectroscopy for mechanistic understanding of photochromism is described in the literature.[124] The photocolouration mechanism of benzopyran and naphthopyran was kinetically monitored using UV and visible irradiation. UV-irradiation of ring closed form **(118)** leads mainly to the isomer **(120)** as observed from kinetic analysis. Two parallel pathways were also suggested leading towards isomer **(119)** and product **(121)**. The photoconversion of isomer **(120)** to the ring closed form was also observed along with the photoisomerization between isomer **(119)** and isomer **(120)**. The reaction from isomer **(120)** to product **(121)** was slow and compound **(121)** was photostable. The same procedure was applied after irradiation with visible light. The photomerocyanines were the only photoreactive species. The isomerization of isomer **(119)** led to isomer **(120)** and isomer **(120)** to the ring closed form ultimately. The conversion of isomer **(120)** to the allenylphenol **(121)** by the 1,5-H shift has also been seen. The reaction is given in Scheme 38.

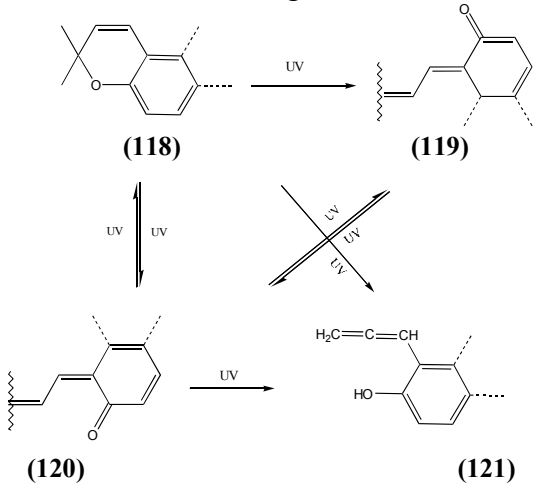

Scheme 38: Mechanism of photocolouration in compound **(118)** under UV-irradiation.

The kinetic and thermal bleaching showed that the *transoid* isomer **(119)** cannot return directly to the closed form. The disappearance of isomer **(119)** requires the isomerization to isomer **(120)**, which then converts to the ring closed form by a single bond rotation. The mechanism is shown in Scheme 39.

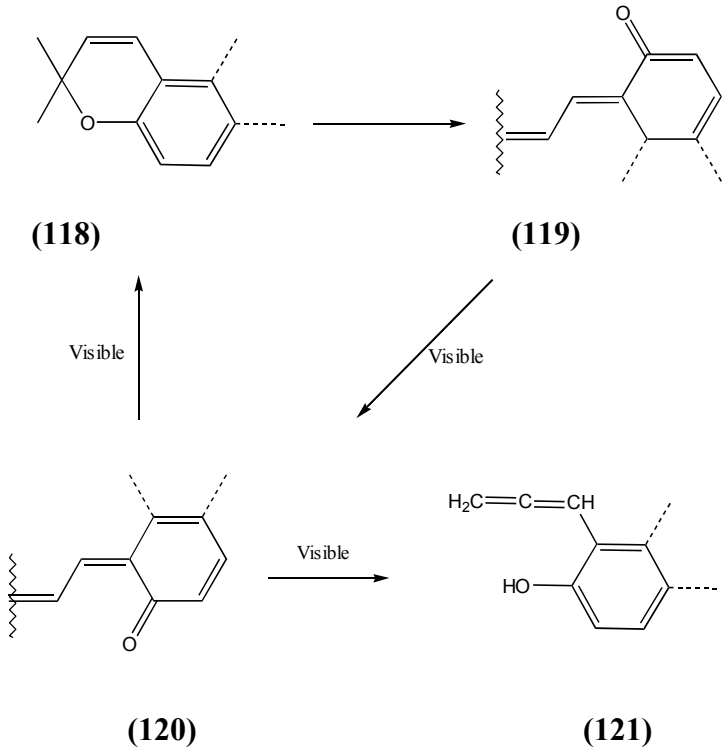

Scheme 39: Mechanism of photo-bleaching in naphtho- and benzopyrans under visible light.

2.6 Molecular modelling

2.6.1 History

The development of molecular modelling started at the beginning of the 20th century. A decisive tool for providing useful information for the development of molecular modelling was X-ray crystallography. Molecular kits were used to provide a 3D impression of a crystal structure. Watson and Crick outlined the structure of the DNA helix through modelling and the subsequent developments in computer science has made it much easier to model molecules and to study their properties using a variety of mathematical

calculations. In the 1930s, computation methods were used in nuclear physics using mathematical modelling techniques. The quantum chemical calculations of systems from the simple hydrogen atom and up to complex systems have been made possible by mathematical approximation techniques. Colour coded and rotatable 3D structures of molecules were introduced in the 1970s. The concepts of force field, geometry optimization and other techniques have been developed for use in molecular modelling.[125]

2.6.2 Sketch approach

The sketch approach was the simplest method of structure generation. The 2D structure of a molecule is drawn which is then converted to a 3D structure. The resulting geometry is optimized at the end to relax the molecular geometry. The sketch approach uses the conversion of a single formula drawn into three dimensional information using programmes such as CONCORD [9, 126] and CORINA.[127] The automatic generation of a 3D structure is carried out by these programmes using a rule and data based system which is reliable and powerful enough to convert huge databases of hundreds of compounds. The CONCORD programme generates the 3D structure by the use of a detailed table of bond lengths. The atomic numbers, bond type and hybridization states are also taken into account before assigning the bond lengths. After the construction of the molecule, the strain is distributed over the molecule to provide a relaxed geometry.

2.6.3 Molecular Mechanics

Molecular mechanics is a widely accepted computational method employed to calculate molecular geometries and energies. Molecular mechanics is a fast computational method practicable for small as well as the large molecules. In molecular mechanics, classical Newtonian mechanics is effectively applied to the atoms in a molecule which are treated as balls of different sizes (atom type) joined together by springs of varying lengths (bonds). The atomic composition of a molecule is considered to be a collection of masses interacting with each other via harmonic forces. The total energy is minimized with respect to the atomic coordinates and can be written as:

$$\mathbf{E_{tot} = E_{str} + E_{ben} + E_{tor} + E_{vdw} + E_{elec}}$$

where E_{tot} is the total energy of the molecule, E_{str} is the bond stretching energy, E_{ben} is the angle-bending energy, E_{tor} is the torsional energy, E_{vdw} is the van der Waals energy, and E_{elec} is the electrostatic energy. The total steric energy of the molecule is calculated with reference to the unstrained molecule using molecular mechanics. A collection of these unstrained values with the force constants is known as a "force field". Molecular mechanics considers that the bonds have natural lengths and angles and the equilibrium values of these bonds and angles correspond to the force constants. The potential energy functions are defined in the force field and are called force field parameters. A deviation from these standard values results in an increase in the total energy of the molecule. The total energy is the measure of intramolecular strain in a hypothetical molecule with an ideal geometry. It is necessary to have a precise description of the molecule to perform molecular mechanics calculations. Different file formats are used for this which contains coordinates for all the atoms, a list of bond connections and a description of each atom. The description of each atom in a molecule is not a simple process as carbon, for example, has an atomic number 6 but it can have tetrahedral, trigonal planar or a linear structure depending on the hybridisation. As a result there are more atom types than the elements. A molecule can be described using simplifications, e.g., a methyl group is more or less spherical and it can be represented as if it was a single large atom instead of a carbon and three hydrogens. Different force fields provide different choices for the size and hardness of atoms. In general, it is not possible to take a parameter for one force field and use it in another because these parameters are non-transferable. A force field can provide the possible information about the conformational properties of a molecule. The flow diagram of a general molecular mechanics computer program is given in Scheme 40.[128]

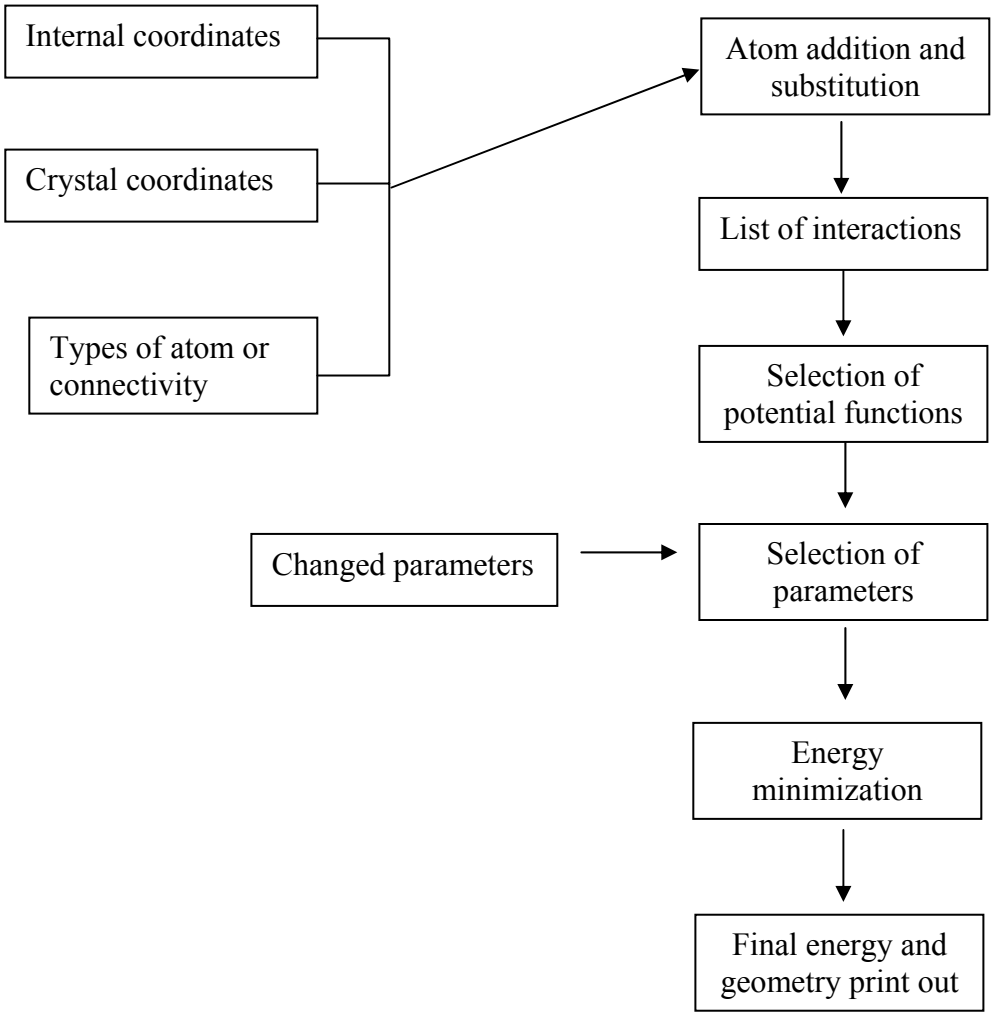

Scheme 40: Flow diagram of a general molecular mechanics computer procedure.

2.6.4 Quantum Mechanics

The quantum theory was introduced in the early part of the twentieth century. The application of quantum mechanics has been developed with the realization that electrons can behave like waves as well as particles. It is possible to carry out calculations of a molecule by assuming that the molecular orbitals are formed from linear combinations of atomic orbitals. The atomic orbitals on the same atom are orthogonal to each other,

and do not interact. The atomic orbitals on different atoms may not be orthogonal but interact to form molecular orbitals. The total number of orbitals is conserved. If there is an overlap between more than two atomic orbitals then they interact with each other and it makes the situation complicated. To provide a clear picture, the strong interactions are taken into account first and are paired according to the strength of interaction. The multiple interactions can then be considered and the remaining weak interactions can be introduced later. Schrödinger's equation is used to determine the allowed energy levels within quantum mechanical systems. The associated wavefunction gives the probability of finding the particle at a certain position. The orbitals containing the electrons do not have clearly defined edges and the probability of finding the electron diminishes with the distance. In order to calculate the structure of a molecular orbital, a reasonable assumption is made which states that molecular orbitals can be expressed as a linear combination of atomic orbitals (LCAO) as shown in the equation given below.

$$\psi = c_1\phi_1 + c_2\phi_2 + c_3\phi_3 \ldots\ldots\ldots\ldots + c_n\phi_n$$

where ϕ_i are the atomic orbitals; ψ is a molecular orbital and c_i are the coefficients. Schrödinger's wave equation can be used to describe the energy of an orbital by the equation.

$$H\psi = E\psi$$

The absolute energy of a system can be calculated from a molecular orbital calculation. The calculations are commonly more complex than molecular mechanics but molecular orbital theory can deal with bond formation and breaking so that it can be used to study reactions as well as the ground state molecular properties.

Properties such as molecular geometry and relative conformation energies with high accuracy can be calculated for a broad variety of structures using a well parameterized general force field using molecular mechanics. Quantum chemical methods can also be used for geometry optimization if the force field parameters for a certain structure are not available. The calculations of transition states or the determination of geometries influenced by polarization or unusual electron distribution in a molecule is a domain of quantum mechanical calculations.[129] The basic concept of semiempirical approaches to quantum mechanics is that the molecular properties are mainly influenced by the valence electrons of the corresponding atoms. If only the valence electrons are taken into account this ultimately reduces the complexity and hence the time in calculation. Semiempirical methods such as AM1 [130] and PM3 [131] provide an effective compromise between the accuracy of the results and the time required for the calculations. Semiempirical methods offer the advantage over the *ab initio* approach as they can perform calculations of systems with up to 200 atoms with reasonable ease. The use of molecular orbital approaches in the prediction of spectral properties has been discussed in section 3.1.2.

3. Results and discussion

This chapter is divided into two sections. The first section deals with the spirooxazines and the second with naphthopyrans. The spirooxazine section is further subdivided into five subsections which discuss the spirooxazines based on different types of the starting material used, involving different permanent chromophore types, which includes dihydroxynaphthalene-based azospirooxazines, anthraquinone-based spirooxazines, naphthoquinone-based spirooxazines, nitrosospirooxazines and pyrazolone-based spirooxazines. Each section starts with the application of computer-aided molecular modelling to provide molecular geometries followed by the PPP-MO calculations to assess the spectral properties of the compounds. The synthesis of selected molecules is discussed subsequently.

3.1 Dihydroxynaphthalene-based azospiroxazines

3.1.1 Molecular modelling

Molecular modelling techniques were used as a predictive tool to account for the properties of all the systems studied. A range of new potentially photochromic materials were modelled with a view to understanding the photochromic properties and the relative stabilities of molecules. Selected azospirooxazines **(122 -127)** were subjected to computer–aided molecular modelling to provide a prediction of their photochromic behaviour and the stabilities of the merocyanine forms. CAChe, a computer aided application system [132] was used to carry out the molecular mechanics (MM2) and the quantum mechanics (AM1) calculations. The molecular mechanics (MM2) calculations are helpful in the optimization of molecular geometry, which provides a structure which corresponds to a minimum energy. An optimum geometry is found by molecular mechanics by moving all the atoms until the net force acting on each atom is zero. The final energy values were used to provide a comparison of the relative stabilities of the merocyanine forms of the molecules. A reasonable assumption that can be made from the comparison of the MM2 final energy values is that the lower the value, the more stable is the photomerocyanine. MM2 final energy values are generally regarded as a good indicator of the stability of similar structures. The heat of formation values calculated from the quantum mechanics (AM1)

are used to predict the potential photochromic behaviour of the molecule by a comparison of the heat of formation values of the ring closed form and the merocyanine forms of a molecule. If the heat of formation of the ring closed form is lower than the values for all the merocyanine forms then the compound is predicted to have the potential to show photochromism. These values are generally regarded as a reasonable indicator of relative stability of structurally different molecules. The modelling results and then prediction of the potential photochromic behaviour of compounds with two different substituents (R) were studied. Based on established knowledge of azonaphthol structures, the molecules were assumed to exist in the ketohydrazone rather than the hydroxyazo tautomeric form because of the intramolecular hydrogen bonding as illustrated in Figure 30.[133]

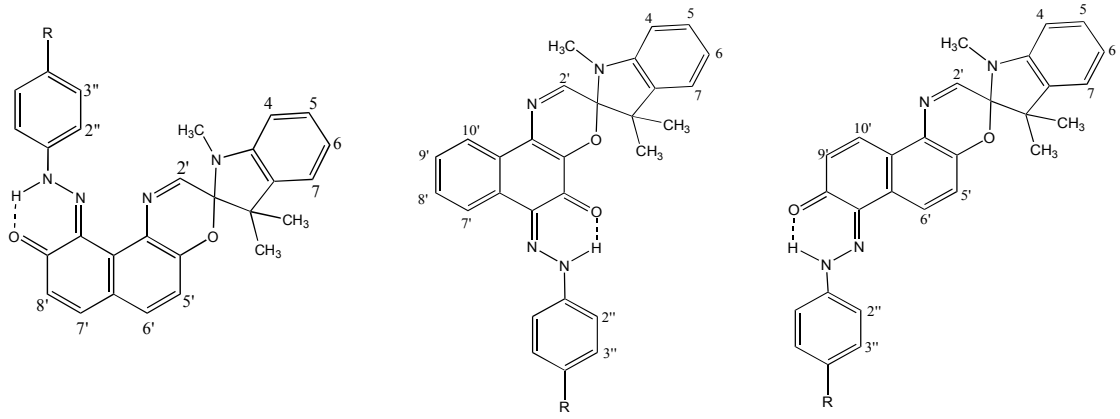

122 (R=NO_2) **124** (R=NO_2) **126** (R=NO_2)

123 (R=CH_3) **125** (R=CH_3) **127** (R=CH_3)

Figure 30: Structures of azospiroxazines **122** – **127**, with numbering scheme for spectral interpretation.

There are eight possible isomers of the photomerocyanines, four of which may be considered as *cisoid* and four as *transoid*. The focus of the investigation was on the *transoid* isomers (**a-d**) because of the high instability due to steric constraints in the *cisoid* isomers. (Figures 31-33).

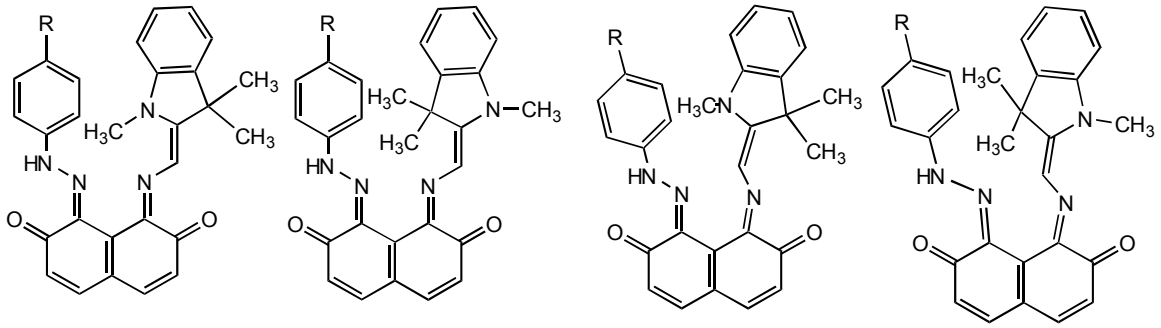

122a ($R=NO_2$) **122b** ($R=NO_2$) **122c** ($R=NO_2$) **122d** ($R=NO_2$)

123a ($R=CH_3$) **123b** ($R=CH_3$) **123c** ($R=CH_3$) **123d** ($R=CH_3$)

Figure 31: The structures of the four possible *transoid* photomerocyanines from compounds **122** and **123**.

The final energy values and heats of formation of the ring closed and merocyanine forms of spiroindolinonaphthoxazines (**122** and **123**) are given in Table 5.

Table 5: Final energy and values of the heats of formation of spirooxazines (**122** and **123**).

Compound	**Final Energy (kcal mol^{-1}) (MM2)**	**Heat of formation (kcal mol^{-1}) (AM1)**
122-Closed form	-1.65	126.83
122a	3.42	137.33
122b	4.47	140.45
122c	3.76	142.79
122d	4.65	140.14
123-Closed form	-2.07	116.51
123a	3.38	125.96
123b	4.30	129.13
123c	3.64	131.05
123d	4.49	128.52

The results suggested that the most stable photomerocyanine forms are likely to be **122a** and **123a** and the order of stability is **122a** > **122c** > **122b** > **122d** and **123a** > **123c** > **123b** > **123d** in the case of compounds **122** and **123** respectively. The order of stability of the merocyanine forms of compound **(122)** and **(123)** can be correlated by visual inspection of the optimized geometric structures, which show the greatest steric hindrance between the two C-methyl groups of the indoline ring when they are in very close proximity to the *p*-nitrophenylhydrazone part of the molecule. The least stable isomers **(122b)** and **(122d)** modelled by MM2 calculations shown in Figure 32, show considerable steric constraint involving the $C(CH_3)_2$ groups. The effect is clearer when the structures are visualised on the computer monitor in three dimensional form, while it is more difficult to show in two dimensions. In the most stable isomer **(122a)**, it is the $N(CH_3)$ which interacts with the phenylhydrazone, and there is much less deviation from planarity.

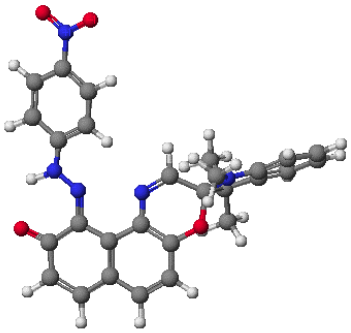

122

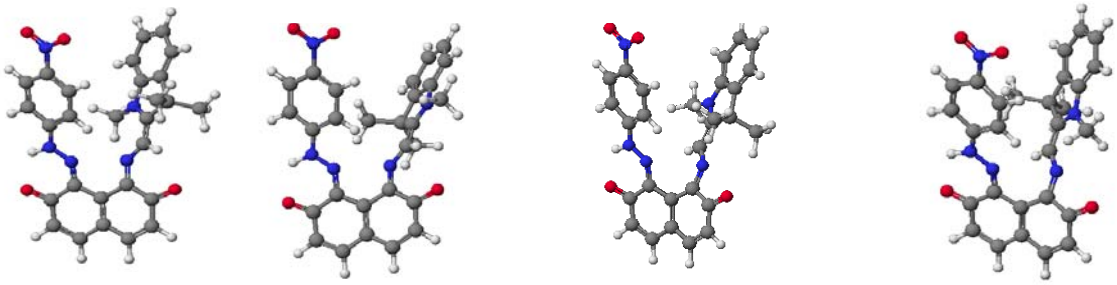

122a **122b** **122c** **122d**

Figure 32: The optimized (MM2) geometric structures of compound **(122)** and its merocyanine forms.

The spiro carbon in compound **(122)** is tetrahedral and the two planes of the molecule are perpendicular to each other. Photochromism in spirooxazines is due to a light-induced ring-opening to form a photomerocyanine, which reverts thermally to the ring-closed form after the removal of the light source. The AM1 calculations given in Table 5, suggest that compounds **122** and **123** after irradiation of UV-visible light have the potential to show photochromism as the heats of formation of ring closed form is lower than all of the photomerocyanine forms. Steric (final) energies from MM2 calculations suggest that isomers **(122a)** and **(123a)** are the lowest energy ring-opened forms and thus are likely to be the most stable photomerocyanines species. Considerable steric congestion is seen in isomers other than **(122a)** and **(123a)**, which results in much more deviation from planarity. The molecular mechanics and the quantum mechanics (AM1) calculations were also carried out for compounds **(124-127)**. The four *transoid* isomers out of the total eight were again considered for these molecules and the structures of these molecules are given in Figures 33 and 34.

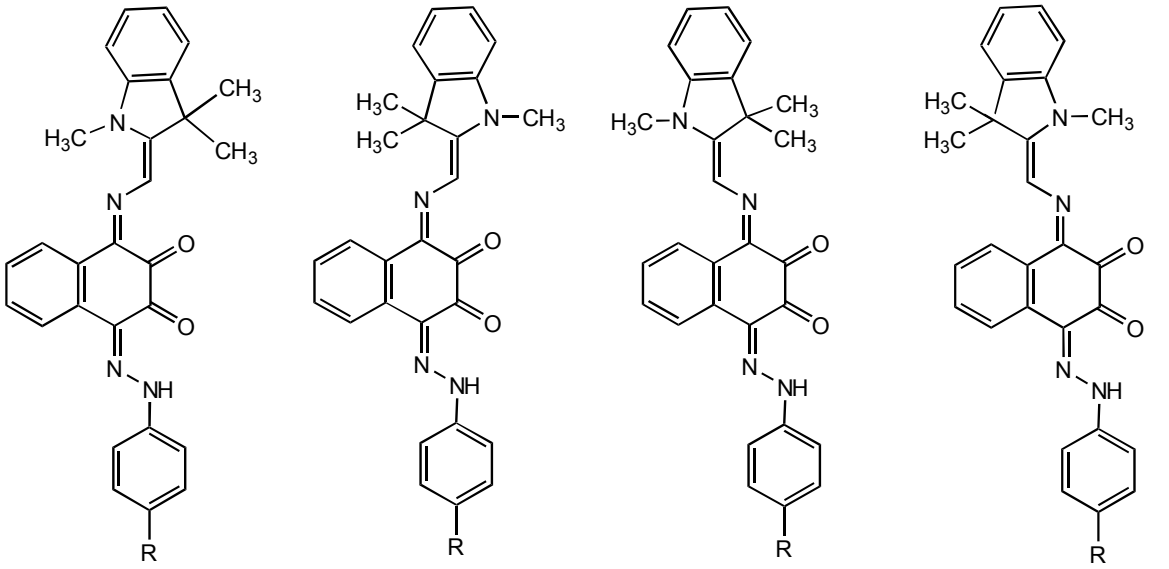

124a (R=NO_2) **124b** (R=NO_2) **124c** (R=NO_2) **124d** (R=NO_2)

125a (R=CH_3) **125b** (R=CH_3) **125c** (R=CH_3) **125d** (R=CH_3)

Figure 33: The structures of the four possible *transoid* photomerocyanines from compounds **124** and **125**.

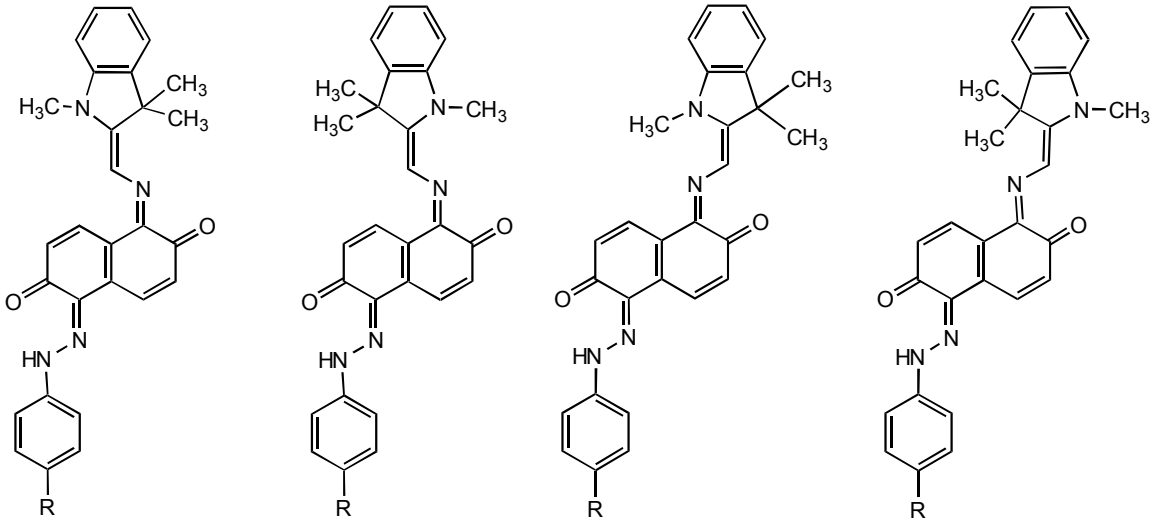

126a (R=NO_2) **126b** (R=NO_2) **126c** (R=NO_2) **126d** (R=NO_2)

127a (R=CH_3) **127b** (R=CH_3) **127c** (R=CH_3) **127d** (R=CH_3)

Figure 34: The structures of the four possible *transoid* photomerocyanines from compounds **126** and **127**.

The molecular geometries of the azospirooxazines **122** - **127** and each of the merocyanine isomers were calculated using standard augmented MM2 within CAChe. The steric energies of molecules **(124-127)** and the photomerocyanines are given in Table 6.

Table 6: Steric energies from MM2 calculations for azospirooxazines **124** – **127** and their ring-opened merocyanine isomers **a** - **d**.

	Final Energy (kcal mol^{-1}) (MM2)			
	124	**125**	**126**	**127**
Closed form	-2.76	-2.93	-2.32	-2.63
A	2.14	1.83	2.53	2.23
B	-0.44	-0.77	-0.05	-0.37
C	3.39	3.06	3.93	3.60
D	5.17	4.84	5.17	5.38

The MM2 calculations predict that merocyanine isomers **(b)** are likely to be the most stable for all compounds **(124-127)**. The heats of formation were calculated from AM1 for compounds **(124-127)** (Table 7). A comparison of the values for the ring closed form and the four photomerocyanines in each case was made. The results show that compounds **(126)** and **(127)** might have the potential to show photochromism by the absorption of UV light to convert to the higher energy merocyanine form, with thermal reversion to the more stable ring-closed form after the removal of the light source. The prediction of photochromism is not clear in the case of compounds **124** and **125**. AM1 calculations suggest that the ring-opened forms are more stable than the ring-closed form, predicting the possibility of a permanent merocyanine form, while MM2 calculations suggest the opposite. However, the calculated values for the both species are very close in these cases. The other relevant comparison is between the different substituents (R) involving the change from nitro group to the methyl group. The results were consistent in both cases. The calculated values for compounds **(124-127)** are given in Table 7.

Table 7: Heats of formation from AM1 calculations for azospirooxazines **124** – **127** and their ring-opened merocyanine isomers **a** - **d**.

	Heat of formation (kcal mol^{-1})			
	124	**125**	**126**	**127**
Closed form	126.99	115.85	124.51	113.46
A	123.20	112.18	135.92	124.50
B	125.75	114.65	138.70	127.11
C	126.62	115.46	141.71	129.80
D	123.78	112.73	137.10	126.94

The minimized structures of the ring closed and photomerocyanine forms of compounds **124** and **126** are given in Figures 35 and 36 respectively.

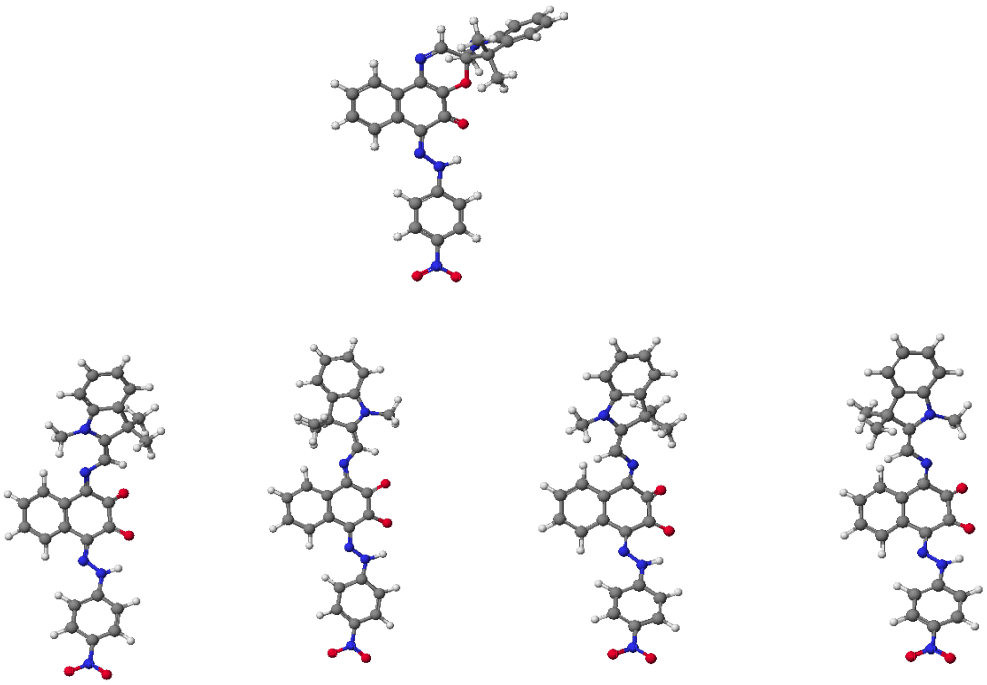

Figure 35: The minimized structures of the ring closed form and the four possible *transoid* photomerocyanines from compounds **124**.

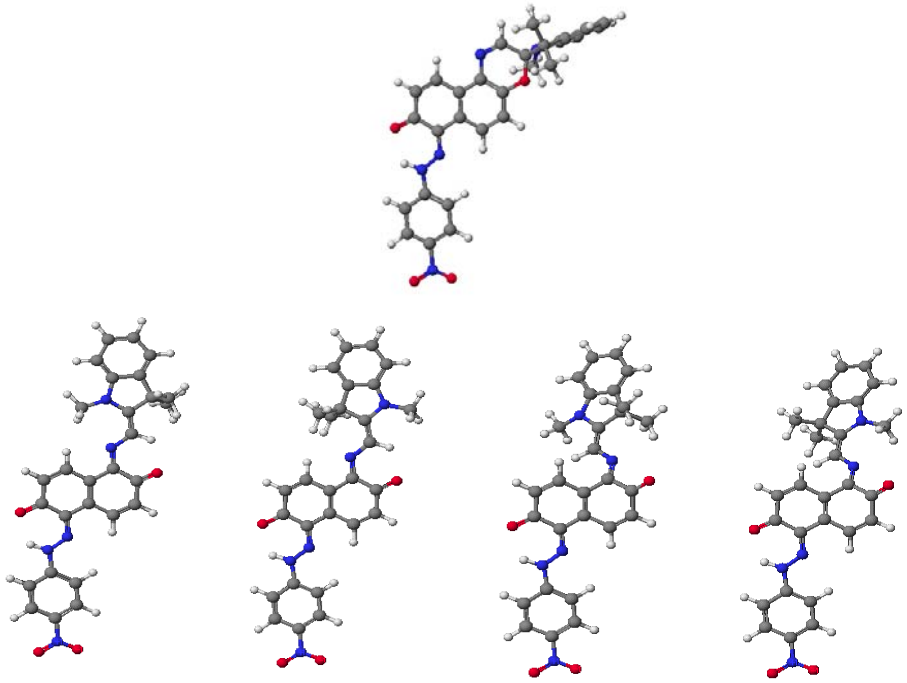

Figure 36: The minimized structures of the ring closed form and the four possible *transoid* photomerocyanines of compound **126**.

Inspection of the modelled structures for compounds **(124)** and **(126)** showed that the merocyanine forms for both compounds are essentially planar. The ring closed forms **(124)** and **(126)** showed less strain in the molecules as compared to compound **(122)**.

3.1.2 PPP-MO Calculations

This section provides a discussion of the results of the PPP-MO calculations for the dihydroxynaphthalene based azospiroindolinonaphthoxazines. The calculations of the ring closed forms of the molecules are discussed first followed by calculations on the merocyanine forms. PPP-MO calculations have proved to be generally useful for the prediction and interpretation of the UV-visible spectra of organic dyes and pigments.[134-138] An attempt was made to predict the colour change arising from these various species using the PPP-MO approach including a correlation with experimental electronic absorption spectral data where available.

Lengthy procedures for synthesis of dyes can be avoided using PPP-MO calculations to predict properties and aid selection of target molecules. For a specific chemical structure, it is possible to input a set of semi-empirical parameters and then using this data to calculate the maximum absorption wavelength (λ_{max}) of a molecule, together with information on the other properties of molecules such as the oscillator strength, an indication of colour strength.

(a) Calculations for the ring closed form

The PPP-MO calculations were carried out for the ring closed and the predicted most stable *transoid* isomer of the molecules assuming planarity of the merocyanine form. For the purposes of the PPP-MO calculations approximations on the ring-closed forms which are non-planar had to be made with respect to the structures. Only the azo-oxazine portions of the structures were regarded as responsible for the colour and the indoline part which is not in conjugation with the other part of the molecule was ignored. The structures assumed for compounds (**122, 124** and **126**) with the numbering scheme used in the calculations are given in Figure 37. The ring closed form and *transoid* merocyanine form predicted from MM2 calculations to be the most stable from compounds **122**, **124** and **126** were selected to run the calculations.

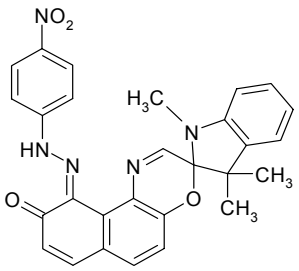

122-Ring closed form

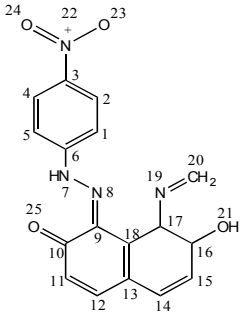

122e

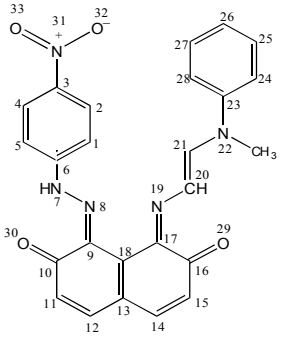

122f

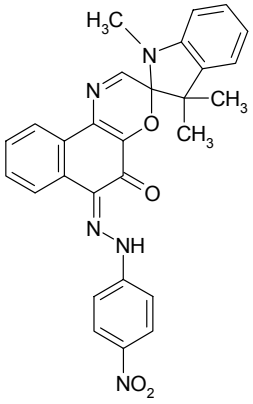

124-Ring closed form

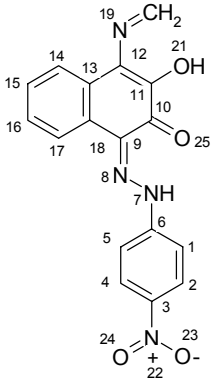

124e

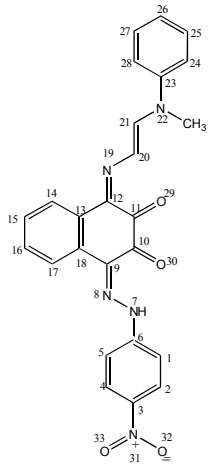

124f

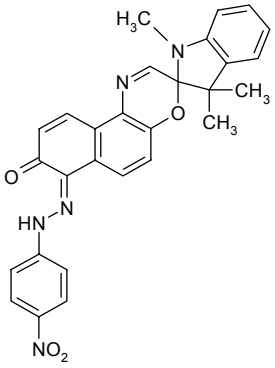

126-Ring closed form

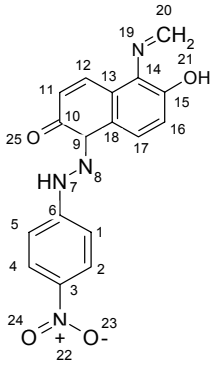

126e

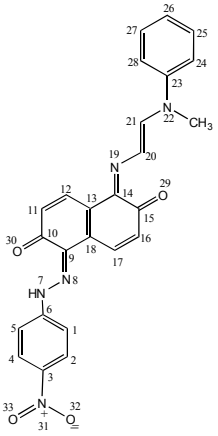

126f

Figure 37: Ring-closed forms and approximation to the ring closed and photomerocyanines forms of spirooxazines **(122, 124** and **126)** used for the PPP-MO calculations.

The parent azonaphthol, which exists in its hydrazone form, was a useful reference molecule as a starting point for the calculations to address that part of the molecule with the permanent chromophore.[139] The structure of the reference molecule **(R-1)** with the numbering scheme used for the calculations is given in Figure 38.

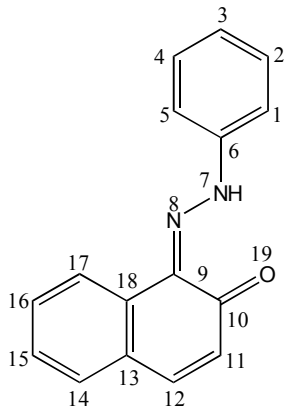

Figure 38: Reference azonaphthol molecule **(R-1)** used for the PPP-MO calculations.

A generalized set of parameters was used to run the PPP-MO calculations and is given in Table 8.

Table 8: A generalized set of parameters used for reference molecule **(R-1)**.

Bond / atom specification	**VSIP eV**	**EA eV**	**Core Charge**	**β value eV**	**Bond length Å**
Aryl ring (C=C)	11.16	0.03	1	-2.4	1.40
C=O	17.7	2.47	1	-2.46	1.22
N=NH	18	8.50	2	**-2.42**	1.35
C=N	15	0.97	1	-2.48	1.33

The experimental λ_{max} value for the reference molecule is reported in the literature [138] as **479** nm while the calculated λ_{max} value by using the set of parameters given in Table 8 was **491** nm. It was considered appropriate to attempt to further adjust the parameters to obtain a closer correlation between the calculated and the experimental values. As a result of adjusting the bond resonance integral (β-value) for the NH-N bond from -2.42 to -2.75 eV, a calculated λ_{max} value of **479** nm (oscillator strength 0.96) was obtained. The PPP-MO calculations were then run for the approximation to the ring closed form **(122e)**. The set of parameters used for the calculations is given in Table 9, where the optimised β value for the N-NH bond (–2.75eV) was used with the remaining parameters from the generalized set.

Table 9: An optimised set of parameters used for approximation to ring closed form **(122e)**.

Bond / atom specification	**VSIP eV**	**EA eV**	**Core Charge**	**β value eV**	**Bond length Å**
Aryl ring C=C	11.16	0.03	1	-2.4	1.40
C=O	17.7	2.47	1	-2.46	1.22
C-OH(H-bonded)	28	10	2	-2.6	1.36
C-N=	11.16	0.03	1	-2.6	1.35
C-NH	18	8.50	2	-2.42	1.35
-NH-N	15	0.97	1	**-2.75**	1.33
(C-N), NO_2gp	24.8	12.5	2	-2.0	1.49
N=O	21	2.5	1	-2.8	1.21

The experimental λ_{max} value for product (**122**, ring closed form) was established as **481 nm**, since compound **(122)** was eventually successfully synthesised (for details see synthesis section 3.1.3, XV). The optimised set of parameters used for the calculations given in

Table 9, gave a calculated λ_{max} value of **522 nm**. In an attempt to correlate the experimental and calculated λ_{max} values more closely, the parameters for the nitro group were changed. The effect of the optimizations on the β value of the nitro group (N-O) for compound **(122e)** showed that by changing the β value from -2.8 to –3.8eV, gave a λ_{max} value of **515 nm** (f_{osc} 0.81). As a final step in the PPP-MO calculations the parameters for the C_6-N_7 bond were optimized. The β value used for C_6-N_7 bond was -2.75 eV instead of -2.42 eV and calculated λ_{max} value obtained was **493 nm** (f_{osc} 0.97).

The calculations were also run for the approximation to the ring closed form of compounds (**124e** and **126e**) using the same optimized set of parameters as derived for structure **(122e)**. A comparison of the experimental and calculated λ_{max} values, since these eventually became available, is given in Table 10.

Table 10: A comparison of λ_{max} values of approximation to compounds **(124e)** and **(126e)**

Compound	**Experimental λ_{max} (nm)**	**Calculated λ_{max} (nm) (f_{osc})**
124	510 **(124)**	501 (0.84) **(124e)**
126	500 **(126)**	515 (1.18), 379 (0.21), 353 (0.37) **(126e)**

The results showed that the calculated λ_{max} values obtained using a set of optimised parameters were in reasonable if not exact agreement to the experimental values. These molecules (ring closed forms) showed wavelength absorptions with significant oscillator strength (0.84-1.18) and experimental λ_{max} values ranging from 481-510 nm.

(b) Calculations for the merocyanine forms

The most stable *transoid* photomerocyanine forms of compounds **122**, **124** and **126** based on prediction from final energy (MM2) calculations to be the most stable were

selected to run the calculations. The reference molecule used for the merocyanine form of spirooxazines was taken from the literature.[140] The structure of the reference molecule **(R-2)** is given in Figure 39.

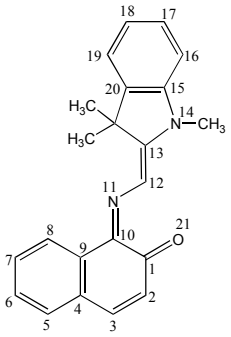

Figure 39: Reference molecule **(R-2)** for modified merocyanine forms, structures **(122f**, **124f** and **126f)**.

A generalized set of parameters used for calculations and is given in Table 11.

Table 11: A generalized set of parameters used for modified merocyanine forms **(f)**.

Group, atom specification	**VSIP eV**	**EA eV**	**Core Charge**	**β value eV**	**Bond length Å**
Aryl ring (C=C)	11.16	0.03	1	-2.4	1.40
C=O	17.7	2.47	1	-2.46	1.22
C-OH (H-bonded)	28	10	2	-2.6	1.36
C-N=	11.16	0.03	1	-2.6	1.35
N-NH	18	8.50	2	-2.42	1.35
-C=N	15	0.97	1	-2.75	1.33
(C-N) NO_2gp	24.8	12.5	2	-2.0	1.49
N=O	21	2.5	1	-2.8	1.21
C=N(17,19)	15	0.97	1	-2.48	1.33
N-C(19,20)	11.16	0.03	1	-2.75	1.40

The experimental λ_{max} value for reference molecule **(R-2)** was **606** nm and the calculated λ_{max} value using generalized parameters was **555** nm (f_{osc} 0.70). Optimised parameters were also described in the literature for this molecule in which the value of VSIP (19.5eV) and EA (6.0eV) for N_{10} were applied. Using these optimised values, the calculated λ_{max} value for the reference molecule was **614** nm (f_{osc} 0. 85). The results are given in Table 12.

Table 12: A comparison of λ_{max} values of reference molecule **(R-2)** (merocyanine form).

Compound	**λ_{max} Using generalized parameters (nm) (f_{osc})**	**λ_{max} Using optimized parameter (nm) (f_{osc})**
Reference molecule	555 (0.70), 414 (0.2), 305 (0.7)	614 (0.85), 431 (0.2), 310 (0.53)

PPP-MO calculations for modified merocyanine structures (**122f**, **124f** and **126f)** were carried out using the generalized parameters (given in Table 11) as well as optimised parameters where the optimised β value for N-NH bond was used. The calculated λ_{max} values using both sets of parameters are given in Table 13.

Table 13: Results of calculated λ_{max} values for modified merocyanines from azospirooxazines.

	Calculated λ_{max} (nm) (f_{osc})		
N-NH bond, β value, eV	**122f**	**124f**	**126f**
(-2.42)	647 (0.42),635 (0.47), 437 (0.55)	597 (0.05), 390 (1.9)	765 (0.8), 704 (2.0)
(-2.75)	649 (0.42), 633 (0.52), 462 (0.44)	676 (0.02), 616 (0.05), 511 (0.06), 416 (2.2)	778 (1.38), 712 (1.56)

Another set of calculations using the optimised β value for the nitro N-O bond was also carried out. The results for compounds (**122f**, **124f** and **126f)** are given in Table 14.

Table14: The results of change in β value of approximation to merocyanine forms **(f)**.

Compound	**β value for N=O group**	**λ_{max} calculated (nm) (f_{osc})**
122f	-3.8	646 (0.50), 628 (0.35), 436 (0.51)
124f	-3.8	608 (0.04), 606 (0.06), 399 (2.09)
126f	-3.8	778 (1.38), 712 (1.56)

As a final step, optimised parameters from the reference molecule were applied. The optimisation was in N_{19} values where the VSIP was changed from 18 to 19.5 eV and EA from 4.5 to 6eV. The calculated λ_{max} values obtained after using these parameters are given in Table 15.

Table15: The results for approximation to merocyanine forms, using optimized parameters from the literature.

Compound	**Calculated λ_{max} (nm) (*f*osc), using optimised parameters**
122f	649(0.40), 605(0.54), 440(0.27)
124f	638(0.67), 495(0.62), 420(0.55)
126f	750(2.2), 561(0.24), 479(0.21)

The results predicted that the merocyanine forms **(122f-126f)** have visible wavelength absorptions with significant oscillator strengths (0.21-2.2) and the calculated λ_{max} values ranging from 638-750 nm. Based on these values a neutral grey colour can be predicted for these merocyanine forms due to multiple absorptions in the visible region. There was a good correlation of predicted and experimental colour in case of compounds (**122f** and

122a). The results of the PPP-MO calculations provide useful information about the π-electronic charge distribution in ground and first excited states of the merocyanine form of spirooxazine **(122b)** predicted to be the most stable. A resonance or valence-bond representation of the structure of compound **(122b)** is given in Figure 40.

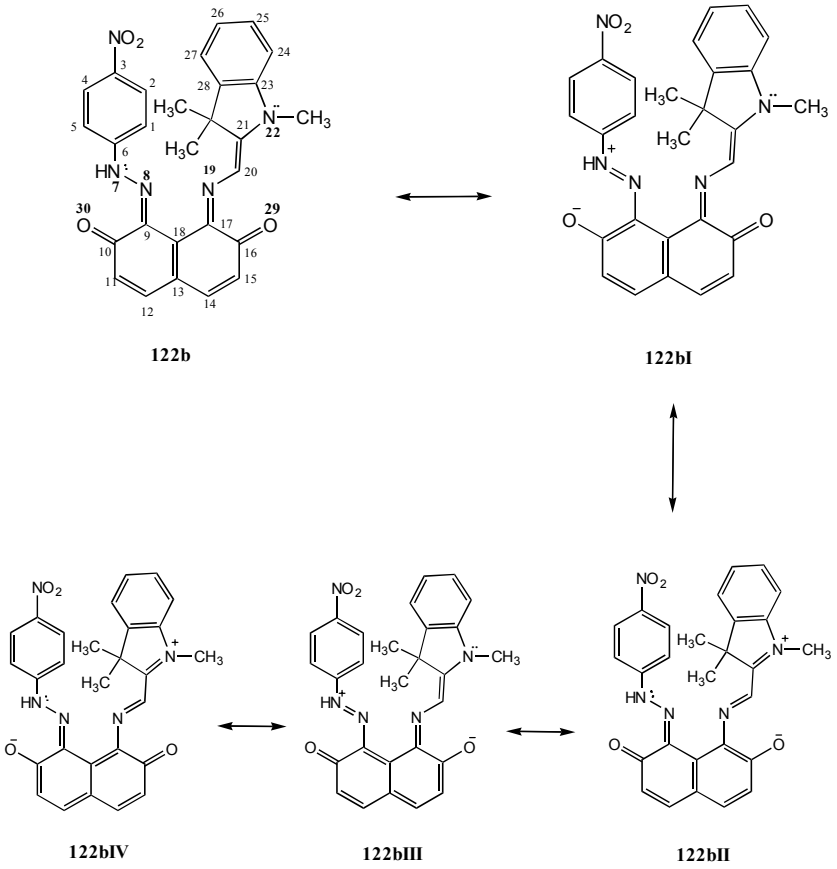

Figure 40: Resonance forms of compound **(122)**.

The relative contribution of the neutral (quinonoid) form and charge separated (zwitterionic) forms to the overall structures of spirooxazines has been mentioned in the literature.[141] Calculated π-electron charge densities for the ground state, first excited state and second excited state of compound **(122b)** are given in Table 16. Four resonance forms (**122bI-122bIV**) were derived by the transfer of charge from N-7 and N-22 to carbonyl oxygens O-29 and O-30 respectively.

Table 16: Calculated π-electron charge densities, for the ground, first excited and second excited states of merocyanine form **(122b)**.

	π-Electron charge densities		
Atom No.	**Ground state**	**1st Excited State**	**2nd Excited State**
1	1.07	1.03	0.99
2	0.96	0.97	0.96
3	1.06	1.08	1.05
4	0.96	0.96	0.96
5	1.03	1.04	1.01
6	1.01	1.03	1.03
7	**1.33**	**1.35**	**1.24**
8	**1.15**	**1.24**	**1.24**
9	1.01	0.98	0.87
10	0.79	0.78	0.79
11	1.01	0.99	1.06
12	0.96	0.97	0.96
13	1.03	0.96	1.07
14	0.97	0.98	0.97
15	1.03	0.98	1.06
16	0.88	0.88	0.89
17	0.82	0.85	0.79
18	0.99	1.03	1.05
19	**1.45**	**1.52**	**1.53**
20	0.94	0.88	0.84
21	0.95	0.99	1.00
22	**1.68**	**1.62**	**1.61**
23	1.01	1.01	1.01
24	1.03	1.02	1.02
25	1.03	0.99	0.99
26	1.02	1.01	1.00
29	**1.23**	**1.24**	**1.34**
30	**1.56**	**1.48**	**1.51**
31	1.12	1.13	1.13
32	1.47	1.48	1.47
33	1.47	1.48	1.47

The ground state charge densities are generally consistent with the valence bond approach. (Table 16) The reduced charge density on N-7 and increased charge density on O-30 is consistent with an important contribution from structure **(122bI)**. The relatively high charge densities on N-8, N-19, O-29 and O-30 and reduced charge densities on C-9, C-17, C-16 and C-10 respectively suggest a polarization of C-N and C-O bonds in structure **(122bI-122bIV)**. Similarly the reduced first excited state charge density on N-22 and increased charge density on O-29 suggest the contribution of structure **(122bII)**. The first excited state charge density on N-7 showed an increase while a decrease in charge densities on N-22 and O-30 suggested the significant participation of structure **(122bIV)** in the excited state. Structure **(122bI)** suggested to make a minor contribution to the first excited state. The comparison of second excited state shows that there is a decrease in second excited state charge density on N-7 and an increase on O-29 indicating a significant possible contribution of structure **(122bIII)** in the second excited state. The contribution of structure **(122bIV)** in the second excited state can be justified by an increase in second excited state charge density on O-30 and a decrease on N-22. An increase in the first excited state charge density on N-7 is not in good agreement to the valence bond interpretation.

3.1.3 Synthesis

Three different isomeric dihydroxynaphthalenes were used as starting materials, namely 2,7-dihydroxynaphthalene, 2,3-dihydroxynaphthalene and 2,6-dihydroxynaphthalene. Attempts were made to synthesize compound **(122)** by three different synthetic routes starting from 2,7-dihydroxynaphthalene as shown in Scheme 41. Each route involved three different stages: nitrosation, reaction with Fischer's base **(70)** and azo coupling of a dihydroxynaphthalene derivative with diazotized *p*-nitroaniline. The routes differ in the sequence in which the reactions were carried out and are discussed individually. (Scheme 41)

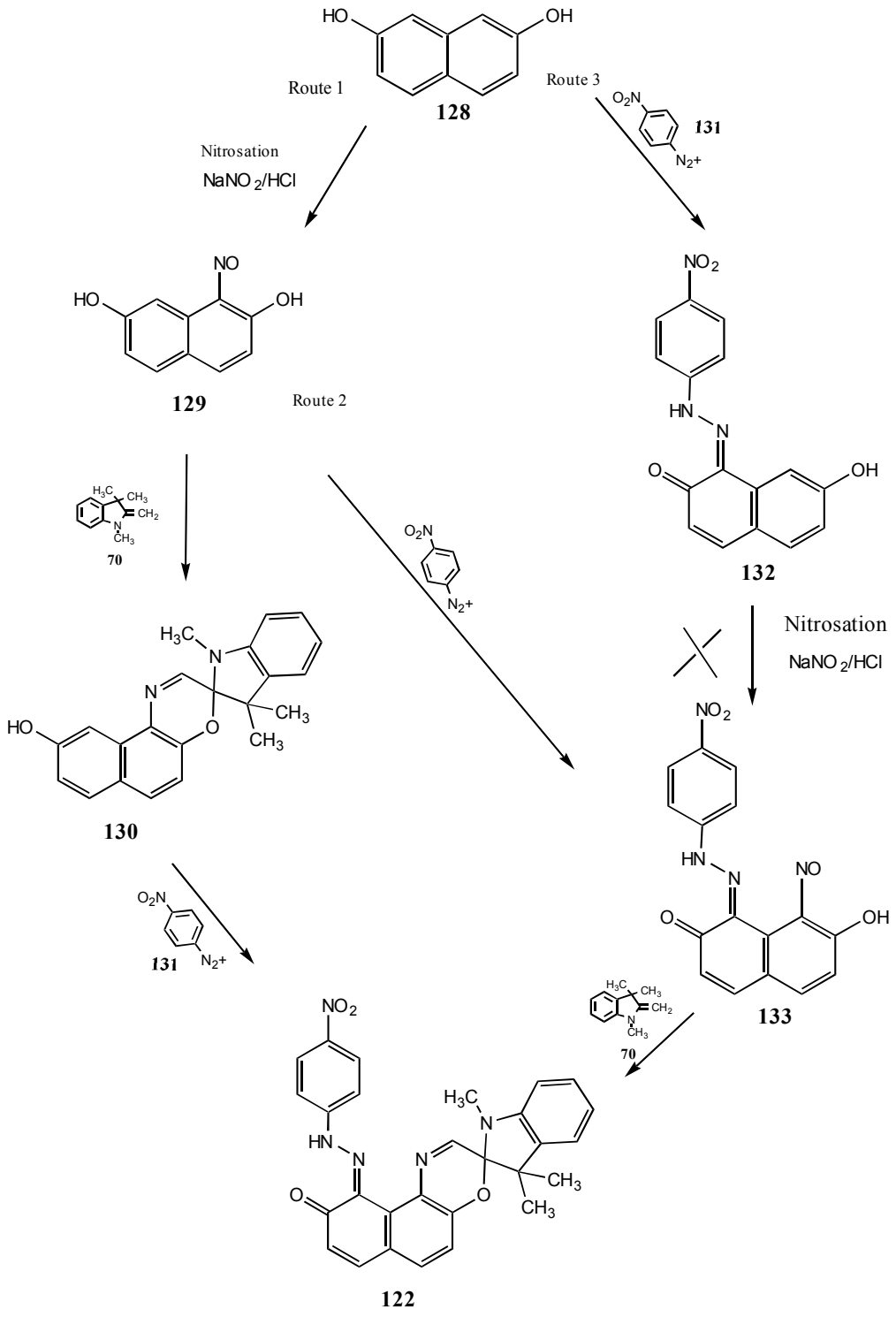

Scheme 41: Synthesis of compound **(122)** by three different routes.

Route 1

(i) Nitrosation

The first step in the synthesis of compound **(122)** was the nitrosation of 2,7-dihydroxynaphthalene **(128)** to give 1-nitroso-2,7-dihydroxynaphthalene **(129)** in 92% yield. (Scheme 41) The experimental details are given in section 5.5.1. The nitroso compound **(129)** is documented in the literature.[133,142]

(ii) Fischer's base reaction

The reaction of *o*-nitrosohydroxyaromatic compounds with Fischer's base **(70)** is the most common route to give spirooxazines. An ethanolic solution of 1-nitroso-2,7-dihydroxynaphthalene **(129)** was reacted with Fischer's base **(70)** to give compound **(130)** as shown in Scheme 41. The details of the synthesis are given in experimental section (5.5.1, b).

(a) Analytical data

A range of analytical techniques was applied to the purified sample to confirm the structure of compound **(130)**. The melting point of compound **(130)** was 218^{o} C. The FTIR spectrum of the compound was obtained as a KBr disc. The absorption bands due to the hydroxy group and the C_{spiro}-O were found at 3401cm^{-1} and 976 cm^{-1} respectively. NMR spectral evidence was used to confirm the structure. For ^{1}H NMR spectroscopy, the numbering scheme used to identify the proton signals is given in Figure 41.

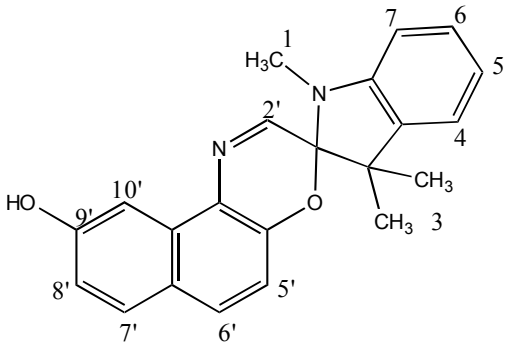

Figure 41: Proton numbering sequence for spiroindolinonaphthoxazine **(130)**.

Table 17: ^{1}H NMR spectral data for spirooxazine **(130)**.

Proton	**NMR signals, Chemical shift (ppm), Coupling constants (Hz)**
N (CH_3)	δ 2.70 (s, 3H, NCH_3)
C $(CH_3)_2$	δ1.25 (s, 6H, $(CH_3)_2$)
H_4	δ7.13 (d, 1H, $J_{4,5}$= 8.6)
H_5	δ6.82 (t, 1H, $J_{5,4}$= 7.6)
H_6	δ7.15 (t, 2H $J_{6,5}$=7.4)
H_7	δ6.63 (d, 1H, $J_{7,6}$=7.5)
$H_{2'}$	δ 7.80 (s, 1H)
$H_{5'}$	δ6.81 (d,1H, $J_{5',6'}$=8.6)
$H_{6'}$	δ7.63 (d, 1H, $J_{6',5'}$=8.6)
$H_{7'}$	δ7.67 (d, 1H, $J_{7',8'}$=9.6)
$H_{8'}$	δ6.95 (dd, 2H, $J_{8',7'}$=9.2)
$H_{10'}$	δ7.72 (m, 1H)

(b) Discussion

1-Nitroso-2,7-dihydroxynaphthalene **(129)** was reacted with Fischer's base **(70)** in an ethanolic solution. The reaction was monitored using TLC (silica, DCM: 0.5% Acetone). Two photochromic products were seen on TLC; both components (major and minor) appeared grey on TLC and turned blue on irradiation with UV-light (254 nm). After recrystallization from ethanol, the minor impurity was removed. It is possible that the minor component has the structure **(130a)**, although no attempt was made to isolate and characterise the compound.

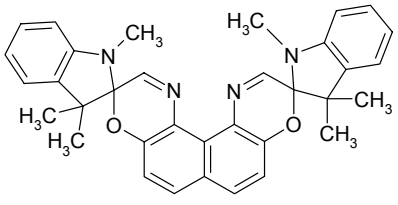

(130a)

Figure 42: Possible structure of photochromic impurity **(130a)**.

A detailed NMR analysis of compound **(130)** is given here because only melting point and CHN analysis are reported in the literature.[98] The NMR spectrum of compound **(130)** showed a distinct singlet at δ1.25 ppm due to two C-methyl groups. Another singlet was found at δ 2.70 ppm due to the $N(CH_3)$ group. The singlet characteristic of the oxazine proton (2′-H) was observed at δ 7.80 ppm. The interpretation of the spectrum of compound **(130)** was useful as a reference for the more complex spirooxazines synthesized subsequently.

The formation of spirooxazine involves a Diels-Alder reaction of the ketooxime tautomer of compound **(129)** with Fischer's base, followed by spontaneous dehydration of the cyclised product as discussed in the literature.[143]

(iii) Coupling of diazotized *p*-nitroaniline with spirooxazine (130)

The synthesis of compound **(122)** was carried out by coupling diazotized *p*-nitroaniline with spirooxazine **(130)**. The product **(122)** was obtained as brown crystals after recrystallization from ethanol.

Analytical data and discussion

Compound **(122)** was obtained in 55% yield and decomposed without melting at 220^{o}C. The FTIR spectrum of the compound was obtained as a KBr disc. The absorption bands due to the N-H stretch and the C_{spiro}-O were found at 3435cm^{-1} and 977 cm^{-1} respectively. A weak absorption band due to the carbonyl group was observed at 1626 cm^{-1}. ^{1}H NMR analysis of the compound was carried out for a solution in deuterated chloroform, $CDCl_3$. The numbering scheme for the identification of the proton signals is given in Figure 43.

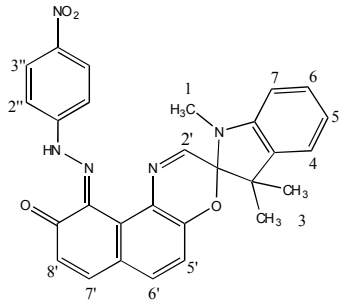

Figure 43: Proton numbering sequence for compound **(122)**.

Table 18: ^{1}H NMR spectral data for azospiroindolinonaphthoxazine **(122)**.

Proton	**NMR signals, Chemical shift (ppm), Coupling constants (Hz)**
$N(CH_3)$	δ 2.86 (s, 3H, NCH_3)
$C(CH_3)_2$	δ1.26 (s, 6H, $(CH_3)_2$)
H_4	δ6.63 (1H, d, 4-H, $J_{7,6}$=8.0 Hz)
H_5 H_7 H_6'	δ7.20-7.45(5-H, 7-H, 5′-H, 6′-H, m, overlapping signals
H_6	δ6.94 (1 H, m, 6-H)
H_2'	δ 7.88 (1H, 2′-H, s)
H_5'	δ6.63 (d,1H, $J_{5',6'}$=8.00)
H_7'	δ7.58 (1H, d, 8′-H, $J_{8',7'}$ = 9.8 Hz)
H_8'	δ6.58 (1H, d, 7′-H, $J_{7',8'}$ = 9.4 Hz)
H_2''	δ7.71 (2H, d, 2″-H, $J_{2'',3''}$ = 9.2 Hz)
H_3''	δ8.31 (2H, d, 3″-H, $J_{3'',2''}$=9.0 Hz)

The ^{1}H NMR spectrum of compound **(122)** showed two distinct singlet peaks at δ1.26 ppm and at δ 2.86 ppm due respectively to the two CH_3 groups and the $N(CH_3)$ group. Two clear signals due to H_2'' and H_3'' were seen at δ7.71 ppm and δ8.31 ppm respectively. The existence of compound **(122)** as the ring-closed azospirooxazine was demonstrated by ^{1}H NMR spectroscopy from the singlet characteristic of the oxazine proton (2′-H) at δ 7.88 ppm. Other identifiable peaks are given in Table 15. Mass spectroscopic analysis showed a molecular ion at m/z 493 which was consistent with the molecular formula $C_{28}H_{23}N_5O_4$. The purification of compound **(122)** proved problematic and different solvents such as dichloromethane and ethanol were used for recrystallization and column chromatography. During purification on a column it was found that the brown compound **(122)** converted to an orange compound. The instability of brown compound **(122)** and conversion to orange compound **(134)** was demonstrated by two dimensional TLC as shown in Figure 44. After first elution, a single brown spot was seen. The TLC was dried and kept for 30 minutes and

then a second elution was run. An orange spot was observed together with some of the original brown material showing the decomposition of compound **(122)**.

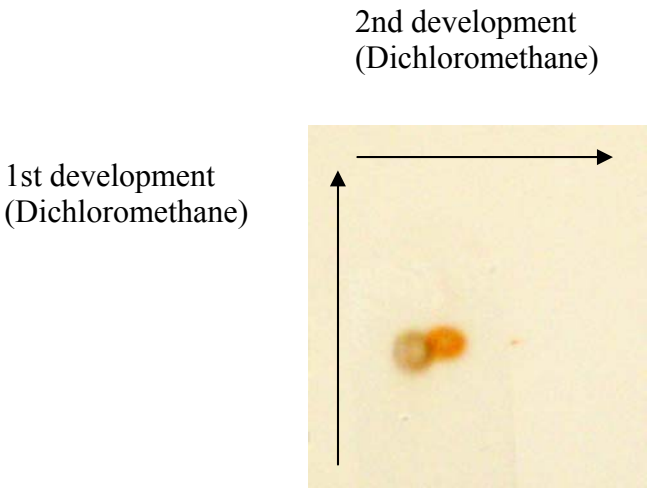

Figure 44: The conversion of brown compound **(122)** to orange compound **(134)** on two dimensional TLC.

(iv) Isolation of Amide (134)

During purification of compound **(122)** (0.27g) in a separate experiment by column chromatography on silica using dichloromethane initially and subsequently DCM / 0.5% acetone, an orange compound was obtained from the eluates (33%) which on analysis proved to be amide **(134)**.

(a) Analytical data

The product decomposed without melting at 287^{o}C. The FTIR spectrum of the compound was obtained as a KBr disc. The main peaks observed were at 3436 cm^{-1} (N-H, st) and 1698 cm^{-1} (C=O st). The ^{1}H NMR spectrum of compound **(134)** in deuterated chloroform was used to confirm the structure and the numbering scheme used to identify the protons is given in Figure 45.

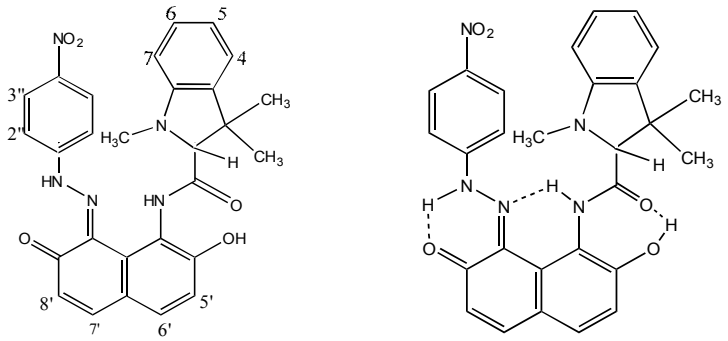

Figure 45: Proton numbering sequence and hydrogen bonding in azoamide **(134)**.

Table 19: ^{1}H NMR spectral data for azoamide **(134)**.

Proton	**NMR signals, Chemical shift (ppm), Coupling constants (Hz)**
$N(CH_3)$	δ 2.51 (s, 3H, NCH_3)
$C(CH_3)_2$	δ1.59 (s, 6H, $(CH_3)_2$)
H_4	δ7.18 (1H, d, 7-H, $J_{7,6}$= 8.3 Hz)
$H_{4'}$	δ3.01 (s, 1H, N-NH)
H_5	δ6.70(1H, m, 6-H)
H_6	δ7.61 (1 H, m, 5-H)
H_7	δ6.61 (1H, 4-H, m)
H_4'	δ 6.56 (d, 1H, $J_{4,3}$= 10.5)
H_5'	δ7.38 (1H,d, 5′-H, $J_{5',6'}$= 7.9 Hz)
H_6'	δ7.65 (1H,d, 6′-H, $J_{6',5'}$= 8.2 Hz)
H_7'	6.50 (1H, d, 7′-H, $J_{7',8'}$= 9.6 Hz)
H_8'	δ7.06 (1H, m, 8′-H)
H_2''	δ7.86 (2H, d, 2″-H, $J_{2'',3''}$ = 9.1 Hz)
H_3''	δ8.43 (2H, d, 3″-H, $J_{3'',2''}$=9.1 Hz)
C-H	δ3.63 (1H, s, C-H)
C-OH	δ9.80 (s, 1H, OH)
N-NH	δ11.65 (br s, 1H, NH)
C-NH	δ12.50 (br s, 1H, NH)

The molecular formula of compound **(134)** is $C_{28}H_{25}N_5O_5$ and showed a molecular ion at m/z 511.

(b) Discussion

It had been noted during the attempts at optimization of the synthesis that compound **(122)** was unstable to TLC on silica and to column chromatography, converting to an orange compound. Compound **(122)** was deliberately exposed to preparative silica column chromatography to obtain the orange product (33%). This compound was demonstrated to be the secondary amide **(134)** on the basis of spectroscopic analysis confirmed by a single crystal X-ray structure determined from crystals grown from ethanol. Compound **(134)** was modelled using CAChe. The MM2 and AM1 calculations were carried out to calculate the energy of the final structure as well as the heat of formation. The energy of the compound after minimization was 10.7 kcal mol^{-1} while the heat of formation was 21.2 kcal mol^{-1}. The X-ray crystal structure and energy minimized structure (MM2 calculation) of compound **(134)** are given in Figure 46.

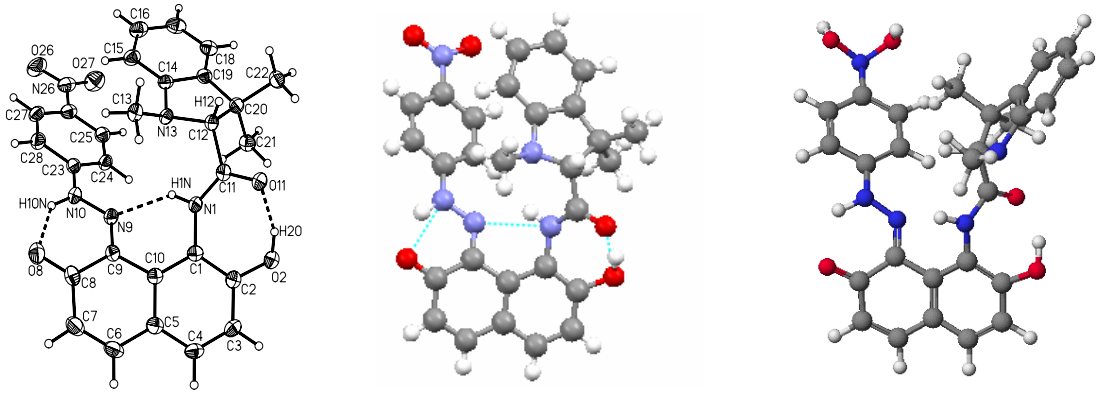

Figure 46: X-ray crystal structure and minimized structure from MM2 calculations of azoamide **(134)**.

The crystal structure (Fig 46) demonstrates that the compound exists in the ketohydrazone form in which there is significant intramolecular hydrogen-bonding in two 6-membered rings (between hydrazone N-H and ketone C=O and between amide N-H and hydrazone

C=N) and in a 7-membered ring (between O-H and amide C=O). Table 20 shows relevant interatomic distances and angles. With regard to intermolecular interactions, there is potential π stacking where the distance between the centroids of the two symmetry equivalent rings C23--C28 related by a centre of inversion is 3.5580(12)Å. The closest intermolecular contacts are three CH..O hydrogen bonds where the C..O distances are in the range 3.206(2) - 3.396(2) Å. X-ray crystal data for compound **(134)** in detail is given in Appendix A.

Table 20: Hydrogen bonds for compound **134** [Å and °].

D-H...A	**d(D-H)**	**d(H...A)**	**d(D...A)**	**<(DHA)**
N(1)-H(1N)...N(9)	0.865(18)	2.025(17)	2.711(2)	135.5(15)
N(1)-H(1N)...N(13)	0.865(18)	2.263(17)	2.734(2)	114.2(14)
N(10)-H(10N)...O(8)	0.93(2)	1.80(2)	2.569(2)	139.1(18)
O(2)-H(2O)...O(11)	0.96(3)	1.63(3)	2.5713(18)	163(2)
C(6)--H(6)..O(26)i	0.95	2.47	3.396(2)	165
C(13)--H(13C)..O(8)ii	0.98	2.49	3.288(2)	139
C(25)--H(25)..O(2)iii	0.95	2.52	3.206(2)	129

Symmetry transformations used to generate equivalent atoms: i: x,-1+y,-1+z; ii: 1-x,2-y,-z; iii: 1-x,2-y,-z.

The molecular structure within the X-ray crystal structure and the structure obtained after molecular mechanics calculations were compared by visual inspection and the geometries are illustrated in a similar way in Figure 46. The analysis showed that these two structures were roughly similar in their geometry, but with differences seen in the relative orientations of two parts of the molecule. The indoline moiety and the diazotized-*p*-nitroaniline unit are closer to each other in the case of the X-ray crystal structure than the modelled structure and the orientation is different. The differences may well be due to constraints due to crystal packing arrangements.

A mechanism for the formation of compound **(134)** is proposed in Scheme 42. The molecular weight of the compound is 511, which is 18 higher than the molecular weight of

the ring closed form **(122)**. This proposition suggests an initial acid-catalysed (by silica) nucleophilic addition of water, presumably from within the silica, followed by ring-opening by cleavage of the weak C_{spiro}-O bond. It has been observed that spirooxazines may be sensitive to aqueous acidic conditions in application [144] and this reaction may provide an insight into the hydrolytic processes involved in the degradation of spirooxazines, the mechanisms of which have not been fully resolved. The ability to isolate a product (**134**) in this case is probably due to the stability provided by the extensive intramolecular hydrogen bonding.

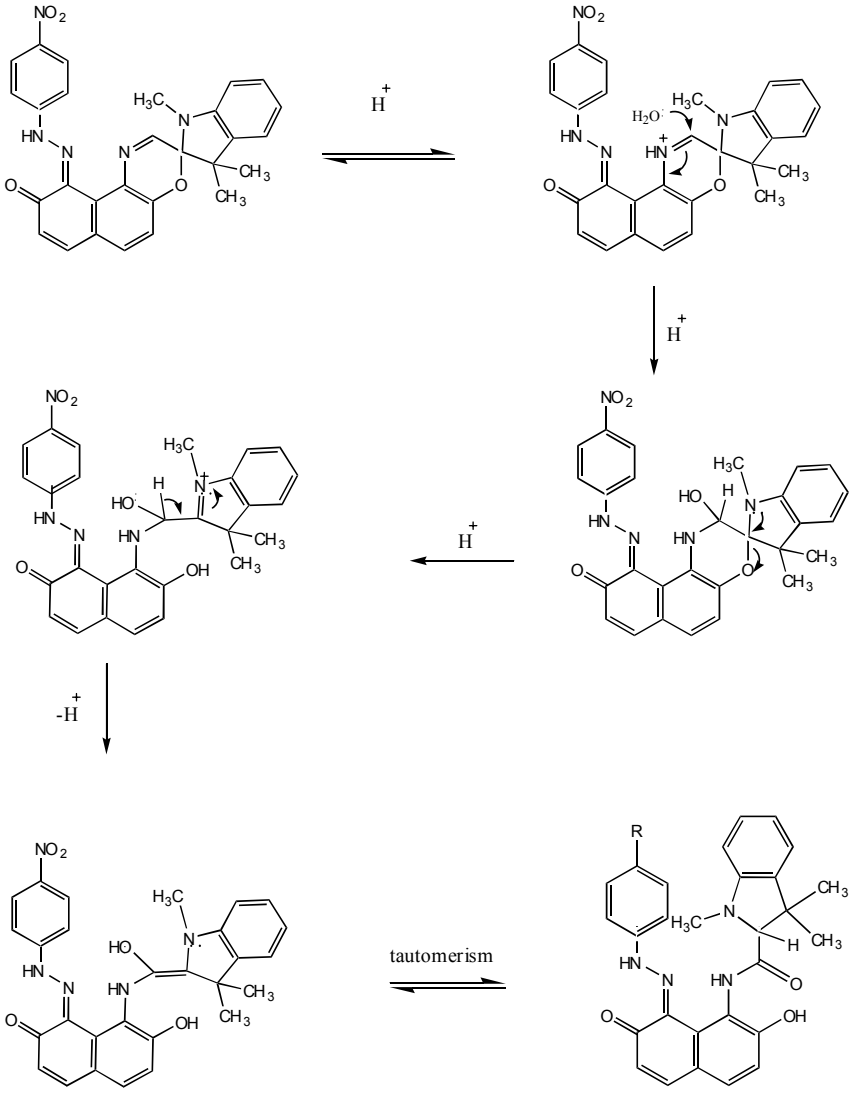

Scheme 42: Proposed mechanism for the synthesis of compound **(134)**.

Route 2

(v) Coupling reaction

The synthesis of 1-nitroso-2,7-dihydroxynaphthalene **(129)** was carried out according to the procedure described in experimental section 5.5.1. Compound **(129)** was coupled with diazotized *p*-nitroaniline **(121)** to give compound **(133)**.

Analytical data

Compound **(133)** obtained was as a highly insoluble brown powder with a yield of 85% and having a melting point of 161^{o}C. FTIR data is given in experimental section 5.5.2. NMR spectral evidence was used to confirm the structure. The ^{1}H NMR spectrum of the compound was recorded in deuterated dimethyl sulfoxide. Figure 47 shows the numbering scheme used to identify the proton signals.

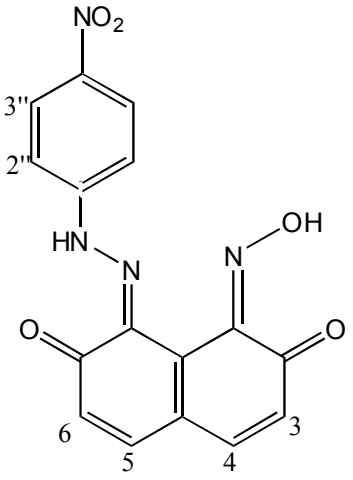

Figure 47: Proton numbering sequence for compound **(133)**.

Table 21: ^{1}H NMR spectral data for nitrosonaphthol **(133)**.

Proton	**NMR signals, Chemical shift (ppm), Coupling constants (Hz)**
H_3	δ6.77 (1H,d, 3-H, $J_{3,4}$=8.3 Hz)
H_4	δ7.32 (1H, d, 4-H, $J_{4,3}$ =8.2 Hz)
H_5	δ7.86 (1H,d, 6-H, $J_{6,5}$= 9.6Hz)
H_6	δ6.24 (1H, d, 5-H, $J_{5,6}$=9.5 Hz)
H_2''	δ7.92 (2H,d, H *o*– to NH, J= 9.0 Hz)
H_3''	δ8.23 (2H,d, H *o*– to NO_2, J= 8.7 Hz)
OH	δ8.71 (1H, br s, OH)

(vi) Fischer's base reaction

The reaction of compound **(133)** with 1,3,3-trimethyl-2-methyleneindoline (Fischer's base) **(70)** gave azospirooxazine **(122)** confirmed by TLC and an identical FTIR spectrum of the product obtained compared with the product obtained by route 1.

Discussion on route 2

The reaction of 1-nitroso-2,7-dihydroxynaphthalene **(129)** with diazotized *p*-nitroaniline was the second step in route 2, to give compound **(133)**, as a brown powder obtained in good yield. The NMR spectrum of compound **(133)** showed two clear signals due to H_2'' and H_3'' at δ7.92 ppm and δ8.23 ppm respectively. A broad singlet due to the hydroxy group was observed at δ8.71 ppm. A reflux reaction of nitrosoazo compound **(133)** in ethanol with 1,3,3-trimethyl-2-methyleneindoline (Fischer's base) **(70)** gave azospirooxazine **(122)**. The yield of the product obtained was 12%.

Route 3

(vii) Coupling reaction

2,7-dihydroxynaphthalene **(128)** was coupled with diazotized *p*-nitroaniline solution and details of the experimental procedure are given in section 5.5.3 (a). Azonaphthol **(132)** was obtained as an insoluble red powder (75% yield).

(a) Analytical data

The melting point of the compound recorded using DSC was 302^{o}C. The FTIR spectrum of the compound showed peaks at 3404 cm^{-1} for N-H, st and 1653 cm^{-1} for C=O. The NMR spectral evidence was used to confirm the structure. The ^{1}H NMR spectrum of the compound was carried out in deuterated dimethylsulfoxide. Figure 48 shows the numbering scheme used to identify the proton signals.

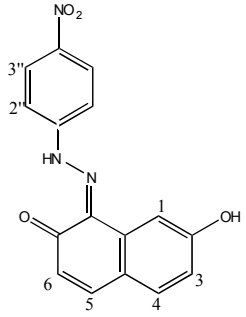

Figure 48: Proton numbering sequence for compound **(132)**.

Table 22: ^{1}H NMR spectral data for azonaphthol **(132)**.

Proton	**NMR signals, Chemical shift (ppm), Coupling constants (Hz)**
H_1 H_6	7.70 – 7.80 (2H, m, 1-H and 6-H, overlapping signals)
H_3	δ6.88 (1H, d, 3-H, $J_{3,4}$= 8.2 Hz)
H_4	δ7.50 (1H, d, 4-H, $J_{4,3}$ = 8.3 Hz),
H_5	δ6.40 (1H,d, 5-H, $J_{5,6}$=9.6 Hz)
H_2''	δ7.86 (2H,d, H *o*– to NH J= 9.2 Hz),
H_3''	δ8.31 (2H,d, H *o*– to NO_2, J= 9.1 Hz)

The molecular formula of compound **(132)** is $C_{16}H_{11}N_3O_4$ and the mass spectrum showed a molecular ion at m/z 309.

(b) Discussion

The coupling reaction of 2,7-dihydroxynaphthalene **(128)** with diazotized *p*-nitroaniline solution gave a red azo compound **(132)** with a good yield (75%). Attempted nitrosation of compound **(132)** using a range of standard procedures led only to recovery of starting material. The synthesis of azospirooxazine **(122)** was successful by both routes 1 and 2. Purification of compound **(122)** was difficult because of its unstable nature, during recrystallization as well as on column chromatography. A reasonably pure product was obtained by optimization of the synthetic procedure and a carefully conducted recrystallization process. Route 1 proved to be the best giving a yield of 55% at the final stage. A much lower yield was obtained by route 2 (12%) with more difficulties at the purification stage. Route 3 failed at the nitrosation stage, probably because of the extreme insolubility of azo compound **(132)** in the acidic media.

The reaction scheme used for the synthesis of compounds **(137)** and **(141)** is given in Scheme 43. The sequence of reactions in Route 1 for compound **(122)** was used as this proved to be the best in that case.

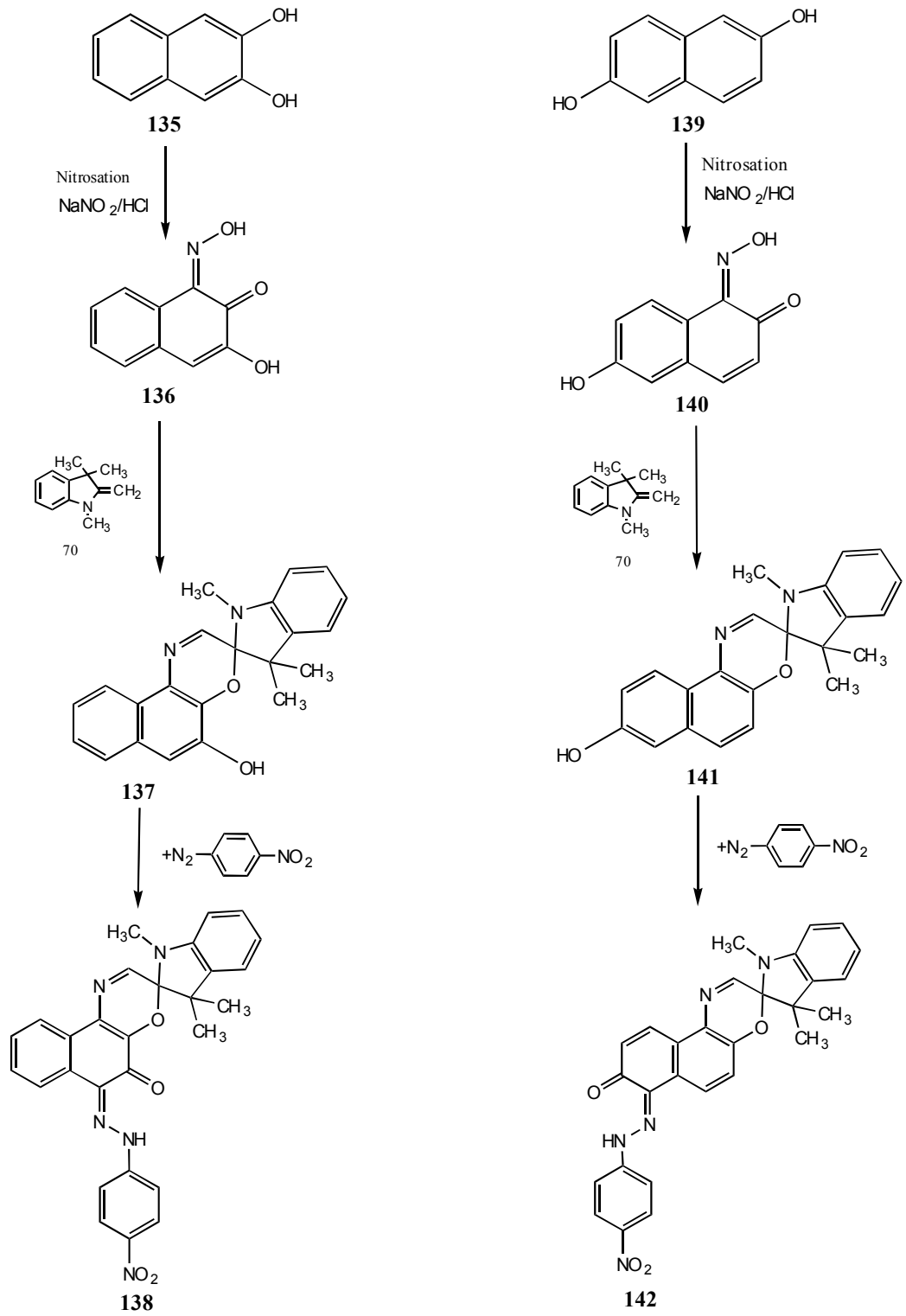

Scheme 43: Synthesis of compounds **(138)** and **(142)**.

(viii) Nitrosation of 2,3-dihydroxynaphthalene (135)

The procedure for synthesis of 2,3-dihydroxy-1-nitrosonaphthalene **(136)** was the same as that used for 1-nitroso-2,7-dihydroxynaphthalene and is described in the experimental section 5.5.1 (a).

Analytical data

Compound **(136)** decomposed without melting at 192^{o} C. The FTIR spectrum of the compound showed a peak at 3348 cm^{-1} for O-H and at 1632 cm^{-1} for C=O. NMR spectral evidence was used to confirm the structure. The ^{1}H NMR spectrum of the compound was carried out in deuterated dimethylsulfoxide. The existence of compound **(135)** in the oxime form as a mixture of geometric isomers (3:1) was suggested by the spectroscopic evidence. The numbering scheme used to identify the proton signals is given in Figure 49.

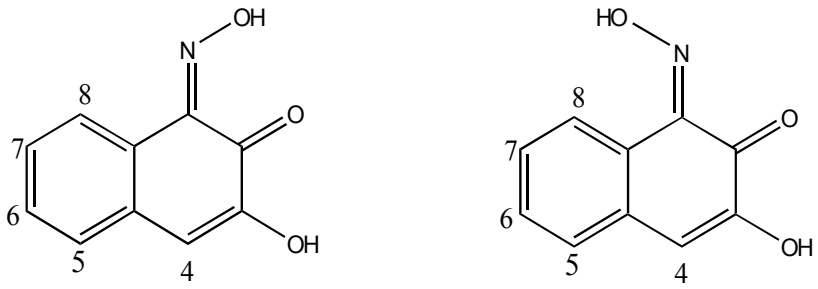

(136a) **(136b)**

Figure 49: Proton numbering scheme in isomer 1 **(136a)** and isomer 2 **(136b)**.

Table 23: ^{1}H NMR spectral data for spirooxazine **(136)**.

Proton	**NMR signals, Chemical shift (ppm), Coupling constants (Hz)**
H_4 (Isomer 1)	δ6.80 (s, 1H, 4-H, major isomer)
H_5, H_6, H_7, H_8	δ7.10 -7.70 (4H, m, 5,6,7,8-H overlapping signals, major and minor isomers)
OH	δ9.75 (1H, br s, OH)
H_4(Isomer 2)	δ 7.08 (s, 1H)
H_5	δ7.40 (m, 1H)
H_6	δ7.23 (m, 1H)

(ix) Fischer's base reaction

2,3-Dihydroxy-1-nitrosonaphthalene **(136)** was reacted with Fischer's base **(70)** to give the spirooxazine **(137)** as a grey solid. The details of synthesis are given in experimental section 5.5.4 (b). The synthesis of spirooxazine **(137)** and some analytical data are given in the literature [66] and are similar to the data given below. A brief ^{1}H NMR analysis is provided in the literature.

Analytical data

The spirooxazine **(137)** showed a melting point of 154^{o} C. The FTIR spectrum of the compound showed peaks at 3368 cm^{-1} for O-H. The ^{1}H NMR spectrum of compound **(137)** in deuterated chloroform was used to confirm the structure and the numbering scheme used to identify the proton signals as given in Figure 50.

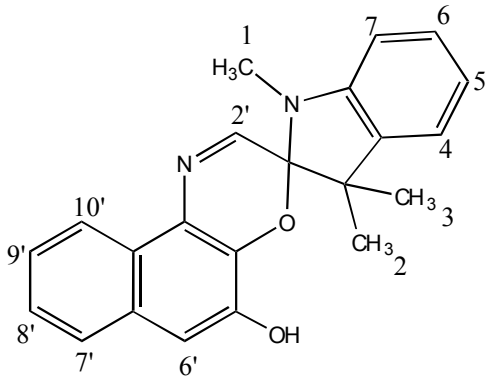

Figure 50: Proton numbering scheme in compound **(137)**.

Table 24: ^{1}H NMR spectral data for spiroindolinonaphthoxazine **(137)**.

Proton	**NMR signals, Chemical shift (ppm), Coupling constants (Hz)**
$N(CH_3)$	δ 2.79 (3H, s, NCH_3)
$C(CH_3)$	δ1.34 (3H, s, C-CH_3)
$C(CH_3)$	δ1.37 (3H, s, C-CH_3)
H_4	δ6.60 (1H, d, 4-H, $J_{4,5}$= 7.5 Hz)
H_5	δ6.92 (1H, t, 5-H, J= 7.5 Hz)
H_6 $H_{8'}$ $H_{9'}$	δ7.38 (3H, m, 6, 8′, 9′-H overlapping peaks)
H_7	δ7.24 (1H, m, 7-H)
$H_{2'}$	δ 7.78 (IH, s, 2′-H)
$H_{6'}$	δ7.09 (1H, s, 6′-H, $H_{6',7'}$=7.05)
$H_{7'}$	δ7.64 (1H, d, 7′H, $J_{7',6'}$=7.08 Hz)
$H_{10'}$	δ8.45 (1H, dd, $J_{10',9}$= 8.30 Hz)

(x) Coupling reaction

Diazotization of *p*-nitroaniline and coupling with spirooxazine **(137)** was carried out as the final step for the synthesis of compound **(138)** by the route shown in Scheme 43. Azospirooxazine **(138)** was obtained as brown crystals after recrystallizations from ethanol (x 2).

(a) Analytical data

The compound **(138)** decomposed without melting at 196^{o}C. The FTIR spectrum of the compound is given in experimental section 5.5.4 (c). The ^{1}H NMR spectrum of compound **(138)** in deuterated chloroform was used to confirm the structure and the numbering scheme used to identify the proton signals is given in Figure 51.

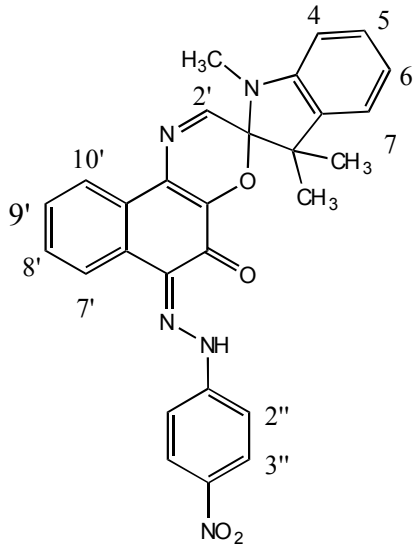

Figure 51: Proton numbering scheme in compound **(138)**.

Table 25: ^{1}H NMR Spectral data for azospiroindolinonaphthoxazine **(138)**.

Proton	**NMR signals, Chemical shift (ppm), Coupling constants (Hz)**
$N(CH_3)$	δ 2.79 (3H, s, NCH_3)
$C(CH_3)$	δ1.30 (3H, s, C-CH_3)
$C(CH_3)$	δ1.42 (3H, s, C-CH_3)
H_4	δ6.52 (1H, d, 4-H, $J_{4,5}$= 7.7 Hz)
H_5	δ6.89 (1H, m, 5-H)
H_6	δ7.20 (1H, m, 6-H)
H_7	δ7.06 (1H, dd, 7-H, $J_{7,6}$=7.79)
H_2'	δ7.97 (s, 1H, 2′-H)
H_7' H_8' H_9' H_{10}'	δ 7.45-7.55 (4H, m, 7′-H, 8′-H, 9′-H, 10′-H)
H_2''	δ7.60 (2H, d, H *o*– to NH , $J_{2'',3''}$=9.16 Hz)
H_3''	δ8.30 (2H, d, H *o*– to NO_2, $J_{3'',2''}$=9.0 Hz)
NH	δ15.8 (1H, br s, NH)

The ^{1}H NMR spectrum of compound **(138)** showed two distinct singlet peaks at δ1.30 and at δ 2.79 because of the two CH_3 groups and the $N(CH_3)$ group. Signals due to H_2'' and H_3'' were seen at δ7.60 and δ8.30 respectively. A clear singlet characteristic of the oxazine proton (2′-H) at δ7.97 ppm was seen. Other identifiable peaks are given in Table 25. Mass spectroscopic analysis gave a molecular ion which was consistent with the theoretical molar mass of 493.

(b) Discussion

Spirooxazine **(137)** was obtained by the reaction of 2,3-dihydroxy-1-nitrosonaphthalene **(136)** with Fischer's base **(70)** in ethanol. TLC (DCM: Acetone 0.5%) of the refluxed mixture showed five components which were yellow, grey, dark blue, green and brown. The spirooxazine **(137)** was obtained by column chromatography (silica, dichloromethane/petroleum ether) (1:1, v/v) and was photochromic in nature as seen from

TLC behaviour. Azospirooxazine **(138)** was obtained by coupling of spirooxazine with diazotized *p*-nitroaniline. A reasonably pure product **(138)** was obtained after recrystallization from ethanol with a yield of 6%.

(xi) Synthesis of compound (142)

The route for the synthesis of compound **(142)** is given in Scheme 43.

(xii) Nitrosation of 2,6-dihydroxynaphthalene (139)

The synthesis of 1-nitroso-2,6-dihydroxynaphthalene **(139)** was carried out using the method as described in experimental section 5.5.1 (a). A brown product **(140)** (97%) was obtained.

Analytical data

The compound **(140)** decomposed without melting at 215^{o} C. The FTIR spectrum of the compound is given in experimental section 5.5.5 (a). NMR spectral evidence was used to confirm the structure. The ^{1}H NMR spectrum of the compound was recorded in deuterated dimethylsulfoxide solution. The numbering scheme used to identify the proton signals is given in Figure 52.

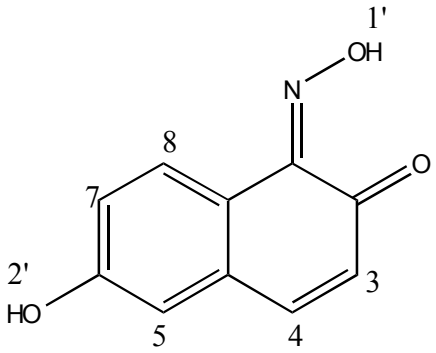

Figure 52: Proton numbering scheme in compound **(140)**.

Table 26: ^{1}H NMR spectral data for spirooxazine **(140)**.

Proton	**NMR signals, Chemical shift (ppm), Coupling constants (Hz)**
H_3	δ6.33 (d, 1H, $J_{4,3}$= 8.2)
H_4	δ 7.60 (d, 1H, $J_{3,4}$= 8.7)
H_5	δ 6.89 (d, 1H, $J_{5,7}$= 9.5)
H_7	δ7.07 (m, 1H)
H_8	δ8.82 (m, 1H)
OH	8.8 (2H, br s)

(xiii) Fischer's base reaction

The spirooxazine **(141)** was obtained by the reaction of compound **(140)** with Fischer's base **(70)**. The method of synthesis is described in experimental section 5.5.5 (b). The light brown powder obtained was identified as spirooxazine **(141)**.

(a) Analytical data

Only melting point and CHN analysis of spirooxazine **(141)** is available in the literature.[98] The FTIR spectrum of the compound showed peaks at 3462 cm^{-1} for O-H. The ^{1}H NMR spectrum of compound **(141)** in deuterated chloroform was used to confirm the structure and the numbering scheme used to identify the proton signals is given in Figure 53. The position of the proton signals and chemical shifts are given in Table 27.

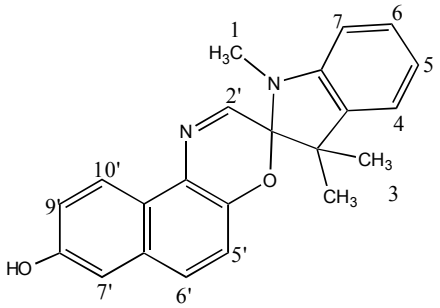

Figure 53: Proton numbering scheme in compound **(141)**.

Table 27: ^{1}H NMR spectral data for spirooxazine **(141)**.

Proton	**NMR signals, Chemical shift (ppm), Coupling constants (Hz)**
$N(CH_3)$	δ 2.65 (3H, s, NCH_3)
$C(CH_3)_2$	δ1.36 (6H, s, $(CH_3)_2$)
H_4	δ6.57 (1H, dd, 4-H, $J_{4,5}$= 7.1 Hz)
H_5	δ6.90 (1H, m, 5-H)
H_6 H_7 $H_5'H_7'$ H_9'	δ7.04-7.16 (5H, 6-H, 7-H, 5′-H, 7′-H, 9′-H, m, overlapping signals)
H_2'	δ 7.75 (IH, s, 2′-H)
H_6'	δ7.52 (1H, d, 6′-H, $J_{6',5'}$=8.7 Hz)
H_{10}'	δ8.41 (1H, d, $J_{10',9'}$= 8.3 Hz)

The molecular formula of compound **(141)** is $C_{22}H_{20}N_2O_2$ with a molecular weight of 344 and was consistent with the molecular ion from the mass spectrum**.**

(xiv) Coupling reaction

The synthesis of azospirooxazine **(142)** was attempted by the coupling reaction of spirooxazine **(141)** with diazotized *p*-nitroaniline. The details of synthesis are given in experimental section 5.5.5 (c). A low yield of a crude brown product was obtained. Attempts to purify by column chromatography and recrystallization showed that the compound is highly unstable, with a tendency to generate new impurities during the purification process. The crude compound was thus investigated spectroscopically.

(a) Analytical data

The FTIR spectrum of the compound is given in experimental section 5.5.5 (c). The ^{1}H NMR spectrum of compound **(142)** in deuterated chloroform was used to confirm the structure and the numbering scheme used to identify the proton signals is given in Figure 54.

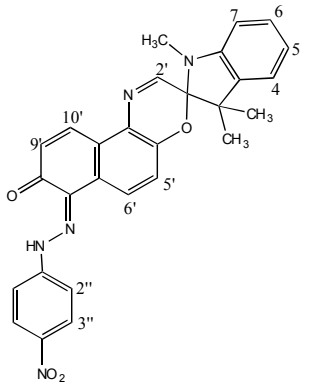

Figure 54: Protons numbering sequence for compound **(142)**.

The assignment of each proton is shown in Table 28. Because of signals due to the presence of impurities in the sample, some of the assignments are tentative.

Table 28: ^{1}H NMR spectral data for compound **(142)**.

Proton	**NMR signals, Chemical shift (ppm), Coupling constants (Hz)**
$N(CH_3)$	δ 2.70 (s, 3H, NCH_3)
$C(CH_3)_2$	δ1.30 (s, 6H, $(CH_3)_2$)
H_2'	δ7.80 (s, 1H)
H_4	δ6.40 (dd, 1H $J_{4,5}$=7.7)
H_5	δ7.15 (t, 1 H, $J_{5,4}$=7.6)
H_6	δ 6.50 (t, 1H, $J_{6,7}$=6.5)
H_7	δ7.35 (d,1H, $J_{7,6}$= 6.5)
H_5'	δ7.12 (m, 1H)
H_6'	δ7.55 (m, 1H)
H_9'	δ7.05 (m, 1H)
H_{10}'	δ8.55 (m, 1H)
H_2''	δ7.75 (m, 2H)
H_3''	δ8.20 (m, 2H)

(b) Discussion

Crude spirooxazine **(141)** was obtained by the reaction of 1-nitroso-2,6-dihydroxynaphthalene **(139)** with Fischer's base **(70)**. Recrystallization from heptane gave 17% of pure photochromic product. The yield of crude product **(142)** obtained was 35%. An attempt was made to recrystallize the product but this was unsuccessful. Column chromatography on silica gel using dichloromethane as the eluent was carried out to give a product (12%) which still contained some impurities. Another attempt was made to recrystallize the compound but because of the highly unstable nature of the compound it was not possible to obtain a completely pure product. The NMR spectrum of the crude compound gave a few characteristic signals identifiable after the analysis of the spectrum. ^{1}H NMR spectrum of compound **(142)** showed two distinct singlet peaks at δ1.30 ppm and at δ 2.70 ppm because of the two CH_3 groups and the $N(CH_3)$ group. Signals due to H_2'' and H_3'' were seen at δ7.67 ppm and δ8.20 ppm respectively. A clear singlet characteristic of the oxazine proton (2′-H) at δ 7.80 ppm was seen. The mass spectrum of the compound did not give meaningful values presumably because of impurities. Further synthesis was abandoned after a few subsequent attempts.

(xv) Photochromism in spirooxazine (122)

Spirooxazines owe their photochromic properties to a light-induced ring-opening to form a photomerocyanine, which reverts thermally to the ring-closed form when the light source is removed. Photochromism of compound **(122)** was studied under different experimental conditions i.e. by change in solvent, light source, temperature as well as concentration. It was seen experimentally that compound **(122)** shows very interesting photochromic properties, converting in ethanolic solution under appropriate UV irradiation conditions from an initial orange to a neutral grey colour, a process which reverses when the light source is removed. This photochromic colour change is unusual. For example, in dilute solution the visual effect as a result of light exposure is from coloured to (virtually) colourless, essentially reversing the normal situation with photochromic spirooxazines.

(a) Irradiation with suitable wavelength using fluorimeter

A solution of the azospirooxazine **(122)**, (0.999mg) in dichloromethane ($100cm^3$) was prepared and was subjected to continuous UV-irradiation with different wavelengths from 352 nm-580 nm using a fluorimeter at room temperature. This technique had been found to induce photochromism in some systems in our laboratory. The λ_{max} values of the compound as measured by the UV-visible spectrum were 481 nm and 352 nm. There was no change in colour in spectral properties after continuous irradiation of the sample for 5, 10, 15, 20 and 30 minutes at any of the wavelengths investigated.

(b) Study of photochromism at low temperature [60]

(i)An azospirooxazine **(122)** ($3.47x10^{-6}$ mol) solution in ethanol was prepared and was cooled using a dry ice-dichloromethane bath in a beaker to -75^oC. The solution was irradiated by a camera flash. No change in colour was observed at this temperature.

(ii) A similar experiment was repeated at -20^oC. No change in colour was observed.

(c) Irradiation using a UV-lamp of mean wavelength 365nm

The solution of azospirooxazine **(122)** (0.999mg) in ethanol ($100cm^3$) was prepared and irradiated continuously for a period of 2 hours at 365 nm (40 watt) to ensure that a steady state was achieved which may be due to the full conversion of one coloured form into the other. The orange solution started to turn grey after 5 minutes and the formation of the grey colour progressed with prolonged irradiation. After 2 hours 20 minutes the samples were kept in the dark, spectra were obtained at intervals before irradiation, during irradiation and after keeping them in the dark. The photochromic effect was observed from orange to grey was demonstrated to be reversible thermally. The photographs of the samples at different stages of the process were recorded and are shown in Figure 55.

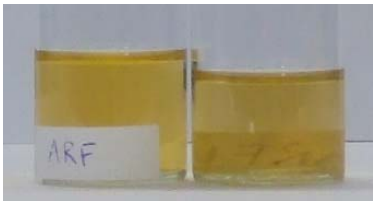

Before irradiation

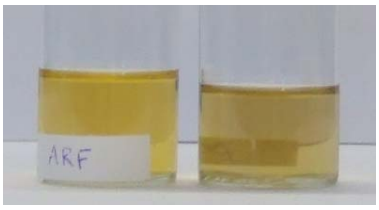

After 5 min

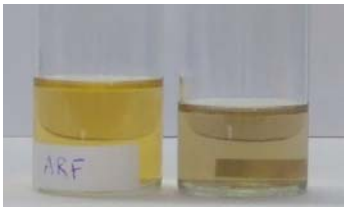

After 10 min

After 20 min

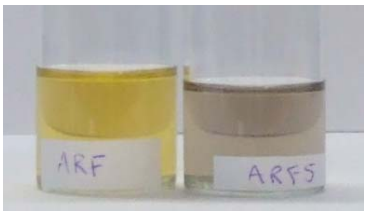

After 30 min

After 40 min

After 55 min

After 65 min

After 120 min

After 140 min

Figure 55: The change in the colour of solution of compound **(122)** before and after UV-irradiation.

The sample irradiated with the maximum length of time (140 minutes) with UV-irradiation (365 nm) was selected to show the reverse change in colour after the removal of the light source. A very slow change from grey to orange was observed. A photographic record showing the stages of the colour change is given in Figure 56.

Before irradiation | After 140 min irradiation | After 17 hrs in dark

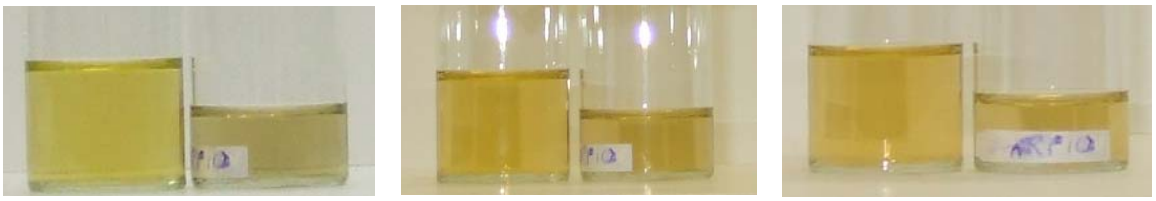

After 41 hrs in dark | After 73 hrs in dark | After 113 hrs in dark

Figure 56: Samples after the removal of light source showing the reverse reaction.

A comparison of the spectrum of the sample before and after UV-irradiation for 140 minutes is given in Figure 57.

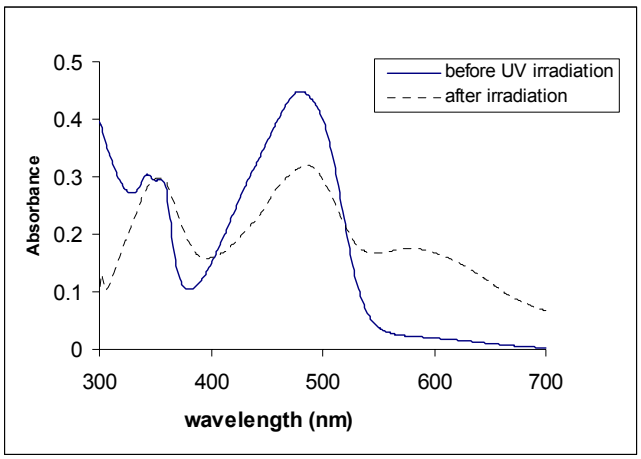

Figure 57: UV/visible spectrum of compound **(122)** before and after UV irradiation.

The change in the spectrum of compound **(122)** during this UV-irradiation is given in Figure 58 (a) and after keeping them in the dark for 17-113 hours is shown in Figure 58 (b). The graph in Figure 58 (a) shows the progressive change of spectra and two isosbestic points indicating equilibrium between the two species.

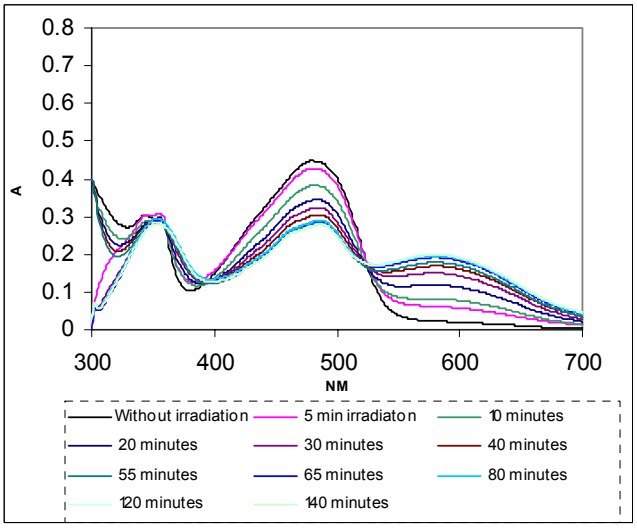

(a)

The reverse reaction appears to show reversion to the original species but probably with some degradation so that the peaks do not return to their original intensity.

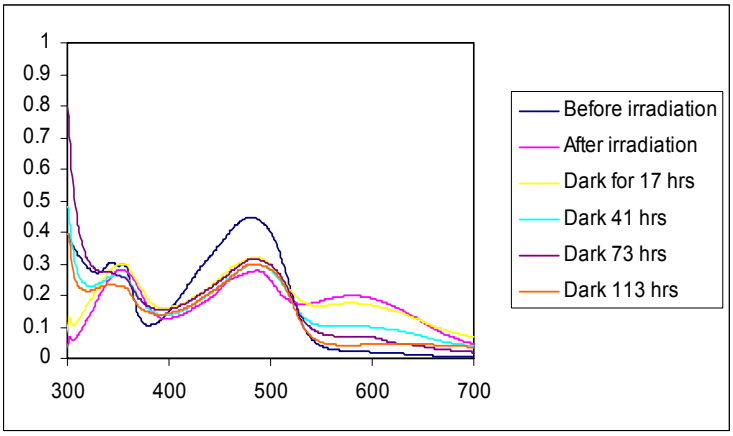

(b)

Figure 58: Graphs to show a change of colour in ethanolic solution of compound **(122)**.

The λ_{max} value for the merocyanine form **(122a)** was obtained experimentally and the experimental details for the calculation of λ_{max} value and the photochromic property of compound **(122)** are given in synthesis section 3.1.3 (xv, c). The experimental λ_{max} value for the merocyanine form was 580, 486 and 353 nm. The spectral properties of compound **(122)** were correlated to the spectrum obtained after running the PPP-MO calculations see section (3.1.2, b). The calculations predicted that the compound may be expected to give λ_{max} values of 646 nm (0.5), 628 nm (0.35) and 352 nm (0.51). The comparison of the experimental and calculated λ_{max} values showed that these values are in reasonable agreement to the calculated values. This difference can be explained on the basis of planarity. The PPP-MO calculations assume the molecule to be planar but after molecular modelling, the structures obtained were not planar.

ZINDO calculations were also run for ring-closed and the most stable merocyanine form of azospirooxazine **(122)**. The calculated λ_{max} values for ring closed form **(122)** were 400 nm, 280 nm and 250 nm which are significantly hypsochromic of the experimental values. In contrast, the most stable merocyanine form **(122a)** gave calculated λ_{max} values of 550 nm, 390 nm and 340 nm. The calculated λ_{max} values for the merocyanine form are in good

agreement to the experimental values. In view of this, future work on correlation with ZINDO calculations for non-planar merocyanines might prove useful.

(xvi) Photochromism in spirooxazine (138)

The investigation after UV irradiation of solutions of azospirooxazine **(138)** was carried out in the same ways as for compound **(122)** but it did not demonstrate photochromic properties. Photochromism can be dependent on a range factors, including the nature of the solvent, the temperature and the irradiation conditions and it is conceivable that the thermal reversion occurs too rapidly to allow observation of photochromism under the conditions we have used.

3.2 Anthraquinone and naphthoquinone-based spirooxazines

In this section, quinone groups was considered as the permanent chromophore.

3.2.1 Molecular Modelling

(a) Molecular Modelling of anthraquinone-based spirooxazine

Ring closed and, merocyanine forms of an anthraquinone-based spirooxazine were modelled using the computer aided CAChe system. As before the molecules were energy minimized using MM2 calculations from these, the final energies were used to compare the relative stabilities of the merocyanine forms. The heats of formation values, obtained by AM1 calculations for the ring closed form as well as the photomerocyanine forms of the anthraquinone-based spirooxazine were used to predict potential photochromic behaviour. The structures of ring closed **(143)** and merocyanine forms **(143, a-d)** are given in Figure 59.

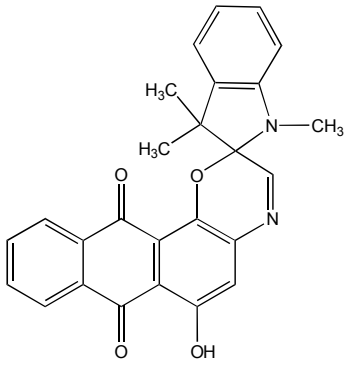

143

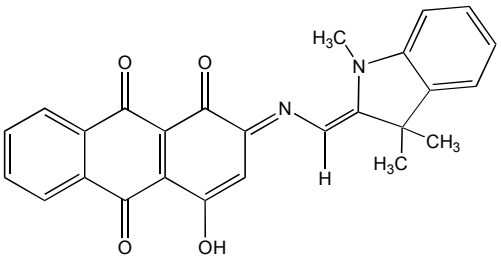

143a

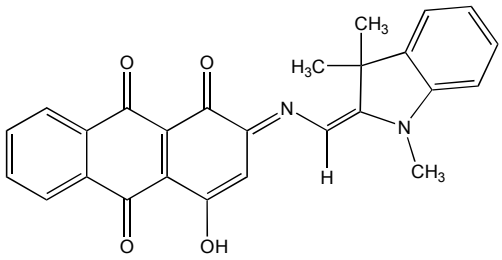

143b

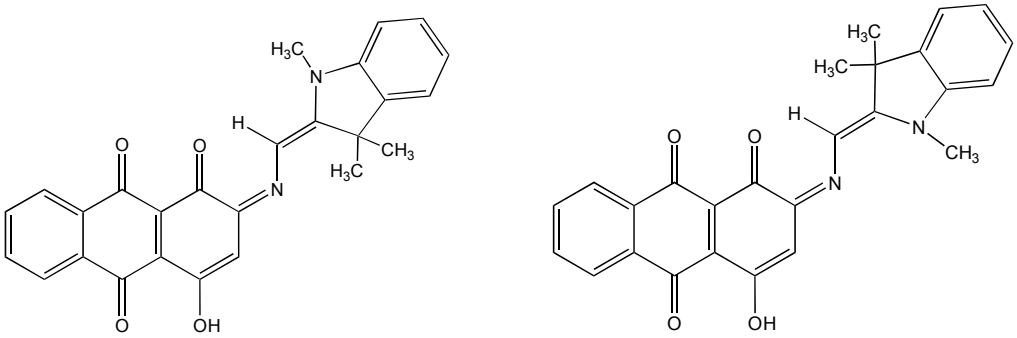

143c **143d**

Figure 59: Ring closed and merocyanine forms of compound **(143)**.

The modelled and energy minimized structures of ring closed **(143)** and merocyanine forms of anthraquinone-based spirooxazine **(143, a-d)** are given in Figure 60.

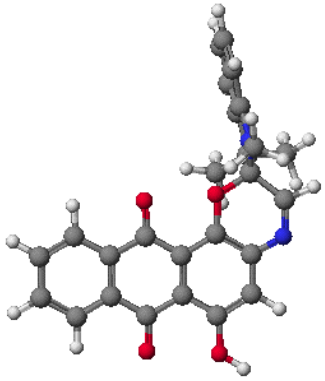

(143)

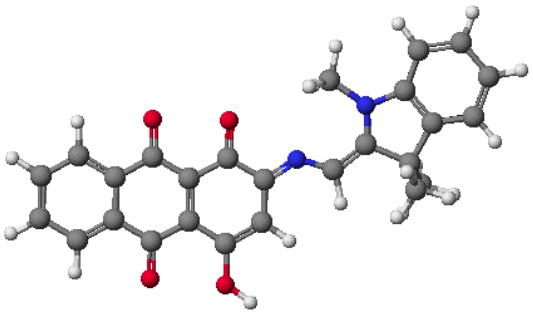

(143a)

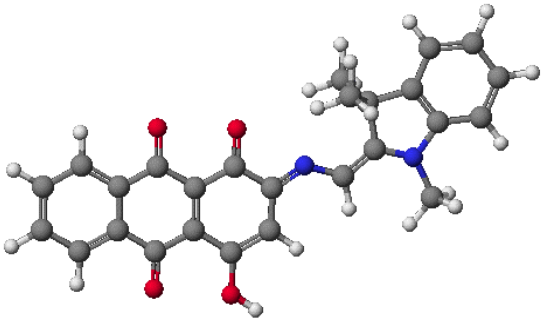

(143b)

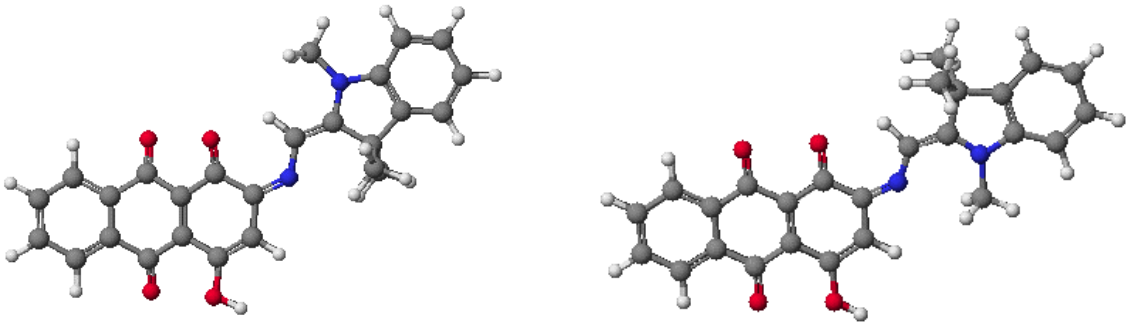

(143c) **(143d)**

Figure 60: The modelled and energy optimized (MM2) geometric structures of compound **143** and its merocyanine forms.

There are other tautomeric possibilities which were not considered at this stage. The final energy and the values of the heats of formation of ring-closed and merocyanine forms of spiroindolinonaphthoxazine **(143)** are given in Table 29.

Table 29: Final energy and heats of formation values of ring-closed and merocyanine forms of anthraquinone based spirooxazine **(143)**.

Compound	**Final Energy (kcal mol^{-1})**	**Heat of formation (kcal mol^{-1})**
(143)- Closed form	-5.32	-0.25
143a	-3.15	14.50
143b	-4.35	17.62
143c	-2.65	15.92
143d	-1.50	13.23

After comparison of final energies, it is suggested that the most stable merocyanine form is **(143b)**. The order of stability of merocyanine forms of compound **(143)** is **143b**>**143a**>**143c**>**143d**. The stability of **(143b)** over other isomers can be correlated to the optimized geometric structures. The hydrogen atom at the azomethine bridge attached

to carbon is in close proximity to the N-methyl group and two C-methyl groups in **(143c)** and **(143d)** respectively which is responsible for higher energy. The strain in these two forms can be clearly seen from the side view of the merocyanine forms (**143c** and **143d**) given in Figure 61 which show non-planarity. In the minimised structures of forms **(143a)** and **(143b)**, the azomethine bridge adopts a different configuration. In **(143b)**, there is reduced steric clash from adjacent NCH_3 with the CH. Both forms are essentially planar.

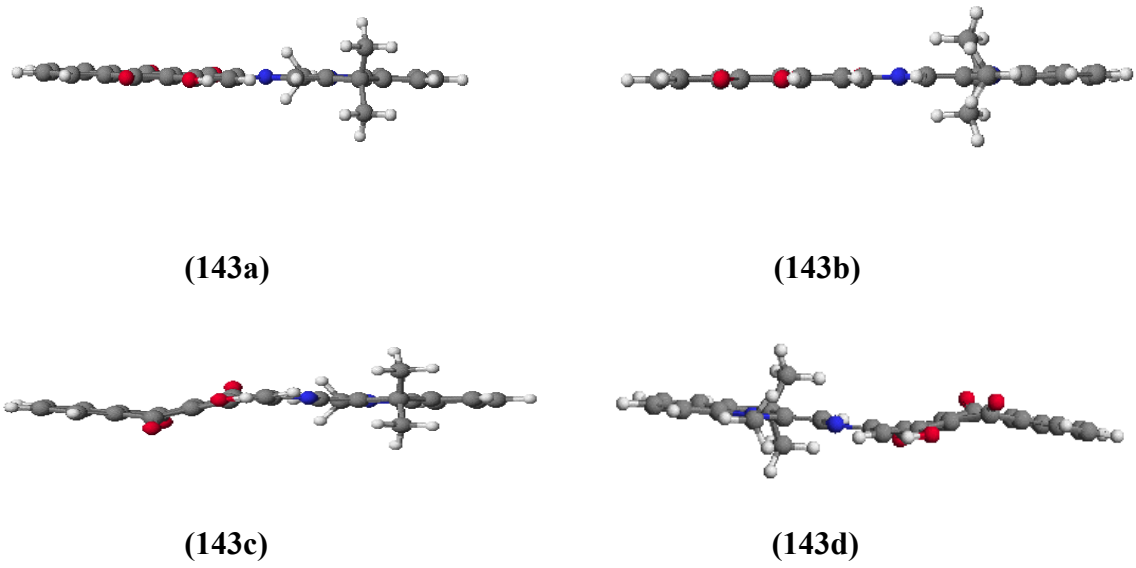

(143a) **(143b)**

(143c) **(143d)**

Figure 61: Side view of the merocyanine forms of anthraquinone based spirooxazine showing strain in geometry of structures (**143c** and **143d**).

The energy minimised structures show that in this case MM2 calculations do not predict the intramolecular hydrogen bonding which would be expected (Figure 60). The heats of formation values suggest isolation of ring closed form **(143)** and the potential for photochromism.

(b) Molecular Modelling of naphthoquinone-based spirooxazine

Final energy and the values of heats of formation of naphthoquinone- based spirooxazine **(144)** were also calculated in terms of the relative stabilities and prediction of potential photochromic behaviour respectively. The structures of ring-closed and merocyanine forms of spirooxazine based on a naphthoquinone are given in Figure 62.

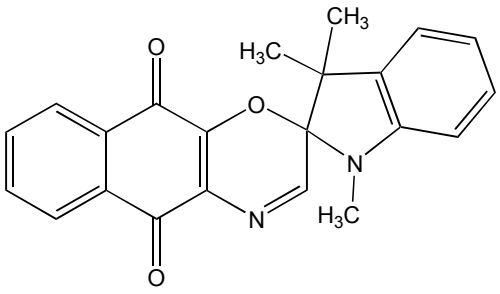

(144)

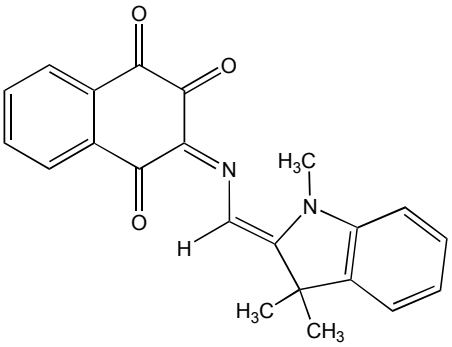

(144a)

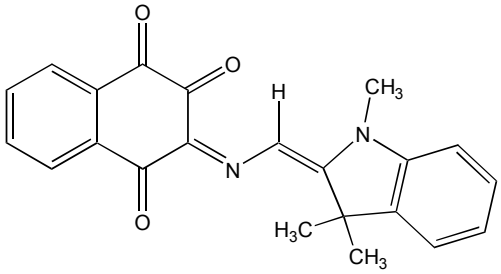

(144b)

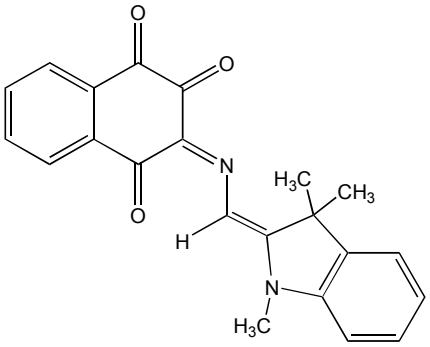

(144c)

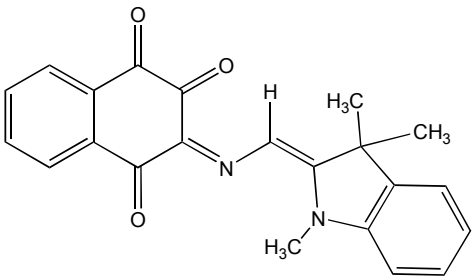

(144d)

Figure 62: Ring-closed and merocyanine forms of compound **(144)**.

The modelled and minimized structures of ring closed **(144)** and merocyanine forms of naphthoquinone-based spirooxazines **(144, a-d)** are given in Figure 63.

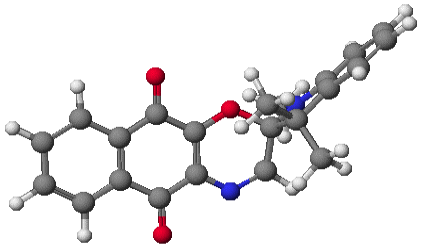

(144)

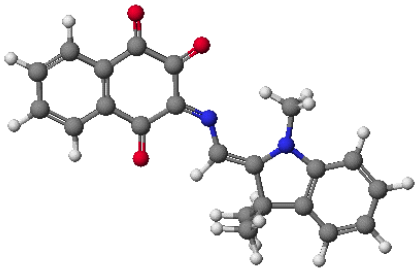

(144a)

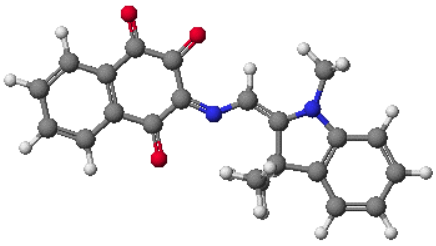

(144b)

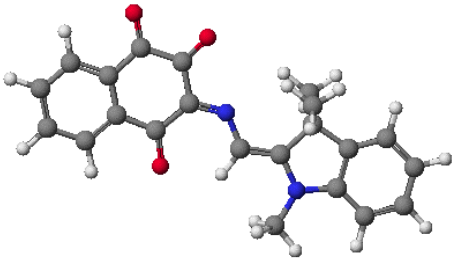

(144c)

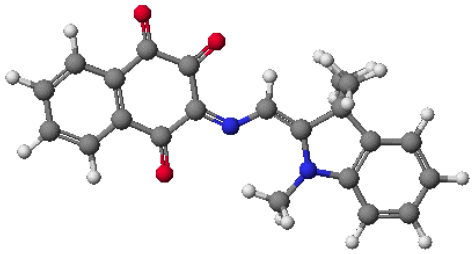

(144d)

Figure 63: The optimized (MM2) geometric structures of compound **(144)** and its four possible *transoid* merocyanine forms

The final energy and values of heats of formation of ring-closed and merocyanine forms of spiroindolinonaphthoxazine **(144)** are given in Table 30.

Table 30: Final energy and heats of formation values of ring-closed and merocyanine forms of naphthoquinone-based spirooxazine **(144)**.

Compound	**Final Energy (kcal mol^{-1})**	**Heat of formation (kcal mol^{-1})**
(144)- Closed form	-0.02	**27.58**
144a	4.58	24.90
144b	1.87	27.55
144c	**1.19**	27.02
144d	4.46	24.96

The molecular modelling results for final energy (MM2 calculations) predict that the most stable form is merocyanine **(144c)**. A comparison of heats of formation of the ring-closed and merocyanine forms showed that the compound might not show photochromism because the heats of formation value of ring closed form **(144)** are higher than the merocyanine forms **(144a-d)**. However, the values for ring-closed and *transoid* merocyanine forms are close and it might not be possible to give a reliable prediction in this case. Based on the heats of formation values there is a possibility of isolating a merocyanine form **(144c)**.

3.2.2 PPP-MO Calculations

In order to study the spectral properties of anthraquinone and naphthoquinone-based spirooxazines, PPP-MO calculations were carried out for ring closed and merocyanine forms of spirooxazines **(143** and **144)**.

(a) PPP-MO Calculations for anthraquinone-based spirooxazine

PPP-MO calculations for ring-closed and merocyanine forms of anthraquinone-based spirooxazine were carried out. The ring-closed and merocyanine forms with their modified structural approximation for PPP-MO calculations are given in Figure 64.

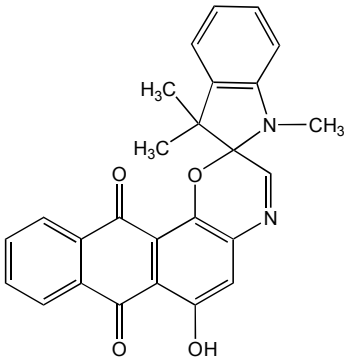

(143)

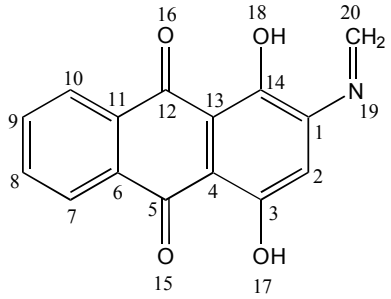

(143e)

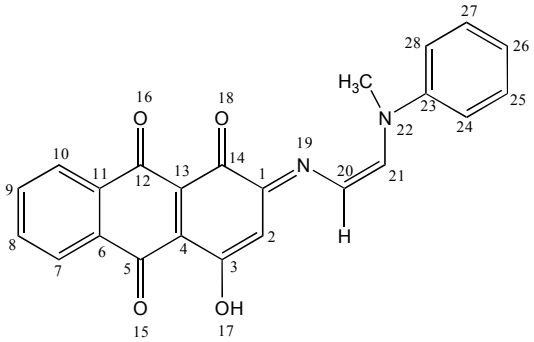

(143f)

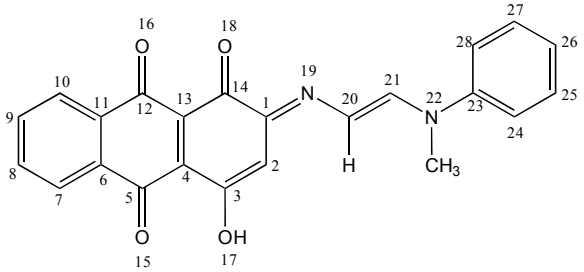

(143g)

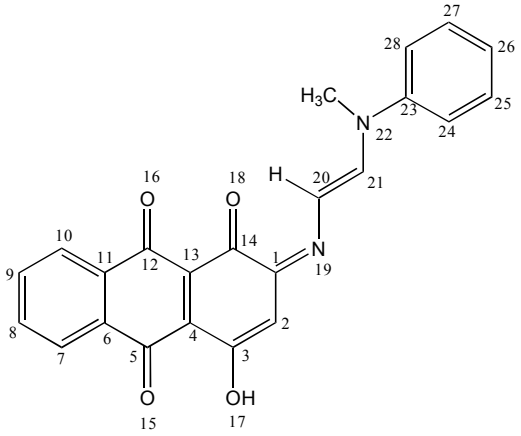

(143h)

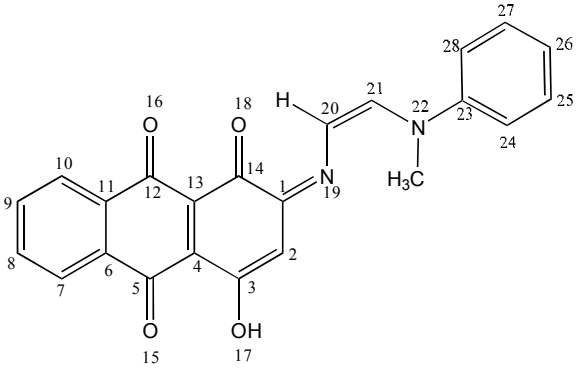

(143i)

Figure 64: Modified ring-closed form and merocyanine forms of anthraquinone based spirooxazine **(143, e-i)**

A generalized set of data was used to run the PPP-MO calculations. The parameters used for the PPP-MO calculations are given in Table 31.

Table 31: A generalized set of parameters for the PPP-MO calculations.

Bond / atom specification	**VSIP eV**	**EA eV**	**Core Charge**	**β value eV**	**Bond length Å**
Aryl ring (C=C)	11.16	0.03	1	-2.4	1.40
Olefinic C=C	11.16	0.03	1	-2.6	1.35
C=O **(Compromise carbonyl)**	18	2.5	1	-2.46	1.22
C-OH	28	10	2	-2.6	1.36
C-N=	19.5	6	1	-2.8	1.33

The results for ring closed and merocyanine forms are given in Table 32.

Table 32: Results of the PPP-MO calculations for anthraquinone-based spirooxazine.

	Calculated λ_{max} (nm) (f_{osc})
Approximation to ring closed form (143e)	484 (0.56), 272 (0.75), 253 (0.37)
143f	695 (0.90), 487 (0.19), 437 (0.19)
143g	672 (0.95), 475 (0.13), 429 (0.18)
143h	704 (0.84), 480 (0.34), 436 (0.20)
143i	699 (0.88), 485 (0.17), 353 (0.45)

The results suggested a bathochromic shift in wavelength from 484-672 nm for the approximation to ring closed **(143e)** to the merocyanine form **(143g)**. The oscillator strength values predict that the merocyanine form is more strongly coloured than the ring closed form. The predicted colour for the ring closed form **(143)** having a λ_{max} value of 484 is orange and for the most stable merocyanine form **(143g)** with absorption at 672 nm and 475 nm might be bluish.

(b) PPP-MO Calculations for naphthoquinone-based spirooxazine

PPP-MO calculations for ring-closed and merocyanine forms of naphthoquinone-based spirooxazine were also carried out using the set of parameters given in Table 33. The approximation to the ring closed and the merocyanine forms of compound **(144, 144 f-i)** are given in Figure 65.

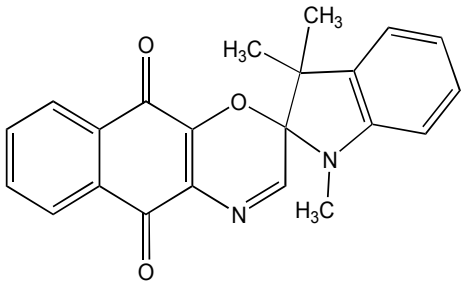

(144)

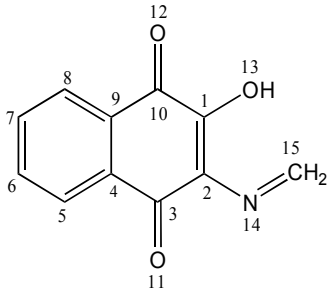

(144e)

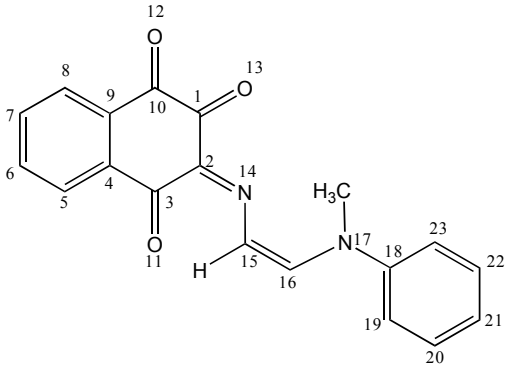

(144f)

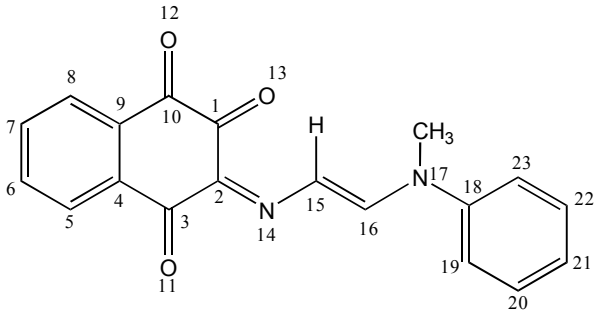

(144g)

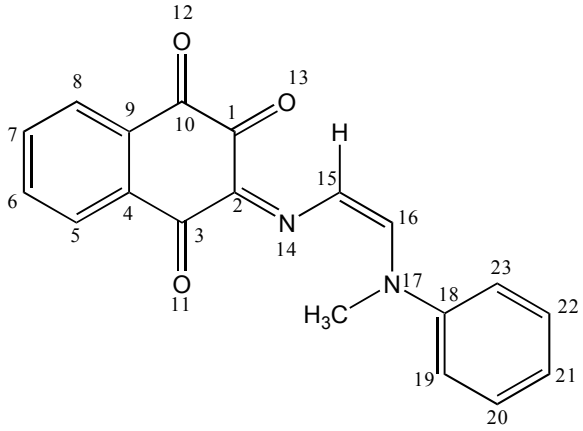

(144h)

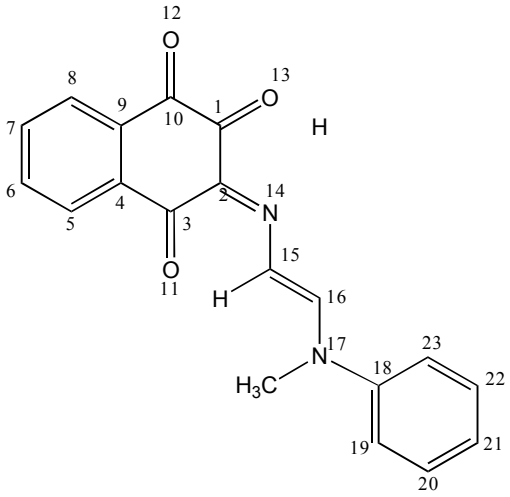

(144i)

Figure 65: Approximation to the ring-closed and merocyanine forms of naphthoquinone based spirooxazine **(144,e-i)**

The set of parameters used for the PPP-MO calculations is given in Table 33.

Table 33: A generalized set of parameters for naphthoquinone- based spirooxazine.

Bond / atom specification	**VSIP eV**	**EA eV**	**Core Charge**	**β value eV**	**Bond length Å**
Aryl ring (C=C)	11.16	0.03	1	-2.4	1.40 (C=C), 1.45 (C-C)
C=O	15.0	0.71	1	-2.46	1.22
C-N=	15.0	0.97	1	-2.48	1.33

The calculation for the ring-closed form **(144e)** and the merocyanine forms **(144, f-i)** were run using compromise carbonyl group values.

The results obtained from the PPP-MO calculations are given in Table 34.

Table 34: Results of the PPP-MO calculations for naphthoquinone-based spirooxazine**.**

	Compromise carbonyl values λ_{max} **(nm) (**f_{osc}**)**
144e	469 (0.11), 322 (0.24), 303 (0.31), 292 (0.67)
144f	542 (0.84), 501 (0.40)
144g	547 (0.67), 478 (0.72), 279 (0.51)
144h	558 (0.67), 494 (0.61), 280 (0.56)
144i	510 (0.97), 494 (0.32)

The PPP-MO calculation suggested that if the compound had a potential to show photochromic properties then there will be a bathochromic shift in absorption maximum value proceeding from approximation to ring closed form **(144e)** to merocyanine form **(144h)**. This was the most stable form according to the molecular mechanic calculations (MM2). The PPP-MO calculations were carried out using the bond angle values from the minimized structure obtained after MM2 calculations. The λ_{max} value for **(144h)** obtained after using these values were 548 nm (0.68), 492 nm (0.66) and 280 nm (0.51). The comparison of λ_{max} values showed that there is no significant difference if the values of standard bond angles or the bond angles from energy minimised structures were used. The predicted colour for ring closed form **(144)** is orange and if the compound had an ability to show photochromism, the predicted colour change is from orange to red or perhaps brown as there are two predicted visible absorptions.

3.2.3 Synthesis

This section covers the attempts to synthesise the modelled anthraquinone and naphthoquinone- based spirooxazines.

(a) Attempted synthesis of anthraquinone-based spirooxazines

The synthesis of compound **(143)** was attempted by the reaction of 1,4-dihydroxy-2-aminoanthraquinone **(147)** with Fischer's Base **(70)** in toluene. The reaction for synthesis of the compound is given in Scheme 44.

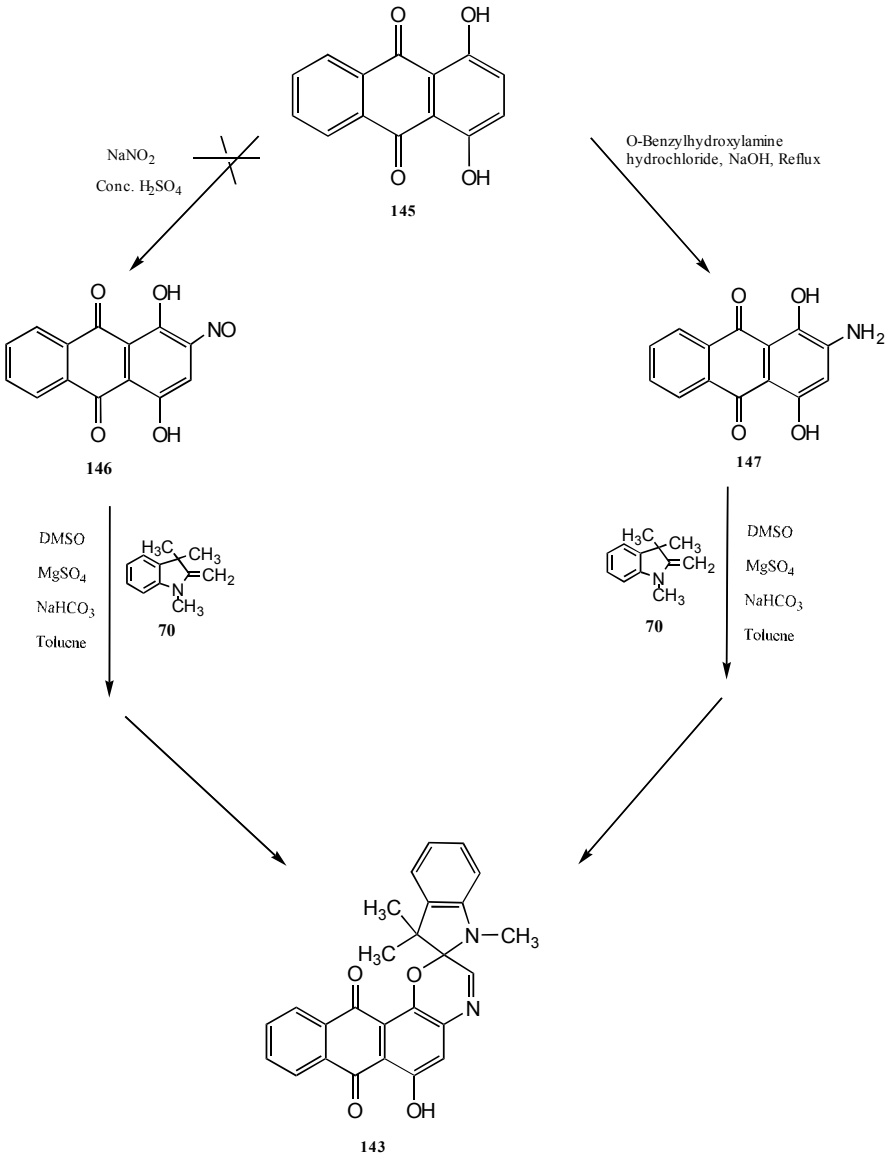

Scheme 44: Attempted synthesis of anthraquinone based-spirooxazine **(143)**.

(i) Attempted synthesis of 1,4-dihydroxy-2-nitrosoanthraquinone (146)

Synthesis of 1,4-dihydroxy-2-nitrosoanthraquinone **(146)** was attempted by reacting quinizarin **(145)** with sodium nitrite and concentrated sulphuric acid. The details of synthesis are given in experimental section 5.5.6 (a). TLC (silica, DCM) showed that the reaction was unsuccessful as no new product developed during the course of reaction and starting material was recovered quantitatively at the end of the reaction. This route was therefore abandoned.

(ii) Attempted synthesis of 1 4-dihydroxy-2-aminoanthraquinone (147)

The reaction of 1,4-dihydroxyanthraquinone was carried out to give amine **(147)** using O-benzylhydroxylamine hydrochloride and an aqueous solution of sodium hydroxide. The product was successfully recrystallized from ethanol.

Analytical data

The product decomposed without melting at 327^{o} C. The FTIR spectrum of compound **(147)** showed absorption bands due to N-H stretch at 3445 cm^{-1} and 3344 cm^{-1}, characteristic of a primary amine and hydroxy group at 3215 cm^{-1}. The ^{1}H NMR analysis of the compound was carried out using deuterated chloroform, $CDCl_3$ which confirmed the presence of the amino group in compound **(147)**. Two broad singlets for NH_2 and OH were observed at 15.35 ppm and δ3.39 ppm respectively. The numbering scheme for the identification of the proton signals is given in Figure 66.

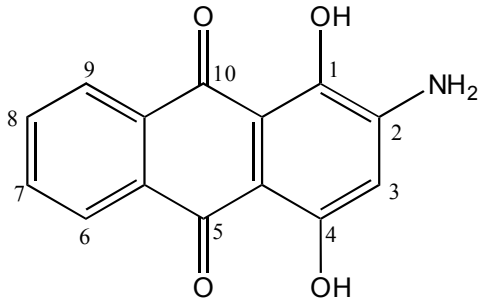

Figure 66: Numbering scheme to identify protons in compound **(147)**.

Positions 1 and 2 in compound **(147)** were occupied and a clear singlet due to H-3 was found at δ6.20 ppm. The positions of other signals are assigned in Table 35.

Table 35: ^{1}H NMR spectral data for 1 4-dihydroxy-2-aminoanthraquinone **(147)**.

Proton	**NMR signals, Chemical shift (ppm), Coupling constants (Hz)**
H_6, H_9	δ 8.20 (dd, 2H, J= 8.3Hz)
H_8, H_7	δ7.79 (t, 2H, J= 5.5Hz)
H_3	δ6.20 (s, 1H)
NH_2	δ15.35
OH	δ3.39

(iii) Attempted synthesis of anthraquinone-based spirooxazine (143)

The reaction of Fischer's Base **(70)** with 2-amino-1,4-dihydroxyanthraquinone was attempted to provide spirooxazine **(143)**. The details of procedures used are given in experimental section 5.5.6 (c). A few attempts were made to synthesize spirooxazine **(143)**. In one attempt a fraction containing a light purple component after column chromatography (silica, DCM) was isolated, although not completely pure.

Analytical data

DSC showed that the melting point of compound was 179^{o}C and it decomposed at 285^{o}C. FTIR absorption bands due to the hydroxy group and carbonyl group were found at 3448 cm^{-1} and 1600 cm^{-1} respectively. ^{1}H NMR spectral evidence was used to investigate the structure. Deuterated pyridine was the unusual choice as NMR solvent because of difficulty in the solubility of the compound. For ^{1}H NMR spectroscopy, the numbering scheme used to identify the proton signals is given in Figure 67 assuming structure **(143)**.

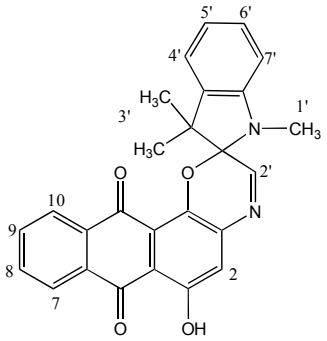

Figure 67: Proton numbering scheme for spirooxazine **(143)**.

Singlets at δ1.47 ppm, δ3.27 ppm and δ7.32 ppm are observed. However, these are not exactly as expected for this structure. The molecular formula of compound **(143)** is $C_{26}H_{20}N_2O_4$ with a molecular weight 424. The mass spectrum was not consistent with structure **(143)**. It was not possible to get a clear mass spectrum due to the unstable nature of the compound. After several attempts to provide the compound further synthesis was abandoned.

(a) Attempted synthesis of naphthoquinone-based spirooxazine

The nitrosation to give 2-hydroxy-3-nitroso-1,4-naphthoquinone **(150)** and the reaction of **(150)** with Fischer's base **(70)** was attempted to obtain spirooxazine **(144)**. (Scheme 45)

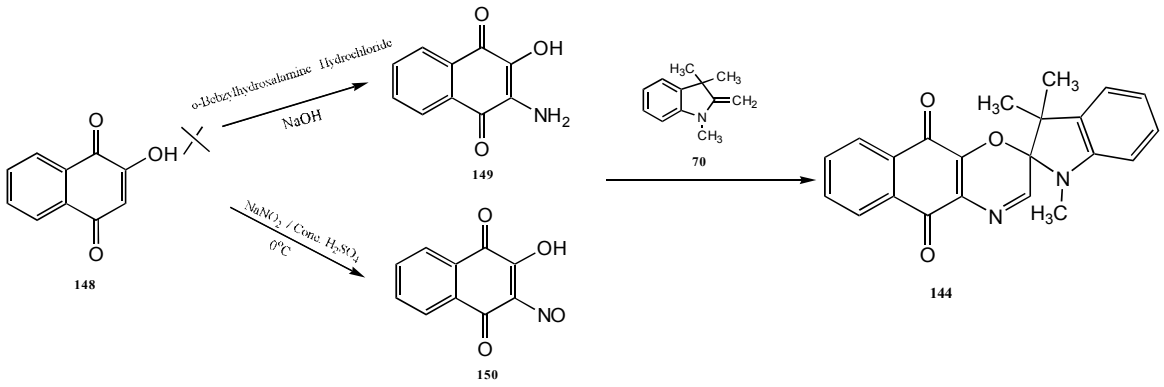

Scheme 45: Attempted synthesis of naphthoquinone- based spirooxazine **(144)**.

(i) Attempted synthesis of 3-amino-2-hydroxynaphthoquinone (149)

2-Hydroxy-1,4-naphthoquinone **(148)** was allowed to react with O-benzylhydroxylamine hydrochloride. The details of attempted syntheses are given in experimental section 5.5.7 (i). After the completion of the reaction no product could be isolated.

(ii) Attempted synthesis of 2-hydroxy-3-nitrosonaphthoquinone (150)

An attempted synthesis of compound **(150)** was carried out by reaction of 2-hydroxy-1,4-naphthoquinone **(148)** with sodium nitrite. The experimental section 5.5.7 (b) gives the detailed procedure for synthesis. A crude brown compound **(150)** was obtained after the completion of reaction as judged by a TLC and decomposed without melting at 133^{o}C. The compound was impure and attempted recrystallisation with DCM:ethanol (2%) did not purify the compound. The ^{1}H NMR spectrum of crude compound was run and it was difficult to assign the exact values to peaks because of the overlapping signals.

(iii) Attempted synthesis of spiro compound (144)

The attempted synthesis of spirooxazine **(144)** was carried out by reaction of the material assumed to be crude compound **(150)** with Fischer's base **(70)**. After reflux, the volume of the reaction mixture was reduced by a rotary evaporator and filtered. The details of synthesis are given in section 5.5.7 (c). Attempts to purify the product **(144)** failed to provide a pure compound. The impure compound was examined spectroscopically. The ^{1}H NMR spectrum of compound **(144)** showed a distinct peak at δ1.40 ppm consistent with two C-methyl groups. Another singlet was observed at δ 2.83 ppm due to the N(CH_3) group. The singlet at δ 7.42 ppm was at lower position than expected for the oxazine proton (2′-H). The molecular formula of compound **(144)** is $C_{22}H_{18}N_2O_3$. The expected molar mass was 358 and mass spectrum failed to show the molecular ion. The mass spectrum did not confirm compound **(144)**. The inconsistency in the mass spectrum could be due to the instable nature of the product. The modelling results suggested that it might be possible to get the merocyanine form because of ring closed form being higher in energy. Further investigation was abandoned.

3.3 Pyrazolone-based spirooxazines

The research on pyrazolone-based spirooxazines discussed in this section is a continuation of some previous work carried out in our laboratory in order to develop a better understanding of reactions, to confirm some questionable results and to in attempts to investigate a photochromic change between two colours (purple and red) in the hope that this might be useful in photochromism.[145,146] The previous study on these spirooxazines showed a red compound which was characterized and detailed analytical data is available in the literature. The purple compound was thought to be a mixture of isomers but not rigorously characterised. The identification of the purple compound was thus one of the aims for present research work. This section is divided into three subsections dealing with three different types of pyrazolone-based spirooxazines separately, according to the nature of the starting material used which includes 3-methyl-1-*p*-tolylpyrazol-5-one, 3-methyl-4-nitroso-1-phenylpyrazol-5-one and 3-ethoxycarbonyl-4-nitroso-1-*p*-phneylpyrazol-5-one. Molecular modelling and the PPP-MO calculations are discussed collectively while the discussion on synthesis is given separately.

3.3.1 Molecular Modelling of pyrazolone-based spirooxazines

Molecular Modelling of the spirooxazines based on pyrazolones was carried out. Three different kinds of spirooxazines were modelled which were based on 3-methyl-1-*p*-tolylpyrazol-5-one, 3-methyl-4-nitroso-1-phenylpyrazol-5-one and 3-ethoxycarbonyl-4-nitroso-1-phenylpyrazol-5-one. The heats of formation values calculated from the quantum mechanics (AM1) are used to predict the potential photochromic behaviour of the molecule by a comparison of the heats of formation values of the ring-closed form and the merocyanine forms of a molecule. The study of the relative stabilities of the merocyanine forms and the existence of the most stable form of the molecules used molecular mechanics (MM2) calculations. Two other compounds, isolated during the synthesis of spirooxazine based on 3-methyl-1-*p*-tolylpyrazol-5-one were also modelled and calculations for the final energy of molecules and the heat of formation of the molecule were also done. The structures of ring-closed form and merocyanine forms of compound **(151)** are given in Figure 68.

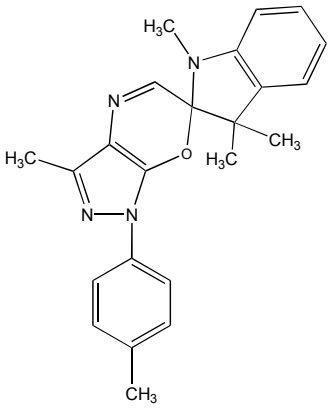

(151)

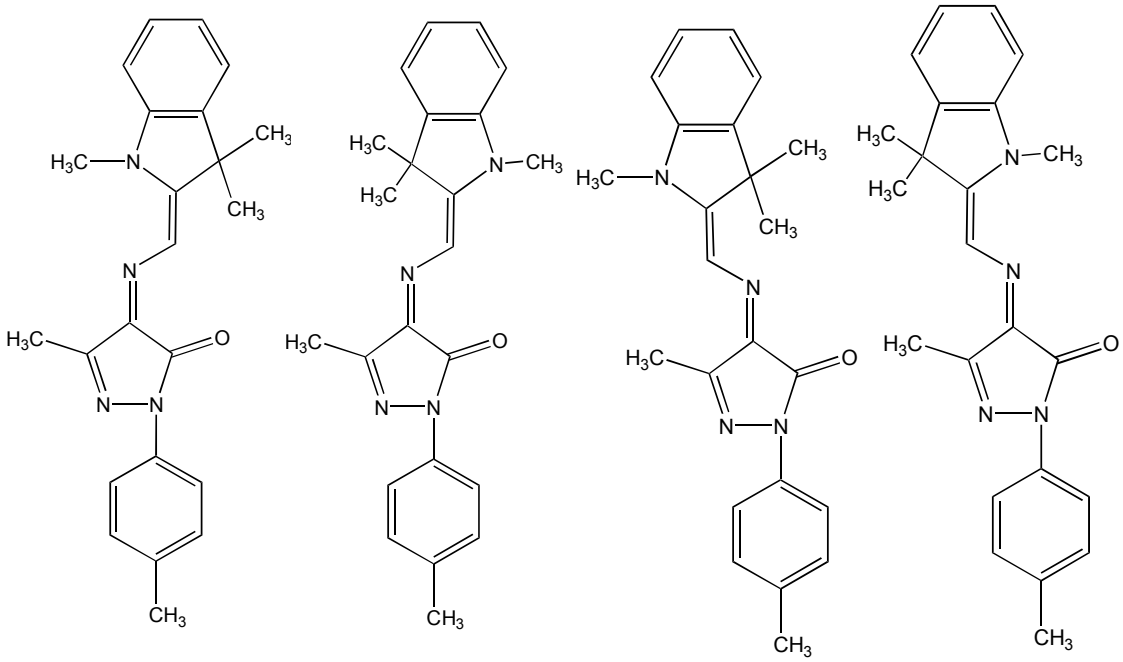

(151a) **(151b)** **(151c)** **(151d)**

Figure 68: Structures of ring-closed and merocyanine forms of compound **(151)**.

The minimized structures of the ring-closed and the merocyanine forms of the spirooxazines based on 3-methyl-1-*p*-tolylpyrazol-5-one **(151)** are given in Figure 69.

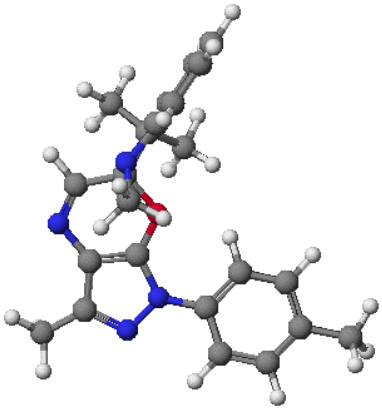

(151)

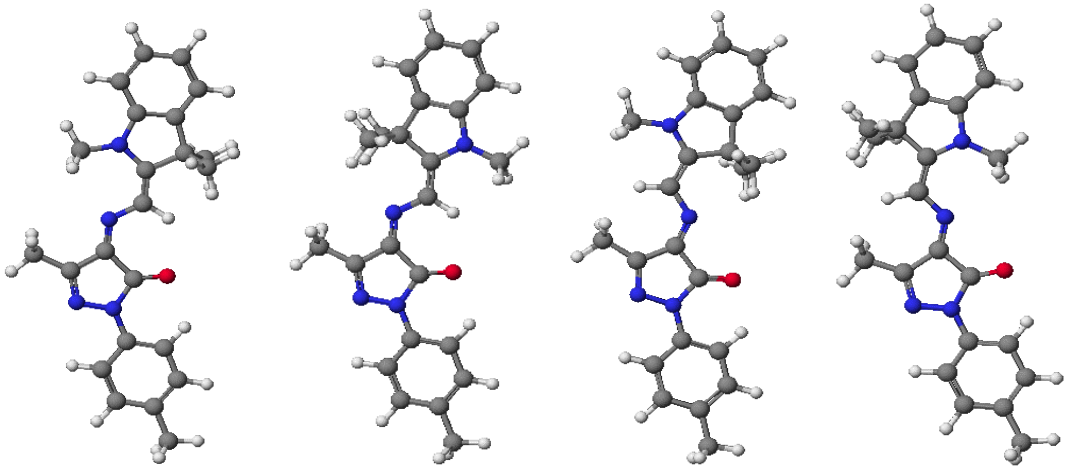

(151a) **(151b)** **(151c)** **(151d)**

Figure 69: The energy minimized structures of the ring-closed form and the four possible *transoid* photomerocyanines forms of compound **(151)**.

The modelling results suggested that the most stable isomer is merocyanine **(151b)**. The lower heat of formation values of merocyanine forms **(151 a-d)** compared with the ring closed form **(151)** suggested that the compound might not be photochromic and that the ring-opened form would be isolated. The modelling results are given in the Table 36.

Table 36: Final energy and heats of formation values for spirooxazines **(151)** and the ring-opened merocyanine isomers **a - d**.

Structure	**Final energy** **kcal mol^{-1}**	**Heat of formation** **kcal mol^{-1}**
(151)-Ring closed	13.88	136.27
(151a)	11.46	121.31
(151b)	**9.61**	123.91
(151c)	11.50	127.07
(151d)	13.34	123.86

The prediction for photochromism was similarly negative for spirooxazines based on 3-methyl-4-nitroso-1-phenylpyrazol-5-one and 3-ethoxycarbonyl-4-nitroso-1-*p*-phenylpyrazol-5-one, as the heats of formation of the ring-closed forms **(152** and **153)** was higher than the ring-opened forms **(a-d)**. The most stable forms were **(152b)** and **(153b)** in case of methyl phenyl and ethoxycarbonyl phenyl pyrazolones-based spirooxazines respectively. Based on the final energy values the isolation of merocyanine forms was again predicted.

The structures of ring-closed and merocyanine forms of compounds **(152)** and **(153)** are given in Figure 70.

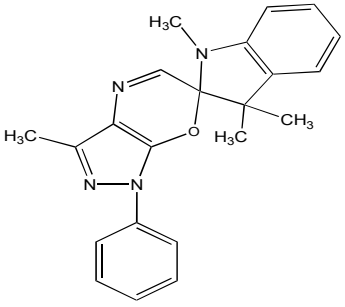

(152)

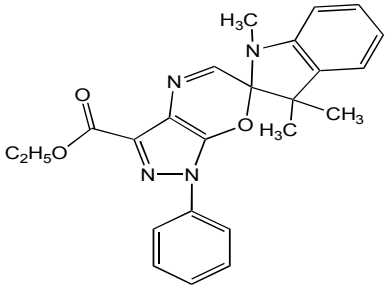

(153)

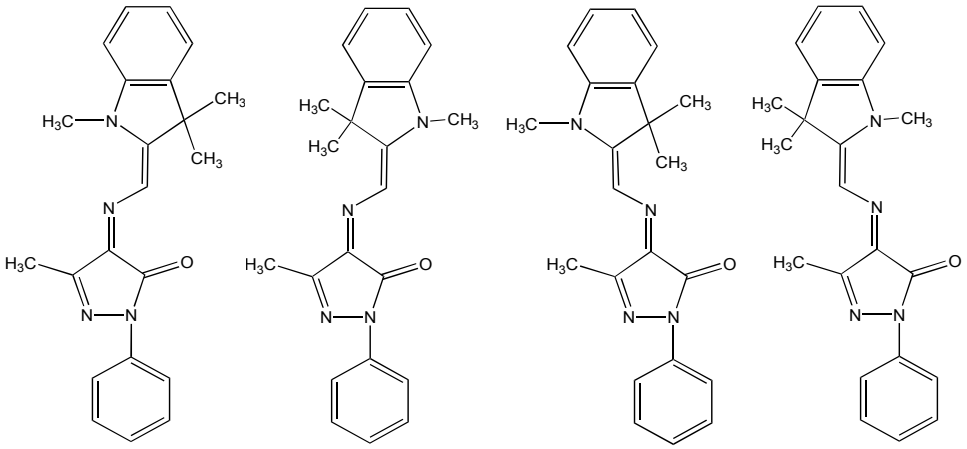

(152a) **(152b)** **(152c)** **(152d)**

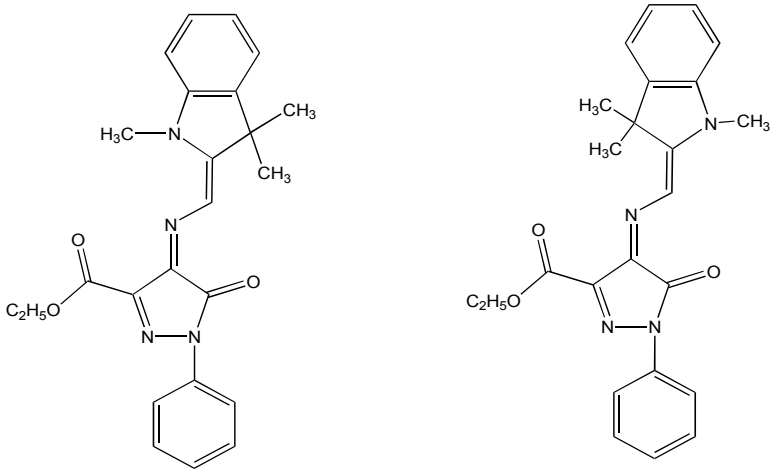

(153a) **(153b)**

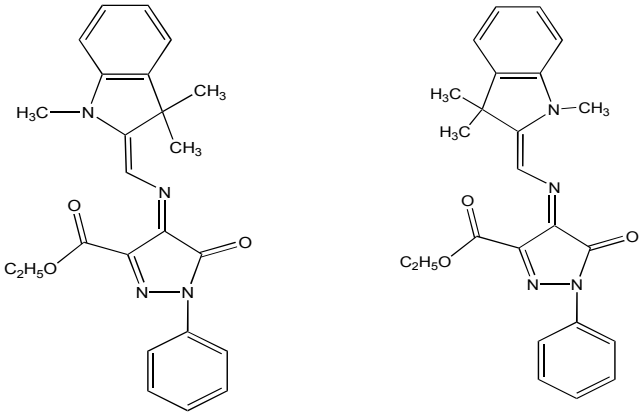

(153c) **(153d)**

Figure 70: Ring-closed and merocyanine forms of compounds **(152)** and **(153b)**.

The energy minimized structures of ring-closed and merocyanine forms of spirooxazines **(152)** and **(153)** are given in Figure 71.

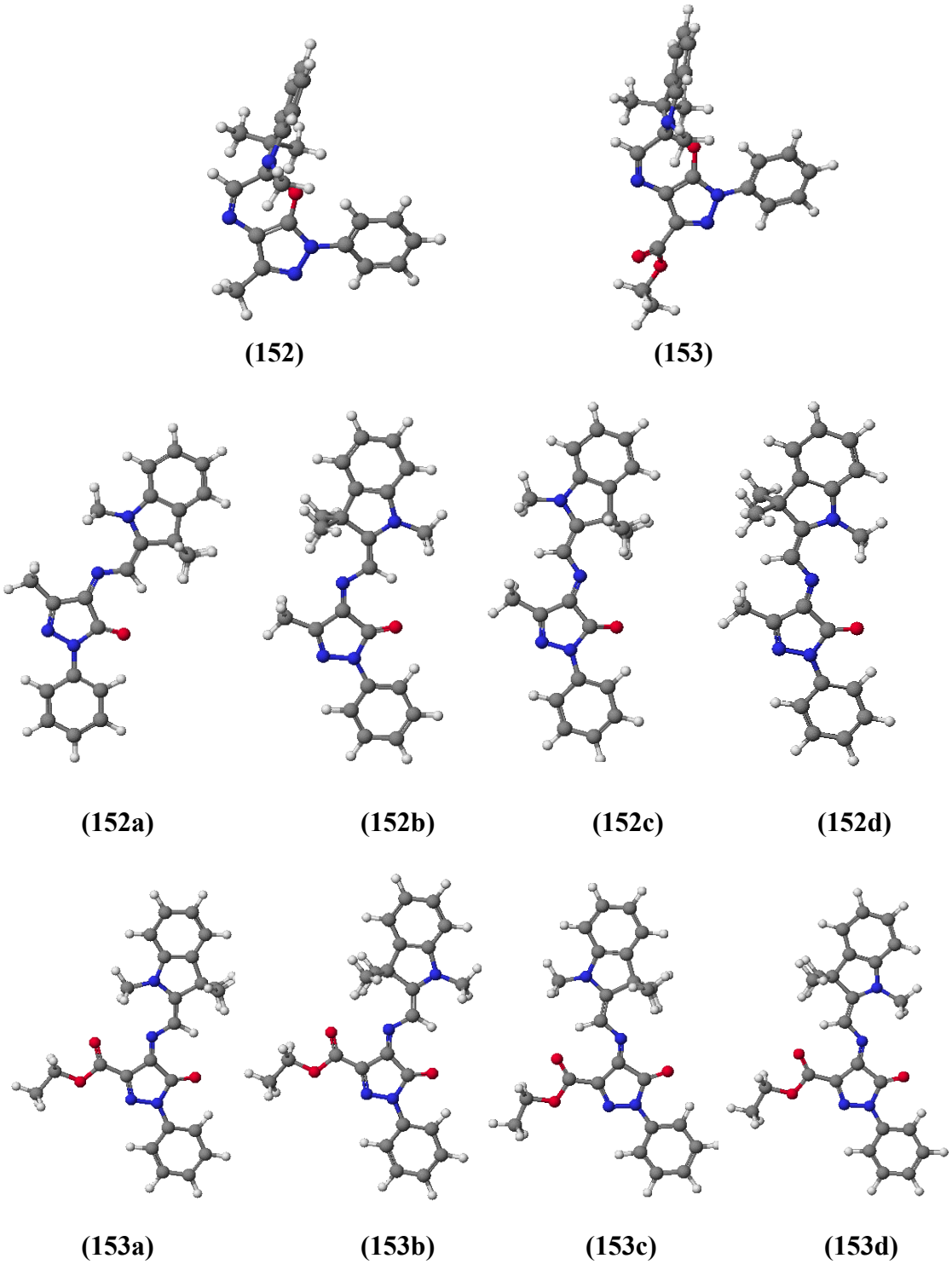

Figure 71: The minimized structures of ring-closed form and four possible *transoid* photomerocyanines forms of compounds **(152)** and **(153)**.

The modelling results (final energy and heats of formation) for spirooxazines **(152)** and **(153)** are given in Table 37.

Table 37: Final energy and heats of formation values for spirooxazines **152** and **153** and their ring-opened merocyanine isomers **a** - **d**.

Structure	**Final energy, kcal mol^{-1}**	**Heat of formation, kcal mol^{-1}**
(152)-Ring closed	12.57	144.20
152a	12.16	131.54
152b	10.32	134.65
152c	12.20	134.66
152d	14.03	131.48
(153)-Ring closed	14.57	68.38
153a	14.32	52.48
153b	12.35	55.70
153c	18.50	58.05
153d	20.21	54.91

3.3.2 PPP-MO Calculations

The PPP-MO calculations for spirooxazines based on pyrazolones (**151**- **153**) were carried out for the prediction of the colour of the molecules. The calculation for the spirooxazines based on 3-methyl-1-*p*-tolylpyrazol-5-one and 3-methyl-4-nitroso-1-phenylpyrazol-5-one are the same as the methyl group is not participating in the π-system. The calculations for compounds **152** and **153** are discussed separately. The ring-closed and the four *transoid* merocyanine forms **(a-d)** were studied in each case and the structures were modified in that the carbon atom attached to two methyl groups is not included in calculations with an assumption that the molecules have planar geometry. UV-Visible spectra of compounds **(152b)** and **(153b)** which were isolated (see section 3.3.3, b&c) were also recorded in order to establish the accuracy of the PPP-MO calculations.

(a) Calculations for spirooxazines based on 3-methyl-1-*p*-tolylpyrazol-5-one

The approximation to the ring-closed and merocyanine forms of the spirooxazine based on 3-methyl-1-*p*-tolylpyrazol-5-one used for the PPP-MO calculations is given in Figure 72.

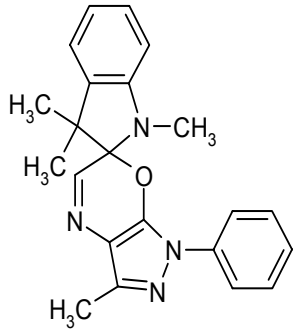

(152)

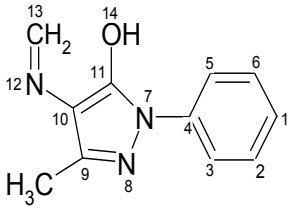

(152e)

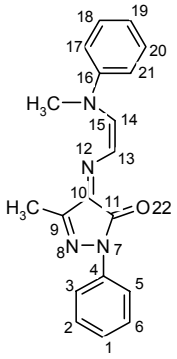

(152f)

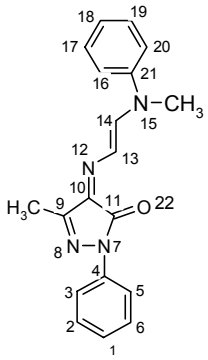

(152g)

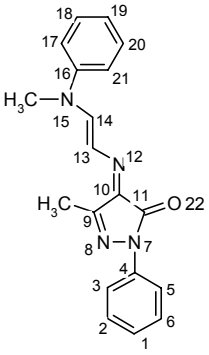

(152h)

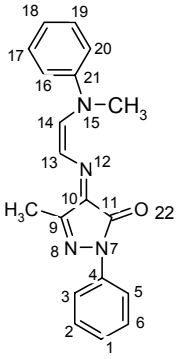

(152i)

Figure 72: Ring-closed form and approximation to the ring closed and merocyanine forms of spirooxazine **(152)** used for the PPP-MO calculations.

A generalized set of parameters used to calculate the λ_{max} value of the ring-closed and the merocyanine forms of spirooxazines based on pyrazolones is given in Table 38.

Table 38: Generalised set of parameters for the PPP-MO calculations for compound **(152)** and its merocyanine forms.

Bond / atom specification	**VSIP eV**	**EA eV**	**Core Charge**	**β value eV**	**Bond length Å**
Aryl ring (C=C)	11.16	0.03	1	-2.4	1.40
C_4-N_7π-Excessive–*N*-heterocyclic	21	10	2	-2.4	1.35
N_7-N_8 N-N- pyrazolone	14.0	2.0	1	-2.3	1.40
N_8-C_9 pyrazolone N=C	10	0.75	1	-2.6	1.40
C-N_{12}	14.0	2.0	1	-2.6	1.40
N=C_{13}	10	0.75	1	-2.6	1.40
C-OH_{14} (H-bonded)	28	10	2	-2.6	1.36
C_{13}-C_{14} C-C olefinic	11.16	0.03	1	-2.4	1.40
C_{14}-N_{15} C=N pyrazolone	14.0	2.0	1	-2.6	1.40
N_{15}-C_{16} N=C pyrazolone	10.0	0.75	1	-2.6	1.40
C=O_{22}	17.7	2.47	1	-2.46	1.22

The results of these calculations were compared to the experimental λ_{max} values when these became available (see section 3.3.3., c i).

(b) Calculations for spirooxazines-based on 3-ethoxycarbonyl-4-nitroso-1-*p*-phenylpyrazol-5-one (153).

The approximation to the ring closed and merocyanine forms of spirooxazine-based on 3-ethoxycarbonyl-4-nitroso-1-*p*-phenylpyrazol-5-one used for the PPP-MO calculations are given in Figure 73.

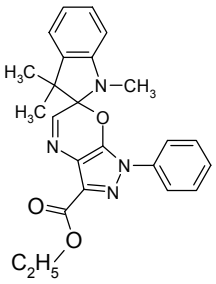

(153)

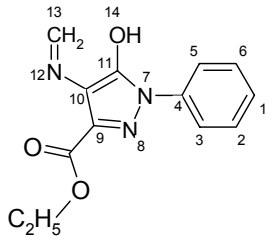

(153e)

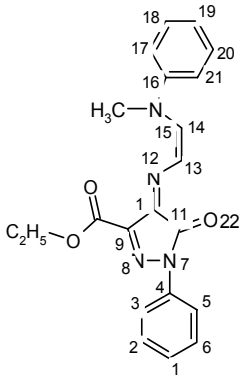

(153f)

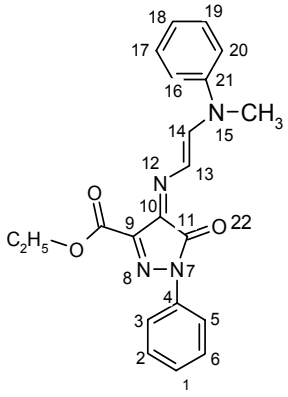

(153g)

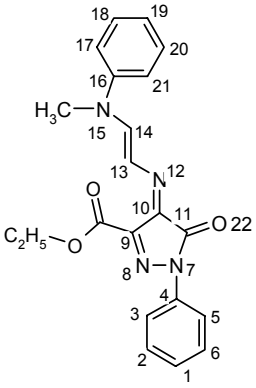

(153h)

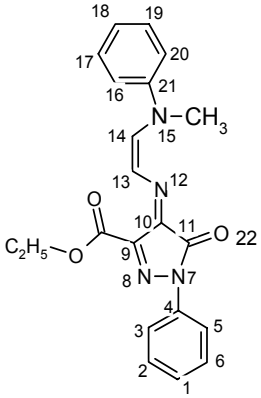

(153i)

Figure 73: Ring-closed forms and the approximation to the photomerocyanines forms of spirooxazines-based on 3-ethoxycarbonyl-4-nitroso-1-*p*-phenylpyrazol-5-one.

All the parameters are given in Table 39. The values selected for the carbonyl group were of free carbonyl group and values used for C-OR group were "electron donor methoxy group". The values used for both groups are given in Table 39.

Table 39: The generalized set of parameters used for PPP-MO calculations for compound **(153)**.

Bond / atom specification	**VSIP eV**	**EA eV**	**Core Charge**	**β value eV**	**Bond length Å**
C=O, free carbonyl group	15	0.71	1	-2.46	1.22
C-O C_2H_5	32.9	11.14	2	-2.6	1.36

The results of calculations and the comparison of these values with the experimental values are given in section 3.3.3 (c, i).

3.3.3 Synthesis

(a) Attempted synthesis of spirooxazine (151b) based on 3-methyl-1-*p*-tolylpyrazol-5-one

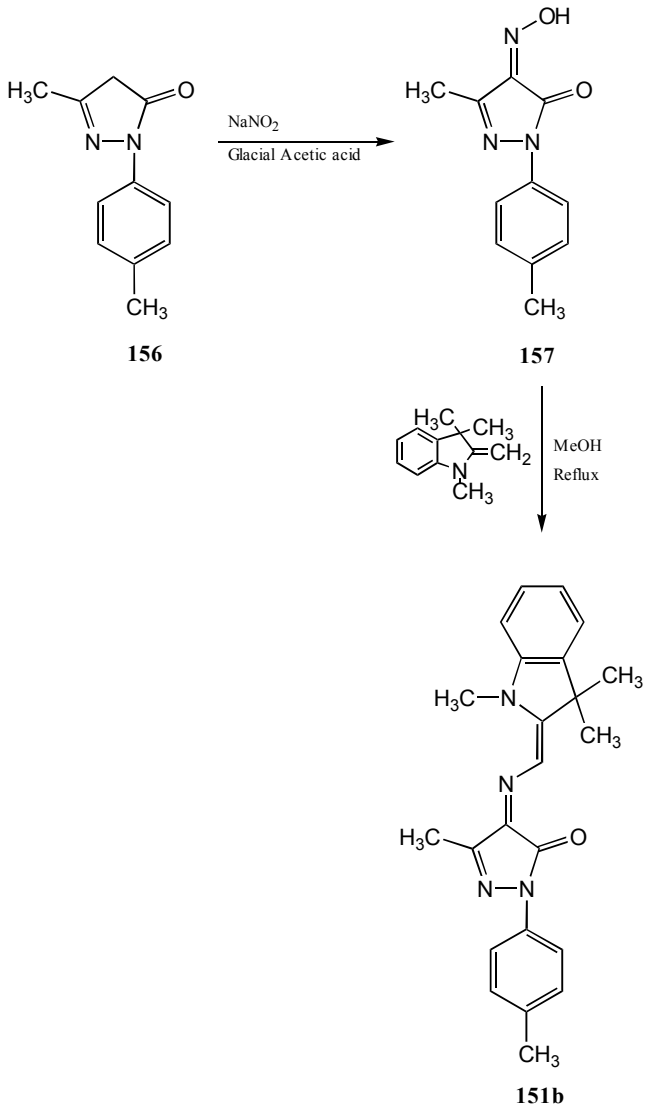

Scheme 46: Synthesis of merocyanine **(151b)**.

(i) Synthesis of 3-methyl-4-nitroso-1-*p*-tolylpyrazol-5-one (157)

The nitrosation of 3-methyl-1-*p*-tolylpyrazol-5-one **(156)** was carried out by reaction with sodium nitrite to obtain an orange compound. The details of synthesis are given in experimental section 5.5.8 (a). Spectral data and melting point were consistent with literature data.[147]

(ii) Reaction of 3-methyl-4-nitroso-1-*p*-tolylpyrazol-5-one (157) with 1,3,3-trimethyl-2-methyleneindoline (70)

In order to study the behaviour of the reaction, compound **(157)** was refluxed with Fischer's Base **(70)** in methanol for 70 minutes. The product obtained was mainly a mixture of red, purple, orange and yellow compounds as seen on TLC (silica, toluene: ethanol, 80:20). The details of synthesis are given in experimental section 5.5.8 (b, i). Two separate reactions were also carried out to by changing the reflux time from 70 minutes to 21 hours and 31 hours respectively in order to observe the effect of time of reaction. Again, a mixture of red, purple, orange and yellow compounds was observed on TLC. The details of reactions are given in experimental section 5.5.8 (b,ii). An image of TLC showing these compounds is given in Figure 74.

Figure 74: TLC (toluene:ethanol, 80:20) of reaction mixture showing all products (Orange, red, purple and yellow).

(iii) Synthesis of orange, purple and red compounds (155, 154 and 151b)

Reaction of 3-methyl-4-nitroso-1-*p*-tolylpyrazol-5-one **(157)** and Fischer's base **(70)** was carried out for 67 hours using the procedure given in experimental section 5.5.8 (b, i). The crude brown product obtained was submitted to a silica gel column chromatographic separation using toluene as eluent. The eluates were evaporated under reduced pressure to provide orange product **(155)** (6%), purple compound **(154)** (1%) and the column under these conditions was unable to separate red and purple compounds giving a mixture of red **(151b)** and purple **(154)** (39%).

Orange compound (155)

Spectroscopic techniques and X-ray crystallography were used to identify the orange compound. The detailed analysis is given below.

Analytical data

The melting point of orange product **(155)** determined by DSC was 250^{o} C and the product decomposed at 290^{o} C. The NMR spectral evidence was used to confirm the structure. For ^{1}H NMR spectroscopy, the numbering scheme used to identify the proton signals is given in Figure 75.

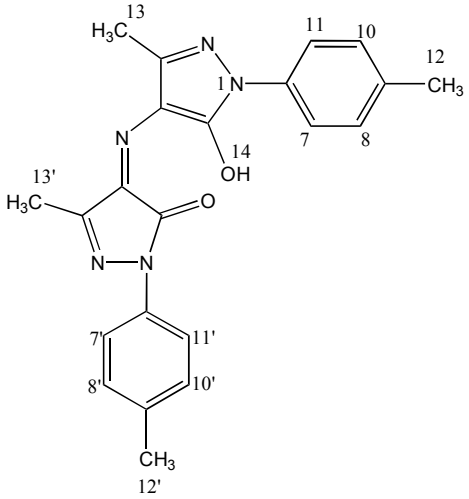

Figure 75: Proton numbering sequence for orange compound **(155)**.

Table 40: ^{1}H NMR spectral data for orange compound **(155)**.

Proton	**NMR signals, Chemical shift (ppm), Coupling constants (Hz)**
H_{12}, $H_{12'}$, H_{13}	δ2.33 (s, 9H, C-CH_3)
$H_{13'}$	δ2.37 (s, 3H, C-CH_3)
H_{14}	δ14.53 (s, 1H, C_2-OH)
H_7, H_{11} $H_{7'}$, $H_{11'}$	δ 7.70- δ 7.80 (m, 4H)
H_8, H_{10}, $H_{8'}$, $H_{10'}$,	δ7.10-δ7.30 (m, 4H)

The NMR spectrum of compound **(155)** showed a broad signal for OH at δ14.53 ppm and peaks for CH_3 groups. The rest of the signals with coupling constants are given in Table 40. The molecular formula of the compound is $C_{22}H_{21}N_5O_2$ and mass spectroscopic analysis gave a molecular ion which was consistent with the theoretical mass of 387. The crystals of orange compound **(155)** were grown from dichloromethane and hexane. The structure obtained by single crystal X-ray crystallography is shown in Figure 76**.**

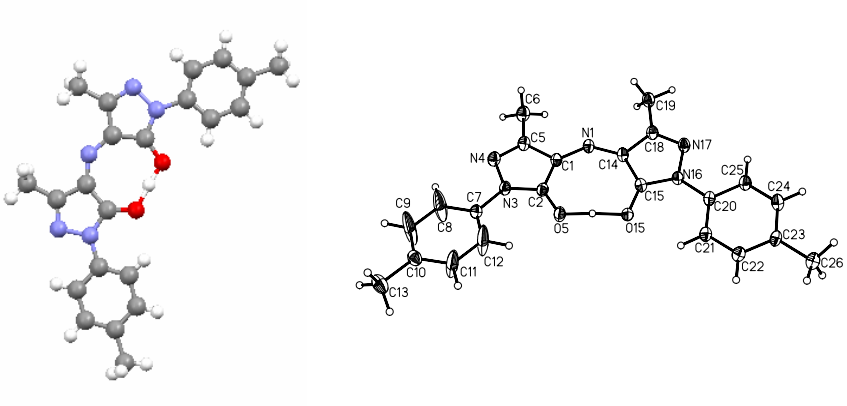

Figure 76: X-Ray crystallographic structure of compound **(155)**.

Crystal structure data for compound **(155)** is given in Appendix C. The crystals were triclinic and the packing of the crystals is shown in Figure 77.

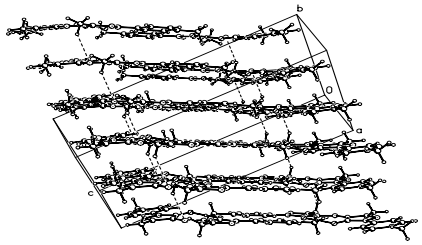

Figure 77: Crystal packing of orange compound **(155)**.

There is significant intramolecular hydrogen-bonding in 8-membered ring between O-15 and O-5. The bond length for hydrogen bonded O5-H5 is 1.26 (5). A comparison of bond angles between N1-C1-C2 and N1-C14-C15 showed that it is an asymmetric molecule. Table 41 shows relevant interatomic distances and bond angles. X-ray crystal data for compound **(155)** in detail is given in Appendix C.

Table 41: Bond lengths [Å] and angles [°] for orange compound **(155)**.

D-B-A	**d(D-B)**	**d(B-A)**	**<(DBA)**
N(1)-C(1)-C(2)	1.321(4)	1.448(4)	135.7(3)
C(5)-C(1)-C(2)	1.438(4)	1.448(4)	103.6(3)
C(14)-N(1)-C(1)	1.319(4)	1.321(4)	134.0(3)
O(5)-C(2)-N(3)	1.282(4)	1.342(4)	122.5(3)
O(5)-C(2)-C(1)	1.282(4)	1.448(4)	131.3(3)
C(2)-O(5)-H(5)	1.282(4)	1.16(5)	113(2)
O(15)-C(15)-N(16)	0.95	2.52	123.8(3)
O(15)-C(15)-C(14)	1.268(4)	1.451(5)	130.7(3)
N(16)-C(15)-C(14)	1.351(4)	1.451(5)	105.5(3)
C(15)-O(15)-H(5)	1.268(4)	1.26(5)	115(2)
O(5)-H(5)...O(15)	1.16(5)	1.26(5)	177(5)
N(1)-C(14)-C(15)	1.319(4)	1.451(5)	134.7(3)

Symmetry transformations used to generate equivalent atoms:

(iv) Synthesis of red merocyanine (151b)

Synthesis was carried out to obtain red merocyanine form **(151b)** as a major product. The details of synthesis are given in experimental section 5.5.8 (e, i). The reaction mixture was refluxed for a month. It was observed that the longer the time given to the reaction, which was a mixture of red and purple compounds, the more is the conversion of the purple compound to the red. The reaction mixture was kept in a freezer for two days and the precipitate was filtered and recrystallization from methanol. Red product **(151b)** with an improved yield (32%) was obtained. The melting point of compound **(151b)** was 182^{o}C. Only FTIR spectrum of the compound was run because detailed characterization of compound **(151b)** is available in the literature.[147] The development of different products during the course of reaction is shown in Figure 78.

start

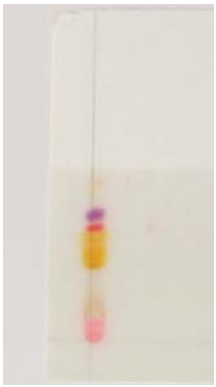

10 min

20 min

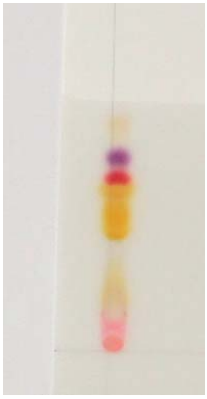

30 min

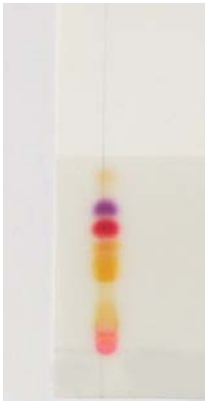

1 hour

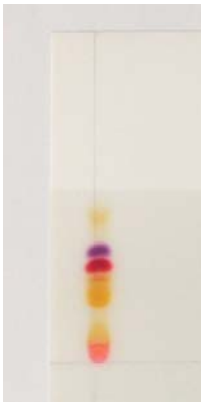

2 hours

3 hours | 4 hours | 5 hours

After 16 hours | After a week | After a month

Figure 78: Development of different products during reflux reaction of compound **(157)** with Fischer's base **(70)**.

(v) Synthesis of purple N-oxide (154)

The N-oxide **(154)** was synthesized by the procedure described in experimental section 5.5.8 (f, i). The reaction was carried out for 18 hours at room temperature using acetone as solvent. Water was added to the reaction mixture which was then left for two days. A precipitate of pure product **(154)** (9%) was obtained.

Analytical data

DSC showed that compound **(154)** decomposed without melting at 200°C. The FTIR spectrum of the compound is given in experimental section (5.5.8, d). Deuterated chloroform, $CDCl_3$ was used for ^1H NMR analysis of the compound. The numbering scheme for the identification of proton signals is given in Figure 79.

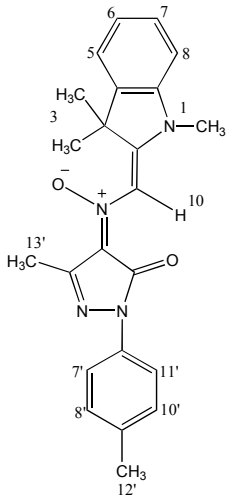

Figure 79: Proton numbering sequence for purple compound **(154)**.

Table 42: ^1H NMR spectral data for purple compound **(154)**.

Proton	**NMR signals, Chemical shift (ppm), Coupling constants (Hz)**
H_1	δ 3.51 (s, 3H, N-CH_3)
H_3	δ1.81 (s, 6H, (C-CH_3)$_2$
$H_{13'}$	δ 2.33 (s, 3H, C-CH_3)
$H_{12'}$	δ 2.53 (s, 3H, C-CH_3)
H_8	δ6.99 (d, 1H, $J_{6,7}$= 6.23)
$H_{5,6,7}$	δ7.1-7.3 (m, 3H)
H_{10}	δ9.33 (s, 1H)
$H_{7',8',10',11'}$	δ7.80 (m, 4H)

The NMR spectrum showed a clear singlet due to H-10 at δ9.33 ppm. Other proton signals used to identify the structure are given in Table 42. The molecular formula of the compound is $C_{23}H_{24}N_4O_2$ and mass spectroscopic analysis gave a molecular ion which was consistent with the theoretical mass of 388. X-Ray crystallography of the purple compound was also run to confirm the structure using crystals grown from dichloromethane and hexane. X-ray crystal data for compound **(154)** in detail is given in Appendix B while the crystal structure is given in Figure 80.

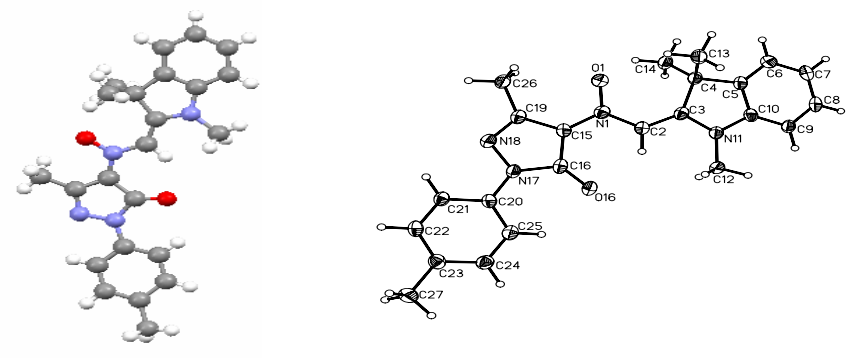

Figure 80: Single crystal X-Ray crystallographic structure of purple N-oxide **(154)**.

Relevant interatomic distances and bond angles are given in Table 43.

Table 43: Bond lengths [Å] and angles [°] for purple compound **(154)**.

D-B-A	**d(D-B)**	**d(B-A)**	**<(DBA)**
O(1)-N(1)-C(15)	1.274(2)	1.356(3)	119.32(19)
O(1)-N(1)-C(2)	1.274(2)	1.374(3)	121.3(2)
C(15)-N(1)-C(2)	1.356(3)	1.374(3)	119.4(2)
C(3)-C(2)-N(1)	1.373(3)	1.374(3)	126.3(2)
C(3)-C(2)-H(2)	1.373(3)	0.9500	116.9
N(1)-C(2)-H(2)	1.374(3)	0.9500	116.9
N(11)-C(3)-C(2)	1.355(3)	1.373(3)	117.9(2)
H(13B)-C(13)-H(13C)	0.9800	0.9800	109.5

Symmetry transformations used to generate equivalent atoms

Products (**154** and **155**) isolated from the column chromatography of spirooxazines based on 3-methyl-1-*p*-tolylpyrazol-5-one **(151)** were also modelled and final energy and heats of formation of the molecules was calculated, (for more details see experimental section 3.3.3 a, iv). The modelled and energy minimized structures of compounds (**154** and **155**) are given in Figure 81 and the results of final energy and heats of formation are given in Table 44. The modelled structures were more or less in agreement with the X-ray structures.

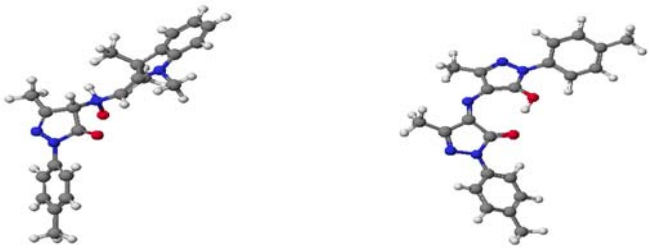

(154) **(155)**

Figure 81: Energy minimized structures of compounds **154** and **155**.

Table 44: Modelling results of compounds **154** and **155**

Compound	**Final energy, kcal mol^{-1}**	**Heat of formation, kcal mol^{-1}**
154	39.38	130.17
155	5.13	125.97

(vi) Attempted isolation of unstable yellow compound (158)

A number of attempts were made to obtain a yellow unstable compound **(158)** which was observed in the early stages of the reaction. 3-Methyl-4-nitroso-1-*p*-tolylpyrazol-5-one **(157)** was refluxed for 5 minutes with Fischer's base **(70),** poured in to ice cooled water and allowed to stand for 4 hours to give precipitate which was then filtered. The filtered product proved to be the starting nitroso compound **(157)**. The filtrate showed a yellow spot on TLC on silica. The details of the experiment are given in section 5.5.8 (c, ii). To provide the yellow compound **(158)** sodium chloride was added to the filtrate and the solution was left overnight. A precipitate was then filtered, dried in the freeze drier and weighed. The yellow compound obtained was unstable and converted

rapidly to a mixture of red and purple compounds on TLC. Because of the unstable nature of compound **(158)** further attempts to isolate it were abandoned. The unstable nature of the yellow compound is shown in the images of two dimensional TLC given in Figure 82. TLC after first elution was dried and kept for 30 minutes; it showed yellow, red, orange and purple compounds. After second elution the diagonal pattern of colour change was observed due to the conversion of yellow compound into red and purple compounds. After 16 hours of reflux a TLC was run which showed traces of the unstable yellow compound which disappear in the last TLC recorded after the reflux reaction carried out for a month. A clear change of yellow to a mixture of red and purple and subsequently from purple to red is shown in Figure 82.

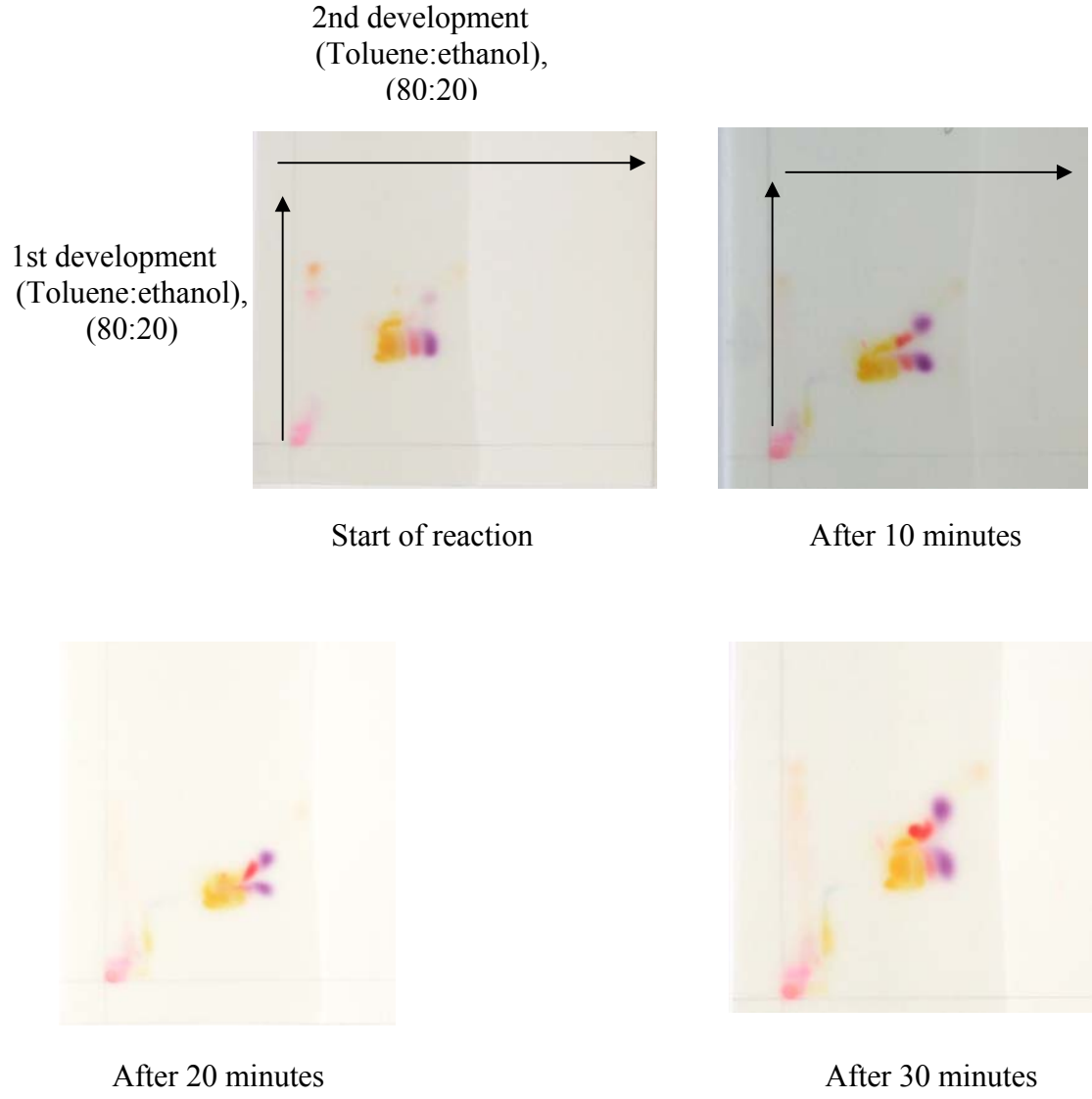

After 1hour

After 2hours

After 3 hours

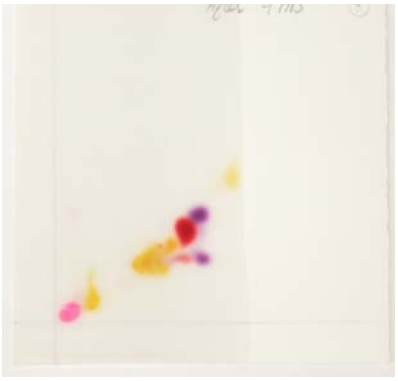

After 4 hours

After 5 hours

After 16 hours

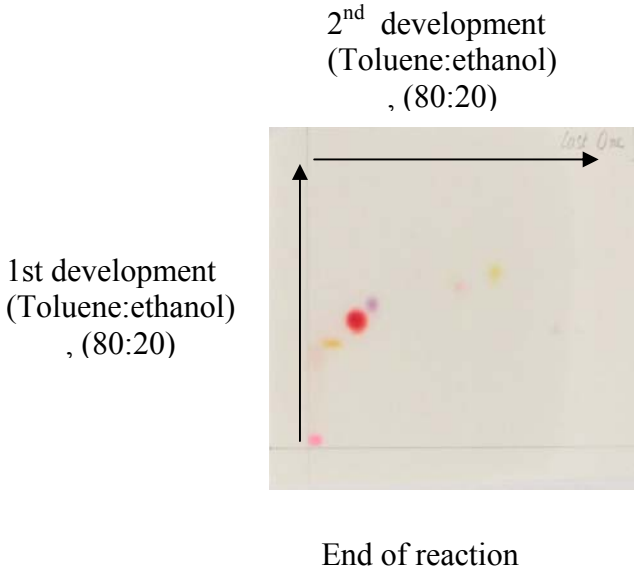

Figure 82: Two dimensional TLC showing the instability of yellow compound **(158)**.

(vii) Attempted oxidation of merocyanine form (151b) to provide N-oxide (154).

An attempted synthesis of N-oxide **(154)** was carried out by the oxidation of merocyanine form **(151b)** using hydrogen peroxide. (Scheme 47) The details of the reaction are given in experimental section 5.5.8 (f, iii). The reaction mixture was heated to 85^{o}C and then refluxed for an hour. The solution turned yellow but no conversion of red product **(151b)** to purple N-oxide **(154)** was observed on a TLC. Only a yellow spot was observed.

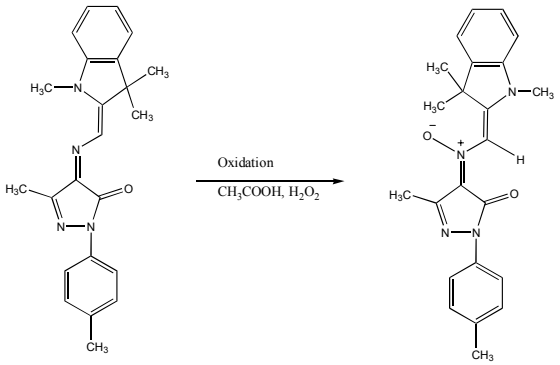

(151b) **(154)**

Scheme 47: Attempted synthesis of N-oxide (purple compound) by the oxidation of merocyanine form **(151b)**.

(viii) Conversion of purple N-oxide (154) to red merocyanine (151b)

N-oxide **(154)** was converted to red merocyanine form **(151b)** by refluxing for 504 hours (21 days) in acetone. The yield of the red product obtained was (95%). The reaction is given in Scheme 48.

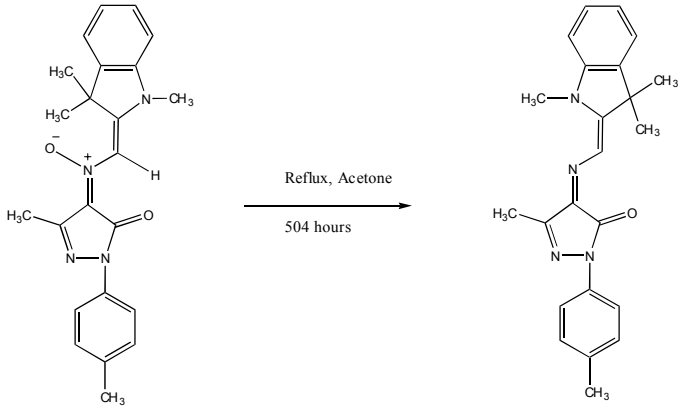

Scheme 48: The conversion of purple N-oxide **(154)** to red merocyanine **(151b)**.

(b) Attempted synthesis of spirooxazine (152b) based on 3-methyl-4-nitroso-1-phenylpyrazol-5-one

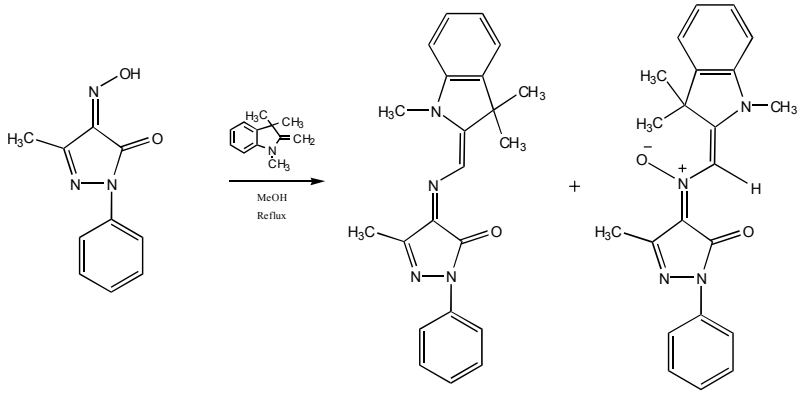

(159) **(152b)** **(160)**

Scheme 49: Reaction scheme for synthesis of compound **(152b)**.

(i) Synthesis of merocyanine (152b)

The reaction of 3-methyl-4-nitroso-1-phenylpyrazol-5-one **(159)** with Fischer's base **(70)** was attempted to obtain merocyanine **(152b)**. The details of the experiment are given in section 5.5.9 (a). The reflux reaction was carried out for 168 hours (7 days) and red

merocyanine **(152b)** was the main product as judged by TLC. The refluxed mixture was cooled in a refrigerator overnight, filtered and recrystallized from methanol to give red merocyanine (73%). The melting point determined by DSC was 240^{o}C. The FTIR spectrum of the compound was compared to the reference spectrum and the complete characterization of the compound is discussed in the literature.[144]

(ii) Synthesis of Purple N-oxide (160)

3-Methyl-4-nitroso-1-phenylpyrazol-5-one **(159)** was allowed to react with Fischer's base **(70)** to obtain N-oxide **(160)**. The detailed procedure is provided in experimental section 5.5.9 (b). The crude compound was submitted to silica gel column using toluene as eluent to provide a pure sample of the purple N-oxide **(160).** The yield of the compound was low (0.53%) because of the unstable nature of the compound.

Analytical data

The melting point of the compound as determined by DSC was 202^{o}C. The peaks observed in the FTIR spectrum of the compound are given in experimental section (5.5.9, b). The molecular formula of the compound is $C_{22}H_{22}N_4O_2$ and mass spectroscopic analysis gave a molecular ion which was consistent with the theoretical mass of 374. The values are given in section (5.5.9, b). The ^{1}H NMR spectrum of the compound in deuterated chloroform showed the signals given in Table 45. Figure 83 shows the numbering scheme used to identify the proton signals.

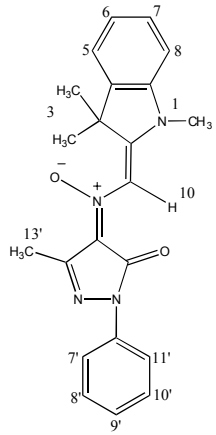

Figure 83: Proton numbering sequence for purple compound **(160)**.

Table 45: ^{1}H NMR spectral data for purple compound **(160)**.

Proton	**NMR signals, Chemical shift (ppm), Coupling constants (Hz)**
H_1	δ 3.4 (s, 3H, N-CH_3)
H_3	δ1.6 (s, 6H, (C-CH_3)$_2$
H_5	δ7.15 (d, 1H, $J_{6,7}$= 6.3)
$H_{6,7}$	δ7.2-7.35 (m, 2H)
H_8	δ6.95 (d, 1H, $J_{6,7}$= 8.5)
H_{10}	δ9.33 (s, 1H)
$H_{13;}$	δ 2.5 (s, 3H, C-CH_3)
$H_{7',11'}$	δ7.94 (d, 4H, J= 7.5)
$H_{8',9',10'}$	δ7.41 (m, 3H)

(c) Synthesis of spirooxazines based on 3-ethoxycarbonyl-4-nitroso-1-*p*-phenylpyrazol-5-one (153b).

The synthesis of red merocyanine **(153b)** and N-oxide **(162)** was attempted by the reaction scheme given below.

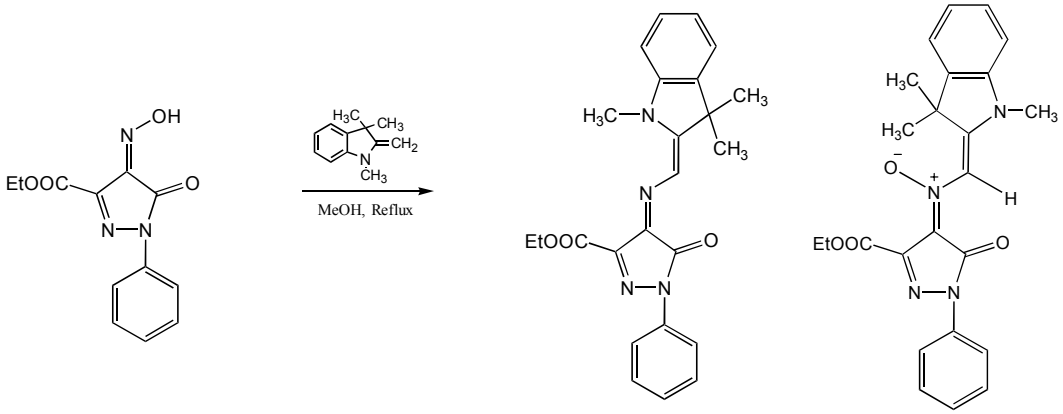

(161) **(153b)** **(162)**

Scheme 50: Synthesis of red merocyanine compound **(153b)**.

(i) Synthesis of red merocyanine (153b)

The synthesis of spirooxazine **(153b)** was carried out by the method described in experimental section 5.5.8 (b, i) using 3-ethoxycarbonyl-4-nitroso-1-phenylpyrazol-5-one **(161)** and Fischer's base **(70)**. A TLC of the filtered product on silica using toluene: ethanol (20%) as eluent showed that it was a mixture of red merocyanine **(153b)** and purple N-oxide **(162)**. The product was recrystallized with ethanol to give pure red product **(153b)** (69%). Melting point determined by DSC was 236^{o}C.

After synthesis, PPP-MO calculations were run to correlate the experimental data with calculated values for compounds **(151-154)** and the comparison of compounds (**151** and **152**) is given in Table 46.

Table 46: A comparison of λ_{max} values for compounds **(151)** and **(152)** using generalized parameters.

Compound	**Experimental λ_{max} (nm) (dichloromethane)**	**Calculated λ_{max}, using generalized parameters, (nm) (f_{osc})**
152- Ring closed		370 (0.08), 296 (0.45)
152f		472 (0.57), 397 (0.83), 260 (0.43)
152g	495 **(152b)**	**469 (0.53), 391 (0.94), 259 (0.44) (152g)**
151g	500 **(151b)**	**469 (0.53), 391 (0.94), 259 (0.44) (151g)**
152h		466 (0.60), 384 (0.96), 260 (0.40)
152i		470 (0.61), 395 (0.83), 260 (0.42)

The results given in Table 46 showed that λ_{max} values calculated using the PPP-MO approach for merocyanines **(151)** and **(152)** are 26-31 nm hypsochromic of the experimental values. The calculated values obtained show oscillator strength values from 0.44 to 0.94, predicting good strength of colour. The only difference between these two compounds is the methyl group on the N-phenyl substitutent and a bathochromic shift was seen when moving from compound **152g** to **151g** (as methyl group is not playing any role in absorption so structures **151g** and **152g** are similar). The calculations for two side products (**154** and **155**) isolated after during column chromatography of the crude compound of spirooxazines based on 3-methyl-1-*p*-tolylpyrazol-5-one were also carried out, (for more details see experimental section 3.3.3 a, iii). One of them was purple in colour **(154)** and other orange **(155)**. The UV-Visible spectra of both compounds were run to compare the experimental values with the calculated values. The experimental λ_{max} values for compound **(154**) were 550 nm and 365 nm while calculated values were 530 nm (f_{osc} 0.47), 449 nm (f_{osc} 0.20), 284 nm (f_{osc} 1.08). The structures of both compounds with the numbering scheme used to run the PPP-MO calculations are given in Figure 84.

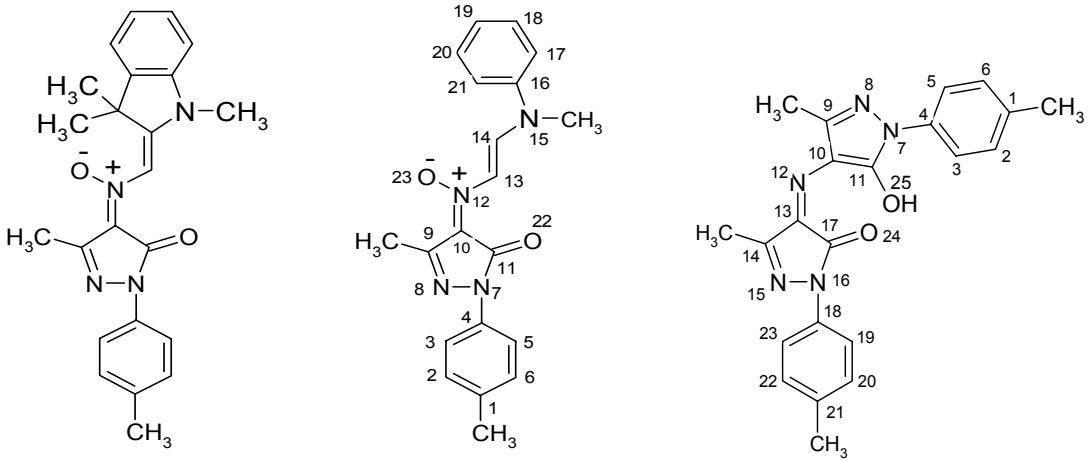

(154) **(154a)** **(155)**

Figure 84: N-Oxide **(154)**, approximation to compound **(154)** and compound **(155)**, for the PPP-MO calculations.

The data used for the PPP-MO calculation for compounds **(154)** and **(155)** is almost the same as used for the calculations of spirooxazines based on methyl phenyl pyrazolones

(Table 38). The only difference was the modification for the N-oxide group. The parameters for the N-oxide were taken from the literature [147] and are given in Table 47.

Table 47: Generalised set of the N-oxide parameters for the PPP-MO calculations for compound **(154)**.

Bond/atom specification	**VSIP eV**	**EA eV**	**Core Charge**	**β value eV**	**Bond length Å**
C-C ring	11.22	0.62	1	-2.37	1.39
C-N	24.24	8.03	1	-2.57	1.39
N-O	22.45	4.38	2	-2.0	1.28

The results obtained after using these values are given in Table 48.

Table 48: Results of calculated and experimental λ_{max} values of compounds **(154** and **155)**.

Compound	**Experimental λ_{max} (nm) (dichloromethane)**	**Calculated λ_{max} (nm) (f_{osc})**
(154) (Purple)	550, 365	530 (0.47), 449 (0.20), 284 (1.08)
(155) (Orange)	450, 335	459 (0.0004), 446 (0.43), 370 (0.20)

The calculations for compound **(154)** using a generalized set of parameters and for N-oxide using values of the N-O of the nitro group gave a higher λ_{max} value. The parameters for N-oxide from the literature gave a better value than the generalized parameters but still it was higher than the expected value which could be due to the fact that this calculation considers the molecule as planar while the actual molecules deviate from planarity.

In case of compound **(153b)**, the comparison of experimental and calculated λ_{max} values showed that the calculated values are in good agreement to the experimental values. There

is a difference of 18 nm between the experimental and calculated values which can be accounted due to the non-planarity of the compound. The results are given in Table 49.

Table 49: A comparison of λ_{max} values of compound **(153)** using generalized parameters.

Compound	**Experimental λ_{max} (nm) (dichloromethane)**	**Calculated λ_{max} using generalized parameters (nm) (f_{osc})**
153-Ring closed		368 (0.09), 346 (0.03), 299 (0.43)
153f		563 (0.53), 474 (0.71), 394 (0.05)
153g **(most stable isomer)**	540 **(153b)**	558 (0.53), 469 (0.83), 262 (0.83) **(153g)**
153h		522 (1.07), 438 (0.28), 265 (0.84)
153i		532 (0.99), 449 (0.21), 264 (0.83)

(ii) Attempted synthesis of N-oxide (162)

The reaction scheme used to synthesize N-oxide is given in Scheme 51.

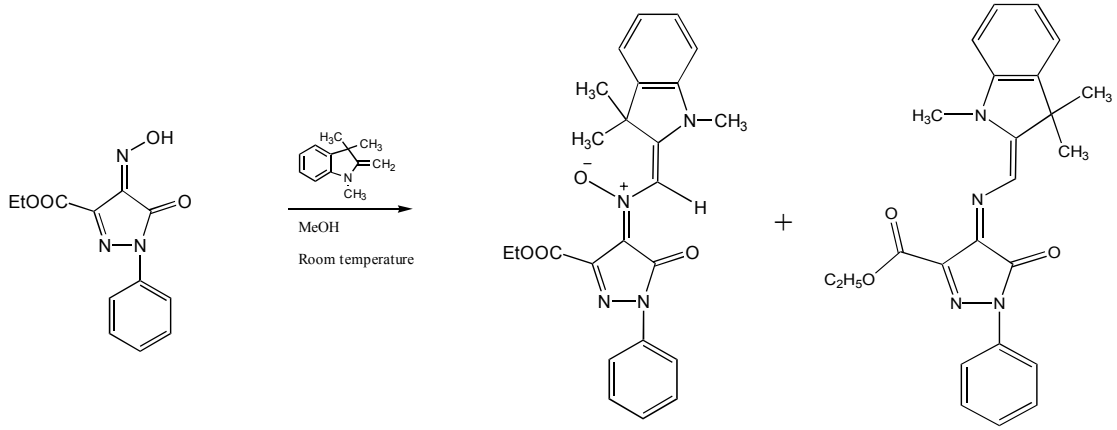

(161) **(162)** **(153a)**

Scheme 51: Synthesis of N-oxide **(162)**.

A room temperature reaction was carried out in an attempt to synthesize N-oxide **(162)**. The attempted synthesis of purple compound **(162)** was carried out using the same amount of starting materials as described in experimental section 5.5.10 (a). The reaction was carried out for a month. The mixture was cooled in a refrigerator for several hours and crystals of the compound were filtered. TLC of the filtered product showed that it contained red merocyanine form **(153a)** as the major product (75%) with only a trace of the purple compound **(162)**.

Mechanisms:

The formation of merocyanine **(151b)** and N-oxide **(154)** is proposed tentatively by the following mechanism.

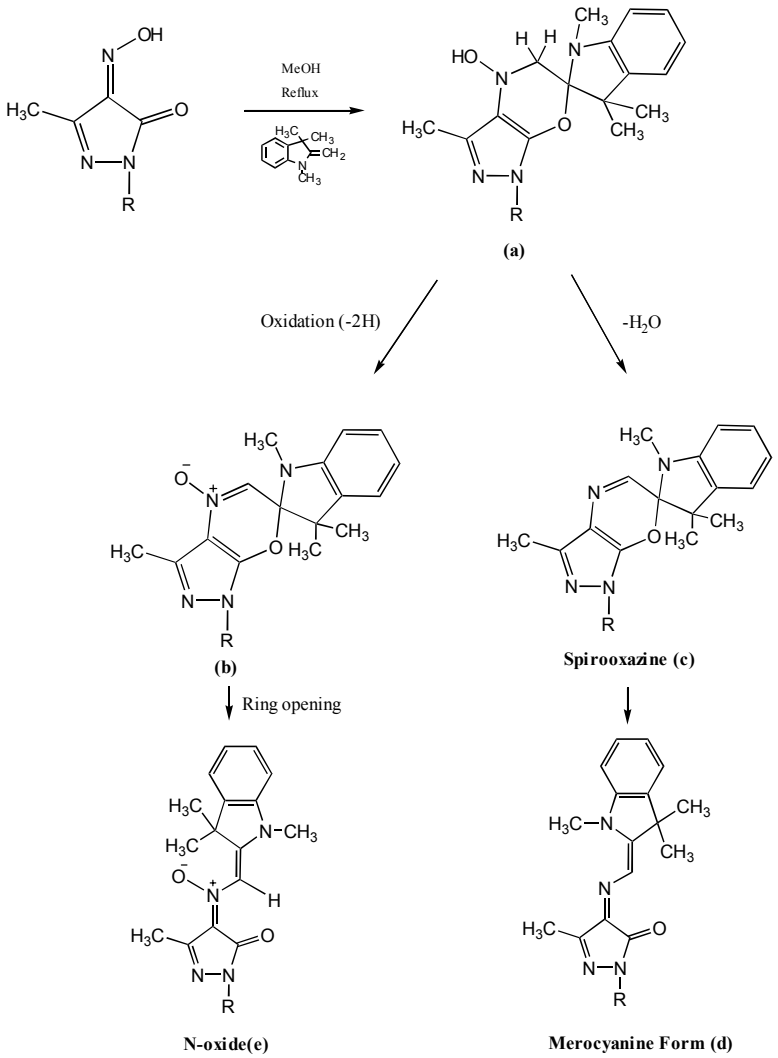

Scheme 52: Proposed mechanism for synthesis of N-oxide.

It is suggested that the reaction of isonitrosospyrazolone with Fischer's base provides an intermediate which can form the merocyanine form **(d)** as well as the N-oxide depending upon the reaction sequence. Dehydration of intermediate **(a)** can lead to spirooxazine **(c)** which provides the merocyanine form after ring opening of the weak C_{spiro} to oxygen bond. N-oxide formation was suggested as a result of oxidation of intermediate **(a)**. Intermediate **(b)** can give an N-oxide upon ring opening. The yellow product may be one of or a mixture of these. The formation of orange compound **(155)** probably results from a reductive self-condensation of **(157)**, the mechanistic details remain unclear. However, the reduction would be consistent with the need for an oxidation to form N-oxide **(154)**.

3.4 Nitrosospirooxazines

3.4.1 Molecular Modelling of nitrosospirooxazine

Molecular modelling techniques were used as a predictive tool to account the photochromic properties and the relative stabilities of the various species derived from quinoneoximespirooxazine **(163)**, the quinone oxime group being considered as a permanent chromophore. Ring closed and the merocyanine forms of nitrosospirooxazine **(163, a-d)** were subjected to computer–aided molecular modelling using the CAChe system as before. The structures of the ring closed form and the four possible merocyanine forms of compound **(163)** are given in Figure 85.

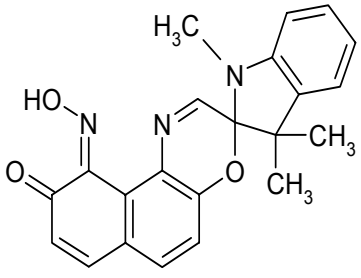

(163)

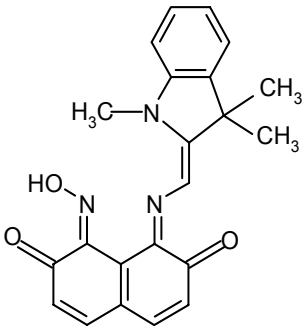

(163a)

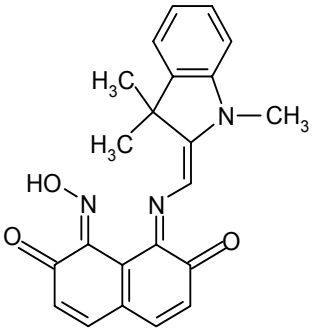

(163b)

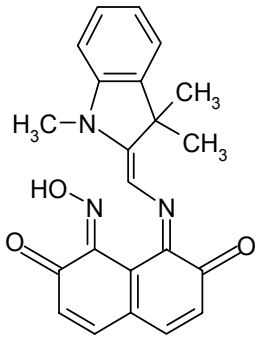

(163c)

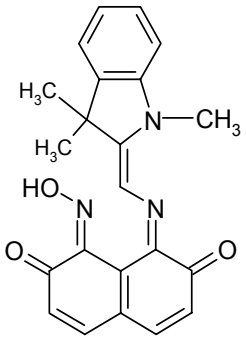

(163d)

Figure 85: The structures of ring closed and the four possible photomerocyanines from compound **(163)**.

The final energy (MM2 values) and heats of formation (AM1 values) of ring-closed and merocyanine forms of quinoneoximespirooxazine **(163)** are given in Table 50.

Table 50: Final energy values and heats of formation of compound **(163)**.

Compound	**Final energy (kcal mol^{-1})**	**Heat of formation (kcal mol^{-1})**
163-Closed form	2.62	64.17
163a	2.92	72.52
163b	6.91	76.00
163c	12.14	75.44
163d	10.30	78.22

The results given in Table 52 suggested that the most stable photomerocyanine form is **163a** and the order of stability in merocyanine forms of compound **(163)** is **163a** > **163b** > **163d** > **163c**. The energy minimized structures of compounds derived from MM2 calculations are shown in Figure 86.

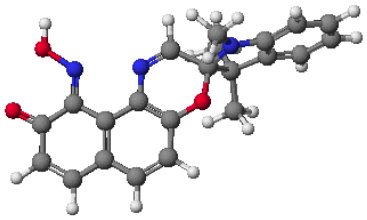

(163)

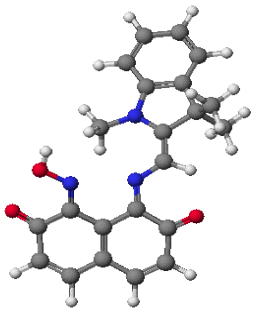

(163a)

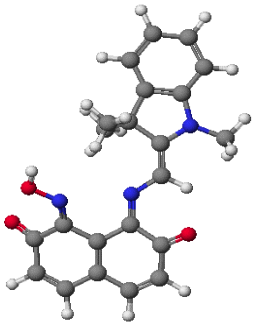

(163b)

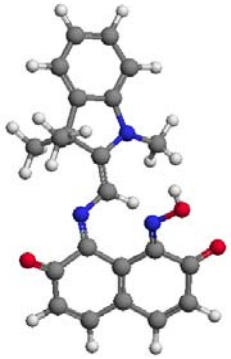

(163c)

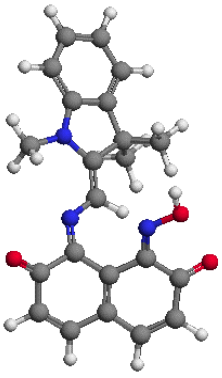

(163d)

Figure 86: The energy optimized (MM2) geometric structures of compound **(163)** and its merocyanine forms.

The comparison of stability can be correlated to inspection of the minimized structures of the merocyanine forms of compound **(163)**. The geometry of merocyanine form **(163a)** is the form in which there is the least steric constraint and thus least deviation from planarity as shown in Figure 87. Forms (**163c** and **163d**) are especially highly twisted out of planarity.

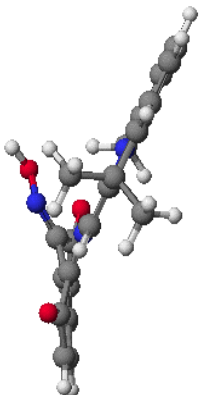

(163a)

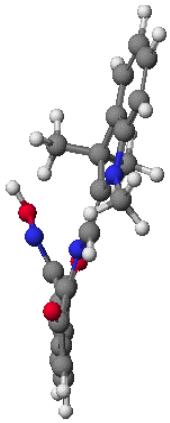

(163b)

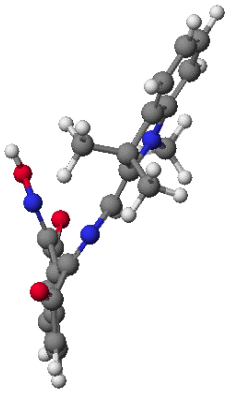

(163c)

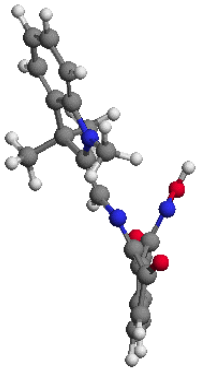

(163d)

Figure 87: The optimized (MM2) geometric structures of merocyanine form of compound **(163)** showing steric constrain in **163c** and **163d**.

3.4.2 PPP-MO Calculations

PPP-MO calculations for the ring-closed form and the merocyanine forms of compounds (**163)** were run. The modified structures making the approximations to the ring-closed form and merocyanine forms of compound **(163)** with numbering scheme used in the calculations are given in Figure 88.

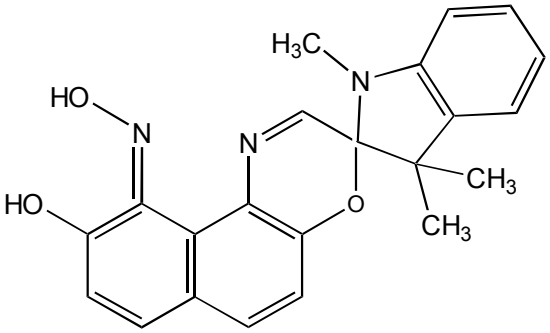

(163)

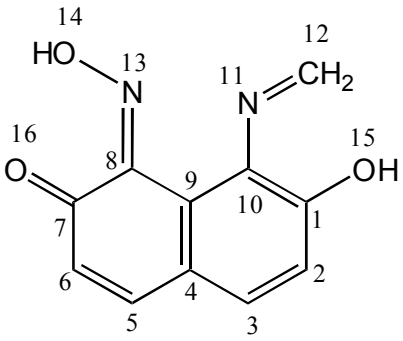

(163e)

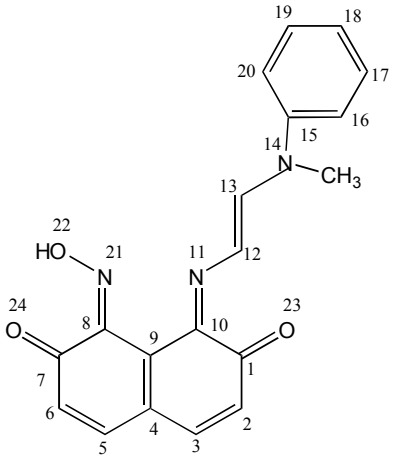

(163g)

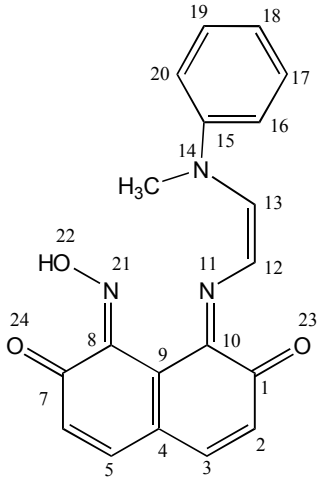

(163h)

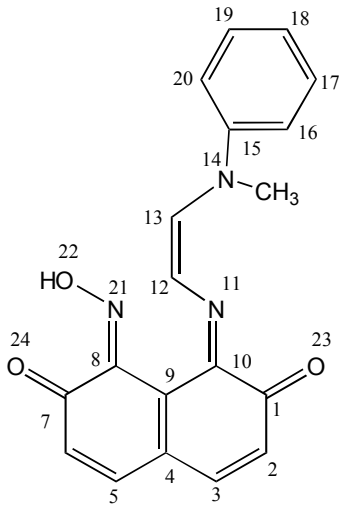

(163i)

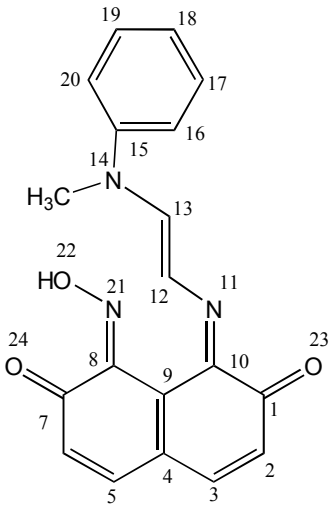

(163j)

Figure 88: Approximation to the ring closed form and photomerocyanine forms of spirooxazine **(163)** used for PPP-MO calculations.

A generalized set of parameters was used to run the calculations and is given in Table 11. The results obtained after the application of generalized parameters are given in Table 51.

Table 51: The results for the PPP-MO calculations for compound **(163)** using generalized parameters.

Compound	**Calculated λ_{max} (nm) (f_{osc})**
163e	433 (0.18), 350 (0.92), 284 (0.1), 232 (0.56)
163g	707 (0.2), 424 (1.9), 280 (0.34)
163h	660 (0.17), 453 (0.21), 417 (1.6)
163i	515 (0.15), 430 (0.68), 402 (1.03)
163j	511 (0.12), 450 (0.25), 395 (1.40)

The results of the PPP-MO calculations showed a bathochromic shift from the ring closed to the merocyanine forms. The λ_{max} values in the visible region ranged from 433-707 nm with low oscillator strength. The calculations were rechecked to confirm the unusual λ_{max} values of 707 nm and 660 nm but the results were the same after every calculation. The predicted colour for the ring closed form having λ_{max} value of 433 nm is yellow and if the compound shows photochromism the colour change will be from yellow to yellowish green.

3.4.3 Synthesis

The synthesis of nitrosospirooxazine **(163)** was attempted by the nitrosation of spirooxazine **(130)** and the details of the synthesis are given in experimental section 5.5.11. A crude brown product with moderate yield was obtained (21%). A flash column using toluene: ethanol (5%) as eluent was run to provide a reasonable product **(163)** (7%) but still with some impurities. The reaction is illustrated in Scheme 53.

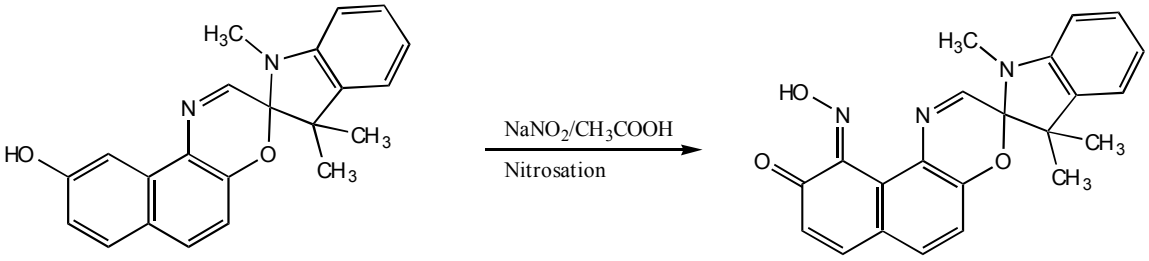

(130) **(163)**

Scheme 53: Attempted synthesis of nitrosospirooxazine **(163)**.

Analytical data

The compound decomposed without melting at 247^{o} C. The FTIR spectrum of the compound is given in experimental section 5.5.11. The absorption bands due to OH and C_{spiro}-O were observed at 3394 cm^{-1} and 932 cm^{-1} respectively. The ^{1}H NMR spectrum of compound **(163)** was run in deuterated chloroform. The spectral evidence was used to

confirm, in this case to a certain extent tentatively, the structure and numbering scheme used to identify the proton signals is given in Figure 89.

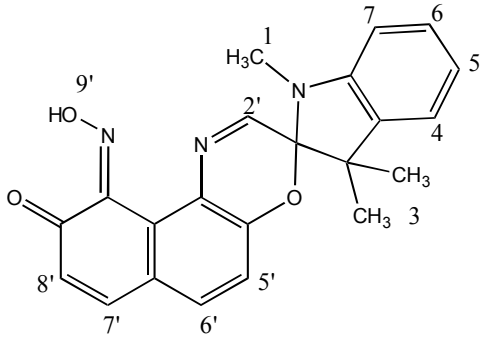

Figure 89: Proton numbering sequence for quinoneoximespirooxazine **(163)**.

The values assigned to each peak are given in Table 52.

Table 52: ^{1}H NMR spectral data for spirooxazine **(163)**.

Proton	**NMR signals, Chemical shift (ppm), Coupling constants (Hz)**
$N(CH_3)$	δ 2.87 (s, 3H, NCH_3)
$C(CH_3)_2$	δ1.49 (s, 6H, $(CH_3)_2$)
H_4	δ7.36 (d, 1H, $J_{4,5}$= 8.8)
H_5	δ6.72 (t, 2H $J_{6,5}$=7.9)
H_6	δ7.10 (t, 1H, $J_{5,6}$= 7.9)
H_7	δ6.60 (d, 1H, $J_{7,6}$=7.4)
$H_{2'}$	δ 7.80 (s, 1H)
$H_{5'}$	δ6.81 (d,1H, $J_{5',6'}$=8.6)
$H_{6'}$	δ7.62 (d, 1H, $J_{6',5'}$=9.2)
$H_{7'}$	δ7.86 (d, 1H, $J_{7',8'}$=8.3)
$H_{8'}$	δ6.79 (m, 2H)
$H_{9'}$	δ10.10 (s, 1H)

The NMR spectrum of compound **(163)** showed a distinct peak at δ1.49 ppm due to two C-methyl groups. Another singlet observed was at δ 2.87 ppm because of the $N(CH_3)$ group. The singlet characteristic of the oxazine proton (2′-H) was at δ 7.80 ppm. The interpretation of compound **(163)** is based on the values assigned to spirooxazine **(130)** (section 3.1.3, ii, a). The molecular formula of compound **(163)** is $C_{22}H_{19}N_3O_3$, with a molar mass of 373. The mass spectrum of compound did not show the expected molecular ion which could be due to the unstable nature of compound as well as being impure. The UV-visible spectrum of the compound showed a weak featureless absorption throughout the visible region. Further attempts failed to produce a product in higher yield and purity.

3.5 Azo-based naphthopyrans

3.5.1 Molecular Modelling of azo based naphthopyran

The successful synthesis of azospirooxazines is described in section 3.1.3. The analogous potentially photochromic dyes based on azonaphthopyrans were modelled using CAChe to provide final energy (MM2) and heats of formation (AM1). Two variations of three isomeric dihydroxynaphthopyran derivatives were modelled, without substituents and one with methoxy groups at the *para* positions to the two phenyl rings (which was ultimately used for the attempted synthesis). Only the nitro group on the phenylhydrazone ring was considered in this case. The comparative stability of the different forms and prediction of the potential photochromic behaviour were studied by comparing the energy values obtained from MM2 and AM1 calculations respectively. The structures of compounds (**165**, **167** and **169**) are given in Figure 90 together with the possible *transoid* photoproducts, only two in each case because of molecular symmetry.

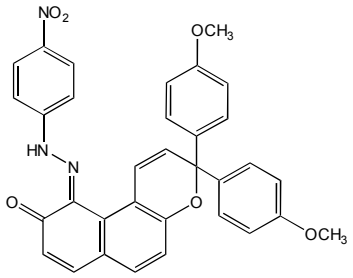

(165)

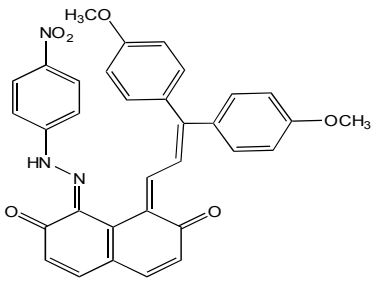

(165a)

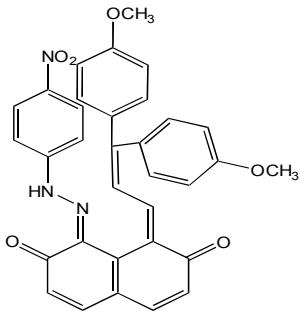

(165b)

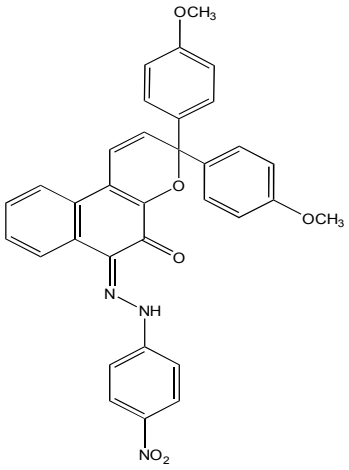

(167)

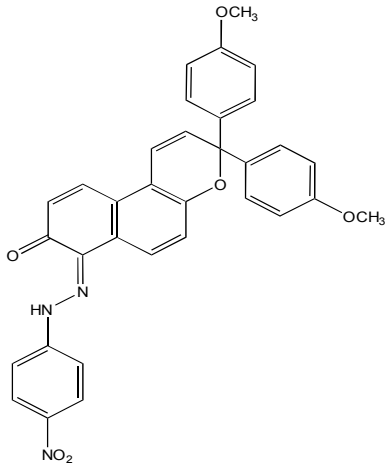

(169)

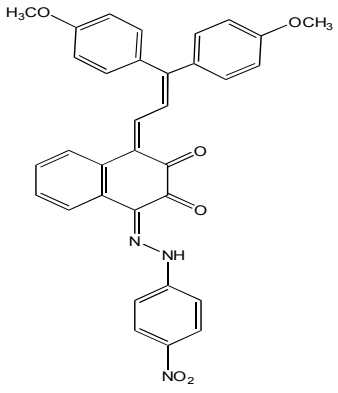

(167a)

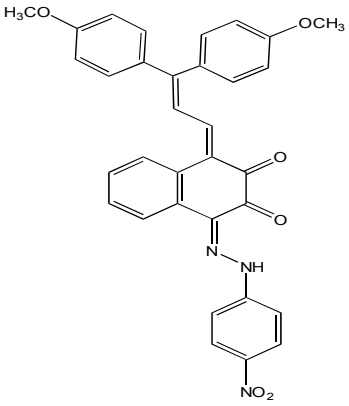

(167b)

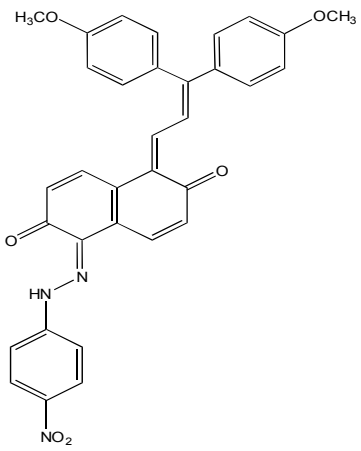

(169a)

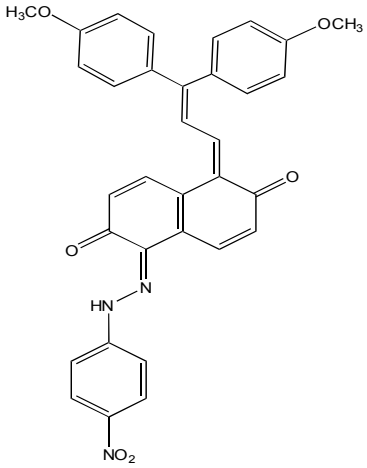

(169b)

Figure 90: Structures of dihydroxynaphthalene-based azonaphthopyrans (**165**, **167** and **169**)

The energy minimized structures of the naphthopyrans and their ring-opened forms are given in Figures 91-93.

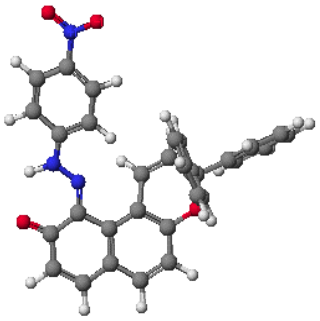

(164)

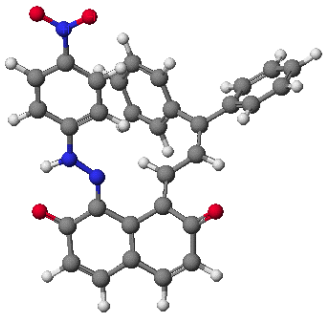

(164a)

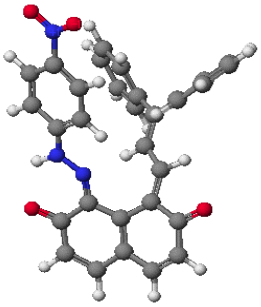

(164b)

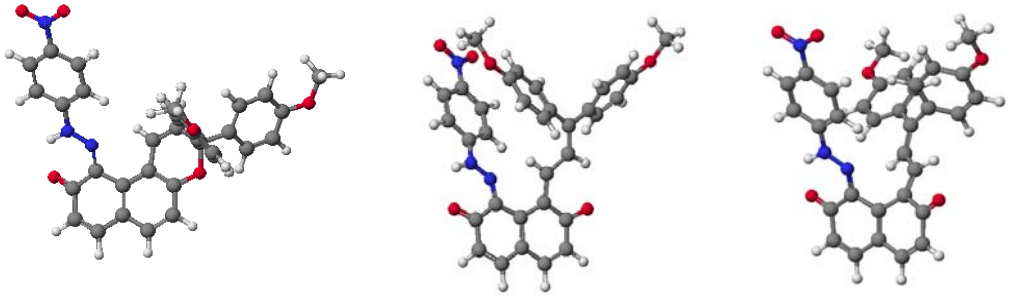

(165) **(165a)** **(165b)**

Figure 91: 2,7-Dihydroxynaphthalene-based, unsubstituted and substituted naphthopyran **(165)** and **(165)** with two *transoid* forms **(165a)** and **(165b)**.

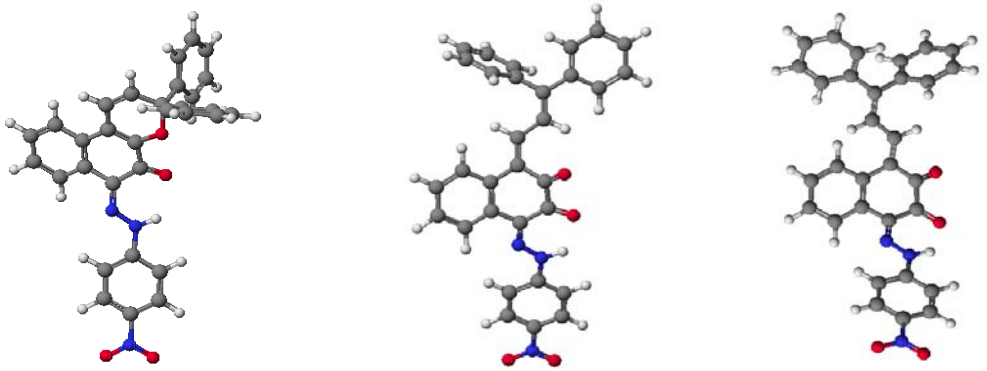

(166) **(166a)** **(166b)**

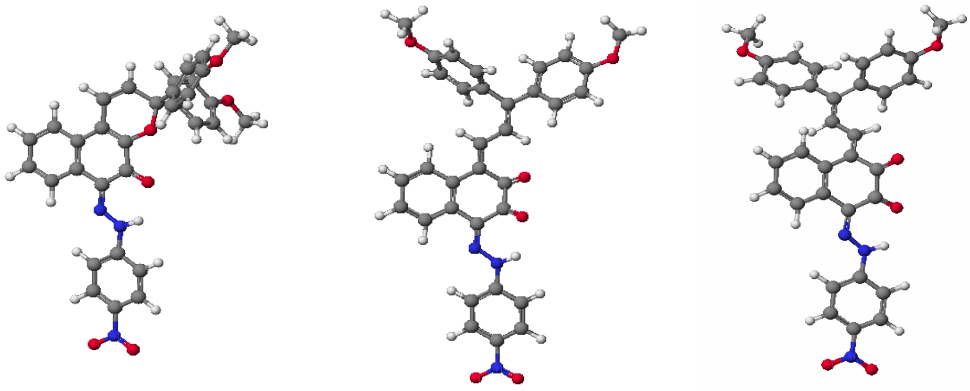

(167) **(167a)** **(167b)**

Figure 92: The structure of unsubstituted and substituted compounds **(166)** and **(167)** and the *transoid* forms.

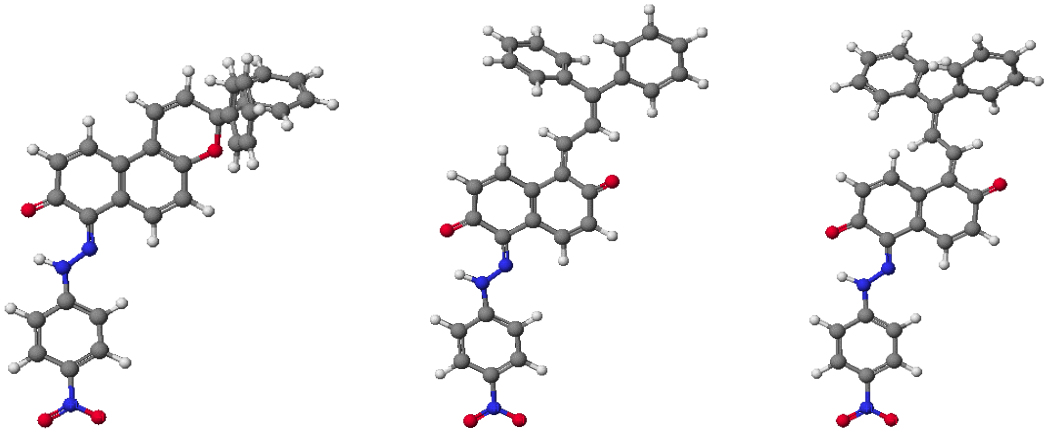

(168) **(168a)** **(168b)**

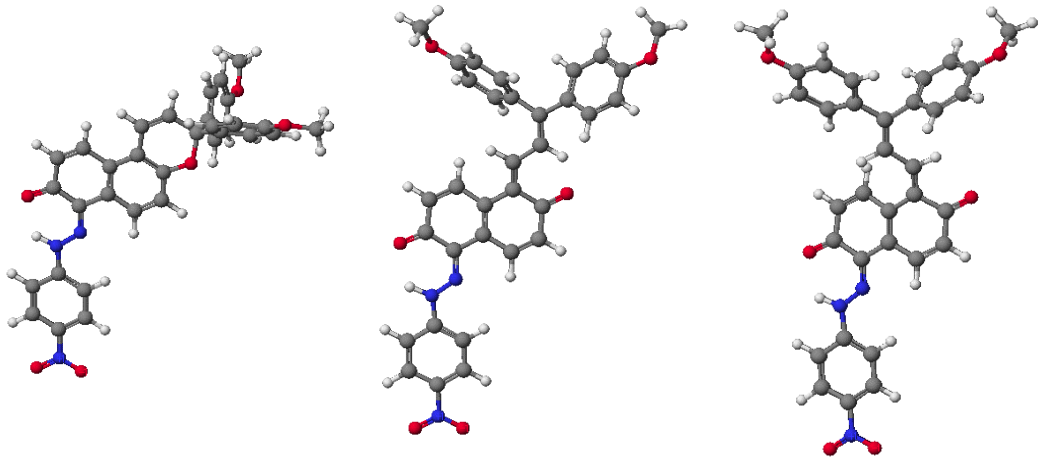

(169) **(169a)** **(169b)**

Figure 93: The structures of compounds **(168)** and **(169)** with the two-*transoid* isomers (**a-b**) of *transoid* forms.

The results of the calculations for compounds **(164-167)** are given in Table 53.

Table 53: Comparison of calculated MM2 and AM1 values of azo-based naphthopyran **(164-167)** and its *transoid* forms.

	2,7-dihydroxynaphthalene based azonaphthopyran				**2,3-dihydroxynaphthalene based azonaphthopyran**			
	Compound (164)		**Compound (165)**		**Compound (166)**		**Compound (167)**	
	MM2	**AM1**	**MM2**	**AM1**	**MM2**	**AM1**	**MM2**	**AM1**
	kcal mol^{-1}		**kcal mol^{-1}**		**kcal mol^{-1}**		**kcal mol^{-1}**	
Closed	-23.14	136.46	-20.41	60.45	-25.32	136.76	-22.60	60.78
a	-21.59	143.68	-19.60	67.26	-21.07	130.35	-20.66	53.57
b	-20.38	144.39	-16.81	69.54	-20.31	130.34	-18.13	54.72

For compounds **(168)** and **(169)**, the results are given in Table 54.

Table 54: Final energy and heats of formation of naphthopyrans **(168)** and **(169)**.

Compound	**Final energy (kcal mol^{-1})**	**Heat of formation (kcal mol^{-1})**
168-Closed form	-25.52	135.15
168a	-21.15	143.65
168b	-20.38	143.65
169-Closed form	-22.67	59.06
169a	-20.77	66.33
169b	-18.20	67.51

From the results given in Table 54 referring to Figure 93 (2,7-dihydroxynaphthalene based-azonaphthopyrans) showing each structure, final energy values (MM2) calculations predict that isomers (**164a** and **165a**) are the most stable of the two ring opened forms. The heat of formation values predict that compounds **(164)** and **(165)** might be photochromic in nature as the heat of formation values for the *transoid* forms are higher than the ring closed forms. Energy optimization calculations involving molecular mechanics (MM2) predicts

that structures **(166a)** and **(167a)** respectively are the most stable structures of two isomers (compounds **166** and **167**). The calculation of heats of formation (AM1) predicts that compound (**166** and **167**) might not show photochromic behaviour as the energy of the ring closed isomer is higher than the ring opened-isomers. In these cases the *transoid* forms might be isolated. In the case of compounds **(168)** and **(169)**, the prediction for photochromism is positive, which is similar to the prediction for the compound **(164)** and **(165)**. All the energy values from MM2 and AM1 calculations are given in Tables 55 and 56. Isomer **(a)** is the most stable in compounds **(164-169)** and the stability of these molecules can be correlated to the optimised geometric structures. In the case of compounds (**164** and **165**), the stability of isomers **(a)** can be explained by visual assessment of these structures which show the naphthopyran rings in close proximity to the *p*-nitrophenylhydrazone part of the molecule. The instability of isomers **(b)** in the case of compounds **(166-169)** can be explained by the close interaction of hydrogen of naphthopyran ring to the hydrogen of dihydroxynaphthalene part of the molecule.

3.5.2 PPP-MO Calculations

The theoretical data for electronic absorption spectra of the ring closed and the ring-opened forms of azonaphthopyrans were studied before proceeding to synthesis. The PPP-Molecular Orbital approach was used for that purpose. These structures were modified and assumed to be planar. Approximation to the structures of dihydroxynaphthalene-based azonaphthopyrans along with the numbering scheme used for the PPP-MO calculations are given in Figure 94.

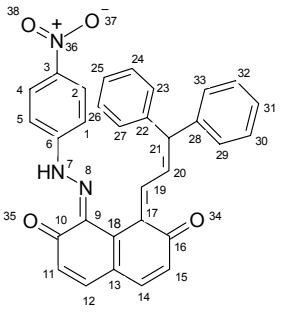

(164)

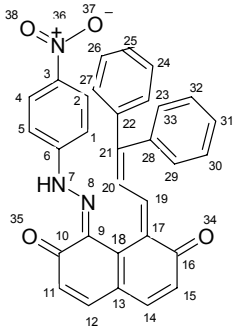

(164c)

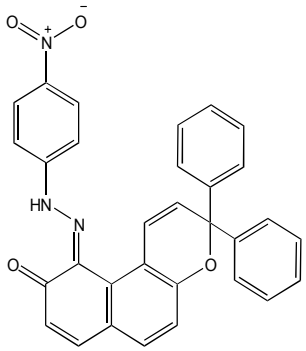

(164d)

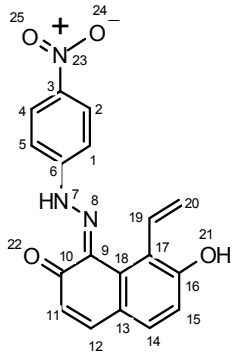

(164e)

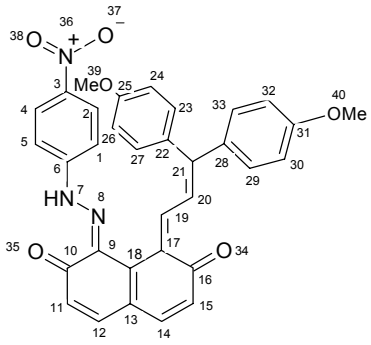

(165c)

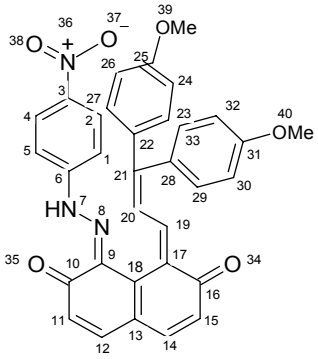

(165d)

Figure 94: 2,7-Dihydroxynaphthalene-based azo naphthopyrans, approximation to ring closed form and *transoid* forms.

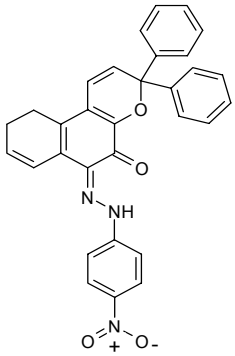

(166)

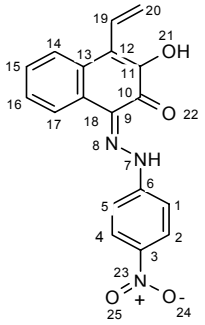

(166c)

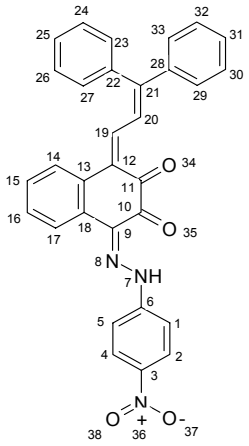

(166d)

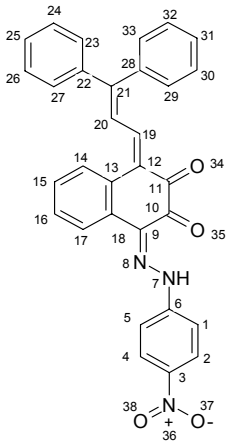

(166e)

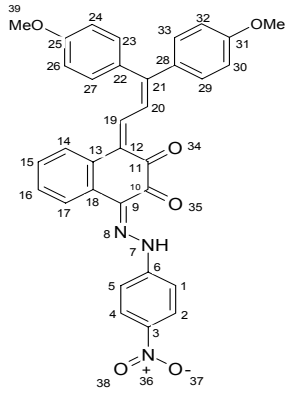

(167c)

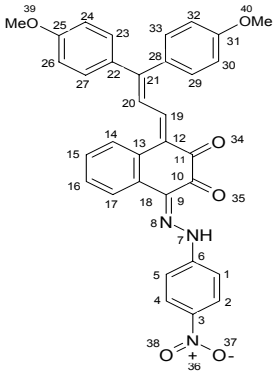

(167d)

Figure 95: Structures of 2,3-dihydroxynaphthalene-based azo naphthopyrans ring closed form, approximation to the ring closed and *transoid* forms for the PPP-MO calculations.

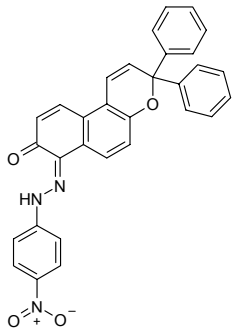

(168)

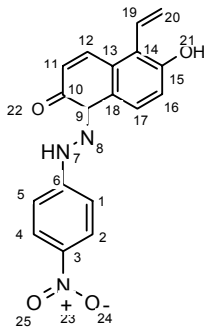

(168c)

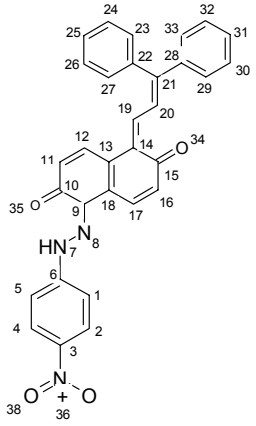

(168d)

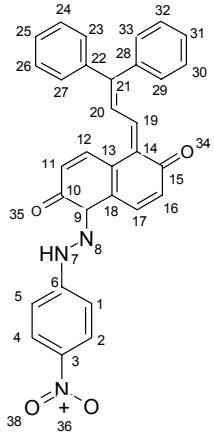

(168e)

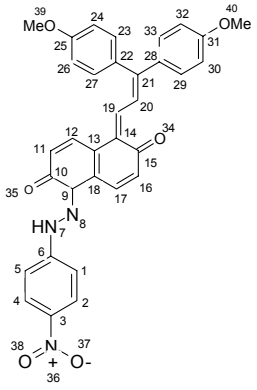

(169c)

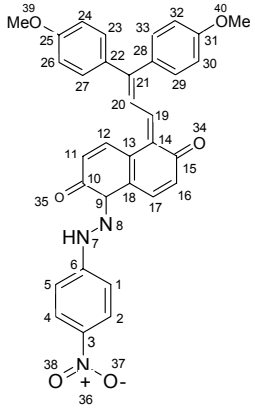

(169d)

Figure 96: 2,6-Dihydroxynaphthalene-based azo naphthopyrans, ring-closed, approximation to the ring-closed and *transoid* forms.

Two sets of calculations were run, one for the unsubstituted and other for the substituted azonaphthopyrans where the (-OCH_3) group is attached to the *para* position to each benzene ring. As the *p*-nitrophenylhydrazone unit of the molecules **(164-169)** was the same as azospirooxazines (see section 3.1.2), it was decided to use the optimised set of parameters for this part of molecule used for azospirooxazines. The optimised set of parameters used for the PPP-MO calculations are given in Table 55.

Table 55: An optimised set of parameters for the PPP-MO calculation.

Group, atom specification	**VSIP eV**	**EA eV**	**Core Charge**	**β value eV**	**Bond length Å**
Aryl ring (C=C)	11.16	0.03	1	-2.4	1.40
C=O	17.7	2.47	1	-2.46	1.22
C-OH (H-bonded)	28	10	2	-2.6	1.36
C-N=	11.16	0.03	1	-2.6	1.35
C-NH	18	8.50	2	-2.42	1.35
-C=N	15	0.97	1	-2.75	1.33
NO_2gp (C-N)	24.8	12.5	2	-2.0	1.49
N=O	21	2.5	1	**-3.8**	1.21
C=N(17,19)	15	0.97	1	-2.48	1.33
N-C(19,20)	11.16	0.03	1	-2.75	1.40

The reference molecule for the naphthopyran part of the molecule was taken from the literature.[149] The structure of the reference molecule and the relevant numbering scheme are given in Figure 97. The values used for PPP-MO calculations for the naphthopyran part of molecule are given in Table 56.

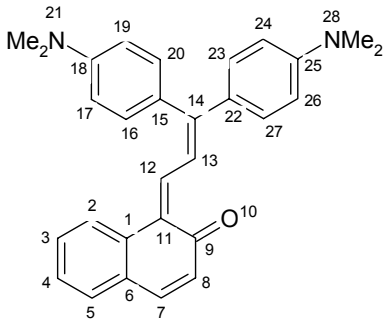

Figure 97: Reference molecule for the PPP-MO calculations of naphthopyran with numbering scheme **(R-3)**.

Table 56: The specified values for different bonds used for the PPP-MO calculations for the reference molecule

Bond and Parameters	**Specified value**
C=O (O 10), VSIP	16.0
C=O (O 10), EA	1.7eV
Alternating Carbon- Carbon β values	-2.35, -2.50eV
Carbonyl Carbon β value	-2.50eV

The results for the ring closed form in methoxy substituted and unsubstituted molecules are the same as the substituted part was not included in the calculations. The results of the optimization of the azo-based naphthopyrans are given in Table 57.

Table 57: Results of the PPP-MO calculations for naphthopyrans **(164-169)**.

Compound	**λ_{max} calculated (nm)**
164c (ring closed form)	480 (0.71), 398 (0.20), 335 (0.50), 312 (0.47)
164a (Unsubstituted isomer 1)	551 (0.43), 425 (0.36), 350 (1.04)
164b(Unsubstituted isomer 2)	601 (0.28), 521 (0.43), 367 (0.90)
165a (Substituted isomer 1)	535 (0.51), 508 (0.23), 427 (0.18), 373 (0.38)
165b (Substituted isomer 2)	565 (0.37), 524 (0.14), 436 (0.21)
166c (ring closed form)	474 (0.58), 445 (0.60), 332 (0.56)
166a (Unsubstituted isomer 1)	460 (1.97), 331 (0.16)
166b (Unsubstituted isomer 2)	459 (2.0)
167a (Substituted isomer 1)	456 (1.37), 453 (0.51)
167b (Substituted isomer2)	455 (1.45), 452 (0.52)
168c (ring closed form	472 (1.01), 395 (0.44), 329 (0.40), 307 (0.45)
168a (Unsubstituted isomer 1)	548 (1.31), 433 (0.13), 401 (0.32), 388 (0.38)
168b (Unsubstituted isomer 2)	546 (1.31), 400 (0.58), 385 (0.25)
169a (Substituted isomer 1)	550 (1.22), 433 (0.13), 400 (0.33), 384 (0.38)
169b (Substituted isomer 2)	547 (1.23), 396 (0.52), 381

The calculations predict an orange colour for the ring closed forms and red for the *transoid* form in the case of compound **(164-169)**. The potential photochromic behaviour might show the reversible conversion of the orange to red and vice versa. The values for both sets of naphthopyrans (unsubstituted and substituted) are given in Table 57.

3.5.3 Synthesis

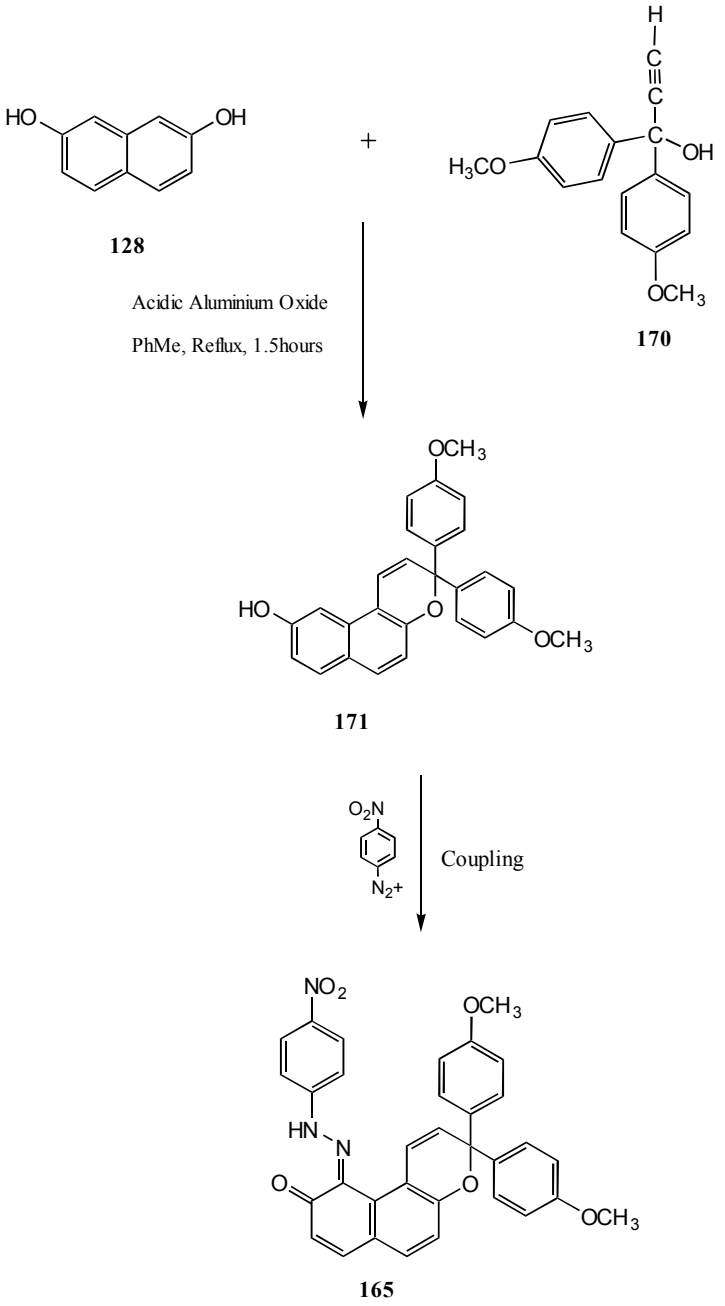

Scheme 54: Attempted synthesis of azonaphthopyran **(165)**.

(i) Synthesis of compound (171)

The synthesis of compound **(165)** was attempted by a two step reaction sequence. The first reaction was the synthesis of compound **(171)** which was coupled with diazotized *p*-nitroaniline. Compound **(171)** was synthesized by the reaction of 2,7-dihydroxynaphthalene **(128)** with 1,1-bis(4-methoxyphenyl)prop-2-yn-1-ol **(170)** using toluene as solvent. The experiment is explained in detail in section 5.5.11. The reaction gave a crude which was submitted to silica gel column chromatography using ethylacetate: hexane (20%) as eluent to give colourless product **(171)** (41%).

(a) Analytical data

DSC of the photochromic compound **(165)** showed the melting point of the compound was 210^{o} C and decomposed at 266^{o}C. The compound has been synthesised previously.[150] The FTIR spectrum of compound is given in experimental section (5.5.12, a). The molar mass of compound **(171)** was 410. Mass spectrum of compound **(171)** confirmed the compound. The ^{1}H NMR spectrum of compound **(171)** in deuterated dimethylsulphoxide was used to confirm the structure and the numbering scheme used to identify the proton signals is given in Figure 98.

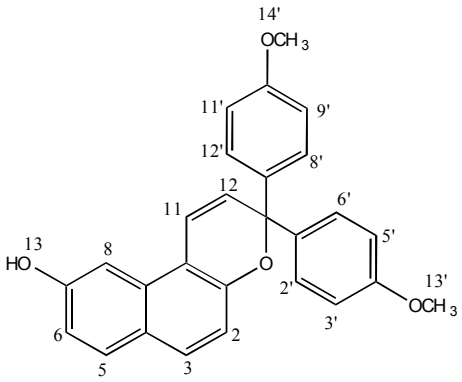

Figure 98: Proton numbering scheme of compound **(171)** for NMR analysis.

The assignment of each proton is shown in Table 58.

Table 58: ^{1}H NMR spectral data for compound **(171)**.

Proton	**NMR signals, Chemical shift (ppm), Coupling constants (Hz)**
$H_{13'}, H_{14'}$	δ 3.70 (s, 6H, -OCH_3)
O-H_{13}	δ9.77 (s, 1H, -OH)
$H_{2'}, H_{6'}, H_{8'}, H_{12'}$	δ7.33 (d, 4H, J= 8.7)
$H_{3'}, H_{5'}, H_{9'}, H_{11'}$	δ6.87 (d, 4H, J= 9.1)
H_8	δ7.15 (d, 1H, $J_{8,6}$=9.6)
H_6	δ6.97 (d, 1H, $J_{6,8}$= 8.8)
H_5	δ7.64 (d, 1H, $J_{5,3}$=4.8)
H_3	δ7.59 (d, 1H, $J_{3,5}$=4.7)
H_2	δ6.87 (d, 1H, J=9.1)
H_{11}	δ6.87 (d, 1H, $J_{11,12}$=9.9)
H_{12}	δ6.38 (d, 1H, $J_{12,11}$=9.9)

(b) Reaction Mechanism

The synthesis of compound **(171)** can be explained by the mechanism given in Scheme 55, which involves the protonation and loss of water from the propynol and generates the carbocation. The accepted mechanism is route A where the 2,7-dihydroxynaphthalene reacts with the carbocation. As a result of Claisen rearrangement (allyl aryl ethers, when heated, rearrange to o-allylphenols) and subsequent enolization the allenylnaphthalenediol is formed. The 1,5-H shift and an electrocyclization of intermediate gave the naphthopyran. It has been seen that by using the Lewis acid catalyst both the aromatic electrophilic substitution and a Claisen cyclic mechanism are in operation.[151]

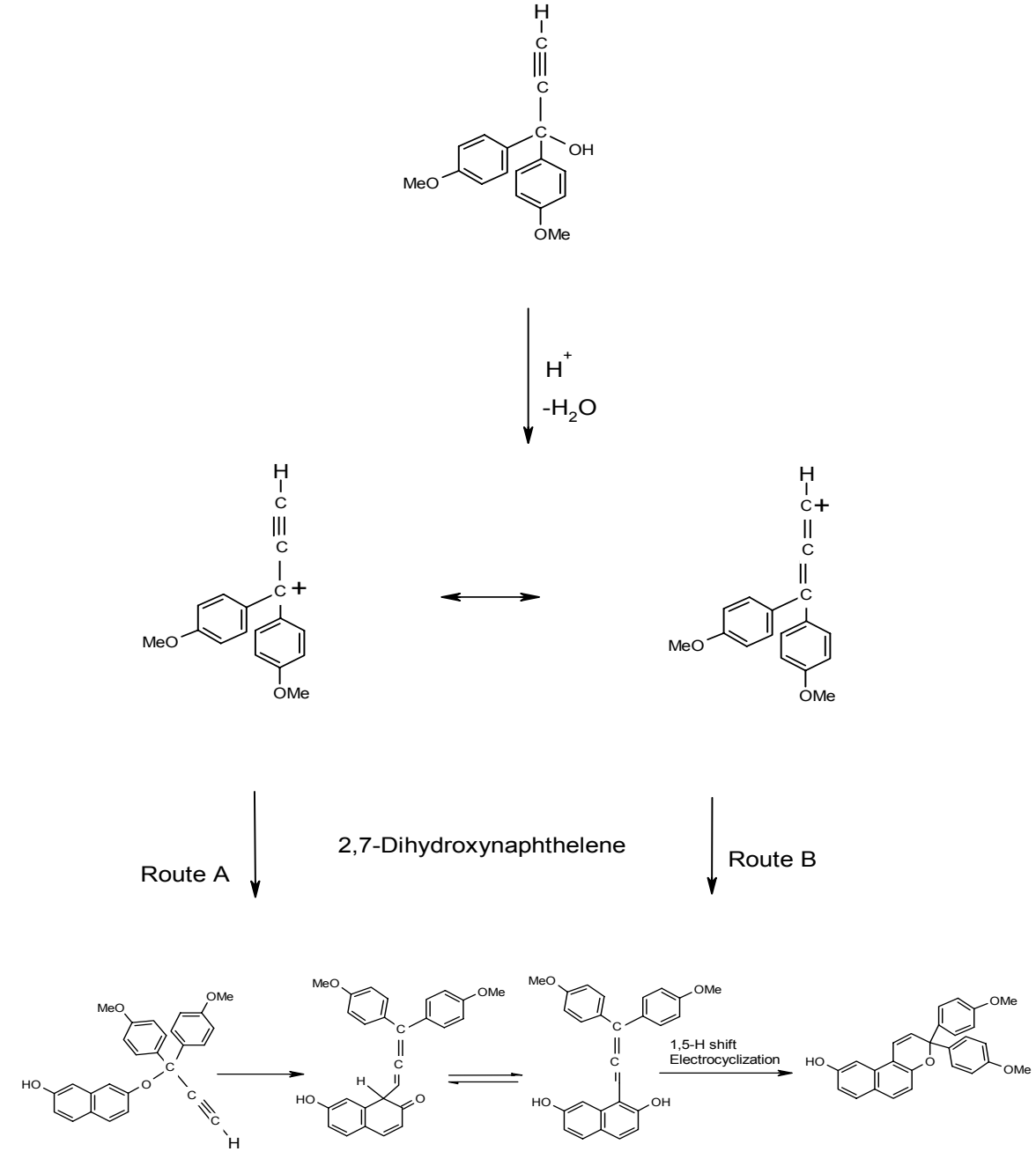

Scheme 55: Reaction mechanism for the synthesis of compound **(171).**

(ii) Synthesis of final product (165)

The attempted synthesis of azocompound **(165)** was carried out by the coupling of compound **(171)** with diazotized *p*-nitroaniline solution. The procedure is described in

detail in experimental section 5.5.12. The reaction mixture was allowed to stir overnight and pH at the end of reaction was 6.03. The precipitate were filtered, washed with water and weighed. The crude product (230mg) showed a red and an orange component by TLC. Recrystallization from ethanol was unsuccessful. Flash column chromatography of the crude product was run on silica using dichloromethane: acetone (10%) as an eluent. Two products, the minor red (10mg) and the major orange (90mg, 33%) were separated.

(a) Structural Analysis of Orange product

The orange compound decomposed without melting at 212^{o} C. The ^{1}H NMR spectrum of compound in deuterated dimethylsulphoxide was run and data are given in experimental section 5.5.12 (b). ^{1}H NMR data are not consistent with compound **(165)** so that its structure remains uncertain.

(b) Structural Analysis of Red product

A possible structure of the red compound is tentatively assigned as **(172)** in Figure 99. The FTIR spectrum of the compound is given in experimental section (5.5.12, b). Peaks due to OH and C=O were observed at 3448 cm^{-1} and 1680 cm^{-1} respectively. The molecular formula of the compound is $C_{33}H_{25}N_3O_7$ and consistent with a clear molecular ion in the mass spectrum at 575. An attempt was made to obtain single crystal for X-ray crystallography but the product was fibrous in nature and was not useful for the crystal structure determination. The ^{1}H NMR spectrum of the compound was measured in deuterated chloroform and the numbering scheme used to identify the proton signals is given in Figure 99. This compound is a potential oxidation product of compound **(165)**.

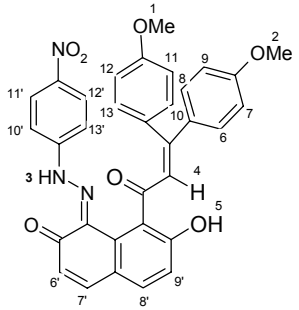

Figure 99: Proton numbering scheme for product **(172)**.

The assignment of each proton is shown in Table 59.

Table 59: ^{1}H NMR spectral data for red compound **(172)**.

Proton	**NMR signals, Chemical shift (ppm), Coupling constants (Hz)**
H_1	δ 3.86 (s, 3H, -OCH_3)
H_2	δ3.82 (s, 3H, -OCH_3)
H_3	δ3.62 (s, 1H N-NH)
H_4	δ7.28 (s, 1H C-H)
H_5	δ15.81 (s, 1H,C-OH)
$H_{6'}$	δ7.08 (d, 1H, $J_{5',4'}$= 8.2)
$H_{7'}$	δ7.59 (d, 1H, $J_{6',7'}$=9.5)
$H_{8'}$	δ7.36 (d, 1H, $J_{7',6'}$=8.2)
$H_{9'}$	δ6.5 (d, 1H, $J_{7',6'}$=9.9)
$H_{6,8,10,13}$	δ7.30 (d, 4H, J=8.27)
$H_{7,9,11,12}$	δ6.88 (m,4H)
$H_{10'13'}$	δ7.67 (d, 2H, J=9.4)
$H_{11'12'}$	δ8.27 (d, 2H, J=9.0)

4 Conclusions

A series of photochromic dyes containing a permanent chromophore were modelled and attempt was made to synthesize selected compounds. Two different classes of photochromic dyes selected were spirooxazines and naphthopyrans although most of the work centred on the former. Molecular modelling of molecules was carried out using CAChe and the potential colour of photochromic dyes was also predicted using the PPP-MO calculations. Synthesis of selected molecules was carried out.

Molecular modelling of dihydroxynaphthalene-based azospirooxazines (in the hydrazone form) suggested that isomer **(a)** is the most stable photomerocyanine form in case of compounds 2,7-dihydroxynaphthalene-based azospirooxazines while isomer **(b)** was the most stable in the case of 2,3- and 2,6-dihydroxynaphthalene-based azospirooxazines. The prediction for photochromism was ambiguous in the case of azospirooxazines based on 2,3-dihydroxynaphthalene because of heats of formation values being close to each other and the other compounds were potentially photochromic according to the comparison of heats of formation values. The calculated λ_{max} values using the PPP-MO approach showed a bathochromic shift when moving from isomer based on 2,7-dihydroxynaphthalene to spirooxazines based on 2,6-dihydroxynaphthalene. The calculated values were in reasonable agreement with the experimental values. Synthesis of all three isomers of dihydroxynaphthalene based spirooxazines was attempted using the azo group derived from *p*-nitroaniline as a permanent chromophore. 2,7-dihydroxynaphthalene-based azospirooxazines and 2,3-dihydroxynaphthalene-based azospirooxazines isomers were successfully synthesized in their ring closed form while 2,6-dihydroxynaphthalene-based azospirooxazines in its crude form was isolated and identified as the ring closed form by a clear proton NMR signal obtained at δ7.82 ppm. Three different synthetic routes were used for the synthesis of 2,7-dihydroxynaphthalene-based azospirooxazines. All the routes involved nitrosation, reaction with Fischer's base and coupling with diazotized *p*-nitroaniline but differ in the sequence of reactions and the successful route which gave high yield and purity was selected for the synthesis of other isomers. The nitrosation reaction of starting materials provided oximes. The reaction of these oximes with Fischer's base provided photochromic spirooxazines which showed a reversible transformation upon UV-irradiation from blue to colourless.

2,7-dihydroxynaphthalene-based azospirooxazine was converted on a silica chromatography column to an azoamide, whose structure was confirmed by a single-crystal X-ray crystallography. A mechanism was proposed for the conversion which may provide an insight into the reasons underlying the instability of spirooxazines towards aqueous acidic conditions.

Interesting and unusual photochromic behaviour was observed in the case of azospirooxazine-based on 2,7-dihydroxynaphthalene, a reversible colour change from orange to grey upon UV-irradiation was observed, and the grey colour turned back to orange after the removal of light source. It was a slow reversible change illustrated by the UV-visible spectra of the samples run before and after irradiation and also after keeping them in the dark. The photochromic behaviour was unusual because a dilute ethanolic solution of the sample on exposure to UV-irradiation of the orange solution was observed almost colourless. Some degradation of photochromic azospirooxazine was also observed when solution in ethanol was irradiated with UV-light for 120 minutes and then kept in the dark for 113 hours.

The comparison of relative stabilities of the merocyanine forms in case of anthraquinone and naphthoquinone-base spirooxazines was also made and it was observed that MM2 calculations does not adequately predict hydrogen bonding in theses molecules because energy minimised structures showed an unexpected hydrogen position. The prediction of photochromism was negative in both cases. PPP-MO calculations for the ring closed forms of spirooxazines based on anthraquinone and naphthoquinone suggested an orange colour for both ring closed forms. Synthesis of spirooxazines was attempted but isolation of products proved problematic.

A stable merocyanine **(b)** was isolated from attempts to synthesise spirooxazines based on pyrazolones. A correlation was found between the molecular modelling and the spectral properties of the product obtained. The predicted λ_{max} values from the PPP-MO calculations were in reasonable agreement to the experimental values and the compounds were predicted to show strong colours (high oscillator strength) in the range red to purple (500 nm – 550 nm). Reaction of nitrosopyrazolone compounds with Fischer's base provided a crude product which on TLC showed red, yellow, orange and purple

compounds. The yellow compound was unstable which, during attempted isolation converted to a mixture of red and purple compounds. The analysis of red compound proved that it is a merocyanine while the purple compound was an N-oxide whose structure was confirmed by X-ray crystallography. The isolation of red and purple compounds proved difficult in case of spirooxazines based on 3-ethoxycarbonyl-4-nitroso-1-*p*-phenylpyrazol-5-one. An orange compound was isolated during the synthesis of spirooxazines based on 3-methyl-4-nitroso-1-*p*-tolylpyrazol-5-one and identified by X-ray crystal structure. Mechanisms for formation of the N-oxide and orange compound were also proposed.

Nitrosospirooxazines were modelled and the results suggested that the most stable isomeric photomerocyanine form is **(163a)** and the compound has potential to show photochromism. Nitrosation of 2,7-dihydroxynaphtahalene provided a crude compound. A clear proton NMR signal for position 2′ was observed at δ7.80 ppm which confirmed the existence of the nitrosospirooxazine in the ring closed form. The mass spectrum of the compound showed some unexpected signals and after a few attempts to obtain a pure compound further investigation was not carried out.

Two types of azo (hydrazone)-based naphthopyrans were modelled. Three isomers of methoxy-substituted and unsubstituted naphthopyrans were modelled. The results showed isomer **(a)** was the most stable photomerocyanine forms in each case. Isomers based on 2,3-dihydroxynaphthalene-based naphthopyrans were potentially non-photochromic while the rest of the isomers were predicted to be photochromic. The PPP-MO calculations in case of 2,7-dihydroxynaphthalene-based naphthopyrans predicted orange colour for the ring-closed from and red for the *transoid* merocyanine form.

Synthesis of 2,7-dihydroxynaphthalene-based naphthopyrans was attempted and an intermediate with a good yield was obtained. Coupling of the intermediate with diazotized *p*-nitroaniline provided an orange product which upon characterization could not be identified as compound **(165)** and its structure remains unknown. A red product was also isolated during this reaction which after characterization is suggested to be an oxidation product of the naphthopyran **(165)**.

The only photochromic colour change observed was in case of compound **(122)** showing a reverse colour change from orange to grey. A very significant aspect of the future work could be the introduction of other chromophores to the photochromic systems to achieve colour change for a wide range of colours. Before proceeding to synthesis, it is quite reasonable to run the PPP-MO calculations to predict the potential colour of molecule.

It can be concluded overall that the molecular modelling technique provided a reasonable account of the relative stabilities as well as the prediction on photochromism for most of the molecules. After running the MM2 calculations a clear pattern of the most stable molecules was observed. The visual assessment of azospirooxazines showed that structures having the $C(CH_3)_2$ group of indoline ring in very close proximity to the *p*-nitrophenylhydrazone part of the molecule show considerable steric constraint involving the interaction of hydrogens. The structures having the N- CH_3 group of indoline ring close to the *p*-nitrophenylhydrazone part are more stable because of less steric constraint. Similar pattern was observed in most of the energy minimised molecules. Exact results can not be expected from the PPP-MO calculations because of the assumption that the molecules are planar while in fact the molecules are non-planar, though the degree of non-planarity may vary from molecule to molecule. Synthesis of selected molecules was carried out and purification of the final products proved problematic in many cases. The instability of compounds caused problems during purification and conversion to other side products was commonly observed. Photochromic properties of some azospirooxazines were also tested. An azospirooxazine proved to be photochromic and a reversible change from orange to grey was observed after irradiation of UV-light showing a slow thermal reverse reaction.

5 Experimental

5.1 Health and safety

The potential hazards were assessed before carrying out the reactions. Appropriate documentation for the Control of Substances Hazardous to Health (COSHH) Regulations was completed. A laboratory coat, safety glasses and gloves were worn as a safety measure in the laboratory and a fume cupboard was used to carry out all the reactions.

5.2 Instrumentation

5.2.1 DSC (Differential Scanning Calorimetry)

The melting points were determined as peak temperatures on a Mettler DSC 12E using a heating rate of $10^{o}C\ min^{-1}$ from 30-400^{o}C.

5.2.2 FTIR (Fourier Transform Infrared Spectroscopy)

Infrared spectra were recorded as KBr discs with a Nicolet Protégé 460 Fourier Transform Spectrophotometer and a Nicolet Avatar 370 DTGS spectrometer from Thermo Electron. The software used for both instruments was EZ OMNIC.

5.2.3 NMR (Nuclear Magnetic Resonance Spectroscopy)

NMR spectra were recorded on a Bruker AC 200 instrument, ^{1}H at 200 MHz and a Bruker DPX400 instrument for ^{1}H at 400 MHz.

5.2.4 Mass Spectroscopy

Mass spectra were recorded at 180^{o} C, on a Kratos Concept 1S spectrometer which was operated in low resolution EI (Electron Impact) mode.

5.2.5 CHN Analysis (Elemental Analysis, EA)

Microanalysis for C, H and N was carried out on an Exeter Analytical CE440 analyser with the industry standard error of +/- 0.3% on each of the three elements analysed.

5.2.6 UV-Visible Spectroscopy

UV-Visible Spectra were recorded on a Perkin-Elmer UV-VIS LAMBDA 2 spectrophotometer for solutions in dichloromethane.

5.2.7 Single X-ray crystallography

Single crystal X-ray diffraction data were collected on a Bruker Nonius X8-Apex 2 CCD diffractometer at 100K cooled with an Oxford Cryosystems Cryostream.

5.2.8 Fluorescence spectrometer

The spectrophotometer used for irradiation of samples for assessing photochromic properties was a Perkin Elmer LS-3 Fluorescence Spectrometer.

5.2.9 UV-Lamps

Two different UV-lamps were used for irradiation to examine photochromism; a Philips 365 nm (40 Watt) and Philips 254 nm (40 Watt).

5.3 Molecular Modelling Calculations (CAChe Computational Applications)

The molecules were modelled in CAChe [132] Work Space in order to view atomic properties such as hybridization. MM2 (molecular mechanics) force field calculations provided final energy values of the molecules which were used to compare the stability of isomers. AM1 (Austin Model 1) semi-empirical calculations were used to determine the heats of formation. These values were use to predict the potential photochromic behaviour of the molecules. ZINDO calculations were used for selected molecules to calculate UV-visible spectra.

5.4 PPP-MO Calculations

The Pariser-Pople-Parr (PPP) approach was used for the calculation of the UV/visible spectral properties of the ring closed and merocyanine forms. A standard method for PPP-MO calculations was initially used using a generalized set of parameters within the fixed β approximation [152] A modified set of parameters for the spirooxazines derived from previous investigations in these laboratories was also used.[153] Two-centre

repulsion integrals were determined using the Nishimoto-Mataga relationship [154] and electronic excitation energies were refined by a limited configuration interaction treatment which involved nine singly-excited configurations obtained by promoting an electron from the three highest occupied molecular orbitals to the three lowest unoccupied molecular orbitals.

5.5 Synthesis

5.5.1 Synthesis of spirooxazine dye (122) (Route 1)

(a) Synthesis of 2,7-dihydroxy-1-nitrosonaphthalene (129) [133,142]

To a 250cm^3 three- necked flask equipped with a mechanical stirrer and addition funnel 2,7-dihydroxynaphthalene **(128)** (6.95g, 0.043mol) and sodium hydroxide solution (75cm^3, 0.6 M) were added. The mixture was cooled to 0^{o}C with an ice-salt bath and sodium nitrite (3g, 0.043mol) was added. With stirring, concentrated sulphuric acid (5cm^3, 0.18mol) was slowly added to the mixture such that the temperature was maintained at 0^{o}C. 2,7-Dihydroxy-1-nitrosonaphthalene **(129)** precipitated out during the addition as a dark brownish precipitate. The mixture was allowed to stir for 1 hour at low temperature after the addition of sulphuric acid. The precipitate was suction-filtered, thoroughly washed with water and allowed to air dry for 2-3 days. 2,7-Dihydroxy-1-nitrosonaphthalene **(129)** (7.47g, 92%) was obtained. The compound decomposed without melting at 228^{o}C (lit m.p. 285^{o}C).

(b) Synthesis of Spirooxazine (130) [98, 133]

2,7-Dihydroxy-1-nitrosonaphthalene **(129)** (4g, 0.022mol) and absolute ethanol (40cm^3) were added to a 100cm^3 round bottom flask equipped with a condenser, addition funnel and stirring bar. The mixture was gently refluxed and stirred while a solution of 1,3,3-trimethyl-2-methyleneindoline (Fischer's base) **(70)** (7.0g, 0.024 mol) and absolute ethanol (24cm^3) was added over a 30-minute period. The mixture was refluxed for 3 hours and then rotary evaporated to approximately one third of the original volume. The dark viscous material was allowed to stand overnight, suction filtered and the residue rinsed with

cold ethanol to give the crude spirooxazine compound **(130)** (4.03g, 56%). Two recrystallizations from ethanol gave 3.4g (47%) of a light brown product **(130)**, m.p. 218^{o}C (lit m.p. 167-173^{o} C). ν_{max}(KBr)/cm^{-1}: 3401 (O-H st), 2967 (C-H st), 1485, 1448 (aromatic C-C st), 1353 (O-H), 1247, 976 (C_{spiro}-O st), 838 (Ar-H).

(c) Synthesis of Spirooxazine (122)

(i) Preparation of diazotized *p*-nitroaniline solution

p-Nitroaniline (1.04g, 0.0075mol) was stirred with concentrated hydrochloric acid (7.5cm^3). With stirring over 2 minutes, a solution of sodium nitrite (0.53g, 0.0075mol) in water (6.8cm^3) was added while keeping the temperature below 5^{o}C by the addition of ice. An excess of nitrous acid was demonstrated by starch/KI paper. The mixture was stirred for 20 minutes at 5^{o}C during which time the suspension converted into a solution. Just before coupling, a few drops of sulphamic acid solution were added to remove the excess of nitrous acid. Because of the difficulty of handling small amounts of the reactants, a solution of diazotized *p*-nitroaniline **(131)** (0.0075mol) was prepared and one fifth of the total solution was used for the reaction with the spirooxazine solution.

(ii) Reaction of spirooxazine (130) with diazotized *p*-nitroaniline

The spirooxazine **(130)** (0.34g, 0.001mol) was dissolved in ethanol (25cm^3) and heated gently at 40^{o}C for 2-3 minutes, to dissolve the compound and then the solution was cooled. A solution of sodium hydroxide (0.6g, 0.15mol) in water (3.2cm^3) was added and the mixture was stirred for 20 minutes. After that, anhydrous sodium acetate (2.5g) was added and the mixture stirred for 30 minutes. The diazonium salt solution **(131)** was run into the coupling component solution **(130)** over about 30 minutes and no excess of the diazo was observed as confirmed by the H-acid test. The pH of the reaction after complete addition of the diazo solution was 13.3. After overnight stirring the pH had dropped to 12.1 and was lowered further with dilute acetic acid to give a pH of 6. The precipitate was filtered and dried. A brown product **(122)** (0.52g) was obtained. Recrystallization from ethanol gave compound **(122)** (0.27g, 55%) as a brown product which decomposed without melting at 220^{o}C. ν_{max}(KBr)/cm^{-1}: 3435 (N-H st), 2975 (C-H st), 1626 (C=O, weak), 1595,

1572 (aromatic C-C st), 1487, 1334 (NO_2 st), 1160, 977 (C_{spiro}-O st), 845, 745 (Ar-H); m/z (EI) (relative intensity, %): 493 (M^+, 5), 356 (38), 340 (39), 158 (56), 138 (79), 108 (4), 83 (100), 65 (57), 48 (92). The UV-Visible spectrum in dichloromethane gave λ_{max} values of 481 nm, 355 nm and 343 nm with respective molar extinction coefficients of 2.42 x 10^4 $M^{-1}cm^{-1}$, 1.42 x 10^4 $M^{-1}cm^{-1}$and 1.58 x 10^4 $M^{-1}cm^{-1}$.

The product was chromatographed on a column of silica using dichloromethane initially and later using dichloromethane: acetone (0.5%). The brown compound (0.27g, 0.0005mol) was unstable on the column and converted to an orange product. The orange product **(134)** (0.17g, 33%) was obtained from the eluates and was recrystallized from ethanol. The yield obtained after recrystallization was 45mg (9%). The product decomposed without melting at 287^{o}C. ν_{max}(KBr)/cm^{-1}: 3436 (N-H, st), 1698 (C=O st), 1594, 1490 (Aromatic C-C st), 1336 (NO_2 st), 910 (C_{spiro}-O st), 746; m/z (EI) (relative intensity, %): 511 (M^+, 7), 509 (79), 481 (15), 372 (40), 359 (18), 344 (11), 331 (4), 254 (6.5), 158 (100), 144 (45). Found C, 64.23; H, 4.53; N, 12.09; $C_{28}H_{25}N_5O_5$ requires C, 65.74; H, 4.93; N, 13.69%. The UV-visible spectrum in dichloromethane showed λ_{max} values of 500 nm, 340 nm and 340 nm with respective molar extinction coefficients of 2.36 x 10^4 $M^{-1}cm^{-1}$, 1.33 x 10^4 $M^{-1}cm^{-1}$ and 1.54 x 10^4 $M^{-1}cm^{-1}$.

5.5.2 Synthesis of spirooxazine dye (122) (Route 2)

2,7-dihydroxynaphthalene **(128)** (0.39g, 0.002mol) was nitrosated with sodium hydroxide (0.66g, 0.016mol) and sodium acetate (2.76g) using the same procedure as described in section 5.5.1 (a). A solution of diazotized *p*-nitroaniline was prepared as described in section 5.5.1. (c, i) using *p*-nitroaniline (0.276g, 0.002mol) and sodium nitrite (0.14g, 0.002mol). The azo coupling reaction was carried out in the same manner as described in section 5.5.1 (c, i). The pH at the end of the coupling reaction was 9.3. The yield of the product **(129)** obtained was 0.59g (85%). ν_{max}(KBr)/cm^{-1} 3431 (N-H, st), 3167 (C-H st), 1636 (C=O), 1576, 1437 (Aromatic C-C st), 1343 (NO_2 st), 749 (Ar-H)

(i) Compound **(130)** was synthesized by reacting compound **(129)** (0.338g, 0.001mol) in absolute ethanol (3.8cm^3) under reflux with a solution of 1,3,3-trimethyl-2-methyleneindoline **(70)** (0.19g, 0.0011mol) in absolute ethanol (0.65cm^3) which was added

over a period of 30 minutes. After refluxing for 2 hours the reaction mixture was rotary evaporated to approximately one third of the original volume. The dark viscous material was allowed to stand overnight, suction filtered and rinsed with cold ethanol to give crude product **(122)**. The yield of product **(122)** was 0.06g (12%).

(ii) Synthesis of compound **(122)** with 50% excess *p*-nitroaniline was also carried out. The yield obtained by using the increased amount of the *p*-nitroaniline was 0.028g (6%). The product decomposed without melting at 230^{o}C.

5.5.3 Attempted synthesis of spirooxazine dye (122) (Route 3)

(a) Synthesis of compound (132)

2,7-Dihydroxynaphthalene **(128)** (3.88g, 0.024mol) was dissolved in water (200 cm^3) to which had been added sodium hydroxide (5.48g). The solution was stirred for 30 minutes after the addition of anhydrous sodium acetate (22.85g).

The diazonium salt solution was prepared by the same procedure as described in section 5.5.1.c (i). *p*-Nitroaniline (3.04g, 0.022mol) and sodium nitrite (1.6g, 0.023mol) were used. To the coupling component **(128)** solution was added an equimolar amount of an aqueous solution of the diazotized *p*-nitroaniline **(131)** dropwise over about 30 minutes at such a rate that no excess diazo was observed (H-acid test). The reaction pH after the complete addition of *p*-nitroaniline was 4.2. The solution was stirred for 75 minutes, heated to 80-90^{o}C, the product was filtered, washed and dried at 60^{o}C. The yield of the product **(132)** was 5.53g (75%). The melting point of compound was 302^{o} C. ν_{max}(KBr)/cm^{-1}: 3404 (O-H, st), 3117 (C-H st), 1653 (C=O), 1590, 1497 (Aromatic C-C st), 1375 (NO_2 st), 748(Ar-H); found C, 61.9; H, 3.4; N, 13.6; $C_{16}H_{11}N_3O_4$ requires C, 62.1; H, 3.6; N, 13.6.

(b) Attempted nitrosation of Compound (132)

Compound **(132)** (0.618g, 0.002mol) was dissolved in sodium hydroxide solution (0.6 mol, 17.2cm^3). After cooling the mixture down to 0^{o}C with an ice salt bath sodium nitrite (0.137g, 0.002mol) was added crystal by crystal. Concentrated sulphuric acid (1.15cm^3) was added dropwise maintaining the temperature at 0^{o}C and the mixture was

stirred overnight. After the addition a red precipitate with a recovery of 0.60g was obtained after filtration and oven drying. TLC on silica using dichloromethane as eluent showed that the precipitate was unreacted starting material.

(c) Attempted nitrosation of compound (132) in acetic acid [155]

Nitrosation of compound **(132)** (0.618g, 0.002mol) was attempted using acetic acid ($20cm^3$) in a $100cm^3$ round bottom flak. The mixture was cooled to 16^o C with an ice bath and sodium nitrite (0.137g, 0.002mol) was added slowly crystal by crystal and stirred overnight. The solid was separated by suction filtration, thoroughly washed with water and dried in air for two days to give a recovery of 0.54g, of starting material.

5.5.4 Synthesis of spirooxazine dye (138)

(a) Nitrosation of 2,3-dihydroxynaphthalene (135)

2,3-Dihydroxy-1-nitrosonaphthalene **(136)** was synthesized by the same method as described in section 5.5.1 (a). 2,3-Dihydroxynaphthalene **(135)** (1.74g, 0.011mol) and sodium nitrite (0.75g, 0.011mol) were used. The mixture was stirred for one hour and 2,3-dihydroxy-1-nitrosonaphthalene precipitated out. Filtration was followed by washing and then drying in a vacuum desiccator to give compound **(136)** (1.58g, 83%) which decomposed without melting at 192^oC. ν_{max}(KBr)/cm^{-1}: 3348 (O-H st), 1632 (C=O st), 1517, 1483, 743, 760. Found C, 63.6; H, 3.6; N, 6.8; $C_{10}H_7NO_3$ requires C, 63.5; H, 3.7; N, 7.4%.

(b) Reaction of 1,3,3-trimethyl-2-methyleneindoline (70) with 2,3-dihydroxy-1-nitrosonaphthalene (137)

To a warm solution of 2,3-dihydroxy-1-nitrosonaphthalene **(136)** (1.89g, 0.01mol) in 1,2-dichloroethane ($50cm^3$), an equimolar solution of 1,3,3-trimethyl-2-methylene indoline **(70)** (1.73g, 0.01mol) in dichloroethane ($10cm^3$) was added gradually over 15 minutes. The mixture was then refluxed for 1 hour and was then cooled at room temperature. Rotary evaporation of the solvent from the mixture to half of its original volume and then filtration gave a crude product. The crude product was subjected to silica

gel column chromatography using dichloromethane/petroleum ether (1:1, v/v) as eluent. A brown product **(137)** (0.15g, 5%) was obtained. The melting point of compound **(137)** was 154^{o} C. ν_{max}(KBr)/cm^{-1}: 3368 (O-H, broad), 1608, 1509, 1466, 992 (C_{spiro}-O st), 750, 738.

(c) Synthesis of azospirooxazine (138)

The spirooxazine **(137)** (0.25g, 0.00073mol) was dissolved in ethanol (18.38cm^3). A solution of sodium hydroxide (0.44g) in water (2.34cm^3) was added and the mixture was stirred for 20 minutes. Anhydrous sodium acetate (1.82g) was added and allowed to stir for half an hour to dissolve entirely. The diazonium salt solution was prepared by the method described in section 5.5.1 (c, i) using *p*-nitroaniline (0.75g, 0.0054mol) and sodium nitrite (0.38g, 0.0055mol). The method of the coupling reaction was the same as described in section 5.5.1 (c, iii). The product **(138)** obtained (0.27g, 77%) was recrystallized twice from ethanol and the yield of the product **(138)** after recrystallization was 0.02g (6%). The compound decomposed without melting at 196^{o} C. ν_{max}(KBr)/cm^{-1}: 3436 (N-H st), 1610 (C=O st, weak), 1599, 1572, 1493, 1334 (NO_2 st), 1299, 1150, 930 (C_{spiro}-O st), 760, 747 ; m/z (EI) (relative intensity, %): 493 (M^+, 80), 477 (71), 369 (30), 353 (72), 343 (31), 309 (13), 160 (100), 138 (90), 69 (64). The UV-Visible spectrum in dichloromethane showed λ_{max} values of 495 nm and 345 nm with respective molar extinction coefficients of 2.91 x 10^4 M^{-1}cm^{-1} and 1.33 x 10^4 M^{-1} cm^{-1}.

5.5.5 Synthesis of spirooxazine dye (142)

(a) Synthesis of 1-nitroso-2,6-dihydroxynaphthalene (140)

The synthesis of compound **(140)** was carried out using the same method as used in section 5.5.1 (a). 2,6-Dihydroxynaphthalene **(139)** (1.76g, 0.011mol) and sodium nitrite (0.76g, 0.01mol) were used. A brown product **(140)** (2.0g, 97%) was obtained which decomposed without melting at 215^{o}C. ν_{max}(KBr)/cm^{-1}: 3192 (O-H st), 1654 (C=O st), 1565, 1517, 1444, 868, 820, 700.

(b) Synthesis of the spiro compound (141)

A method similar to that described in section 5.5.1 (b) was used for synthesis. The reflux was carried out using 1,3,3-trimethyl-2-methyleneindoline **(70)** (0.368g, 0.002mol) and compound **(140)** (0.375 g, 0.0019mol). The product was filtered and the main photochromic compound **(141)** was present in the filtrate with only a trace in the filtered product. The filtrate was evaporated under reduced pressure. A grey crude product **(141)** (0.34g) was obtained which was recrystallized from heptane to give a yield of 0.10g (17%). The melting point of the compound was 289^{o}C. ν_{max}(KBr)/cm^{-1}: 3462 (O-H st), 1607, 1576, 1519, 1488, 1462, 1153 (C-N, st), 932 (C_{spiro}-O st), 736. m/z (EI) (relative intensity, %): 344 (M^{+}, 1.2), 243 (0.6), 185 (12.9), 175 (67.2), 160 (100), 132 (16.3), 117 (12.5).

(c) Attempted synthesis of final product (142)

A solution of spirooxazine **(141)** was prepared by the same method as described in section 5.5.4 (c). Spirooxazine **(141)** (0.37g, 0.001mol) and sodium hydroxide (0.65g, 0.016mol) were used. The same method was used for the preparation of diazotized *p*-nitroaniline solution as that described in section 5.5.1 (c, i) using *p*-nitroaniline (1.11g, 0.008mol) and sodium nitrite (0.65g, 0.009mol). The method for the coupling reaction was the same as described in section 5.5.1 (c, iii). The yield of the product **(142)** obtained was 0.17g (35%). An attempt was made to recrystallize the product but this was unsuccessful. The residue (0.07g) was chromatographed on silica gel column using dichloromethane as the eluent to give a reasonably pure product (0.06g, 12%). Another attempt was made to recrystallize the compound but because of the highly unstable nature of the compound it was not possible to obtain a pure product. Synthesis of **(142)** was abandoned after three unsuccessful attempts. Crude compound was analysed. ν_{max}(KBr)/cm^{-1}: 3435 (N-H st), 1606 (C=O st), 1570, 1486 (Aromatic C-C st), 930 (C_{spiro}-O st), 736. The UV-Visible spectrum was also run for the compound **(142)** showed a λmax value of 499 nm and 254 nm with respective values of molar extinction coefficient 2.36x10^{4} M^{-1}cm^{-1} and 7.49x10^{4}M^{-1}cm^{-1}.

5.5.6 Attempted synthesis of anthraquinone-based spirooxazine (143)

(a) Attempted synthesis of 1,4-dihydroxy-2-nitrosoanthraquinone (146)

The synthesis of 1,4-dihydroxy-2-nitrosoanthraquinone was attempted by the same procedure as described in section 5.5.1 (a). Quinizarine **(145)** (5.15g, 0.02mol) and sodium nitrite (1.48g, 0.02mol) were used. After stirring for an hour the precipitate was filtered, washed and oven dried to provide an orange brown solid (5.03g). A TLC on silica using dichloromethane as eluent showed that this was recovered starting material.

(b) Synthesis of 2-amino-1,4-dihydroxyanthraquinone (147)[156]

1,4-Dihydroxyanthraquinone **(145)** (2.88g, 0.01mol) was dissolved in water ($300cm^3$). After stirring for a few minutes, O-benzylhydroxylamine hydrochloride (1.8g) and an aqueous sodium hydroxide solution (40%, $6.6cm^3$) were added. The mixture was heated for 10 hours at 95-100^oC. After careful acidification of the mixture, the precipitate was filtered, dried and the yield of product **(147)** recorded was 2.76g (90%). The product was recrystallized from ethanol and decomposed without melting at 327^oC. ν_{max}(KBr)/ cm^{-1}: 3445, 3344 (N-H st), 3215 (O-H), 1645 (C=O), 1579, 1471 (Aromatic C-C).

(c) Attempted synthesis of Spirooxazine (143)

(i) A mixture of 1,3,3-trimethyl-2-methyleneindoline **(70)** (0.58g, 0.0036mol), 2-amino-1,4-dihydroxyanthraquinone, **(147)** (1g, 0.0039mol), dimethylsulfoxide (0.89g), magnesium sulphate (1.07g), sodium bicarbonate (1.43g) and toluene ($54cm^3$) was heated at 80^oC for 11 hours. The precipitate was filtered and a TLC of the filtered product and the filtrate on silica showed a red product as the major component with several other coloured impurities in the filtrate while the filtered product proved to be the starting material. The filtrate was concentrated by evaporating the solvent under reduced pressure to give 0.80g of the red product which was recrystallized from ethanol but this did not remove impurities.

(ii) A further reaction using the procedure described in section 5.5.6 (c, i) was attempted to provide spirooxazine **(143)**. 2-Amino-1,4-dihydroxyanthraquinone **(147)** was recrystallized

from ethanol for use in the synthesis. The purification of the starting material did not eliminate the impurities.

(iii) Two similar reactions using the same quantities of starting materials as described above were attempted; in one reaction time was reduced to 45 minutes and the other by increasing the amount of 1,3,3-trimethyl-2-methyleneindoline **(70)**. A TLC of the reaction mixture on silica using dichloromethane as eluent showed the same range of impurities and the reaction was abandoned. The melting point of the compound was 179^{o} C. ν_{max}(KBr)/cm^{-1}: 3448 (O-H st), 1600 (C=O), 1499, 1458, (Aromatic C-C st), 970 (C_{spiro}-O st).

5.5.7 Attempted synthesis of naphthoquinone based spirooxazine (144)

(a) Synthesis of 3-amino-2-hydroxynaphthoquinone (149)

Two different strategies for the synthesis of 3-amino-2-hydroxynaphthoquinone **(149)** were attempted**.**

(i) First attempted synthesis of 3-amino-2-hydroxynaphthoquinone (149)

The synthesis of 3-amino-2-hydroxynaphthoquinone was attempted by the procedure described in section 5.5.6 (b). 2-Hydroxy-1,4-naphthoquinone **(148)** (2.09g, 0.012mol), O-benzylhydroxylamine hydrochloride (1.8g) and aqueous caustic soda (4.8cm^3, 0.01mol) were used. After stirring for 10 hours, no precipitation occurred. The volume of the reaction mixture was reduced to one fourth using the rotary evaporator. The precipitate was suction filtered and washed with water. A TLC of the filtered product and filtrate on silica using dichloromethane as eluent showed a yellow component in the filtrate and unreacted starting material in the filtered product. Due to the difficulty in isolating product **(149)** as a filtered product, another method of 3-amino-2-hydroxynaphthoquinone synthesis was attempted.

(ii) Second attempted synthesis of 3-amino-2-hydroxynaphthoquinone (149) [157]

To a cooled (3^{o}C) solution of O-benzylhydroxylamine hydrochloride (1.25g, 0.0075mol) in ethanol (30cm^{3}) was added triethylamine (0.83g, 0.0075mol). The mixture was stirred continuously and a solution of 2-hydroxy-1,4-naphthoquinone (1.95g, 0.011mol) in ethanol (12.5cm^{3}) was added dropwise. The mixture was stirred at room temperature for four hours and then filtered. The filtered product proved to be starting material while an orange product was in the filtrate. 2-Hydroxy-3-nitrosonaphthoquinone **(150)** was decided to synthesize with an aim to get it as a filtered product.

(b) Synthesis of 2-hydroxy-3-nitrosonaphthoquinone (150)

(i) First synthesis of 2-hydroxy-3-nitrosonaphthoquinone (150)

Synthesis of 2-hydroxy-3-nitrosonaphthoquinone **(150)** was attempted in the same way as described in section 5.5.1 (a). 2-Hydroxynaphthoquinone **(148)** (3.82g, 0.022mol) and sodium nitrite (1.5g, 0.022mol) were used. The product **(150)** was dried in a desiccator and the yield recorded was 1.00g (23%).

(ii) Second synthesis of 2-hydroxy-3-nitrosonaphthoquinone (150)

The method and the scale for the synthesis of 2-hydroxy-3-nitrosonaphthoquinone **(150)** was the same as used in section 5.5.1 (a) and section 5.5.7 (b, i) respectively. A reasonably pure brown product **(150)** with a yield of 2.04g (46%) was obtained. The compound decomposed without melting at 133^{o}C. ν_{max}(KBr)/cm^{-1}: 3430 (O-H st), 1328 (N-H), 1693 (C=O), 1589, 1484 (Aromatic C-C st), 864 (Ar-H).

(c) Attempted synthesis of spirooxazine (144) [158]

A solution of 1,3,3-trimethyl-2-methyleneindoline **(70)** (1.04g, 0.006mol) was reacted with 2-hydroxy-3-nitroso-1,4-naphthoquinone **(150)** (1.12g, 0.005mol) in the same manner as described in section 5.5.1 (b). The recrystallization of the product from ethanol gave a product with 0.08g (4%) yield. The product decomposed without melting. ν_{max}(KBr)/cm^{-1}: 3433 (O-H st), 1699 (C=O), 1585, 1482, 1437 (Aromatic C-C st).

5.5.8 Synthesis of pyrazolone-based spirooxazines

(a) Nitrosation of 3-methyl-1-*p*-tolylpyrazol-5-one (156)[159]

3-Methyl-1-*p*-tolylpyrazol-5-one **(156)** (18.8g, 0.1mol) was dissolved in glacial acetic acid (60cm^3) and water (340cm^3) was added over 20 minutes. A solution of sodium nitrite (13.8g, 0.2mol) in water (20cm^3) was added over 20 minutes maintaining the temperature at 10-20^{o}C. The mixture was stirred for 2 hours at room temperature. Orange crystals formed after the addition of nitrite. Sulphamic acid (5g) was used to remove the excess nitrite. The product was filtered, washed with water and dried in the vacuum oven at 80^{o}C. The yield of the product **(157)** obtained was 20.03g (92%). Melting point determined by DSC was 179^{o}C.

(b) Reaction of 3-methyl-4-nitroso-1-*p*-tolylpyrazol-5-one with 1,3,3-trimethyl-2-methyleneindoline [160]

(i) 3-Methyl-4-nitroso-1-*p*-tolylpyrazol-5-one **(157)** (2.17g, 0.01mol) was dissolved in methanol (30cm^3). The solution was warmed to boiling to dissolve and the reaction was carried out under nitrogen to avoid an oxidation. To this solution was added quickly 1,3,3-trimethyl-2-methyleneindoline **(70)** (1.73g, 0.01mol) in ethanol (10 cm^3) and the mixture heated to reflux for 70 minutes. The crude product was a mixture of red, orange, purple and yellow compounds as seen from TLC using toluene: ethanol (80:20) as an eluent. The recrystallization of this material from methanol was attempted but this was unsuccessful in providing a pure product.

(ii) Two similar reactions were also attempted with different reflux times, one with 21 hours and the other with 31 hours using half the reaction scale as described above. A mixture of red merocyanine **(151b)** and purple N-oxide **(154)** was obtained in both cases as judged by TLC.

(c) Attempted isolation of unstable yellow compound (158)

(i) The reaction was attempted in the same manner as described in section 5.5.8 (b, i) using 3-methyl-4-nitroso-1-*p*-tolylpyrazol-5-one **(157)** (1.08g, 0.005mol) and 1,3,3-trimethyl-2-methyleneindoline **(70)** (0.86g, 0.005mol). The reaction mixture was refluxed for 10 minutes, chilled in a freezer overnight and then filtered. The yellow compound was obtained but was unstable in solution and rapidly converted to a mixture of red and purple compounds as seen from a two dimensional TLC on silica using toluene: ethanol (80:20) as eluent. (see discussion in section 3.3.3, a, vi)

(ii) A further reaction with the same amount of the starting materials was carried out as discussed above. The reaction mixture was heated to reflux for 5 minutes, poured in to ice cooled water ($100cm^3$) and allowed to stand for 4 hours to give precipitate which was then filtered. The filtered product proved to be the starting nitroso compound and a yellow spot in the filtrate was seen from a TLC on silica. Sodium chloride (20g) was added to the filtrate; the solution was left overnight. A precipitate was then filtered and dried in freeze drier. The yield of the yellow solid was 0.13g (7%).

(d) Synthesis of the Red, Orange and Purple compounds (151b, 155, and 154)

3-Methyl-4-nitroso-1-*p*-tolylpyrazol-5-one **(157)** (2.16g, 0.01mol) and 1,3,3-trimethyl-2-methyleneindoline **(70)** solution (1.72g, 0.01mol) were refluxed for 67 hours using the same procedure as used in section 5.5.8 (b, i). The crude brown product (1.91g) obtained was submitted to a silica gel column chromatographic separation using toluene as eluent. The solvent was evaporated under reduced pressure to provide the orange product **(155)** (0.13g, 6%), purple **(154)** (20mg, 1%) and a mixture of red **(151b)** and purple **(154)** (720mg, 39%). The melting point of orange product **(155)** was 250°C and product decomposed at 290°C as determined by DSC. ν_{max}(KBr)/cm^{-1}: 3432 (O-H st), 2956 (C-H, st), 1710 (C=O), 1580 (Aromatic C=C st). m/z (EI) (relative intensity, %): 387 (M^+, 100), 231 (90.1), 216 (42.1), 200 (40.7), 184 (92.5), 172 (48.2), 149 (34.5), 105 (49). The UV-visible spectrum in dichloromethane showed λ_{max} values of 449 nm and 329 nm with respective molar extinction coefficients of 7.75 x 10^3 $M^{-1}cm^{-1}$and 6.2 x 10^3 $M^{-1}cm^{-1}$. The

purple compound **(154)** decomposed without melting at 200°C. ν_{max}(KBr)/cm^{-1}: 2965 (C-H, st), 1644 (C=O), 1510, 1491 (Aromatic C=C st) and 821 (Ar-H). m/z (EI) (relative intensity, %): 388 (M^+, 99.3), 373 (100), 355 (61.2), 330 (75.2), 288 (30.1), 214 (62.7), 200 (84.2), 160 (45.7). The UV-visible spectrum in dichloromethane showed λ_{max} values of 550 nm and 365 nm with respective molar extinction coefficients of 2.22 x 10^4 $M^{-1}cm^{-1}$ and 5.8 x 10^3 $M^{-1}cm^{-1}$.

(e) Synthesis of red merocyanine (151b)

(i) The amount of the material used was the same as used in section 5.5.8 (c) and the solution in methanol was refluxed under nitrogen for a month. The refluxed mixture was kept in the freezer for two days and the precipitate was filtered. The yield of the product **(26)** after recrystallization from methanol was 0.59g (32%). The melting point of compound **(151b)** was 182°C.

(ii) The reaction was carried out using half the scale used originally in section 5.5.8 (c). The reaction mixture was kept in the freezer overnight and the precipitate was filtered. The product **(151b)** was recrystallized from methanol to give a yield of 270mg (29%). The melting point recorded by DSC was 182°C.

(f) Synthesis of N-oxide (154)

(i) The procedure and the reaction conditions were the same as described in section 5.5.8 (e, ii). The reaction was carried out for 16 hours. The precipitate was filtered and a TLC on silica using toluene: ethanol (20%) as eluent showed that purple N-oxide **(154)** (0.67g, 73%) was the main product along with some starting material.

(ii) 3-Methyl-4-nitroso-1-*p*-tolylpyrazol-5-one **(157)** (0.27g, 0.0012mol) in acetone (3.75cm^3) was reacted with 1,3,3-trimethyl-2-methyleneindoline **(70)** (0.22g, 0.0013mol) solution in acetone (1.25cm^3) at room temperature for 18 hours. The reaction mixture was kept in the freezer but no precipitation was seen. Water was added to the reaction mixture

which was left for two days. A precipitate of pure product **(154)** (0.041g, 9%) was obtained. DSC showed that compound decomposed without melting at 200^{o}C.

(iii) Attempted oxidation of merocyanine form (151b) to provide N-oxide (154)

The synthesis of purple N-oxide **(154)** was attempted by the oxidation of red compound **(151b)**.[160] Compound **(151b)** (0.151g, 0.0004mol) was dissolved in glacial acetic acid (3cm^3) at room temperature. Hydrogen peroxide (29%, 0.048g, 0.0048mol) was added slowly. The reaction mixture was heated to 85^{o}C and then refluxed for an hour. The solution turned yellow but no conversion of red product **(151b)** to the purple N-oxide **(154)** was observed on TLC.

(iv) A further oxidation reaction using the same reaction conditions was attempted using hydrogen peroxide (0.0048mol, 12%). Again, no N-oxide formation was observed by TLC on silica using toluene: ethanol (80:20) as eluent.

(g) Conversion of purple N-oxide (154) to red merocyanine (151b)

Conversion of purple N-oxide **(154)** to red merocyanine **(151b)** was carried out by refluxing 10mg (0.000025mol) of the purple compound **(154)** in acetone (7.5cm^3) under nitrogen. The purple N-oxide **(154)** was converted completely into red merocyanine **(151b)** after 504 hours giving a yield of 9.2mg (95%).

5.5.9 Attempted synthesis of Spirooxazine (152b) based on 3-methyl-1-phenylpyrazol-5-one

(a) Synthesis of merocyanine (152b)

Using half the scale as used in section 5.5.8 (b), the reflux reaction was carried out for 168 hours. Red merocyanine **(152b)** was the main product as judged by TLC. The refluxed mixture was cooled in a refrigerator overnight and crystals of the product **(152b)** were filtered. The yield of the product **(152b)** after recrystallization from methanol was 1.30g (73%). The melting point determined by DSC was 240^{o}C.

(b) Synthesis of Purple N-oxide (160)

The reaction of 3-methyl-4-nitroso-1-phenylpyrazol-5-one **(159)** (1.01g, 0.005mol) in acetone (12.5cm^3) with 1,3,3-trimethyl-2-methyleneindoline **(70)** (0.86g, 0.005mol) solution in acetone (2.5cm^3) was carried out at room temperature. The mixture was then cooled at room temperature, kept in the freezer overnight and water (12.5cm^3) was added in the reaction mixture to get a precipitate. The product (66mg, 3.5%) obtained was a mixture of red, purple and orange components. This mixture was again submitted to silica gel column using toluene as eluent to provide a pure sample of the purple N-oxide **(160)** (10mg, 0.53%). The melting point of the compound as determined by DSC was 202^{o}C. ν_{max}(KBr)/cm^{-1}: 2919 (C-H st), 1655 (C=O), 1560, 1491 (Aromatic C=C st), 1287 (N-oxide) and 835. m/z (EI) (relative intensity, %): 374 (M$^+$, 8.0), 358 (64.5), 343 (11.1), 200 (10.3), 160 (30.1), 144 (33.1), 77 (34.8), 69 (53.5). The UV-visible spectrum in dichloromethane showed λ_{max} value of 549 nm with molar extinction coefficients of 1.24 x 10^4 M^{-1}cm^{-1}.

5.5.10 Synthesis of red merocyanine (153b) based on 3-ethoxycarbonyl-1-p-phenylpyrazol-5- one

(a) Synthesis of red merocyanine (153b)

The synthesis of spirooxazine **(153b)** was carried out by the same method as described in section 5.5.8 (b, i) using 3-ethoxycarbonyl-4-nitroso-1-phenylpyrazol-5-one **(161)** (1.3g, 0.005mol) and 1,3,3-trimethyl-2-methyleneindoline **(70)** (0.86g, 0.005mol). The reaction mixture was refluxed overnight and was then chilled in the freezer. The product was filtered and a TLC on silica using toluene: ethanol (20%) as eluent showed that it was a mixture of red merocyanine **(153b)** and purple N-oxide **(162)**. The product was recrystallized with ethanol to give pure red product **(153b)** (1.42g, 69%). The melting point determined by DSC was 236^{o}C.

(b) Attempted synthesis of N-oxide (162)

The synthesis of purple compound **(162)** was carried out using the same amount of starting materials as described in section 5.5.10 (a). The reaction was carried out at room

temperature over a month. The mixture was cooled in a refrigerator for several hours and crystals of the compound were filtered. TLC of the filtered product showed that it contained red merocyanine form **(34)** as the major product (1.72g, 75%) with only a trace of the purple compound **(162)**.

5.5.11 Attempted synthesis of quinoneoximespirooxazine (163)

The nitrosation of spirooxazine **(130)** was carried out using the same synthetic method as used in section 5.5.3 (c). Compound **(130)** (0.344g, 0.001mol) and sodium nitrite (0.084g, 0.001mol) were used. The yield of the brown product obtained was 76mg (21%). A flash column using toluene: ethanol (5%) as eluent was run to get a reasonably pure product **(7)** (26mg, 7%). The compound **(163)** decomposed without melting at 247^{o} C as measured on a melting point apparatus. ν_{max}(KBr)/cm^{-1}: 3394 (O-H st), 2970 (C-H, st), 1620 (C=O), 1607, 1490, 1445 (aromatic C=C st), 1348 (O-H bending), 1213, 1125 (C-N stretch), 932 cm^{-1} (C $_{spiro}$-O) and 832 (Ar-H, bd).

5.5.12 Attempted synthesis of photochromic dye based on naphthopyran (165)

(a) Synthesis of Intermediate (171) [161]

2,7-Dihydroxynaphthalene **(128)** (1.6g, 0.01mol) and 1,1-bis(4-methoxyphenyl)prop-2-yn-1-ol **(170)** (2.7g, 0.01mmol) solution was stirred in toluene (125cm^3), warmed to 50^{o}C and acidic alumina (7.8g) was added. The mixture was refluxed for 1.5 hours until no 1,1-bis(4-methoxyphenyl)prop-2-yn-1-ol remained as judged by TLC on silica using dichloromethane: acetone (2%) as eluent. The mixture containing acidic alumina was cooled, filtered off and washed with hot toluene (2x156cm^3). A red product obtained after washing the acidic alumina with toluene and then evaporating the solvent under reduced pressure was submitted to a silica gel column chromatography using ethylacetate: hexane (20%) as eluent to give product **(171)** (0.72g, 41%). Melting point of compound was 210^{o} C and it decomposed at 266^{o}C. ν_{max}(KBr)/cm^{-1}: 3393 (O-H st), 1610, 1584, 1508 (Aromatic C-C st) and 730. m/z (EI) (relative intensity, %): 410 (M^{+}, 100), 303 (75), 287 (5.4), 251 (6.8, 205 (6.0), 135 (8.3), 84 (27.4), 55 (9.7).

(b) Attempted synthesis of compound (165)

The diazonium salt solution was prepared using half the scale but otherwise the same procedure as described in section 5.5.1(c, i).

Naphthopyran **(171)** (0.205g, 0.05mmol) in ethanol (12.5cm^3) was heated gently at 40^oC and added to a solution of sodium hydroxide (0.3g) in water (1.6cm^3). The procedure for the synthesis as well as for coupling was the same as described in section 5.5.1 (c, ii). The crude product (230mg) showed a red and an orange component on TLC. A flash column of crude product on silica using dichloromethane: acetone (10%) as an eluent was run. Two products, the minor red (10mg) and the major orange (90mg, 33%) were separated. The orange compound decomposed without melting at 212^oC. ν_{max}(KBr)/cm^{-1}: 3432 (N-H st), 1591, 1509 (Aromatic C=C st), and 778 (Ar-H). δ_H (200 MHz, d_6-DMSO): δ1.3 (s, 1H, N-NH), δ3.70 (s, 3H, OCH_3), δ 3.86 (s, 3H, OCH_3), δ5.99 (d, 1H, J=10.3), δ6.49 (d,4H J=9.9), δ6.58 (d, 1H, J=8.7), δ6.87 (d, 1H, J=5.5), δ6.91 (d,1H, J=4.9), δ7.13 (d, 4H, J= 9.1), δ7.22 (d, 2H, J=3.7) ,δ 7.49 (d, 1H, J=9.6), δ7.69 (d, 2H, J=9.5)

Red compound **(172)** was also analysed. ν_{max}(KBr)/cm^{-1}: 3448 (O-H st), 1680 (C=O), 1610, 1560, 1521 (Aromatic C=C st). m/z (EI) (relative intensity, %): 575 (M^+, 41), 559 (50.4), 439 (23.1), 387 (100), 373 (23), 357 (13), 341 (31.5), 251 (41.6), 239 (18), 189 (17), 161 (27), 135 (15), 57 (36.2). UV-Visible spectrum showed a λ_{max} value of 483 nm and 290 nm.

References

1. J. C. Crano & R. J. Guglielmetti, editors, *Organic Photochromic and Thermochromic compounds,* Vol **1:** Main photochromic families, Plenum Press, New York (1999).
2. G. H. Brown, *editor, Photochromism,* John Wiley & Sons, New York, First edition (1971).
3. A.V. El'tsov, *editor, Organic Photochromes,* Plenum Publishing Corporation, New York (1990).
4. J. J. P. Stewart, *editor, Semiempirical molecular orbital methods. In: Reviews in Computational Chemistry,* 1, VCH New York, 45-81 (1990).
5. C. B. Mcardle & Blackie, *editor, Applied Photochromic Systems,* Glasgow and London, (1992).
6. V. Krongauz, V. Weiss & G. Berkovic, Chem. Rev., **100** 1741 (2000).
7. J. K. Hurst, K. Giertz, R. F. Khairutdinov, E. N. Voloshina, N. A. Voloshina & V. I. Minkin, J. Amer. Chem. Educ., **120**, 12707 (1998).
8. C. M. Bowen, J. D. Winkler & V. Michelet, J. Amer. Chem. Educ., **120** 3237 (1998).
9. R. S. Pearlman, *editor, 3D Molecular Structures: Generation and use in 3D searching In: 3DQSAR in Drug Design, Kubinyi, H. (Ed),* Escom Science Publishers:Leiden; 41-79 (1993).
10. J. Mater, H. Schmidt & L.S. Hou, Sci. Lett, **16**, 435 (1997).
11. M. J. Def Maunder, C. B. Mcardle, & J. M. Kelly, *editors, Photochemistry and polymeric systems,* Royal Society of Chemistry, Cambridge (1993).
12. P. Gregory & P. F. Gordon, *editor, Organic chemistry in colour,* New York, Springer-Verlay Berlin Heidelberg, 121 (1983).
13. C. Graebe & C. Liebermann, Ber., **1**, 106 (1868).
14. O. N. Witt, *Zur kentniss des Baues und der Buildung farbender Kohlenstoffverbindungen,* Ber. Deut. Chem. Ges., **1**, 522-527 (1876).
15. R. M. Christie, *Colour Chemistry,* Royal Society of Chemistry, Cambridge, 26 (2001).

16. P. F. Gordon & P. Gregory, *editors, Organic Chemistry in Colour,* New York, Springer-Verlay Berlin Heidelberg, 122 (1983).
17. H. E. Armstrong, Philos. Mag., **23**, 73 (1887).
18. M. Gomberg, *On the preparation of triphenylchloromethane*, J. Amer. Chem. Soc., **22**, 757 (1900).
19. A. Baeyer, Liebigs Ann. Chem. , **354**, 152 (1907).
20. E. R. Watson, J. Chem. Soc., **30**, 759 (1914).
21. E. Q. Adams & L. Rosenstein, *The colour and ionization of crystal-violet*, J. Amer. Chem. Soc., **36**, 1452 (1914).
22. C. R. Bury, *Auxochromes and Resonance*, J. Amer. Chem. Soc., **57**, 2116 (1935).
23. G. N. Lewis, *The atom and the molecule,* J. Amer. Chem. Soc., **38**, 762 (1916).
24. R. Pariser & R. G. Parr, Chemical Physics, **21**, 466, 767 (1953).
25. J. A. Pople, Trans. Faraday Soc., **49**, 1375 (1953).
26. J. Griffiths, Chemistry in Britain, **22**, 997 (1986).
27. J. Griffiths et al, *An approach to the prediction of absorption bandwidths of dyes using the PPP-MO procedure*, Dyes and Pigments, **10**, 123 (1989).
28. J. Griffiths, Rev. Prog. Colouration, **11**, 37 (1981).
29. J. A. Pople & G. A. Segal, J. Phys. Chem., **43**, 136 (1965).
30. J. A. Pople & G. A. Segal, J. Phys. Chem., **44**, 3289 (1966).
31. J. M. S. Dewar & G. Klopman, *Ground states of .sigma.-bonded molecules. I. Semiempirical S.C.F. molecular orbital treatment of hydrocarbons*, J. Amer. Chem. Soc., **89**, 3089 (1967).
32. R. N. Dixon, Molecular Physics, **12**, 83 (1967).
33. N. C. Baird & M. J. S. Dewar, J. Phys. Chem., **50**, 1262 (1969).
34. M. Fritsche, Comptes Rendues, **69**, 1035 (1867).
35. E. ter Meer, Leibigs Ann. Chem., **181**, 1 (1876).
36. W. Wislicenus, Leibigs Ann. Chem., **277**, 366 (1893).
37. H. Biltz, Leibigs Ann. Chem., **305**, 170 (1899).
38. A. Wienaanda & H. Biltz, Leibigs Ann. Chem., **308**, 1 (1899).
39. H. Biltz, Z. Phys. Chem. (Leipzig), **30**, 527 (1899).
40. W. Marckwald, Z. Phys. Chem. (Leipzig), **30**, 140 (1899).

41. G. H. Brown, *editor, Photochromism,* John Wiley & Sons, New York, **3**, 1 (1971).
42. Y. Hirshberg, J. Amer. Chem. Soc., **68**, 2304 (1956).
43. G. H. Brown, *editor, Photochromism,* John Wiley & Sons, New York, **3**, 8 (1971).
44. A.V. El′tsov, *editor, Organic Photochromes,* Plenum Publishing Corporation, New York, (1990).
45. H. Durr & H. Bouas-Laurent, *editor, Photochromism: Molecules and Systems,* Elsevier, New York, (1990).
46. Blackie & C. B. McArdle, *editor, Applied Photochromic Systems,* Glasgow and London (1992).
47. D. S. Tyson, C. A. Bignozzi. & F. N. Castellano, *Metal-Organic Approach to Binary Optical Memory*, J. Amer. Chem. Soc., **124**, 4562-4563. (2002).
48. I. Willner, Acc. Chem. Res., **30**, 347-356 (1997).
49. H. Durr & H. Bouas-Laurent, *Organic Photochromism*, IUPAC, 639-665 (2001).
50. G. H. Brown, *Photochromism,* John Wiley & Sons, New York, **3**, 472-474 (1971).
51. A. Hass, M. R. C. Gerstenberger, B. Kirste, C. Kruger & H. Kurreck, Chem. Ber., **115**, 2540 (1982).
52. G. H. Brown, *editor, Photochromism,* 3, John Wiley & Sons, New York, 557 (1971).
53. H. Durr & H. Bouas-Laurent, *Photochromism, Molecules and systems,* Elsevier, New York, 654 (1990).
54. J. C. Crano, R. J. Guglielmetti & B. V. Gemert, *Organic photochromic and thermochromic compounds,* **1**, 125 (1999).
55. R. E. Fox, *Research reports and test items pertaining to eye protection of air crew personnel,* Final report on Contract A F41 (657)-215, (1961).
56. A. Samat, J. P Reboul, P. Lareginie, V. Lokshin, R. Guglielmetti & G. Pepe, Acta Crystallographica, **C51**, 817 (1995).
57. M. C. Norman, W. Clegg & T. Flood et al, *Structure of three photochromic compounds and three non-photochromic derivatives: the effect of methyl substituents,* Acta Crystallographica, **C47**, 817-824 (1991).
58. *Molecular Structure and Dimensions,* Utrecht, Netherlands, **A1**, (1972).

59. I. I. Chuev, S. M. Aldoshin, O. S. Filipenko, A. N. Utenyshev, V. Lokshin, P. Laregenie, A. Smat & R. Guglielmetti, *Structure and photochromic properties of substituted spiroindolinonaphthoxazines,* Russian Chemical Bulletin, **47**, 1089-1097 (1998).

60. N. Y. C. Chu, *Photochromism of spiroindolinonaphthoxazine, I. Photophysical properties*, Can. J. Chem., **61**, 300-305 (1983).

61. Jinliang Li, Xiaoliu Li, Y. Wang, T. Matsuura & J. Meng, *Synthesis of functionalized spiropyran and spirooxazine derivatives and their photochromic properties,* J. Photochem. Photobiol. A, **161**, 210-213 (2004).

62. Pei-li Chen, Ting-feng Tan, Huaming Huang & Ji ben Mengs, *Synthesis, characterization and photochromic studies in films of heterocycle-containing spirooxazines,* Tetrahedron, **61**, 8192-9198 (2005).

63. T. Asahi & H. Masuhara, *Chemistry letters,* 1165 (1997).

64. N. Y. C. Chu., *editor, 4N+2 Systems, spirooxazines,* in H. Durr & H. B. Laurent, *Photochromism, molecules and systems*, Elseiver, Amsterdam (1990).

65. N. W. Tyer & R. S. Becker, *Photochromic spiropyrans. I. Absorption spectra and evaluation of the .pi.-electron orthogonality of the constituent halves*, J. Amer. Chem. Soc., **92**, 1289-1294 (1970).

66. S. Minkovska, T. Deligergive, B. Jeliazkovs & S. Rakovsky, *Synthesis of photochromic chelating spironaphthoxazines,* Dyes and Pigments, **53**, 101-108 (2002).

67. J. C. Micheau, A. V. Metelitsa, S. O. Besugliy, E. B. Gaeva, N. A. Voloshin, E. N. Voloshina, A. Samat & V. I. Minkin, *Photochromic properties of six 5-O-n-alkyl,-6'-CN substituted spironaphthoxazines,* International Journal of Photoenergy, **6**, 199-200 (2004).

68. F. Tfibel, A. Kellmann, R. Dubset, P. Levoir, J. Aubard, E. Pottier & R. J. Guglielmetti, *Photophysics and kinetics of two photochromic indolinospironaphthoxazines and one indolinospironaphthopyran,* J. Photochem. Photobiolo.A, **49**, 63-67 (1989).

69. S. Schenider, *Investigation of the photochromic effect of spiro-[indolino-naphthoxazine] derivatives by time resolved spectroscopy,* Z. Phys. Chem., **154**, 91-119 (1987).

70. A. Samat, J. L. Pozzo, R. Guglielmetti & D de Keukeleire, *Solvatochromic and photochromic characteristics of new 1,3-dihydrospiro[2H-indole-2,2'-[2H]-bipyrdo[3,2-f][2,3-h][1,4]benzoxazines],* J. Chem. Soc, **2**, 1327-1332 (1993).

71. M. Rickwood, S. D. Marsden, M. E. Ormby, A. L. Stunton & D. W. Wood, *Red colouring photochromic 6'-substituted spiroindolinonaphth[2,1-b][1,4]oxazines,* Mol. Cryst. Liq. Cryst., **246**, 17-24 (1994).

72. Aramaki & G. H. Atkinson, *Spirooxazine photochromism: picosecond time-resolved Raman and absorption spectroscopy,* Chem. Phys. Lett, **170**, 181-186 (1990).

73. N. Tamai & H. Masuhara, *Intersystem crossing of benzophenone by femtosecond transient grating spectroscopy,* Chem. Phys. Lett, **198**, 413-418 (1992).

74. S. Schneider, F. Baumann, U. Kluter & M. Melzig, *Photochromism of spirooxazines, II. CARS-investigation of solvent effects on the isomeric distribution,* Ber. Bunzenges Phys. Chem, **91**, 1225-1228 (1987).

75. F. Wilkinson, D. R. Worrall, J. Hobley, L. Janzen, S. L. Williams, A. J. Langley & P. Matousek, *Picosecond time-resolved spectroscopy of the photocolouration reaction of photochromic naphthoxazine-spiro-indolines,* J. Chem. Soc., Faraday Trans, **92**, 1331-1336 (1996).

76. J. C. Crano, R. J. Guglielmetti & V. Malatesta, *editor, "Photodegradation of organic photochromes" in organic Photochromic and Thermochromic compounds,* **2**, Plenum, New York, (1999).

77. S. A. Kaysanov & M. V. Alfimov, Chem. Phys. Lett, **91**, 23-26 (1982).

78. Ya. N. Malkin, T. B. Krasieva & V. A. Kuzmin, Izv, Akad. Nauk. SSSR. Ser. Khim, 236-243 (1990).

79. Y. Hirshburg, E. Fischer & R. Heiligoman-Rim, *Photochromism in spiropyrans, part IV, Evidence for the existence of several forms of the coloured modification,* J. Chem. Soc, 2465-2470 (1962).

80. R. S. Becker & C. Lenoble, *Photophysics, photochemistry, kinetics, and mechanism of the photochromism of 6'-nitroindolinospiropyran*, J. Phys. Chem., **90**, 62-65 (1986).

81. R. Gautron, *Photochromisme des indolinospiropyranes IV-Etude de la degradation par voie physique. Relation avec la structure,* Bull. Soc. Chim. Fr., (1968).

82. R.Guglielmetti, G. Giusti & G. Baillet, *Comparative photodegradation study between spiro[indoline-oxazine] and spiro[indoline-pyran] derivatives in solution,* J. Photochem. Photobiolo.A, **70**, 157-161 (1993).

83. M. Milosa, V. Malatesta, R. Millini, L. Lanzini, P. Bortolus & S. Monti, *Oxidative degdration of organic photochromes,* Mol. Cryst. Liq. Cryst., **246**, 303-310 (1994).

84. C. Froute, V. Pimienta, M. H. Deniel, D. Lavabre, R. Guglielmetti & J. C. Micheau, *Kinetic modelling of the photochromism and photodegradation of a spiro[indoline-naphthoxazine],* J. Photochem. Photobiol. A, **122**, 199-204 (1999).

85. V. Malatesta, G. Favaro, U. Mazzucato, G. Ottavi & A. Romani, *Thermally reversible photoconversion of spiroindoline- naphthhoxazine to photomerocyanine: A photochemical and kinetic study,* J. Photochem. Photobiol. A, **87**, 235-241 (1995).

86. J. H. Day, *Thermochromism,* Chem. Rev., **63**, 65-80 (1963).

87. V. Lokshin, A. Samat, J. C. Crano & R. J. Guglielmetti *editor, Thermochromism of organic compounds" in organic photochromic and thermochromic compounds,* **2**, Plenum, New York, (1999).

88. V. Lokshin, P. Lareginie, A. Samat, R. Guglilemetti & G. Pepe, *First permanent opened forms in spiro[indoline-oxazine] series: Synthesis and structural elucidation* J. Chem. Soc., Perkin Trans, **2**, 107-111 (1996).

89. J. G. Kim, Y. S. Lee, Y. D. Huh & M. K. Kim, *Thermochromism of spiropyran and spirooxazine derivatives,* J. Korean. Chem. Soc, **38**, 864-872 (1994).

90. V. Malatesta, P. Allegrini & L. L. Montanari, *A solid-state (CP-MAS) 13C nuclear magnetic resonance study of selected photo (thermo) chromic spiro (indolinonaphthoxazines,.* Appl. Magn. Reson,. **7**, 551-557 (1994).

91. F. Garnier, P. Appriou & R. Guglielmetti, *Etdude du processus photochimique implique dans la reaction d ouverture du cycle benzopyrannique des spiropyrans photochromicques,* J. Photochem. Photobiol. A., **8**, 145 (1978).
92. H. Yoshida, S. Kawauchi, N. Yamashina, M. Ohira, S. Saeda & M. Irie, *A new photochromic spiro[3H-1,4-oxazine],* Bull. Soc. Jpn., **63**, 267-268 (1990).
93. C. Reichardt, *Solvents and solvents effect in organic chemistry,* VCH, Weinheim, **3**, 285-286 (1990).
94. P. Suppan & N. Ghoneim, *Solvatochromism,* Royal Society of Chemistry Cambridge, (1997).
95. V.Gutmann, *editor, The donor-acceptor approach to molecular interaction,* Plenum Press, (1978).
96. V. Lokshin, A. V. Metelitsa, J. C. Micheau, A. Samat, R. Guglielmetti & V. I. Minkin, Phys, Chem. Chem. Phys., **4**, 4340 (2002).
97. C. H. Hoelscher & D. S. McBain, *Methods for preparing spiro(indoline) type photochromic compounds*, 4,634,767, United States Patent, (1987).
98. Masahiro & Hosoda., *Photochromic compounds*, 0,186,364, European Patent Application, (1986).
99. Yamamoto S. Taniguchi, 63,301,885, Japanese Patent*,* Toray Industrial (1988).
100. V. I. Minkin, V. A. Chelepin, N. E. Paltchkov, N. S Trofimova &. O. A Zoubkov,. WO 96/03368.
101. J. Chung-Chun Lee, C. Wang & A. Teh Hu, *Microwave assisted synthesis of photohcromic spirooxazine dyes under solvent free conditions,* Materials letters, **58**, 535-538 (2004).
102. P. Griess, Liebigs Ann. Chem., **106**, 123 (1858).
103. P. Griess, Liebigs Ann. Chem., **113**, 205 (1860).
104. H. Gies & E. Pfeil, Liebigs Ann. Chem., **578**, 11 (1952).
105. H. Zollinger, *editor, Diazo Chemistry:Aromatic and Heteroaromatic Compounds* VCH Publishers, New York, Vol **I**, 13 (1994).
106. H. Zollinger, *editor, Diazo Chemistry I, Aromatic and Heteroaromatic compounds,* VCH Publishers, New York, Vol **I**, 307 (1994).
107. R. M. Christie, *Colour Chemistry,* Royal Society of Chemistry, 58-59 (2001).

108. M. S. Salvador, P. J. Coeliho, B. M. Heron & L. M. Carvalho, *Spectrokinetic studies on new biphotochromic molecules containing two naphthopyran entities,* Tetrahedron, **61**, 11730-11743 (2005).

109. J. Micheall, S. Delbaere & G. Vermeersch, J. Org. Chem., *NMR Kinetic Investigations of the Photochemical and Thermal Reactions of a Photochromic Chromene,* **68**, 8968-8973 (2003).

110. J. C. Crano, V. Gemert & R. Guglielmetti, editors, *Organic photochromic and thermochromic compounds,* Plenum, New York, **1**, 111-140 (1999).

111. M. Melzig & C. M. Weigand, 03/080595, U. PCT WO (2003).

112. M. Bezer & D. W. McCallien, *Methods for marking liquids and compounds for use in said method*, 2344599, GB Patent (2000).

113. M. Camus, *Security document including a security element having photochromic properties*, 488902, European Patent, (1992).

114. E. M. Carreira & W. Zhao, *A Smart Photochromophore through Synergistic Coupling of Photochromic Subunits,* J. Am. Chem. Soc., **124**, 1582-1583 (2002).

115. E. M. Carreira & W. Zhao, 0078441, United States Patent (2003).

116. T. Imura, T. Tanaka, K. Tanaka & Y. Kita, *Spiropyran compounds and its manufacturing method*, 02,69,471, Japanese Patent (1990).

117. C. D. Gabbutt, J. D. Hepworth, B. M. Heron & M. M. Rehman, *Allenes from 3-bromo-2H-1-benzopyrans,* J. Chem. Soc, **1**, 1733-1737 (1994).

118. R. S. Becker & J. Michel, *Photochromism of synthetic and naturally occuring 2H-chromenes and 2-H-pyrans,* J. Am. Chem. Soc., **88**, 5931-5933 (1966).

119. H. Zinner & M. Melzig, *Photochromic spiropyran compounds*, 95/00504, World Patent Appl. WO, (1995).

120. B. V. Gemert, *Photochromic naphthopyrans*, 5,340,857, United States Patent, (1994).

121. J. D. Hepworth, C. D. Gabbutt, B. M. Heron, S. M. Partington & D. A. Thomas, *Synthesis and spectroscopic properties of some merocyanine,* Dyes and Pigments, **49**, 65-74 (2001).

122. B. M. Heron, C. D. Gabbutt, A. C. Instone, P.N. Hotron & M. B. Hursthouse, *Synthesis and photochromic properties of substituted 3H-naphtho[2,1-b]pyrans,* Tetrahedron, **61**, 463-471 (2005).

123. C. D. Gabbutt, B. M. Heron, A. C. Instone, D. A. Thomas, S. M. Partington, M. B. Hursthouse & T. Gelbrich, *Observation on the synthesis of photochromic naphthopyrans,* J. Org. Chem., 1220-1230 (2003).

124. J. C. Micheall, S. Delbaere, J. Berthet & G. Vermeersch, *Contribution of NMR spectroscopy to the mechanistic understanding of photochromism,* International Journal of Photoenergy, **6**, 151-158 (2004).

125. J. M. Goodman, *editor, Chemical application of molecular modelling,* Department of Chemistry, University of Cambridge, UK, Royal Society University Research Fellow (1998).

126. R. S. Pearlman, in. *CDA News* 1987. p. 1-7.

127. J. Rudolph, C. Gasteiger, & J. Sadowski, *Comput. Methodol.,* Tetrahedron, **3**, 537-547 (1990).

128. N. L. Allinger & U. Burkert, *Molecular Mechanics, ACS Monograph,* **177**, 62 (1982).

129. W. Sippl, H-D Holtje, D. Rognan & G. Folkers, *Molecular Modelling: Basic principles and applications* 23 (2003).

130. M. J. S. Dewar, E. G. Zoebisch, E. F. Healy & J. J. P. Stewart, *Development and use of quantum mechanical molecular models. 76. AM1: a new general purpose quantum mechanical molecular model,* J. Amer. Chem. Soc., **107**, 3902-3909 (1985).

131. J. J P. Stewart, *editor, Semiempirical molecular orbital methods. In: Reviews in Computational Chemistry,* 1, VCH New York, 45-81 (1990).

132. CAChe Work space, CAChe Ab Initio, Oxford Molecular Group Limited (1989-2000).

133. B. Osterby, R. D. McKelvey & L. Hill, *Photochromic Sunglasses, A patent-Based Advanced Organic Synthesis Project and Demonstration* J. Chem. Educ., **68**, 425 (1991).

134. J. Griffiths, *Practical aspects of colour prediction of organic dye molecules,* Dyes and Pigments, **3**, 211-233 (1982).
135. J. Griffiths, Chemistry in Britain, **22**, 997 (1986).
136. R. Pariser & R. G. Parr, Chemical Physics, **21**, 466, 767 (1953).
137. J. A. Pople, *Electron interaction in unsaturated hydrocarbons,* Translations of the Faraday Society, **49**, 1375-85 (1953).
138. J. L. Mchale, H. B. Lueck & W. D. Edward, *Symmetry-breading solvent effects on the electronic structure and spectra of a series of triphenylmethane dyes,* J. Amer. Chem. Soc., **114**, 2342-2348 (1992).
139. R. M. Christie, C-H Chang, H-Y Huang & M. Vincent, *Colour and constitution relationships in organic pigments: Part 6 Azonaphtharylamide Pigments,* Surface coating international Part B: Coating Transactions, **89**, 1-10 (2006).
140. R. M. Christie, L. J. Chi, R. A. Spark, K. M. Morgan, A. S. F. Boyd & A. Lycka, *The application of molecular modelling techniques in the prediction of the photochromic behaviour of spiroindolinonaphthoxazines,* J. Photochem. and Photobiolo. A: chemistry, **169**, 41 (2005).
141. S. Nakamura M. Aoto, S. Maeda, Y. Tomotake, T. Matsuzaki & T. Murayama, MRS International Meeting on Adv. Mats, **12**, 219 (1989).
142. P. K. Porter & C. S. Marvel, *Based on the preparation of 1-nitroso-2-naphthol* Org. Synth. Coll., **I**, 411 (1941).
143. R. M. Christie, C. Agyako, K. D. Mitchell & A. Lycka, *The formation of Dihydroxyspiro[1,2]oxazines from the reaction of Fischer's base with some isonitroso compounds. A multinuclear NMR study,* Dyes and Pigments, **131**, 155-170 (1995).
144. S. M. Reduwan Billah, *Molecular design and synthesis of photochromic dyes for direct application of textiles and leather substrates*, PhD thesis, School of Textiles and Design, Heriot-Watt University, p-122 (2007).
145. K. D. Mitchell, *Synthesis and structural investigation of potentially photochromic spirooxazines and their ring opened forms,* PhD thesis, School of Textiles and Design, Heriot-Watt University: Galashiels, p-202 (1997).

146. Li-Jen Chi, *Synthesis and Computer aided structural investigation of potentially photochromic spirooxazines* PhD thesis, Scottish Borders Campus, Heriot-Watt University (2000).

147. K. D. Mitchell, *Synthesis and structural investigation of potentially photochromic spirooxazines and their ring opened forms*, PhD thesis, School of Textiles, Heriot-Watt University: Galashiels, p-116 (1997).

148. T. Kubota, M. Yamakawa & Hideko, *Electronic Structure of Aromatic Amine N-Oxide,* Theoretical Chemistry Accounts: Theory, Computation and Modeling, **15**, 245-251 (1969).

149. D. Hepworth, A. John, R. M. Christie, C. D. Gabbutt & S. Rae, *An investigation of the electronic spectral properties of the coloured photoproducts derived from some photochromic naphtho[2,1-b]pyrans,* Dyes and Pigments, **35**, 343 (1997).

150. B. M. Heron, *Private communication*, University of Leeds, U.K (2005).

151. C. D. Gabbutt, B. M. Heron, A. C. Instone, D. A. Thomas, S. M. Partington, M. B. Hursthouse & T. Gelbrich, *Observations on the synthesis of Photochromic Naphthopyrans,* Eur. J. Org. Chem., 1222 (2003).

152. J. Griffiths, Rev. Prog. Colouration, **11**, 37 (1981).

153. R. M.Christie, C. K. Agyako & K.D. Mitchell, *An investigation of the electronic spectral properties of the merocyanines derived from photochromic spiroindolinonaphth[2,1-b][1,4]oxazines,* Dyes and Pigments, **29**, 241 (1995).

154. K. Nishimoto & N. Mataga, Zeitschrift Fur Physical Chemistry, **12**, 335 (1957).

155. W. Dettwyler, United State Patent, 3,051,750 (1962).

156. P. Grossmann, *Polyhydroxy-b-acylaminoanthraquinones*, 2,819,288, Switzerland, 2 (1958).

157. D. Lempert & S. Bittner, *Reaction of Hydroxylamines with 1,4-Quinones: A new direct synthesis of aminoquinones,* Synthesis, 917 (1994).

158. A. Samat, R. Guglielmetti & V. Lokshin, *Synthesis of photochromic spirooxazines from 1-amino-2-naphthol,* Tetrahedron, **53**, 9675 (1997).

159. K .D. Mitchell, *Synthesis and structural investigation of potentially photochromic spirooxazines and their ring open forms*, PhD thesis, Scottish College of Textile, Department of Textile, Heriot-Watt University, p-176 (1997).

160. K. D. Mitchell, *Synthesis and structural investigation of potentially photochromic spirooxazines and their ring open forms*, PhD thesis, Scottish College of Textile, Department of Textile, Heriot-Watt University, p-183 (1997).

161. B. M. Heron, C. D. Gabbutt, A. C. Instone, D. A. Thomas, S. M. Partington, M. B. Hursthouse & T. Gelbrich, *Observations on the synthesis of Photochromic Naphthopyrans,* Eur. J. Org. Chem., 1222 (2003).

Appendix A

X-ray crystal structure data and structure refinement for compound (134).

Empirical formula	C28 H25 N5 O5	
Formula weight	511.53	
Temperature	100(2) K	
Wavelength	0.71073 Å	
Crystal system	Triclinic	
Space group	P-1	
Unit cell dimensions	a = 9.3585(14) Å	α=111.358(8)°.
	b = 11.1009(17) Å	β= 03.385(8)°.
	c = 13.201(2) Å	γ = 95.229(8)°.
Volume	1219.1(3) $Å^3$	
Z	2	
Density (calculated)	1.394 Mg/m^3	
Absorption coefficient	0.098 mm^{-1}	
F(000)	536	
Crystal size	0.16 x 0.10 x 0.08 mm^3	
Theta range for data collection	2.44 to 29.93°.	
Index ranges	-13<=h<=13, -15<=k<=15, -18<=l<=17	
Reflections collected	39435	
Independent reflections	6927 [R(int) = 0.0753]	
Completeness to theta = 25.00°	98.3 %	
Absorption correction	Semi-empirical from equivalents	
Max. and min. transmission	0.9922 and 0.9845	
Refinement method	Full-matrix least-squares on F^2	
Data / restraints / parameters	6927 / 0 / 358	
Goodness-of-fit on F^2	0.973	
Final R indices [I>2sigma(I)]	R1 = 0.0507, wR2 = 0.1073	

R indices (all data)	R1 = 0.1283, wR2 = 0.1319
Largest diff. peak and hole	0.265 and -0.295 e.Å^{-3}

(i) Bond lengths [Å] and angles [°] for compound (134)

C(1)-C(2)	1.400(2)
C(1)-C(10)	1.412(2)
C(1)-N(1)	1.428(2)
N(1)-C(11)	1.343(2)
N(1)-H(1N)	0.865(18)
C(2)-O(2)	1.3669(19)
C(2)-C(3)	1.393(2)
O(2)-H(2O)	0.96(3)
C(3)-C(4)	1.371(2)
C(3)-H(3)	0.9500
C(4)-C(5)	1.396(2)
C(4)-H(4)	0.9500
C(5)-C(10)	1.418(2)
C(5)-C(6)	1.444(2)
C(6)-C(7)	1.335(3)
C(6)-H(6)	0.9500
C(7)-C(8)	1.443(2)
C(7)-H(7)	0.9500
C(8)-O(8)	1.248(2)
C(8)-C(9)	1.476(2)
C(9)-N(9)	1.324(2)
C(9)-C(10)	1.469(2)
N(9)-N(10)	1.3325(18)
N(10)-C(23)	1.400(2)
N(10)-H(10N)	0.93(2)
C(11)-O(11)	1.2469(18)

C(11)-C(12)	1.518(2)
C(12)-N(13)	1.472(2)
C(12)-C(20)	1.567(2)
C(12)-H(12)	1.0000
C(13)-N(13)	1.460(2)
C(13)-H(13A)	0.9800
C(13)-H(13B)	0.9800
C(13)-H(13C)	0.9800
N(13)-C(14)	1.417(2)
C(14)-C(15)	1.390(2)
C(14)-C(19)	1.389(2)
C(15)-C(16)	1.387(2)
C(15)-H(15)	0.9500
C(16)-C(17)	1.387(3)
C(16)-H(16)	0.9500
C(17)-C(18)	1.388(2)
C(17)-H(17)	0.9500
C(18)-C(19)	1.388(2)
C(18)-H(18)	0.9500
C(19)-C(20)	1.515(2)
C(20)-C(22)	1.533(2)
C(20)-C(21)	1.541(2)
C(21)-H(21A)	0.9800
C(21)-H(21B)	0.9800
C(21)-H(21C)	0.9800
C(22)-H(22A)	0.9800
C(22)-H(22B)	0.9800
C(22)-H(22C)	0.9800
C(23)-C(24)	1.392(2)
C(23)-C(28)	1.397(2)
C(24)-C(25)	1.379(2)

C(24)-H(24)	0.9500
C(25)-C(26)	1.382(2)
C(25)-H(25)	0.9500
C(26)-C(27)	1.387(2)
C(26)-N(26)	1.459(2)
N(26)-O(27)	1.231(2)
N(26)-O(26)	1.2324(19)
C(27)-C(28)	1.377(3)
C(27)-H(27)	0.9500
C(28)-H(28)	0.9500

C(2)-C(1)-C(10)	119.64(15)
C(2)-C(1)-N(1)	121.10(15)
C(10)-C(1)-N(1)	119.22(14)
C(11)-N(1)-C(1)	128.08(15)
C(11)-N(1)-H(1N)	114.8(12)
C(1)-N(1)-H(1N)	114.5(12)
O(2)-C(2)-C(3)	117.38(15)
O(2)-C(2)-C(1)	122.15(15)
C(3)-C(2)-C(1)	120.40(16)
C(2)-O(2)-H(2O)	105.8(14)
C(4)-C(3)-C(2)	120.13(16)
C(4)-C(3)-H(3)	119.9
C(2)-C(3)-H(3)	119.9
C(3)-C(4)-C(5)	121.19(16)
C(3)-C(4)-H(4)	119.4
C(5)-C(4)-H(4)	119.4
C(4)-C(5)-C(10)	119.37(16)
C(4)-C(5)-C(6)	120.95(16)
C(10)-C(5)-C(6)	119.63(16)
C(7)-C(6)-C(5)	123.43(17)

C(7)-C(6)-H(6)	118.3
C(5)-C(6)-H(6)	118.3
C(6)-C(7)-C(8)	120.96(17)
C(6)-C(7)-H(7)	119.5
C(8)-C(7)-H(7)	119.5
O(8)-C(8)-C(7)	122.37(16)
O(8)-C(8)-C(9)	120.83(16)
C(7)-C(8)-C(9)	116.66(16)
N(9)-C(9)-C(10)	117.09(15)
N(9)-C(9)-C(8)	122.05(15)
C(10)-C(9)-C(8)	120.24(15)
C(9)-N(9)-N(10)	120.38(15)
N(9)-N(10)-C(23)	118.64(15)
N(9)-N(10)-H(10N)	114.4(13)
C(23)-N(10)-H(10N)	126.6(13)
C(1)-C(10)-C(5)	118.95(15)
C(1)-C(10)-C(9)	124.49(15)
C(5)-C(10)-C(9)	116.54(15)
O(11)-C(11)-N(1)	124.24(16)
O(11)-C(11)-C(12)	119.65(15)
N(1)-C(11)-C(12)	116.03(15)
N(13)-C(12)-C(11)	113.68(13)
N(13)-C(12)-C(20)	105.95(13)
C(11)-C(12)-C(20)	112.17(13)
N(13)-C(12)-H(12)	108.3
C(11)-C(12)-H(12)	108.3
C(20)-C(12)-H(12)	108.3
N(13)-C(13)-H(13A)	109.5
N(13)-C(13)-H(13B)	109.5
H(13A)-C(13)-H(13B)	109.5
N(13)-C(13)-H(13C)	109.5

H(13A)-C(13)-H(13C)	109.5
H(13B)-C(13)-H(13C)	109.5
C(14)-N(13)-C(13)	117.09(13)
C(14)-N(13)-C(12)	106.15(13)
C(13)-N(13)-C(12)	115.39(13)
C(15)-C(14)-C(19)	121.44(16)
C(15)-C(14)-N(13)	127.49(16)
C(19)-C(14)-N(13)	111.06(14)
C(16)-C(15)-C(14)	117.72(17)
C(16)-C(15)-H(15)	121.1
C(14)-C(15)-H(15)	121.1
C(15)-C(16)-C(17)	121.46(17)
C(15)-C(16)-H(16)	119.3
C(17)-C(16)-H(16)	119.3
C(18)-C(17)-C(16)	120.22(17)
C(18)-C(17)-H(17)	119.9
C(16)-C(17)-H(17)	119.9
C(19)-C(18)-C(17)	119.04(17)
C(19)-C(18)-H(18)	120.5
C(17)-C(18)-H(18)	120.5
C(18)-C(19)-C(14)	120.05(16)
C(18)-C(19)-C(20)	129.66(16)
C(14)-C(19)-C(20)	110.29(14)
C(19)-C(20)-C(22)	113.23(14)
C(19)-C(20)-C(21)	109.87(14)
C(22)-C(20)-C(21)	110.20(14)
C(19)-C(20)-C(12)	100.45(12)
C(22)-C(20)-C(12)	110.00(14)
C(21)-C(20)-C(12)	112.82(13)
C(20)-C(21)-H(21A)	109.5
C(20)-C(21)-H(21B)	109.5

H(21A)-C(21)-H(21B)	109.5
C(20)-C(21)-H(21C)	109.5
H(21A)-C(21)-H(21C)	109.5
H(21B)-C(21)-H(21C)	109.5
C(20)-C(22)-H(22A)	109.5
C(20)-C(22)-H(22B)	109.5
H(22A)-C(22)-H(22B)	109.5
C(20)-C(22)-H(22C)	109.5
H(22A)-C(22)-H(22C)	109.5
H(22B)-C(22)-H(22C)	109.5
C(24)-C(23)-C(28)	120.65(17)
C(24)-C(23)-N(10)	121.78(15)
C(28)-C(23)-N(10)	117.56(16)
C(25)-C(24)-C(23)	119.61(16)
C(25)-C(24)-H(24)	120.2
C(23)-C(24)-H(24)	120.2
C(24)-C(25)-C(26)	119.22(17)
C(24)-C(25)-H(25)	120.4
C(26)-C(25)-H(25)	120.4
C(25)-C(26)-C(27)	121.76(17)
C(25)-C(26)-N(26)	118.95(17)
C(27)-C(26)-N(26)	119.29(16)
O(27)-N(26)-O(26)	122.85(17)
O(27)-N(26)-C(26)	118.66(16)
O(26)-N(26)-C(26)	118.48(17)
C(28)-C(27)-C(26)	119.18(17)
C(28)-C(27)-H(27)	120.4
C(26)-C(27)-H(27)	120.4
C(27)-C(28)-C(23)	119.56(18)
C(27)-C(28)-H(28)	120.2

C(23)-C(28)-H(28) 120.2

Symmetry transformations used to generate equivalent atoms:

(ii) Torsion angles [°] for compound (134)

C(2)-C(1)-N(1)-C(11)	-44.5(3)
C(10)-C(1)-N(1)-C(11)	137.63(18)
C(10)-C(1)-C(2)-O(2)	175.32(15)
N(1)-C(1)-C(2)-O(2)	-2.6(3)
C(10)-C(1)-C(2)-C(3)	-1.6(2)
N(1)-C(1)-C(2)-C(3)	-179.51(15)
O(2)-C(2)-C(3)-C(4)	-179.17(15)
C(1)-C(2)-C(3)-C(4)	-2.1(3)
C(2)-C(3)-C(4)-C(5)	1.5(3)
C(3)-C(4)-C(5)-C(10)	2.7(3)
C(3)-C(4)-C(5)-C(6)	-174.69(16)
C(4)-C(5)-C(6)-C(7)	175.19(18)
C(10)-C(5)-C(6)-C(7)	-2.2(3)
C(5)-C(6)-C(7)-C(8)	6.3(3)
C(6)-C(7)-C(8)-O(8)	178.02(18)
C(6)-C(7)-C(8)-C(9)	2.4(3)
O(8)-C(8)-C(9)-N(9)	-20.1(3)
C(7)-C(8)-C(9)-N(9)	155.58(17)
O(8)-C(8)-C(9)-C(10)	169.19(16)
C(7)-C(8)-C(9)-C(10)	-15.1(2)
C(10)-C(9)-N(9)-N(10)	178.61(14)
C(8)-C(9)-N(9)-N(10)	7.6(2)
C(9)-N(9)-N(10)-C(23)	-167.32(15)
C(2)-C(1)-C(10)-C(5)	5.8(2)
N(1)-C(1)-C(10)-C(5)	-176.31(15)

C(2)-C(1)-C(10)-C(9)	-172.69(16)
N(1)-C(1)-C(10)-C(9)	5.2(2)
C(4)-C(5)-C(10)-C(1)	-6.3(2)
C(6)-C(5)-C(10)-C(1)	171.12(15)
C(4)-C(5)-C(10)-C(9)	172.28(15)
C(6)-C(5)-C(10)-C(9)	-10.3(2)
N(9)-C(9)-C(10)-C(1)	26.2(2)
C(8)-C(9)-C(10)-C(1)	-162.63(16)
N(9)-C(9)-C(10)-C(5)	-152.25(16)
C(8)-C(9)-C(10)-C(5)	18.9(2)
C(1)-N(1)-C(11)-O(11)	12.0(3)
C(1)-N(1)-C(11)-C(12)	-171.27(15)
O(11)-C(11)-C(12)-N(13)	-164.35(14)
N(1)-C(11)-C(12)-N(13)	18.8(2)
O(11)-C(11)-C(12)-C(20)	75.47(19)
N(1)-C(11)-C(12)-C(20)	-101.40(17)
C(11)-C(12)-N(13)-C(14)	-148.67(14)
C(20)-C(12)-N(13)-C(14)	-25.03(16)
C(11)-C(12)-N(13)-C(13)	79.86(18)
C(20)-C(12)-N(13)-C(13)	-156.50(14)
C(13)-N(13)-C(14)-C(15)	-32.3(2)
C(12)-N(13)-C(14)-C(15)	-162.76(17)
C(13)-N(13)-C(14)-C(19)	148.96(15)
C(12)-N(13)-C(14)-C(19)	18.46(18)
C(19)-C(14)-C(15)-C(16)	2.3(3)
N(13)-C(14)-C(15)-C(16)	-176.40(16)
C(14)-C(15)-C(16)-C(17)	0.2(3)
C(15)-C(16)-C(17)-C(18)	-1.8(3)
C(16)-C(17)-C(18)-C(19)	0.9(3)
C(17)-C(18)-C(19)-C(14)	1.6(3)
C(17)-C(18)-C(19)-C(20)	-179.08(17)

C(15)-C(14)-C(19)-C(18)	-3.2(3)
N(13)-C(14)-C(19)-C(18)	175.67(15)
C(15)-C(14)-C(19)-C(20)	177.32(15)
N(13)-C(14)-C(19)-C(20)	-3.80(19)
C(18)-C(19)-C(20)-C(22)	52.1(2)
C(14)-C(19)-C(20)-C(22)	-128.52(16)
C(18)-C(19)-C(20)-C(21)	-71.6(2)
C(14)-C(19)-C(20)-C(21)	107.79(16)
C(18)-C(19)-C(20)-C(12)	169.30(17)
C(14)-C(19)-C(20)-C(12)	-11.29(17)
N(13)-C(12)-C(20)-C(19)	21.73(16)
C(11)-C(12)-C(20)-C(19)	146.32(14)
N(13)-C(12)-C(20)-C(22)	141.33(14)
C(11)-C(12)-C(20)-C(22)	-94.09(16)
N(13)-C(12)-C(20)-C(21)	-95.17(15)
C(11)-C(12)-C(20)-C(21)	29.41(19)
N(9)-N(10)-C(23)-C(24)	8.5(2)
N(9)-N(10)-C(23)-C(28)	-172.41(15)
C(28)-C(23)-C(24)-C(25)	1.4(3)
N(10)-C(23)-C(24)-C(25)	-179.48(15)
C(23)-C(24)-C(25)-C(26)	-1.4(3)
C(24)-C(25)-C(26)-C(27)	0.6(3)
C(24)-C(25)-C(26)-N(26)	-179.92(15)
C(25)-C(26)-N(26)-O(27)	-5.4(2)
C(27)-C(26)-N(26)-O(27)	174.18(16)
C(25)-C(26)-N(26)-O(26)	175.34(16)
C(27)-C(26)-N(26)-O(26)	-5.1(2)
C(25)-C(26)-C(27)-C(28)	0.2(3)
N(26)-C(26)-C(27)-C(28)	-179.28(16)
C(26)-C(27)-C(28)-C(23)	-0.2(3)
C(24)-C(23)-C(28)-C(27)	-0.6(3)

N(10)-C(23)-C(28)-C(27)	-179.76(15)

Symmetry transformations used to generate equivalent atoms:

(iii) Hydrogen bonds for compound (134)

___ D-H...A	d(D-H)	d(H...A)	d(D...A)	<(DHA)
___ N(1)-H(1N)...N(9)	0.865(18)	2.025(17)	2.711(2)	135.5(15)
N(1)-H(1N)...N(13)	0.865(18)	2.263(17)	2.734(2)	114.2(14)
N(10)-H(10N)...O(8)	0.93(2)	1.80(2)	2.569(2)	139.1(18)
O(2)-H(2O)...O(11)	0.96(3)	1.63(3)	2.5713(18)	163(2)

__

Symmetry transformations used to generate equivalent atoms:

Appendix B

X-ray crystal structure data and structure refinement for compound (154).

Empirical formula	C23 H24 N4 O2	
Formula weight	388.46	
Temperature	100(2) K	
Wavelength	0.71073 Å	
Crystal system	Triclinic	
Space group	P-1	
Unit cell dimensions	a = 8.376(2) Å	α= 102.077(7)°.
	b = 11.003(3) Å	β= 108.494(6)°.
	c = 11.447(3) Å	γ = 97.143(6)°.
Volume	957.4(4) $Å^3$	
Z	2	
Density (calculated)	1.347 Mg/m^3	
Absorption coefficient	0.088 mm^{-1}	
F(000)	412	
Crystal size	0.40 x 0.26 x 0.03 mm^3	
Theta range for data collection	2.62 to 29.28°.	
Index ranges	-11<=h<=11, -14<=k<=15, -15<=l<=15	
Reflections collected	24595	
Independent reflections	5070 [R(int) = 0.0696]	
Completeness to theta = 25.00°	98.5 %	
Absorption correction	Semi-empirical from equivalents	
Max. and min. transmission	0.997 and 0.682	
Refinement method	Full-matrix least-squares on F^2	
Data / restraints / parameters	5070 / 0 / 267	
Goodness-of-fit on F^2	1.003	
Final R indices [I>2sigma(I)]	R1 = 0.0646, wR2 = 0.1454	
R indices (all data)	R1 = 0.1400, wR2 = 0.1878	

Largest diff. peak and hole	0.330 and -0.259 e.Å^{-3}

(i) Bond lengths [Å] and angles [°] for compound (154)

N(1)-O(1)	1.274(2)
N(1)-C(15)	1.356(3)
N(1)-C(2)	1.374(3)
C(2)-C(3)	1.373(3)
C(2)-H(2)	0.9500
C(3)-N(11)	1.355(3)
C(3)-C(4)	1.535(3)
C(4)-C(5)	1.520(3)
C(4)-C(13)	1.529(3)
C(4)-C(14)	1.533(3)
C(5)-C(6)	1.372(3)
C(5)-C(10)	1.378(3)
C(6)-C(7)	1.393(3)
C(6)-H(6)	0.9500
C(7)-C(8)	1.371(3)
C(7)-H(7)	0.9500
C(8)-C(9)	1.383(3)
C(8)-H(8)	0.9500
C(9)-C(10)	1.379(3)
C(9)-H(9)	0.9500
C(10)-N(11)	1.405(3)
N(11)-C(12)	1.449(3)
C(12)-H(12A)	0.9800
C(12)-H(12B)	0.9800
C(12)-H(12C)	0.9800
C(13)-H(13A)	0.9800
C(13)-H(13B)	0.9800
C(13)-H(13C)	0.9800

C(14)-H(14A)	0.9800
C(14)-H(14B)	0.9800
C(14)-H(14C)	0.9800
C(15)-C(19)	1.423(3)
C(15)-C(16)	1.445(3)
C(16)-O(16)	1.233(3)
C(16)-N(17)	1.387(3)
N(17)-N(18)	1.398(3)
N(17)-C(20)	1.403(3)
N(18)-C(19)	1.299(3)
C(19)-C(26)	1.480(3)
C(20)-C(25)	1.383(3)
C(20)-C(21)	1.391(3)
C(21)-C(22)	1.376(3)
C(21)-H(21)	0.9500
C(22)-C(23)	1.383(3)
C(22)-H(22)	0.9500
C(23)-C(24)	1.386(3)
C(23)-C(27)	1.502(3)
C(24)-C(25)	1.385(3)
C(24)-H(24)	0.9500
C(25)-H(25)	0.9500
C(26)-H(26A)	0.9800
C(26)-H(26B)	0.9800
C(26)-H(26C)	0.9800
C(27)-H(27A)	0.9800
C(27)-H(27B)	0.9800
C(27)-H(27C)	0.9800

O(1)-N(1)-C(15)	119.32(19)
O(1)-N(1)-C(2)	121.3(2)

C(15)-N(1)-C(2)	119.4(2)
C(3)-C(2)-N(1)	126.3(2)
C(3)-C(2)-H(2)	116.9
N(1)-C(2)-H(2)	116.9
N(11)-C(3)-C(2)	117.9(2)
N(11)-C(3)-C(4)	108.93(19)
C(2)-C(3)-C(4)	133.2(2)
C(5)-C(4)-C(13)	109.98(19)
C(5)-C(4)-C(14)	109.73(19)
C(13)-C(4)-C(14)	111.4(2)
C(5)-C(4)-C(3)	100.63(18)
C(13)-C(4)-C(3)	111.59(19)
C(14)-C(4)-C(3)	113.0(2)
C(6)-C(5)-C(10)	119.7(2)
C(6)-C(5)-C(4)	130.5(2)
C(10)-C(5)-C(4)	109.8(2)
C(5)-C(6)-C(7)	118.8(2)
C(5)-C(6)-H(6)	120.6
C(7)-C(6)-H(6)	120.6
C(8)-C(7)-C(6)	120.3(2)
C(8)-C(7)-H(7)	119.9
C(6)-C(7)-H(7)	119.9
C(7)-C(8)-C(9)	121.9(2)
C(7)-C(8)-H(8)	119.0
C(9)-C(8)-H(8)	119.0
C(10)-C(9)-C(8)	116.6(2)
C(10)-C(9)-H(9)	121.7
C(8)-C(9)-H(9)	121.7
C(5)-C(10)-C(9)	122.8(2)
C(5)-C(10)-N(11)	109.12(19)
C(9)-C(10)-N(11)	128.1(2)

C(3)-N(11)-C(10)	111.35(19)
C(3)-N(11)-C(12)	124.9(2)
C(10)-N(11)-C(12)	123.74(18)
N(11)-C(12)-H(12A)	109.5
N(11)-C(12)-H(12B)	109.5
H(12A)-C(12)-H(12B)	109.5
N(11)-C(12)-H(12C)	109.5
H(12A)-C(12)-H(12C)	109.5
H(12B)-C(12)-H(12C)	109.5
C(4)-C(13)-H(13A)	109.5
C(4)-C(13)-H(13B)	109.5
H(13A)-C(13)-H(13B)	109.5
C(4)-C(13)-H(13C)	109.5
H(13A)-C(13)-H(13C)	109.5
H(13B)-C(13)-H(13C)	109.5
C(4)-C(14)-H(14A)	109.5
C(4)-C(14)-H(14B)	109.5
H(14A)-C(14)-H(14B)	109.5
C(4)-C(14)-H(14C)	109.5
H(14A)-C(14)-H(14C)	109.5
H(14B)-C(14)-H(14C)	109.5
N(1)-C(15)-C(19)	125.0(2)
N(1)-C(15)-C(16)	127.5(2)
C(19)-C(15)-C(16)	107.3(2)
O(16)-C(16)-N(17)	125.5(2)
O(16)-C(16)-C(15)	131.7(2)
N(17)-C(16)-C(15)	102.76(19)
C(16)-N(17)-N(18)	112.09(19)
C(16)-N(17)-C(20)	129.45(19)
N(18)-N(17)-C(20)	117.84(17)
C(19)-N(18)-N(17)	107.48(18)

N(18)-C(19)-C(15)	110.3(2)
N(18)-C(19)-C(26)	120.4(2)
C(15)-C(19)-C(26)	129.3(2)
C(25)-C(20)-C(21)	118.8(2)
C(25)-C(20)-N(17)	122.4(2)
C(21)-C(20)-N(17)	118.8(2)
C(22)-C(21)-C(20)	120.3(2)
C(22)-C(21)-H(21)	119.9
C(20)-C(21)-H(21)	119.9
C(21)-C(22)-C(23)	122.0(2)
C(21)-C(22)-H(22)	119.0
C(23)-C(22)-H(22)	119.0
C(22)-C(23)-C(24)	117.1(2)
C(22)-C(23)-C(27)	121.5(2)
C(24)-C(23)-C(27)	121.4(2)
C(25)-C(24)-C(23)	122.0(2)
C(25)-C(24)-H(24)	119.0
C(23)-C(24)-H(24)	119.0
C(20)-C(25)-C(24)	119.9(2)
C(20)-C(25)-H(25)	120.1
C(24)-C(25)-H(25)	120.1
C(19)-C(26)-H(26A)	109.5
C(19)-C(26)-H(26B)	109.5
H(26A)-C(26)-H(26B)	109.5
C(19)-C(26)-H(26C)	109.5
H(26A)-C(26)-H(26C)	109.5
H(26B)-C(26)-H(26C)	109.5
C(23)-C(27)-H(27A)	109.5
C(23)-C(27)-H(27B)	109.5
H(27A)-C(27)-H(27B)	109.5
C(23)-C(27)-H(27C)	109.5

H(27A)-C(27)-H(27C)	109.5
H(27B)-C(27)-H(27C)	109.5

Symmetry transformations used to generate equivalent atoms:

(ii) Torsion angles [°] for compound (154)

O(1)-N(1)-C(2)-C(3)	-6.2(4)
C(15)-N(1)-C(2)-C(3)	174.7(2)
N(1)-C(2)-C(3)-N(11)	-179.8(2)
N(1)-C(2)-C(3)-C(4)	-1.6(4)
N(11)-C(3)-C(4)-C(5)	4.3(2)
C(2)-C(3)-C(4)-C(5)	-174.0(3)
N(11)-C(3)-C(4)-C(13)	-112.3(2)
C(2)-C(3)-C(4)-C(13)	69.4(3)
N(11)-C(3)-C(4)-C(14)	121.3(2)
C(2)-C(3)-C(4)-C(14)	-57.1(3)
C(13)-C(4)-C(5)-C(6)	-65.5(3)
C(14)-C(4)-C(5)-C(6)	57.4(3)
C(3)-C(4)-C(5)-C(6)	176.6(3)
C(13)-C(4)-C(5)-C(10)	115.4(2)
C(14)-C(4)-C(5)-C(10)	-121.7(2)
C(3)-C(4)-C(5)-C(10)	-2.4(2)
C(10)-C(5)-C(6)-C(7)	0.5(4)
C(4)-C(5)-C(6)-C(7)	-178.5(2)
C(5)-C(6)-C(7)-C(8)	-0.4(4)
C(6)-C(7)-C(8)-C(9)	0.1(4)
C(7)-C(8)-C(9)-C(10)	0.1(4)
C(6)-C(5)-C(10)-C(9)	-0.3(4)
C(4)-C(5)-C(10)-C(9)	178.8(2)
C(6)-C(5)-C(10)-N(11)	-179.4(2)

C(4)-C(5)-C(10)-N(11)	-0.3(3)
C(8)-C(9)-C(10)-C(5)	0.0(3)
C(8)-C(9)-C(10)-N(11)	179.0(2)
C(2)-C(3)-N(11)-C(10)	173.7(2)
C(4)-C(3)-N(11)-C(10)	-4.9(2)
C(2)-C(3)-N(11)-C(12)	-5.8(3)
C(4)-C(3)-N(11)-C(12)	175.6(2)
C(5)-C(10)-N(11)-C(3)	3.3(3)
C(9)-C(10)-N(11)-C(3)	-175.7(2)
C(5)-C(10)-N(11)-C(12)	-177.2(2)
C(9)-C(10)-N(11)-C(12)	3.8(4)
O(1)-N(1)-C(15)-C(19)	6.2(3)
C(2)-N(1)-C(15)-C(19)	-174.6(2)
O(1)-N(1)-C(15)-C(16)	-169.7(2)
C(2)-N(1)-C(15)-C(16)	9.5(4)
N(1)-C(15)-C(16)-O(16)	-3.5(4)
C(19)-C(15)-C(16)-O(16)	-180.0(2)
N(1)-C(15)-C(16)-N(17)	174.8(2)
C(19)-C(15)-C(16)-N(17)	-1.7(2)
O(16)-C(16)-N(17)-N(18)	-179.4(2)
C(15)-C(16)-N(17)-N(18)	2.2(2)
O(16)-C(16)-N(17)-C(20)	10.0(4)
C(15)-C(16)-N(17)-C(20)	-168.5(2)
C(16)-N(17)-N(18)-C(19)	-1.9(3)
C(20)-N(17)-N(18)-C(19)	170.0(2)
N(17)-N(18)-C(19)-C(15)	0.7(3)
N(17)-N(18)-C(19)-C(26)	-179.3(2)
N(1)-C(15)-C(19)-N(18)	-176.0(2)
C(16)-C(15)-C(19)-N(18)	0.7(3)
N(1)-C(15)-C(19)-C(26)	4.0(4)
C(16)-C(15)-C(19)-C(26)	-179.4(2)

C(16)-N(17)-C(20)-C(25)	-13.1(4)
N(18)-N(17)-C(20)-C(25)	176.7(2)
C(16)-N(17)-C(20)-C(21)	165.7(2)
N(18)-N(17)-C(20)-C(21)	-4.5(3)
C(25)-C(20)-C(21)-C(22)	1.0(4)
N(17)-C(20)-C(21)-C(22)	-177.9(2)
C(20)-C(21)-C(22)-C(23)	0.2(4)
C(21)-C(22)-C(23)-C(24)	-0.9(4)
C(21)-C(22)-C(23)-C(27)	177.7(2)
C(22)-C(23)-C(24)-C(25)	0.4(4)
C(27)-C(23)-C(24)-C(25)	-178.2(2)
C(21)-C(20)-C(25)-C(24)	-1.4(4)
N(17)-C(20)-C(25)-C(24)	177.4(2)
C(23)-C(24)-C(25)-C(20)	0.7(4)

Symmetry transformations used to generate equivalent atoms:

(iii) Hydrogen bonds for compound (154) [Å and °].

D-H...A	d(D-H)	d(H...A)	d(D...A)	<(DHA)
C(25)-H(25)...O(16)	0.95	2.32	2.939(3)	122.2
C(2)-H(2)...O(16)	0.95	2.20	2.931(3)	133.0
C(14)-H(14A)...O(1)	0.98	2.20	2.949(3)	132.3

Symmetry transformations used to generate equivalent atoms:

Appendix C

X-ray crystal structure data and structure refinement for compound (155).

Empirical formula	C22 H21 N5 O2	
Formula weight	387.44	
Temperature	100(2) K	
Wavelength	0.71073 Å	
Crystal system	Triclinic	
Space group	P-1	
Unit cell dimensions	a = 4.6547(9) Å	α= 97.929(7)°.
	b = 10.476(2) Å	β= 91.455(7)°.
	c = 19.556(4) Å	γ = 101.969(7)°.
Volume	922.5(3) $Å^3$	
Z	2	
Density (calculated)	1.395 Mg/m^3	
Absorption coefficient	0.093 mm^{-1}	
F(000)	408	
Crystal size	0.62 x 0.12 x 0.08 mm^3	
Theta range for data collection	2.01 to 32.97°.	
Index ranges	-6<=h<=6, -16<=k<=15, -29<=l<=29	
Reflections collected	16191	
Independent reflections	6091 [R(int) = 0.0483]	
Completeness to theta = 25.00°	95.1 %	
Absorption correction	Semi-empirical from equivalents	
Max. and min. transmission	0.993 and 0.739	
Refinement method	Full-matrix least-squares on F^2	
Data / restraints / parameters	6091 / 0 / 269	
Goodness-of-fit on F^2	1.033	
Final R indices [I>2sigma(I)]	R1 = 0.0863, wR2 = 0.2257	

R indices (all data)	R1 = 0.1832, wR2 = 0.2865
Largest diff. peak and hole	1.005 and -1.005 e.Å^{-3}

(i) Bond lengths [Å] and angles [°] for compound (155)

C(1)-N(1)	1.321(4)
C(1)-C(5)	1.438(4)
C(1)-C(2)	1.448(4)
N(1)-C(14)	1.319(4)
C(2)-O(5)	1.282(4)
C(2)-N(3)	1.342(4)
N(3)-N(4)	1.410(4)
N(3)-C(7)	1.423(4)
N(4)-C(5)	1.300(4)
C(5)-C(6)	1.484(5)
O(5)-H(5)	1.16(5)
C(6)-H(6A)	0.9800
C(6)-H(6B)	0.9800
C(6)-H(6C)	0.9800
C(7)-C(8)	1.333(5)
C(7)-C(12)	1.341(6)
C(8)-C(9)	1.389(6)
C(8)-H(8)	0.9500
C(9)-C(10)	1.341(6)
C(9)-H(9)	0.9500
C(10)-C(11)	1.338(6)
C(10)-C(13)	1.509(5)
C(11)-C(12)	1.379(6)
C(11)-H(11)	0.9500
C(12)-H(12)	0.9500
C(13)-H(13A)	0.9800

C(13)-H(13B)	0.9800
C(13)-H(13C)	0.9800
C(14)-C(18)	1.442(4)
C(14)-C(15)	1.451(5)
C(15)-O(15)	1.268(4)
C(15)-N(16)	1.351(4)
O(15)-H(5)	1.26(5)
N(16)-N(17)	1.417(4)
N(16)-C(20)	1.419(4)
N(17)-C(18)	1.292(4)
C(18)-C(19)	1.484(5)
C(19)-H(19A)	0.9800
C(19)-H(19B)	0.9800
C(19)-H(19C)	0.9800
C(20)-C(21)	1.386(5)
C(20)-C(25)	1.394(4)
C(21)-C(22)	1.385(5)
C(21)-H(21)	0.9500
C(22)-C(23)	1.389(4)
C(22)-H(22)	0.9500
C(23)-C(24)	1.386(5)
C(23)-C(26)	1.504(5)
C(24)-C(25)	1.382(5)
C(24)-H(24)	0.9500
C(25)-H(25)	0.9500
C(26)-H(26A)	0.9800
C(26)-H(26B)	0.9800
C(26)-H(26C)	0.9800

N(1)-C(1)-C(5)	120.5(3)
N(1)-C(1)-C(2)	135.7(3)

C(5)-C(1)-C(2)	103.6(3)
C(14)-N(1)-C(1)	134.0(3)
O(5)-C(2)-N(3)	122.5(3)
O(5)-C(2)-C(1)	131.3(3)
N(3)-C(2)-C(1)	106.1(3)
C(2)-N(3)-N(4)	112.1(3)
C(2)-N(3)-C(7)	130.1(3)
N(4)-N(3)-C(7)	117.8(2)
C(5)-N(4)-N(3)	105.7(3)
N(4)-C(5)-C(1)	112.4(3)
N(4)-C(5)-C(6)	121.5(3)
C(1)-C(5)-C(6)	126.1(3)
C(2)-O(5)-H(5)	113(2)
C(5)-C(6)-H(6A)	109.5
C(5)-C(6)-H(6B)	109.5
H(6A)-C(6)-H(6B)	109.5
C(5)-C(6)-H(6C)	109.5
H(6A)-C(6)-H(6C)	109.5
H(6B)-C(6)-H(6C)	109.5
C(8)-C(7)-C(12)	117.5(4)
C(8)-C(7)-N(3)	119.5(3)
C(12)-C(7)-N(3)	123.0(3)
C(7)-C(8)-C(9)	120.8(4)
C(7)-C(8)-H(8)	119.6
C(9)-C(8)-H(8)	119.6
C(10)-C(9)-C(8)	122.5(4)
C(10)-C(9)-H(9)	118.8
C(8)-C(9)-H(9)	118.8
C(11)-C(10)-C(9)	115.5(4)
C(11)-C(10)-C(13)	121.3(4)
C(9)-C(10)-C(13)	123.1(4)

C(10)-C(11)-C(12)	122.8(5)
C(10)-C(11)-H(11)	118.6
C(12)-C(11)-H(11)	118.6
C(7)-C(12)-C(11)	120.9(4)
C(7)-C(12)-H(12)	119.6
C(11)-C(12)-H(12)	119.6
C(10)-C(13)-H(13A)	109.5
C(10)-C(13)-H(13B)	109.5
H(13A)-C(13)-H(13B)	109.5
C(10)-C(13)-H(13C)	109.5
H(13A)-C(13)-H(13C)	109.5
H(13B)-C(13)-H(13C)	109.5
N(1)-C(14)-C(18)	121.3(3)
N(1)-C(14)-C(15)	134.7(3)
C(18)-C(14)-C(15)	104.0(3)
O(15)-C(15)-N(16)	123.8(3)
O(15)-C(15)-C(14)	130.7(3)
N(16)-C(15)-C(14)	105.5(3)
C(15)-O(15)-H(5)	115(2)
C(15)-N(16)-N(17)	112.2(3)
C(15)-N(16)-C(20)	129.5(3)
N(17)-N(16)-C(20)	118.3(2)
C(18)-N(17)-N(16)	105.8(2)
N(17)-C(18)-C(14)	112.6(3)
N(17)-C(18)-C(19)	121.5(3)
C(14)-C(18)-C(19)	125.9(3)
C(18)-C(19)-H(19A)	109.5
C(18)-C(19)-H(19B)	109.5
H(19A)-C(19)-H(19B)	109.5
C(18)-C(19)-H(19C)	109.5
H(19A)-C(19)-H(19C)	109.5

H(19B)-C(19)-H(19C)	109.5
C(21)-C(20)-C(25)	119.8(3)
C(21)-C(20)-N(16)	121.4(3)
C(25)-C(20)-N(16)	118.8(3)
C(22)-C(21)-C(20)	119.4(3)
C(22)-C(21)-H(21)	120.3
C(20)-C(21)-H(21)	120.3
C(21)-C(22)-C(23)	121.8(3)
C(21)-C(22)-H(22)	119.1
C(23)-C(22)-H(22)	119.1
C(24)-C(23)-C(22)	117.7(3)
C(24)-C(23)-C(26)	121.7(3)
C(22)-C(23)-C(26)	120.6(3)
C(25)-C(24)-C(23)	121.8(3)
C(25)-C(24)-H(24)	119.1
C(23)-C(24)-H(24)	119.1
C(24)-C(25)-C(20)	119.4(3)
C(24)-C(25)-H(25)	120.3
C(20)-C(25)-H(25)	120.3
C(23)-C(26)-H(26A)	109.5
C(23)-C(26)-H(26B)	109.5
H(26A)-C(26)-H(26B)	109.5
C(23)-C(26)-H(26C)	109.5
H(26A)-C(26)-H(26C)	109.5
H(26B)-C(26)-H(26C)	109.5

Symmetry transformations used to generate equivalent atoms:

(ii) Torsion angles [°] for compound (155)

C(5)-C(1)-N(1)-C(14)	179.4(3)

C(2)-C(1)-N(1)-C(14)	4.8(6)
N(1)-C(1)-C(2)-O(5)	-2.4(6)
C(5)-C(1)-C(2)-O(5)	-177.5(3)
N(1)-C(1)-C(2)-N(3)	175.5(3)
C(5)-C(1)-C(2)-N(3)	0.4(3)
O(5)-C(2)-N(3)-N(4)	177.4(3)
C(1)-C(2)-N(3)-N(4)	-0.8(3)
O(5)-C(2)-N(3)-C(7)	-1.8(5)
C(1)-C(2)-N(3)-C(7)	-180.0(3)
C(2)-N(3)-N(4)-C(5)	0.9(3)
C(7)-N(3)-N(4)-C(5)	-179.8(3)
N(3)-N(4)-C(5)-C(1)	-0.6(3)
N(3)-N(4)-C(5)-C(6)	178.5(3)
N(1)-C(1)-C(5)-N(4)	-175.9(3)
C(2)-C(1)-C(5)-N(4)	0.2(3)
N(1)-C(1)-C(5)-C(6)	5.1(5)
C(2)-C(1)-C(5)-C(6)	-178.8(3)
C(2)-N(3)-C(7)-C(8)	-176.1(5)
N(4)-N(3)-C(7)-C(8)	4.7(5)
C(2)-N(3)-C(7)-C(12)	4.4(7)
N(4)-N(3)-C(7)-C(12)	-174.7(5)
C(12)-C(7)-C(8)-C(9)	0.9(10)
N(3)-C(7)-C(8)-C(9)	-178.6(5)
C(7)-C(8)-C(9)-C(10)	-0.9(11)
C(8)-C(9)-C(10)-C(11)	0.3(10)
C(8)-C(9)-C(10)-C(13)	178.6(6)
C(9)-C(10)-C(11)-C(12)	0.3(11)
C(13)-C(10)-C(11)-C(12)	-178.1(7)
C(8)-C(7)-C(12)-C(11)	-0.3(11)
N(3)-C(7)-C(12)-C(11)	179.2(7)
C(10)-C(11)-C(12)-C(7)	-0.3(14)

C(1)-N(1)-C(14)-C(18)	-175.7(3)
C(1)-N(1)-C(14)-C(15)	4.7(6)
N(1)-C(14)-C(15)-O(15)	2.4(6)
C(18)-C(14)-C(15)-O(15)	-177.2(3)
N(1)-C(14)-C(15)-N(16)	180.0(3)
C(18)-C(14)-C(15)-N(16)	0.4(3)
O(15)-C(15)-N(16)-N(17)	177.6(3)
C(14)-C(15)-N(16)-N(17)	-0.2(3)
O(15)-C(15)-N(16)-C(20)	-4.9(5)
C(14)-C(15)-N(16)-C(20)	177.4(3)
C(15)-N(16)-N(17)-C(18)	0.0(3)
C(20)-N(16)-N(17)-C(18)	-177.9(2)
N(16)-N(17)-C(18)-C(14)	0.3(3)
N(16)-N(17)-C(18)-C(19)	180.0(3)
N(1)-C(14)-C(18)-N(17)	179.9(3)
C(15)-C(14)-C(18)-N(17)	-0.4(3)
N(1)-C(14)-C(18)-C(19)	0.3(5)
C(15)-C(14)-C(18)-C(19)	179.9(3)
C(15)-N(16)-C(20)-C(21)	7.7(5)
N(17)-N(16)-C(20)-C(21)	-174.9(3)
C(15)-N(16)-C(20)-C(25)	-172.1(3)
N(17)-N(16)-C(20)-C(25)	5.3(4)
C(25)-C(20)-C(21)-C(22)	1.2(4)
N(16)-C(20)-C(21)-C(22)	-178.6(3)
C(20)-C(21)-C(22)-C(23)	-0.3(4)
C(21)-C(22)-C(23)-C(24)	-0.8(4)
C(21)-C(22)-C(23)-C(26)	179.6(3)
C(22)-C(23)-C(24)-C(25)	1.0(5)
C(26)-C(23)-C(24)-C(25)	-179.4(3)
C(23)-C(24)-C(25)-C(20)	-0.2(5)
C(21)-C(20)-C(25)-C(24)	-0.9(4)

N(16)-C(20)-C(25)-C(24)	178.8(3)

Symmetry transformations used to generate equivalent atoms:

(iii) Hydrogen bonds for compound (155) [Å and °].

___D-H...A	d(D-H)	d(H...A)	d(D...A)	<(DHA)
___ O(5)-H(5)...O(15)	1.16(5)	1.26(5)	2.415(3)	177(5)

___Symmetry transformations used to generate equivalent atoms:

Glossary of Terms

1: Bathochromic Shift

Shift of a spectral band to lower frequencies (longer wavelengths) owing to the influence or a change in environment e.g. solvent. It is informally referred to as red shift.

2: Carbocation

A carbocation is an ion with a positively-charged carbon atom

3: Chromophore

That part of a molecular entity consisting of an atom or group of atoms in which the electronic transition responsible for a given spectral band is approximately localized.

4: Configuration Intigration (CI)

The mixing of many-electron wavefunctions constructed from different electronic configurations to obtain an improved many-electron state.

5: Colourability

The ability of a colourless or a slightly coloured (pale yellow) photochromic material to develop colouration is called colourability

6: Force field

In the context of molecular mechanics, a force field refers to the functional form and parameter sets used to describe the potential energy of a system of particles (typically but not necessarily atoms). Force field functions and parameter sets are derived from both experimental work and high-level quantum mechanical calculations.

7: Hypsochromic shift

A change of spectral band position in the absorption, reflectance, transmittance, or emission spectrum of a molecule to a shorter wavelength.

8: Oscillator strength (f)

A measure of the intensity of a spectral band: a classical concept (giving the effective number of electrons taking part in a certain transition) adapted to wave mechanism.

9: Photochromism

It is defined as a light induced reversible transformation of chemical species between isomers having different absorption spectra.

10: Photodegradation

Due to chemical degradation of a material, the performance is reduced over time and this is termed "fatigue" or degradation and is caused by the absorption of photons, particularly those wavelengths found in sunlight, such as infrared radiation, visible light and ultraviolet light.

11: Spirooxazines

It is an important class of photochromic compounds which can be defined as the molecules containing a condensed ring-substituted 2*H*-[1,4]oxazine, in which the number 2 carbon of the oxazine ring is involved in spiro linkage.

12: Solvatochromism

Solvatochromism is the ability of a chemical substance to change color due to a change in solvent polarity. Negative solvatochromism corresponds to hypsochromic shift and positive solvatochromism corresponds to bathochromic shift with increasing solvent polarity. The sign of the solvatochromism depends on the difference in dipole moment of the molecule of the dye between its ground state and excited state.

***13: Quantum Yield* (Φ)**

The number of defined events which can occur per photon absorbed by the system.

14: Thermochromism

A thermally induced reversible colour change is called thermochromism.

15: Thermosolvatochromism

It is the phenomenon exhibited when the thermochromism of a molecular system results from its association with another chemical species such as metal ion or proton or from modification of the medium by a thermal effect.